



<https://theses.gla.ac.uk/>

Theses Digitisation:

<https://www.gla.ac.uk/myglasgow/research/enlighten/theses/digitisation/>

This is a digitised version of the original print thesis.

Copyright and moral rights for this work are retained by the author

A copy can be downloaded for personal non-commercial research or study, without prior permission or charge

This work cannot be reproduced or quoted extensively from without first obtaining permission in writing from the author

The content must not be changed in any way or sold commercially in any format or medium without the formal permission of the author

When referring to this work, full bibliographic details including the author, title, awarding institution and date of the thesis must be given

Enlighten: Theses

<https://theses.gla.ac.uk/>
research-enlighten@glasgow.ac.uk

ProQuest Number: 10646252

All rights reserved

INFORMATION TO ALL USERS

The quality of this reproduction is dependent upon the quality of the copy submitted.

In the unlikely event that the author did not send a complete manuscript and there are missing pages, these will be noted. Also, if material had to be removed, a note will indicate the deletion.



ProQuest 10646252

Published by ProQuest LLC (2017). Copyright of the Dissertation is held by the Author.

All rights reserved.

This work is protected against unauthorized copying under Title 17, United States Code
Microform Edition © ProQuest LLC.

ProQuest LLC.
789 East Eisenhower Parkway
P.O. Box 1346
Ann Arbor, MI 48106 – 1346

Phosphodiesterases in the cell cycle

A thesis submitted to the

FACULTY OF BIOMEDICAL AND LIFE SCIENCES

for the degree of

DOCTOR OF PHILOSOPHY

by

Catherine Louise Sheppard

Division of Biochemistry & Molecular Biology

Institute of Biomedical and Life Sciences

University of Glasgow

February 2002

© Catherine Sheppard, 2002

Declaration

I declare that the work described in this thesis has been carried out by myself unless otherwise cited or acknowledged. It is entirely of my own composition and has not, in whole or in part, been submitted for any other degree.

Catherine L. Sheppard

February 2001.

Abstract

Phosphodiesterases (PDEs) are of central importance in the regulation of cyclic AMP (cAMP) signalling, since they mediate its degradation. Cyclic AMP and the downstream kinase, protein kinase A (PKA), are central to many cellular processes including cell proliferation, where they exert effects on the cell cycle machinery at a number of levels. The study of PDEs through the cell cycle in mammalian somatic cells has been sparse.

Here, an investigation into the activities of different PDE isoforms through the cell cycle was undertaken. Reproducible methods for arresting Rat-1 fibroblasts in different stages of the cell cycle were developed. These were used to determine the profiles of PDE activity in the different phases of the cycle. It was found that, in Rat-1 cells, there was an increase in total PDE activity during mitosis. This was found to be largely attributable to PDE4 activity since it was sensitive to rolipram inhibition. Selective immunoprecipitation allowed the changes to be attributed to specific PDE4 subfamilies. In particular PDE4D3, when immunoprecipitated from mitotic lysates, exhibited the highest activity. This increased activity of PDE4D3 coincided with a fraction of the protein migrating as a double bandshift when analysed by SDS-PAGE and immunoblotting. Both the increased activity and the bandshifts occurring during mitosis were specific to mitosis and both disappeared within 2 h following a release from mitotic block. Both the increased activity and the bandshifts seen during mitosis were sensitive to the general kinase inhibitor, staurosporine, but insensitive to a range of other more specific inhibitors for kinases such as PKA, PKC, PI 3-kinase, ERK and Cdk2/ Cyclin B. They were also sensitive to treatment with alkaline phosphatase, and could be maintained following release from mitosis using concentrations of okadaic acid characteristic of protein phosphatase 1 inhibition.

HPLC and mass spectrometric analysis of tryptically digested PDE4D3 phosphopeptides, four residues were identified as being highly phosphorylated by kinases that were active in mitotic lysate. Three of these residues Ser⁶¹, Ser⁷⁵ and Ser²³⁹ are previously unknown phosphorylation sites. The fourth phosphorylated residue, Ser⁵⁷⁹, has previously been shown to be phosphorylated by ERK.

When the activity of PKA in cell lysates was assayed, it was noted that in mitosis there was a fall in PKA activity that coincided with the increases in PDE4D3 activity. Upon rolipram-mediated inhibition of PDE4 in these mitotic cells a concomitant increase in PKA

activity was noted. Furthermore, this inhibition of PDE4 in mitotic cells caused an increase in the rate at which the cells left mitosis.

These observations suggest that the phosphorylation and activation of PDE4D3 in mitosis, by an as yet unidentified kinase, may lead to the decrease in PKA activity. The inhibition of PDE4 may cause an increase in the rate at which cells leave mitosis, suggesting a specific regulatory role for PDE4D3 in the control of the transition of cells through mitosis.

Acknowledgements

My thanks go to Prof. M. Houslay, my supervisor, for allowing me to carry out this project in his laboratory, helping me with my thesis and supporting the work that I've done throughout the last three years and more.

Thanks to everyone in the Gardiner Lab., especially Carolynn for bravely taking this project off my hands and U Guy, without whom lunchtimes would have been boring, Boston would not have been any fun and the work days would have been long and lonely – Bunsen and Beaker forever!!!

I would like to thank my mum, dad, grandma and Chris for being there always, giving me all the help, support, love and encouragement that I could ever need and more.

Gilles, thank you for everything, I know I wouldn't have been able to finish this thing without your help, support, guidance and most of all encouragement – onwards and upwards!!!

Special thanks must go to Gopal Sapkota and Dr. N. Morrice for their help with the HPLC and phosphopeptide analysis work.

I should also take this opportunity to mention Dr. R. Owens my joint supervisor from Celltech Plc.

Table of contents

Declaration.....	ii
Abstract.....	iii
Acknowledgements.....	v
Table of contents.....	vi
List of figures	xii
List of tables.....	xv
Abbreviations.....	xvi
Chapter 1	
General Introduction	1
1.1. <i>Cyclic nucleotide signalling pathways.....</i>	<i>2</i>
1.1.1. Cyclic nucleotide generation in cells.....	2
1.1.1.1. G-Protein Coupled Receptors	2
1.1.1.2. Adenylyl cyclases	3
1.1.2. Targets of cAMP generation.....	4
1.1.2.1. Protein Kinase A.....	5
1.1.2.2. A Kinase-anchoring proteins (AKAPs)	6
1.1.2.3. PKA independent mechanisms of cAMP dependent signalling.....	6
1.1.3. Cyclic nucleotide hydrolysis within cells.....	7
1.2. <i>The phosphodiesterase superfamily</i>	<i>7</i>
1.2.1. The PDE1 family of phosphodiesterases	8
1.2.2. The PDE2 family of phosphodiesterases	8
1.2.3. The PDE3 family of phosphodiesterases	9
1.2.4. The PDE4 family of phosphodiesterases	9
1.2.5. The PDE5 family of phosphodiesterases	10
1.2.6. The PDE6 family of phosphodiesterases.....	10
1.2.7. The PDE7 family of phosphodiesterases.....	11
1.2.8. The PDE8 family of phosphodiesterases.....	11
1.2.9. The PDE9 family of phosphodiesterases.....	12
1.2.10. The PDE10 family of phosphodiesterases.....	12
1.2.11. The PDE11 family of phosphodiesterases.....	12
1.3. <i>Biochemistry of the PDE4 cAMP-specific phosphodiesterases</i>	<i>13</i>
1.3.1. The PDE4A subfamily.....	13
1.3.2. The PDE4B subfamily.....	14
1.3.3. The PDE4C subfamily.....	14
1.3.4. The PDE4D subfamily.....	14
1.3.4.1. ‘Short-form’ splice variants of PDE4D	15
1.3.4.2. ‘Long-form’ splice variants of PDE4D.....	15
1.3.4.3. Regulation of PDE4D by PKA	16
1.3.4.4. Regulation of PDE4D by ERK	17
1.3.4.5. Regulation of PDE4D by phosphatidic acid	18
1.4. <i>Cyclic AMP involvement in the cell cycle</i>	<i>18</i>
1.4.1. Cyclic AMP induced inhibition of cell cycle entry	18
1.4.1.1. Cyclic AMP mediated elevation of p27 ^{KIP1} protein levels.....	20
1.4.1.2. Cyclic AMP mediated down regulation of D-type cyclins	21
1.4.1.3. Cyclic AMP mediated interference of the mitogen activated protein kinase cascade.....	21

1.4.1.4. PI3-kinase pathway.....	22
1.4.2. Cyclic-AMP involvement of M phase transition.....	23
1.4.2.1. Cyclic AMP dependent modulation of MPF activity.....	24
1.4.2.2. Cyclic AMP dependent modulation of the anaphase promoting complex activity.....	24
1.5. <i>Phosphodiesterases and the cell cycle</i>	25
1.5.1. Phosphodiesterases and T cell proliferation.....	26
1.5.1.1. PDE4 and T cell proliferation.....	28
1.5.1.2. PDE7 and T cell proliferation.....	29
1.5.2. PDEs and smooth muscle cell proliferation.....	29

Chapter 2

Materials and methods.....46

2.1. <i>Mammalian cell culture</i>	47
2.1.1. Maintenance of cell lines.....	47
2.1.1.1. Rat-1 cell line.....	47
2.1.1.2. HeLa cell line.....	47
2.1.1.3. SK-N-SH cell line.....	47
2.1.1.4. COS-1 and COS-7 cell lines.....	47
2.1.1.5. HuT-78, Molt-3 and Jurkat J6 cell lines.....	48
2.1.1.6. HEK-293, U118 MG, FTC113 and U937 cell lines.....	48
2.1.2. DEAE-Dextran transient transfection.....	48
2.1.3. LipofectAMINE™ transfection of HeLa cells.....	49
2.1.4. Cell cycle arrest.....	49
2.1.4.1. Asynchronous cell isolation.....	49
2.1.4.2. G0 phase arrest.....	50
2.1.4.3. G1/ S phase arrest.....	50
2.1.4.4. S / G2 phase arrest.....	50
2.1.4.5. Mitotic arrest.....	50
2.2. <i>Analysis of cells in the cell cycle</i>	51
2.2.1. Propidium iodide (PI) double stranded DNA staining.....	51
2.2.2. FACS analysis of PI stained cells.....	51
2.2.3. Labelling cells for dual PI and bromo-deoxyuridine (BrdU) DNA analysis.....	51
2.2.3.1. Incorporating BrdU to proliferating cells.....	51
2.2.3.2. Fixing BrdU labelled cells.....	52
2.2.3.3. Staining BrdU labelled cells with FITC conjugated antibody and propidium iodide.....	52
2.2.4. FACS analysis of BrdU-FITC and PI stained cells.....	52
2.2.4.1. FACScalibur acquisition settings.....	53
2.2.4.2. FACS data analysis.....	53
2.2.5. Apoptotic analysis of cells.....	54
2.2.5.1. Labelling cells for apoptotic analysis.....	54
2.2.5.2. FACS analysis of apoptotic cells.....	54
2.3. <i>Protein analysis</i>	55
2.3.1. Harvesting cell lysate.....	55
2.3.1.1. Whole cell lysate production.....	55
2.3.1.2. Crude sub-cellular fractionation by differential centrifugation.....	55
2.2.1.3. Refined sub-cellular fractionation by differential centrifugation.....	56
2.3.2. Quantification of protein (Bradford assay).....	56
2.3.3. Enzyme-linked immunosorbent assay.....	57
2.3.4. Lactate Dehydrogenase (LDH) assays.....	58
2.3.5. SDS-poly-acrylamide gel electrophoresis (SDS-PAGE).....	58
2.3.5.1. Sample preparation.....	58
2.3.5.2. Casting and running a tris-glycine gel.....	58
2.3.6. Visualising protein by coomassie staining.....	59
2.3.7. Visualising protein by silver staining.....	59
2.3.8. Western immuno-blotting.....	60
2.3.8.1. Transfer of protein from acrylamide gel to nitrocellulose.....	60
2.3.8.2. Immunoblotting nitrocellulose.....	60
2.3.9. Phosphodiesterase-4 activity assay.....	61
2.3.9.1. Activation of dowex 1X8-400 anion exchange resin.....	61
2.3.9.2. Assay tube preparation.....	61
2.3.9.3. Determination of PDE3 and PDE4 activity.....	62

2.3.10. Immunoprecipitation	62
2.3.10.1. Pre-clearing agarose beads.....	62
2.3.10.2. Binding target protein to antibody	62
2.4. Kinase assays	63
2.4.1. PKA assay	63
2.4.1.1. Cell lysate extraction for PKA assay	63
2.4.1.2. PKA assay tube pre-incubation.....	63
2.4.1.3. PKA assay reaction.....	64
2.4.1.4. Calculations for PKA assay data.....	64
2.4.2. Alkaline phosphatase treatment of protein	65
2.4.3. MBP fusion protein production	66
2.4.3.1. Induction of E.Coli cells transformed with a recombinant protein-containing construct	66
2.4.3.2. Isolation of recombinant MBP fusion protein from E.Coli cells	66
2.4.3.3. Elution of recombinant MBP fusion protein from amylose resin	67
2.4.3.4. TEV cleavage of MBP fused recombinant protein from amylose resin.....	67
2.4.4. In vivo phosphorylation of protein	67
2.4.5. In vitro phosphorylation of protein.....	68
2.4.5.1. Phosphorylation of a target protein from mammalian cells using a purified kinase	68
2.4.5.2. Phosphorylation of recombinant target protein from E.Coli. using cellular lysate	68
2.4.5.3. Phosphorylation using an isolated kinase	69
2.4.5.4. Radiolabelled analysis of protein.....	69
2.4.5.5. 'Cold' in vitro phosphorylation of proteins	70
2.4.6. Tryptically digested phosphopeptide analysis by 2D TLC.....	70
2.4.6.1. Tryptic cleavage of phosphorylated protein.....	70
2.4.6.2. Isolation of tryptically cleaved peptides	71
2.4.6.3. Loading plates for 2D TLC separation of phosphopeptides	71
2.4.6.4. First dimension thin-layer electrophoresis.....	71
2.4.6.5. Second dimension thin-layer chromatography.....	72
2.4.6.6. Identification radiolabelled phosphopeptides	72
2.4.7. Tryptically digested phosphopeptide analysis by HPLC	72
2.4.7.1. In gel tryptic digest of phosphorylated protein	73
2.4.7.2. HPLC analysis of phosphopeptides	73
2.4.7. Protein binding assay.....	73
2.5. Molecular Biology	74
2.5.1. Large scale production of plasmid DNA	74
2.5.1.1. Ethanol precipitation of DNA.....	74
2.5.1.2. Quantification of DNA	75
2.5.2. Small scale production of plasmid DNA	75
2.5.3. Analysis of plasmid DNA.....	76
2.5.3.1. DNA restriction digest.....	76
2.5.3.2. Agarose gel analysis of DNA	76
2.5.3.3. Gel purification of digested DNA.....	77
2.5.4. Ligation of dsDNA.....	77
2.5.5. Production of Competent Cells.....	77
2.5.6. Transformation of Competent Cells with Target DNA	78
2.5.7. Glycerol Stock Production.....	78
2.5.8. DNA Sequencing.....	78
2.5.9. Site directed mutagenesis of DNA using the QuickChange™ kit	79
2.5.9.1. Isolation and transformation of mutated DNA.....	79
2.5.10. Reverse transcription PCR (RT-PCR)	80
2.5.10.1 RNA isolation	80
2.5.10.2. First strand complementary DNA (cDNA) synthesis.....	80

Chapter 3

Phosphodiesterases and the cell cycle86

3.1. Introduction	87
3.1.1. The cell cycle; a brief overview.....	87
3.1.2. Cyclic AMP control of the cell cycle	87
3.1.2.1. Elevated cAMP induces cell quiescence.....	88
3.1.2.2. Cyclic AMP controls cells in interphase and mitosis.....	88
3.1.3. Phosphodiesterases inhibit cell cycle progression	89

Results

3.2. <i>Characterisation of Rat-1 fibroblast PDE4 profile</i>	91
3.2.1. Western blot analysis of PDE4A splice variants	91
3.2.1.1. RT-PCR analysis of PDE4A isoforms found in Rat-1 fibroblast.....	91
3.2.2. Western blot analysis of PDE4B splice variants.....	92
3.2.2.1. RT-PCR analysis of PDE4B isoforms found in Rat-1 fibroblasts	92
3.2.3. Western blot analysis of PDE4C isoforms	92
3.2.4. Western blot analysis of PDE4D isoforms	93
3.3. <i>Cell cycle analysis in Rat-1 fibroblasts</i>	93
3.3.1. Determination of the rates of proliferation of Rat-1 fibroblasts	93
3.3.2. Method development for the isolation of Rat-1 cells in specific phases of the cell cycle	94
3.3.3. Arresting Cells in G0 phase.....	94
3.3.4. Arresting Cells in G1/S.....	94
3.3.4.1. Alternative means of G1 arrest	95
3.3.5. Inhibition of cells in S-phase	95
3.3.5.1. Alternative means of S phase arrest.....	95
3.3.6. Inhibition of cells in M-phase.....	95
3.3.6.1. Microtubule disruption agents and M-phase arrest.....	96
3.3.6.2. Alternative antimicrotubular agents for M-phase arrest	96
3.3.7. Expression of marker proteins to determine the isolation of Rat-1 cells in cell cycle phases ..96	
3.3.7.1. Detection of Cyclin E in cells isolated at different phases of the cell cycle	97
3.3.7.2. Detection of Cyclin B in cells isolated at different phases of the cell cycle	97
3.3.7.3. Detection of phospho-ERK in cells isolated at different phases of the cell cycle.....	98
3.3.7.4. Detection of phospho-MEK in cells isolated at different phases of the cell cycle.....	98
3.4. <i>Analysing the changes in cAMP phosphodiesterase activity in the cell cycle</i>	99
3.4.1. Determination of cAMP PDE activity in Rat-1 cells isolated at different stages of the cell cycle	99
3.4.1.1. PDE4 activity in Rat-1 cells isolated at different stages of the cell cycle.....	99
3.4.1.2. PDE3 activity in Rat-1 cells isolated at different stages of the cell cycle.....	100
3.4.2. Analysis of PDE4 isoform activity changes in cells isolated at different stages of the cell cycle	100
3.4.2.1. Changes in PDE4A and PDE4C isoform activity in cells isolated at different stages of the cell cycle	100
3.4.2.2. Changes in PDE4B activity in cells isolated at different stages of the cell cycle	101
3.4.2.3. Changes in PDE4D activity in cells isolated at different stages of the cell cycle	101
3.4.2.4. Changes in PDE4D protein expression in cells isolated at different stages of the cell cycle... ..	101
3.4.3. Subcellular localisation of PDE4D protein in cells isolated at different stages of the cell cycle.. ..	102
3.5. <i>Analysis of the changes in PKA activity in the cell cycle</i>	102
3.5.1. Determination of PKA activity in cells isolated at different stages of the cell cycle.....	102
3.5.1.1. Changes in PKA activity in the cell cycle.....	102
3.5.1.2. Detection of phospho-CREB in cell lysates isolated at different phases of the cell cycle .	103
3.5.1.3. Levels of PKA activity controlled specifically by PDE4 dependent mechanisms in Rat-1 cells	103
3.6. <i>The effects of the inhibition of PDE isoforms on cell proliferation</i>	103
3.6.1. Inhibition of PDE4 reduces Rat-1 cell proliferation	104
3.6.1.1. Inhibition of PDE4 alters the distribution of Rat-1 cells within the cell cycle.....	104
3.6.2. Inhibition of PDE3 does not alter the rate of Rat-1 cell proliferation.....	104
3.6.2.1. Inhibition of PDE3 does not alter the distribution of Rat-1 cells within the cell cycle.....	105
3.7. <i>Discussion and conclusions</i>	106

Chapter 4

Investigation of PDE4D3 in mitosis	142
4.1. <i>Introduction</i>	143
4.1.1. PKA and mitotic regulation.....	143
4.1.2. PDE4D3 function, localisation and modification	144

Results

4.2	<i>Characterisation of PDE4D3 in nocodazole-induced mitosis</i>	146
4.2.1.	Changes in PDE4D electrophoretic mobility during mitosis.....	146
4.2.1.1.	Identification of electrophoretically retarded PDE4D species in Rat-1 cells.....	146
4.2.2.	Subcellular distribution of PDE4D3 protein in mitosis	147
4.2.3.	Modification of PDE4D3 as cells accumulate in mitosis	147
4.2.3.1.	Nocodazole induced modification of PDE4D3 is not brought about by disruption of microtubule dynamics	147
4.2.3.2.	Accumulation of Rat-1 cells in mitosis with nocodazole treatment.....	148
4.2.3.3.	Electrophoretic mobility of PDE4D3 is reduced as cells accumulate in mitosis	148
4.2.3.4.	Activity of PDE4D increases as cells accumulate in mitosis.....	148
4.2.4.	Modification of PDE4D3 as cells leave mitosis	149
4.2.4.1.	Cell cycle analysis of Rat-1 cells released from nocodazole block	149
4.2.4.2.	Electrophoretic mobility of PDE4D3 is increased as Rat-1 cells leave mitosis.....	149
4.2.4.3.	Activity of PDE4D decreases as Rat-1 cells leave mitosis	149
4.3.	<i>Identification of the PDE4D3 mitotic modification</i>	150
4.3.1.	Mitotically isolated PDE4D3 is not ubiquitinated.....	150
4.3.2.	In vivo phosphorylation of PDE4D3 with ³² P orthophosphate.....	150
4.3.3.	The mitotic modifications of PDE4D can be maintained by phosphatase inhibition	151
4.3.3.1.	Electrophoretically shifted species of PDE4D3 are maintained upon addition of okadaic acid to mitotically released cells	151
4.3.3.2.	Elevated PDE4D activity is maintained with Okadaic acid addition to mitotically released cells	151
4.3.4.	Phosphatase treatment of mitotic PDE4D3	152
4.3.5.	Utilisation of staurosporine to identify the nature of the mitotic modification of PDE4D3 ..	152
4.3.5.1.	Staurosporine increases the electrophoretic mobility of mitotically modified PDE4D3 ..	153
4.3.5.2.	Staurosporine decreases the activity of mitotically modified PDE4D	153
4.3.5.3.	Staurosporine does not induce premature exit of Rat-1 cells from mitosis.....	154
4.3.6.	Use of specific kinase inhibitors to identify the kinase which targets PDE4D3 in mitosis	154
4.3.6.1.	Protein kinase C inhibitors do not affect the mitotic modification of PDE4D3.....	154
4.3.6.2.	Many commercially available specific kinase inhibitors do not affect the mitotic modification of PDE4D3	155
4.4.	<i>The effect of PKA activation on PDE4D3 in mitotic cells</i>	155
4.4.1.	Forskolin increases the amount of 'mitotic' PDE4D3 showing retarded electrophoretic migration.....	155
4.4.1.1.	Forskolin retarded PDE4D3 is insensitive to H89	156
4.4.2.	Forskolin increases the activity of mitotic PDE4D.....	156
4.4.2.1.	Forskolin-stimulated PDE4D3 activity is insensitive to H89	157
4.5.	<i>Identification of the potential phosphorylation sites in PDE4D3</i>	157
4.5.1.	Analysis packages used for identification of target sequence motifs in PDE4D3	158
4.5.1.1.	Predicted serine, threonine and tyrosine phosphorylation sites of PDE4D3.....	158
4.6.	<i>Mutational analysis of the modification of PDE4D3 during mitosis in alternative cell lines</i>	158
4.6.1.	Endogenous PDE4D3/5 in HeLa cells arrested in mitosis have reduced electrophoretic mobilities	159
4.6.2.	Serine and threonine mutants of PDE4D3 are modified during mitosis.....	159
4.6.2.1.	Electrophoretic mobility of mutants of the PKA phosphorylated sites in PDE4D3 during mitosis	159
4.6.2.2.	Analysis of the activity of Ser13Ala and Ser54Ala PDE4D3 mutants in mitosis.....	160
4.6.2.3.	The electrophoretic mobility of truncated PDE4D mutants in mitosis	160
4.6.2.4.	Analysis of the activity and electrophoretic mobility of other PDE4D3 mutants in mitosis ...	161
4.7.	<i>In vitro phosphorylation of PDE4D3</i>	161
4.7.1.	UCR1 is phosphorylated in vitro by mitotic kinases	161
4.7.2.	Phosphorylation of PDE4D3 by mitotic kinases is within a different peptide to that targeted by PKA	162
4.7.2.1.	Cyanogen bromide cleavage of phosphopeptides	162
4.7.3.	2D analysis of PDE4D3 peptides phosphorylated with mitotic lysate	162
4.7.4.	HPLC identification of PDE4D3 peptides phosphorylated with mitotic lysate.....	163
4.7.4.1.	Mass spectrometry identification of PDE4D3 peptides phosphorylated by mitotic kinases....	164
4.7.4.2.	Cycle burst identification of residues phosphorylated in mitosis.....	164
4.7.5.	The activity of PDE4D3 is increased by in vitro phosphorylation using kinases present in mitotic lysates	164

4.8. <i>The effects of the mitotic increase in PDE4D activity on mitotic processes</i>	165
4.8.1. Rolipram causes an elevation of PKA activity in mitotic cells.....	165
4.8.2. Rolipram increases the rate of M/G1 transition.....	165
4.9. <i>Discussion</i>	166
 Chapter 5	
Characterisation of Phosphodiesterase 7 (PDE7)	223
5.1 <i>Introduction</i>	224
<i>Results</i>	226
5.2. <i>Expression of PDE7A isoforms in cells</i>	226
5.2.1 Screening cell lines for endogenous PDE7A protein.....	226
5.2.2. Expression of recombinant PDE7A protein in a mammalian system	226
5.2.2.1. Cloning PDE7A2 into the pcDNA3.....	227
5.2.2.2. Transfection of COS-7 cells with PDE7A constructs	227
5.2.2.3. PDE7A mRNA is detected in COS-7 cells	228
5.2.2.4. Attempt to transfect T-cell lines with PDE7A1	228
5.2.2.5. Subcellular localisation of PDE7A1 in mammalian cells	228
5.3. <i>Analysis of PDE7A1 Protein Activity</i>	229
5.3.1. Modification of PDE assay to optimise the detection of PDE7 activity	229
5.4. <i>Characterisation of PDE7 specific inhibitors</i>	230
5.4.1. Production of PDE7 specific inhibitors.....	230
5.4.2. Characterisation of PDE7 inhibitors in mammalian cells.....	230
5.5. <i>Modification of PDE7 within cells</i>	231
5.5.1. Prediction of phosphorylation sites within PDE7A1	231
5.5.2. Stimulation of cells in an attempt to phosphorylate PDE7A1	231
5.5.3. Attempted in vitro phosphorylation of PDE7A1	232
5.5.3.1. Efficacy of the PDE7A antibody in the isolation of PDE7A from cell lysates	232
5.5.3.2. In vitro phosphorylation of PDE7A1	232
5.5.4. In vivo phosphorylation of PDE7A1	233
5.5.5. Attempted identification of kinase which co-immunoprecipitates with PDE7A antibody.	233
5.5.5.1. Immunoprobe of the PDE7A1 immunoprecipitate	233
5.5.5.2. Coimmunoprecipitation of RACK1 with PDE7A1.....	234
5.5.5.3. RACK1-GST pulldown of in vitro expressed PDE7A1	234
5.6. <i>Conclusions</i>	235
 Chapter 6	
General discussion and future directions	263
References	272

List of figures

Chapter 1

Figure 1.1. G-protein coupled receptor activation of protein kinase A.....	32
Figure 1.2. The topology of membrane bound adenylate cyclase.....	33
Figure 1.3. Interaction of AKAPs with PKA regulatory domains	34
Figure 1.4. Mammalian PDE isozyme families	35
Figure 1.5. Splice variation of PDE4 isoforms	36
Figure 1.6. Alignment of the deduced amino acid sequences of cDNAs for the human PDE4 families	37
Figure 1.7. Structure of mRNA transcripts from the PDE4A gene.....	40
Figure 1.8. Structure of mRNA transcripts from the PDE4C gene.....	41
Figure 1.9. Structure of mRNA transcripts from the PDE4D gene.....	42
Figure 1.10. Postulated mechanism of 'long form' PDE activation upon PKA phosphorylation.....	43
Figure 1.11. Regulation of G1/S transition	44

Chapter 2

Figure 2.1. FL2-H distribution of cells labelled with propidium iodide	81
Figure 2.2. Doublet discrimination of a Rat-1 cell population.....	82
Figure 2.3. Normal FL1-H distribution of cells from an asynchronous population.....	83
Figure 2.4. Modfit™ analysis of BrdU-FITC and propidium iodide labelled cells.....	84
Figure 2.5. Locations of sample and dye origins for two-dimensional separation of phosphopeptides on 20 x 20 TLC plates.....	85

Chapter 3

Figure 3.1. Stages of the cell cycle	110
Figure 3.2. The changes in chromosome morphology during the different phases of mitosis.....	111
Figure 3.3. Effects of cAMP elevation and PKA activation on G1/S arrest	112
Figure 3.4. Western blot analysis of PDE4A isoforms expressed in Rat-1 cells	113
Figure 3.5. Annealing positions of primers and primer sequences for RT-PCR analysis of rat PDE4A splice variants	114
Figure 3.6. RT-PCR analysis of Rat-1 cell total RNA using PDE4A specific primers.....	115
Figure 3.7. Western blot analysis of PDE4B isoforms expressed in Rat-1 cells.....	116
Figure 3.8. Annealing positions of primers and primer sequences for RT-PCR analysis of rat PDE4B splice variants	117
Figure 3.9. RT-PCR analysis of Rat-1 cell total RNA using PDE4B specific primers.....	118
Figure 3.10. Western blot analysis of PDE4C isoforms expressed in Rat-1 cells.....	119
Figure 3.11. Western blot analysis of PDE4D isoforms expressed in Rat-1 cells	120
Figure 3.12. Analysis of cell cycle distribution of an asynchronous population of Rat-1 cells	121
Figure 3.13. Determination of the duration of a complete cell cycle in Rat-1 cells.....	122
Figure 3.14. Arrest of Rat-1 cells in G0 upon 48 h serum starvation	123
Figure 3.15. Arrest of Rat-1 cells at G1/S upon a double thymidine block	124
Figure 3.16. Treatment of Rat-1 cells with olomucine	125
Figure 3.17. Arrest of Rat-1 cells in S and S/G2 upon incubation with aphidicolin.....	126
Figure 3.18. Treatment of Rat-1 cells with L-mimosine for 24 h	127
Figure 3.19. Arrest of Rat-1 cells in M phase upon 14 h incubation with nocodazole	128
Figure 3.20. Redistribution of Rat-1 cells within the cell cycle upon release of nocodazole block....	129
Figure 3.21. Differential expression and phosphorylation of marker proteins in Rat-1 cells isolated at different phases of the cell cycle.....	130
Figure 3.22. Change in cAMP specific PDE activities in Rat-1 cell lysates isolated at different stages of the cell cycle	131
Figure 3.23. Change in specific PDE4 isoforms activities in Rat-1 cell lysates isolated at different stages of the cell cycle	132
Figure 3.24a. Change in subcellular localisation of PDE4D protein in Rat-1 cells isolated at different stages of the cell cycle	133

Figure 3.24b. Quantification of changes in subcellular localisation of PDE4D protein in Rat-1 cells isolated at different stages of the cell cycle	134
Figure 3.25. Analysis of PKA activity in Rat-1 cell lysates isolated at different phases of the cell cycle	135
Figure 3.26. Analysis of CREB phosphorylation in Rat-1 cell lysates isolated at different phases of the cell cycle	136
Figure 3.27. The effect of PDE4 inhibition on the percentage of active PKA in Rat-1 cell lysates isolated at different phases of the cell cycle.....	137
Figure 3.28. Changes in cell cycle distribution of Rat-1 cells upon incubation with rolipram	138
Figure 3.29. Changes in cell cycle distribution of Rat-1 cells upon incubation with cilostomide	139

Chapter 4

Figure 4.1. PKA activity and mitotic transition	173
Figure 4.2. Change of PDE4D3 electrophoretic mobility during mitosis	174
Figure 4.3. PDE4D5 is not expressed in Rat-1 cells	175
Figure 4.4a. Sub-cellular localisation of PDE4D3 in asynchronous and mitotic Rat-1 cells, determined by crude fractionation	176
Figure 4.4b. Subcellular localisation of PDE4D3 in Rat-1 cells isolated in mitosis, determined by refined fractionation.....	177
Figure 4.5. The effect of short-term incubation of increasing concentrations of nocodazole on PDE4D3 modification	178
Figure 4.6. Change in Rat-1 cell cycle distribution with the addition of nocodazole	179
Figure 4.7. Changes in electrophoretic mobility of PDE4D3 in Rat-1 cells incubated with nocodazole for various times.....	180
Figure 4.8. The increase in PDE4D activity as cells accumulate in mitosis	181
Figure 4.9. Redistribution of Rat-1 cells through the cell cycle upon release of the nocodazole-induced mitotic block	182
Figure 4.10. Increase in electrophoretic mobility of PDE4D3 protein as Rat-1 cells exit nocodazole-induced mitosis	183
Figure 4.11. Decrease in PDE4D activity in cells released from nocodazole-induced mitotic arrest.	184
Figure 4.12. PDE4D3 is not ubiquitinated during mitosis	185
Figure 4.13. <i>In vivo</i> phosphorylation of PDE4D3 in asynchronous and mitotic Rat-1 cells.....	186
Figure 4.14. Okadaic acid maintains bandshifted PDE4D3 modification after release of cells from mitotic block	187
Figure 4.15. Okadaic acid maintains the elevated PDE4D activity after release of cells from mitotic block	188
Figure 4.16. CIAP ablates the bandshifted species of PDE4D3 from nocodazole-induced mitotic lysate	189
Figure 4.17. CIAP reduces the activity of PDE4D in nocodazole-induced mitotic lysate.....	190
Figure 4.18. Staurosporine ablates bandshifted species of PDE4D3 in Rat-1 cells isolated in mitosis	191
Figure 4.19. Staurosporine ablates the nocodazole-induced mitotic bandshift of PDE4D3 in a time dependent fashion	192
Figure 4.20. Staurosporine reduces the activity of PDE4D in nocodazole-induced mitotic Rat-1 cells	193
Figure 4.21. FACs analysis of Rat-1 cells arrested in mitosis and subjected to a further incubation with staurosporine.....	194
Figure 4.22. Commercially available specific kinase inhibitors do not ablate the PDE4D3 bandshift in nocodazole induced mitotic cells	195
Figure 4.23. The increased activity of PDE4D in nocodazole-induced mitotic cells is insensitive to many commercially available specific kinase inhibitors.....	196
Figure 4.24. Change in electrophoretic mobility of PDE4D3 in mitotic and asynchronous cells upon stimulation or inhibition of PKA	197
Figure 4.25. Changes in PDE4D activity upon treatment with forskolin and H89	198
Figure 4.26. The amino acid sequence of rat PDE4D3.....	199
Figure 4.27. A proportion of endogenous PDE4D3/PDE4D5 in nocodazole induced mitotic HeLa cells has reduced electrophoretic mobilities.....	200
Figure 4.28. PDE4D3 Ser ¹³ /Ala mutant behaves as wild-type in nocodazole-induced mitosis	201
Figure 4.29. Analysis of electrophoretic mobilities of PDE4D mutants in mitosis	202
Figure 4.30. Mutant PDE4D3 protein activity in asynchronous and mitotic cells.....	203
Figure 4.31. Mutant forms of PDE4D3 used in this study.....	204

Figure 4.32. Domain sequences of GST-fused recombinant protein used for <i>in vitro</i> phosphorylation reactions.....	205
Figure 4.33. Phosphorylation of recombinant UCR1/UCR2 constructs by mitotic lysate and PKA ..	206
Figure 4.34. Peptides generated from <i>in vitro</i> phosphorylated PDE4D3 cleaved with cyanogen bromide	207
Figure 4.35. Separation of tryptically digested phosphorylated peptides of PDE4D3 by 2D thin layer chromatography	208
Figure 4.36. Separation of tryptically digested PDE4D3 phosphopeptides by HPLC	209
Figure 4.37. Peptides of PDE4D3 phosphorylated <i>in vitro</i> by kinases from mitotic lysates	210
Figure 4.38a. Cycle burst amino acid analysis of residues phosphorylated in the peptide found at the N-terminal of UCR1.....	211
Figure 4.38b. Cycle burst amino acid analysis of residues phosphorylated in the peptide found at the C-terminal of UCR1.....	212
Figure 4.38c. Cycle burst amino acid analysis of residues phosphorylated in the peptide found at the N-terminal of the catalytic domain.....	213
Figure 4.38d. Cycle burst amino acid analysis of residues phosphorylated in the peptide found at the C-terminal of the catalytic domain.....	214
Figure 4.39. Changes in PDE4D activity after <i>in vitro</i> phosphorylation with kinases isolated from asynchronous and mitotic lysate	215
Figure 4.40. Increase in proportion of active PKA in cells arrested in mitosis after incubation with rolipram.....	216
Figure 4.41. The effect of rolipram on cell cycle distribution after the release of cells from nocodazole-induced mitosis	217

Chapter 5

Figure 5.1. Synthetic selective inhibitors of PDE7	238
Figure 5.2. Alignment of PDE7A1, PDE7A2 and PDE7A3 peptide sequences	239
Figure 5.3. Screening cell lines for PDE7A isoforms	241
Figure 5.4. Transfection of COS-1 cells with PDE7A1 and PDE7A2 cDNA constructs	242
Figure 5.5. Attempted lipid-based transfection of COS-7 cells with pCS1	243
Figure 5.6. RT-PCR analysis of pCS1 transfected COS-7 cells	244
Figure 5.7. Attempted transfection of Jurkat J6 and HuT-78 cells with PDE7A1 containing construct	245
Figure 5.8. Subcellular localisation of PDE7A1 in COS-1 cells.....	246
Figure 5.9. Expression of endogenous PDE4 isoforms in COS cell lines.....	247
Figure 5.10. Detection of PDE7 and PDE4 enzymatic activity in the presence of varying cAMP concentrations	248
Figure 5.11. Chemical structures of CT6251 and CT6236	249
Figure 5.12. IC ₅₀ values of CT6251 for PDE4 and PDE7.....	250
Figure 5.13. IC ₅₀ values of CT6236 for PDE4 and PDE7.....	251
Figure 5.14. Activity changes of PDE7A1 upon stimulation of cells with agonists of kinase signalling cascades	252
Figure 5.15. Rabbit anti-PDE7A antibody successfully immunoprecipitates PDE7A1 from COS-1 cell lysate.....	253
Figure 5.16. <i>In vitro</i> phosphorylation of PDE7A1 and PDE7A2.....	254
Figure 5.17. Whole cell labelling of COS-7 cells transfected with the pSM2 construct.....	255
Figure 5.18. High salt and SDS washed remove none specific bound protein from immunoprecipitates	256
Figure 5.19. A protein which cross reacts with the pan-PKC antibody co-immunoprecipitates with PDE7A1 protein.....	257
Figure 5.20. RACK-1 appears to co-immunoprecipitate with PDE7A1	258
Figure 5.21. GST-RACK-1 pulldown of <i>in vitro</i> synthesised PDE7A1 protein.....	259

Chapter 6

Figure 6.1. Proposed mechanism of PDE4D3 phosphorylation in mitosis	270
Figure 6.2. Involvement of PDE4D3 in the progression of cells through mitosis	271

List of tables

Chapter 1

Table 1.1. Effectors which modulate adenylate cyclase isoform activity	45
--	----

Chapter 3

Table 3.1. Quantification of the proportion of apoptotic Rat-1 cells on an FL1-H vs FL2-H density plot when treated with nocodazole.....	140
Table 3.2. Analysis of PDE4D protein expression in Rat-1 cells isolated at different stages of the cell cycle.....	141

Chapter 4

Table 4.1. Panel of kinase inhibitors.....	218
Table 4.2. Probability of residue phosphorylation using NetPhos.	219
Table 4.3. Predicated phosphorylation sites of PDE4D3 using PhosphoBase	220
Table 4.4. Predicted peptides generated upon cyanogen bromide cleavage of PDE4D3.....	222

Chapter 5

Table 5.1. Summary of the expression of PDE7A1 and PDE7A2 protein in different cell lines.....	260
Table 5.2. The IC ₅₀ values of the PDE7 selective inhibitors CT6251 and CT6236.....	261
Table 5.3. Predicted phosphorylation sites of PDE7A1 using PhosphoBase.....	262

Abbreviations

AC	adenylyl cyclase
AKAP	A kinase anchoring protein
APC	Anaphase promoting complex
ASMC	Airway smooth muscle cell
ATP	adenosine triphosphate
Ca ²⁺ /CaM	calcium/calmodulin
cAMP	cyclic 3'5' adenosine monophosphate
CAT	chloramphenicol acetyltransferase
CHO	Chinese hamster ovary
CIAP	Calf intestinal phosphatase
CRE	cAMP response element
CREB	cAMP response element binding protein
Cdk	Cyclin dependent kinase
cDNA	complementary DNA
cGMP	cyclic guanosine monophosphate
DEAE	diethyl aminoethyl
DEPC	diethyl pyrocarbonate
DMEM	Dulbecco's modification of Eagle's Medium
DMSO	dimethylsulphoxide
DNA	deoxyribonucleic acid
DRB	5,6-Dichloro-1-β-D-ribofuranosylbenzimidazole
dNTP	deoxynucleotide triphosphate
DTT	dithiothreitol
ECL	Enhanced chemiluminescence
EDTA	Diaminoethanetetra-acetic acid
EGF	epidermal growth factor
EGTA	Ethylene glycol-bis(β-aminoethyl ether)-N,N,N',N'-tetraacetic acid
ELISA	enzyme linked immunosorbent assay
Epac	Exchange protein directly activated by cAMP
ERK	Extracellular regulated kinase
FCS	foetal calf serum
GEF	Guanine nucleotide exchange factor
GPCR	G-protein coupled receptor
G-protein	guanine nucleotide binding regulatory protein

GRK	G-protein receptor specific kinase
GSK-3	Glycogen synthase kinase-3
GST	Glutathione S-transferase
GTP	guanosine triphosphate
h	hour
HEK	Human embryo kidney
HEPES	N-2-Hydroxyethylpiperazine-N'-2-ethanesulfonic acid
HeLa	Henrietta Lacks
HTLV	Human T-lymphotrophic virus
IBMX	isobutylmethylxanthine
IC ₅₀	Concentration of inhibitor required to inhibit half the specific activity
IPTG	isopropyl-β-D-thiogalactopyranoside
IL	interleukin
IFN γ	Interferon gamma
K _m	Michealis-Menton constant
kb	kilobase
kDa	kiloDaulton
KHEM	potassium (K), HEPES, EGTA, Magnesium
l	litre
LB	Luria-Bertoni
LR	linker region
M	molar
mg	milligram
MAP kinase	mitogen activated protein kinase
MBP	maltose binding protein
MEK	MAPK kinase
MHC	Major histocompatability complex
min	minute
MPF	Maturation promotion factor
mRNA	messenger RNA
ORF	open reading frame
PA	phosphatidic acid
PAGE	Polyacrylamide gel electrophoresis
PBS	phosphate buffered saline
PCR	polymerase chain reaction

PDE	phosphodiesterase
PDGF	Platelet derived growth factor
PHA	Phytohaemagglutinin
PI 3-kinase	Phosphatidyl inositol 3-kinase
PKA	protein kinase A
PKC	protein kinase C
PKG	protein kinase G
PMA	Phorbol myristate
PP1	Protein phosphatase 1
pRb	Retinoblastoma protein
RACK	receptor for activated C kinase
RNA	ribonucleic acid
rpm	revolutions per minute
RT	reverse transcription
SAPU	Scottish antibody production unit
SDS	sodium dodecyl sulphate
sec	second
SH2 domain	Src homology 2 domain
SH3 domain	Src homology 3 domain
TAE	tris/acetate/EDTA
TBS	tris buffered saline
TCR	T cell receptor
TE	tris/EDTA
TEA	triethanolamine
TEMED	N,N,N',N'-Tetramethyl-ethylenediamine
TFA	Trifluoroacetic acid
TGF	Transforming growth factor
TLC	Thin-layer cellulose
TSH	Thyroid stimulating hormone
UCR	upstream conserved region
VSMC	Vascular smooth muscle cell
VSV	vesicular stomatitis virus

Chapter 1

General Introduction

1.1. Cyclic nucleotide signalling pathways

1.1.1. Cyclic nucleotide generation in cells

The cyclic nucleotides cyclic 3'5' guanosine monophosphate (cGMP) and cyclic 3'5'-adenosine monophosphate (cAMP) are intracellular second messengers ubiquitously generated in cells to mediate the physiological responses of a host to specific cellular stimuli. Cyclic nucleotides mediate a diverse range of effects. Since its discovery cAMP (Sutherland and Rall, 1958) has been found to mediate numerous biological responses (Sutherland and Rall, 1958; Shacter et al., 1988). Cyclic AMP can elicit acute, reversible changes in dynamically regulated processes such as neurotransmission, muscle contraction and regulate metabolic processes such as glycogenolysis (Verne et al., 1973; Byus et al., 1976) and lipolysis (Pohl, 1981). Yet, in other contexts, cAMP can have long term effects on, for example, embryonic development, cell growth, proliferation and differentiation. Most of the cellular effects of modulation of cAMP concentrations are due to the stimulatory effect of cAMP on protein kinase A (PKA) activity (Walsh et al., 1968). PKA then phosphorylates key target proteins ultimately leading to alterations in cell functioning (Scott, 1991).

1.1.1.1. *G-Protein Coupled Receptors*

Cyclic AMP is produced within cells, from ATP, by the action of adenylyl cyclase. This enzyme can be either directly activated by forskolin or indirectly activated through interaction of a G-protein coupled cell surface receptor (GPCR) with its cognate ligand. There are over 1000 members of the GPCR family identified to date, classed into groups based on their sequence homology. All GPCRs have common structural features; the N-terminus of the protein is extracellular, there are seven transmembrane helical domains, connected by short loops and the intracellular C-terminal (Milligan, 1998). GPCRs are activated by extracellular signals such as hormones, neurotransmitters, chemokines, odorants and light. Upon activation GPCRs undergo a conformational change and complex with and activate their cognate heterotrimeric G-proteins (Neer, 1995; Gether et al., 1995). Modulation of the cAMP-signalling cascade, to elicit a regulated cellular response to a stimulant, is brought about through the ability of the GPCRs to couple to the C-terminus of one of the multiple $G\alpha_s$ isoforms, the specificity of which is determined by the third intracellular loop of the receptor (Neer, 1995; Gether, 2000). $G\alpha_s$, in its inactive state binds GDP and exists in a complex with cognate $\beta\gamma$ subunits. The ligand bound GPCR induces a $G\alpha_s$ conformational change and the bound GDP is exchanged for GTP while the $\beta\gamma$

subunits dissociate from the G-protein complex (Birnbaumer et al., 1990). The active $G\alpha_s$ -GTP binds to membrane associated adenylyl cyclase (AC) activating it, whereas the released $\beta\gamma$ complex itself goes on to modulate other intracellular signalling cascades (reviewed in (Hamm, 1998), *Fig. 1.1.*). Activation of AC persists until such time as the GTP bound to the $G\alpha_s$ is hydrolysed by the intrinsic GTPase activity of the $G\alpha_s$ and the reassociation of the $\beta\gamma$ subunits (Neer, 1995).

Other intracellular mechanisms can also serve to attenuate the stimulated G-protein response at different levels of the signalling cascade. Phosphorylation of the receptor by a G-protein receptor specific kinase (GRK) increases the affinity of the GPCR for a class of binding proteins called arrestins (Lefkowitz, 1998). The binding of an arrestin to the carboxyl terminal region of the GPCR sterically inhibits receptor interaction with G-proteins, thereby causing desensitisation. The bound arrestin also leads to receptor internalisation by clathrin coated vesicles (Lefkowitz, 1998; Milligan, 1998). Other kinase mediated phosphorylations of the receptor, such as through PKC (Diviani et al., 1997) or PKA (Freedman et al., 1995), inhibit the interaction between the receptor and the G-protein, so aid the desensitisation of the cAMP mediated signal (reviewed in Bunemann and Hosey, 1999). There exists a family of GPCRs, which when stimulated, interact with the inhibitory G protein, $G\alpha_i$. This G-protein, once stimulated, inactivates adenylyl cyclase by binding directly to it (Houslay, 1991).

1.1.1.2. *Adenylyl cyclases*

Adenylyl cyclases (ACs) belong to a multigene family of transmembrane proteins of which there are nine known mammalian isozymes (Patel et al., 2001). They are activated by the stimulation of $G\alpha_s$ coupled receptor by hormones (Hawes et al., 2000), cytokines (Tachibana et al., 1998) or neurotransmitters (Spada et al., 1997). All mammalian ACs are activated by $G\alpha_s$ and their activities are differentially regulated by binding calcium/calmodulin, through phosphorylation by PKC or PKA and by the association of various G-protein subunits (Hurley, 1998). The ligand, which activates the cell-surface receptors, alters cAMP signalling in a way that depends on the family of AC the G-protein is co-localised with. AC enzymes are typically more than 1000 amino acids long with molecular weights of approximately 120 kDa (Taussig and Gilman, 1995). Members of the mammalian AC family all have a similar structure consisting of two sets of six transmembrane helices (M1 and M2) with relatively low sequence homology between AC species. Each transmembrane helix is separated by very short connecting loops except M1

and M2 which are separated by a large intracellular loop called C1 (*Fig. 1.2.*). This loop is subdivided into the highly conserved C1a catalytic domain and C1b, which acts as a specific regulatory site for the AC, that is poorly conserved between isoforms. The carboxyl terminal tail of the ACs, termed C2, is cytoplasmic and contains the well-conserved C2a region, which encodes the second part of the catalytic domain and the terminal C2b domain. C2b is found only within the type I, II, III and VIII AC isoforms (Hurley, 1999) for which it appears to act as a regulatory module. The cytoplasmic loops interact with one another to form a catalytic site for the enzyme (*Fig. 1.2.*).

All but type IX AC are activated by forskolin, a chemical which appears to promote the assembly of the catalytic region by binding to the hydrophobic pocket at one end of the central cleft between the catalytic dimers (Patel et al., 2001; Hurley, 1998). Divalent metal cations play an important role in directly regulating AC. They interact with C2 at the dimer interface so, like forskolin, exert their stimulatory effect by altering the conformation of the catalytic site (Houslay and Milligan, 1997). ACs are activated via a direct interaction between the $G_{s\alpha}$ and the C1a and C2a domains (Patel et al., 2001). However, the different AC forms often have contrasting modulating effectors (Houslay and Milligan, 1997). For example, the activity of the AC I, III and VIII isoforms can be stimulated by binding calcium/calmodulin whereas the AC V, VI and IX isoforms are inhibited by calcium (Taussig and Gilman, 1995; Cooper et al., 1995, for summary of AC isoform modulation see table 1.1.). The different catalytic properties of the AC act in determining cAMP fluxes in the cell (Houslay and Milligan, 1997) and numerous physiological roles of the different isoforms have been identified (reviewed in Patel et al., 2001).

1.1.2. Targets of cAMP generation

Cyclic AMP activates several downstream signalling mechanisms through direct interaction with proteins. It binds to and activates a class of cyclic nucleotide gated ion channels (Sanchez et al., 2001; Viscomi et al., 2001) as well as the guanine nucleotide exchange factors (cAMP-GEFs) for the small G-protein Rap1, also called Epac1 and Epac2 (de Rooij et al., 1998). However the best characterised cAMP receptor in mammalian cells with which the majority of biological effects of cAMP have been associated, is PKA.

1.1.2.1. Protein Kinase A

Protein kinase A was originally classed as a 'third messenger' which was activated by cAMP and conveyed a physiological signal through modulation of substrate activity by phosphorylating them (Walsh et al., 1968). PKA is a heterotetrameric enzyme composed of two regulatory subunits ($RI\alpha$, $RI\beta$, $RII\alpha$ or $RII\beta$) bound to two catalytic subunits ($C\alpha$, $C\beta$ or $C\gamma$). The RI regulatory subunits have high homology with one another, as do the RII subunits (Skalhegg and Tasken, 2000), and further diversification of $RI\alpha$ is brought about by the existence of several splice variants (Solberg et al., 1997). $RI\alpha$ and $RII\alpha$ are expressed ubiquitously, whereas $RII\beta$ is expressed predominantly in endocrine, brain, fat and reproductive cells (Taylor et al., 1992).

Multiplicity of the PKA catalytic subunit occurs, with there being three distinct splice variants of $C\alpha$ and several $C\beta$ variants (Skalhegg and Tasken, 2000). The PKAII ($RII\alpha_2C_2$ and $RII\beta_2C_2$) holoenzymes are assembled preferentially over PKAI ($RI\alpha_2C_2$ and $RI\beta_2C_2$) under physiological conditions (Francis and Corbin, 1994). However, complex mechanisms influenced by multiple factors govern to what extent PKA-I and PKA-II assembly is preferred *in vivo*. The assembly of different catalytic and regulatory subunits gives rise to a number of PKA holoenzymes which possess different biological characteristics (Skalhegg and Tasken, 2000). The PKA type I complex is generally cytoplasmic and is activated transiently by weak cAMP signalling (Houslay and Milligan, 1997). The type II complex, however, is associated with cell particulate fractions and responds only to high and persistent cAMP stimulation (Rubin et al., 1979; Stein et al., 1987). The localisation of PKAII to specific subcellular compartments is mediated by interactions with anchoring proteins called AKAPs (*see below*).

Cyclic AMP binds co-operatively to two sites on each of the PKA regulatory subunits (reviewed in Doskeland et al., 1993). The R subunits binding affinity for cAMP differs between isoforms. $RI\alpha$ has a much higher affinity for cAMP relative to $RII\alpha$ and $RII\beta$ (Taylor et al., 1992). This interaction with cAMP causes a conformational change of the regulatory subunits which mediates their dissociation from the catalytic subunits, enabling the free catalytic subunits to target serine and threonine residues on substrate proteins for phosphorylation (Skalhegg and Tasken, 2000).

1.1.2.2. *A Kinase-anchoring proteins (AKAPs)*

AKAPs represent a functionally related family of regulatory proteins that contain a PKA binding domain and unique targeting sequences that direct the complex to specific subcellular structures (Murphy and Scott, 1998). AKAPs have diverse amino acid sequences but share certain structural features. AKAPs bind to the first 30 amino acids of the N-terminus of the PKA RII subunit, which is also crucial for the promotion of dimerisation of the RII subunits ((Li and Rubin, 1995), *Fig. 1.3.*). AKAPs appear to bind selectively with high affinity to RII dimers (Scott et al., 1990). Recently, several AKAPs have also been shown to interact with RI, similarly targeting them to membranous regions of the cell (Felicciello et al., 2001). The tissue specific expression of AKAPs, their localisation, role in cellular functions and R subunit binding specificities are reviewed in detail in (Felicciello et al., 2001).

1.1.2.3. *PKA independent mechanisms of cAMP dependent signalling*

Cyclic AMP also acts in a fashion independent of PKA, notably through the exchange protein directly activated by cAMP (Epac). Epacs are guanine nucleotide exchange factors (GEFs) for the small GTPase Rap1, which are activated both *in vitro* and *in vivo* by the direct binding of cAMP in an N-terminal domain (de Rooij et al., 1998). This domain contains a motif similar to that found in the cAMP binding pocket of PKA (Kawasaki et al., 1998; de Rooij et al., 1998). There are three known Epac family members, Epac1 and Epac2, and Repac (related to Epac). Epac1 binds cAMP at only one location, Epac2 has two binding sites for cAMP and Repac is constitutively active (de Rooij et al., 2000). Epacs have a C-terminal catalytic region which contains the GEF domain that activates Rap1 and Rap2 (de Rooij et al., 2000) but not the other members of the small G-protein family Ras, Ral, or R-ras (Kawasaki et al., 1998). In the absence of cAMP the catalytic ability of Epac1 is constrained, by a direct interaction of the GEF domain with the high affinity cAMP binding domain (de Rooij et al., 2000). Upon interaction with cAMP, a conformational change of Epac relieves this auto-inhibition and GEF activity is resumed. Epac is tightly associated with cell membranes via its DEP (common to Disheveled, Egl-10 and pleckstrin) domain, a characteristic which is not regulated by cAMP (de Rooij et al., 2000).

1.1.3. Cyclic nucleotide hydrolysis within cells

Termination of cAMP mediated intracellular signal is controlled by phosphodiesterases (PDE), which were first discovered shortly after the identification of cAMP (Butcher and Sutherland, 1962). PDEs act to hydrolyse the 3'-phosphoester bond of the 3', 5'-purine ribose cyclic monophosphate nucleotides leaving the residual 5'-monophosphate, thus terminating the cyclic nucleotide stimulated pathways in cells. This is important not only in the ablation of cellular signalling, but also in the maintenance of tight regulation of downstream effector activity. The isolation of PDEs from preparations of heart tissue were found, initially, to hydrolyse cAMP, however, with further investigation, the preparations were found to hydrolyse both cAMP and cGMP (Nair, 1966). Purification of the PDEs from the tissue homogenate, by ion exchange chromatography, identified several peaks of cAMP and cGMP hydrolytic activity. Each peak had different kinetics for its substrate and could be differentially inhibited or activated (Goren and Rosen, 1972). The peaks were characterised and correlated to different families of PDE (Butcher and Sutherland, 1962).

PDEs serve four major functions within cells: they act as effectors of signal transduction by interacting with receptors and G-proteins; they integrate cAMP signalling with other signalling transduction pathways; they play a role as homeostatic regulators, by acting as feedback regulators of cyclic nucleotide levels; and they act to control the diffusion of cyclic nucleotides and creating subcellular compartmentalisation of cyclic nucleotide signalling.

1.2. The phosphodiesterase superfamily

The PDE family is evolutionarily conserved, homology of the molecule exists in organisms ranging from *Dictyostelium* to human beings (Charbonneau, 1990). The 35 currently known PDEs are encoded for by 21 different genes and classed into 11 families determined by their genetic sequence and functionally by their substrate specificity and kinetic properties, inhibitory profiles and regulation by allosteric activators or inhibitors. From comparative, structural and functional studies PDEs are known to possess a modular architecture. The conserved catalytic domain, containing a sequence of approximately 275 amino acids, which is common to all PDEs, is located proximal to the carboxyl terminus. The catalytic core contains common structural elements which are important for the hydrolysis of cyclic nucleotides which include a PDE-specific motif (H-D-[L/I/V/M/F/Y]-X-H-X-[A/G]-X-X-N-X-[L/I/V/M/F/Y]) and two consensus divalent cation (Zn^{2+} or

Mg²⁺)- binding domains. Family specific regulatory domains or motifs are often found near the amino terminus of the enzyme (*Figure 1.4.*).

1.2.1. The PDE1 family of phosphodiesterases

PDE1 was originally found as a calcium stimulated PDE activity from rat brain (Kakiuchi and Yamazaki, 1970). PDE1s act as one of the key enzymes involved in the complex interactions between cyclic nucleotide and Ca²⁺ second messenger systems. Three different genes code the CaM/Ca²⁺ stimulated PDE1 family, and each gene has at least two different splice variants, which give rise to functionally different isozymes with distinct catalytic and regulatory properties. The PDE1 isoforms have differing affinities for the CaM/ Ca²⁺ complex, which binds within two regions of their N-terminal regulatory domains and determines subtle changes in their activity regulation (reviewed in Kakkar et al., 1999).

The stimulation of enzymatic activity of PDE1 can also be differentially modulated by post-translational events. Phosphorylation of PDE1 isoforms, by PKA and CaM dependent kinase, decreases PDE1 affinity for Ca²⁺/CaM, therefore decreasing the activity of the enzyme (summarised in Kakkar et al., 1999). PDE1s have Michaelis constant (K_m) values of between 1 μM and 40 μM for cAMP and between 1 μM and 3 μM for cGMP with different cyclic nucleotide specificity for each isoform (Yan et al., 1996).

The CaM-dependent PDEs have been localised in the postsynaptic regions in several brain areas, including olfactory neurones. PDE1A has been localised to the cortex, PDE1B to the striated region of the dentate gyrus and PDE1C in the neuronal epithelia (Yan et al., 1996). Inhibitors of PDE1 isoforms include Ginsenoides that are used for the treatment of heart failure, and have antipsychotic, anticonvulsant and antifatigue actions. Amantadine and Deprenyl are both anti-parkinsonian agents that also inhibit PDE1s possibly through disruption of the CaM/PDE interaction (reviewed in Kakkar et al., 1999).

1.2.2. The PDE2 family of phosphodiesterases

PDE2 activity was first identified in rat liver extracts (Beavo et al., 1970). Cyclic AMP and cGMP are hydrolysed by this enzyme with K_m values of 50 μM for both substrates. The protein has an N-terminal non-catalytic binding site for cGMP which when bound causes an increased affinity of the catalytic site for cAMP (Manganiello et al., 1990), providing a point of crosstalk between the cAMP and cGMP signalling pathways (reviewed in Beavo,

1995). One PDE2 gene has been identified to date and this has at least three different splice variants encoding PDE2A1, PDE2A2 and PDE2A3.

PDE2 is localised to the adrenal cortex and several areas of the brain, as well as in goblet cells, olfactory neurones and in capillary and endothelial cells (Sadhu et al., 1999). PDE2 activity has been implicated in cardiac Ca^{2+} channel control, catecholamine secretion in the central nervous system (Beavo, 1995) and in olfactory neurone signalling (Juilfs et al., 1997).

1.2.3. The PDE3 family of phosphodiesterases

Two different genes make up the PDE3 family and further diversification exists since at least two different splice variants of PDE3A are known. The members of the PDE3 family have a low K_m for cAMP and can bind cGMP with high affinity ($K_m = 0.3 \mu M$). However, they hydrolyse cGMP poorly so, in effect, the binding of cGMP inhibits enzymatic activity to cAMP (reviewed in Beavo, 1995). Phosphorylation of PDE3 by PKA has been shown to increase the activity of this enzyme (Smith et al., 1991). PDE3A is found in smooth muscle, platelets and cardiac tissue (Liu and Maurice, 1998). PDE3B is abundant in adipocytes where it is activated upon insulin stimulation and where it participates in the regulation of glucose transport mechanisms and stimulates the antilipolytic and antiglycogenolytic actions of insulin (Degerman et al., 1997; Sano et al., 2001). To achieve this insulin activates PDE3 via an IRS-1, PI 3-kinase, PDK and PKB/Akt dependent mechanism (Ahmad et al., 2000). PDE3 isoforms have also been associated with platelet aggregation, myocardial contractility, relaxation of smooth muscle, and inhibition of T cell and vascular smooth muscle cell proliferation (Manganiello et al., 1995).

1.2.4. The PDE4 family of phosphodiesterases

PDE4 enzymes currently provide the largest known PDE family. The PDE4A1 isozyme was the first PDE to be cloned, it was identified in a screen of a rat brain cDNA library using the product of the *Drosophila melanogaster dunce* gene as a probe (Davis et al., 1989). Four genes encode PDE4s, giving rise to at least 18 different splice variants. These cDNAs can be grouped into long, short and super-short categories (*Fig. 1.5*). All PDE4s have a conserved catalytic region, located within a 360 amino acid domain. The 'long' isoforms have two of the conserved N-terminal regulatory domains, termed UCR1 (for upstream conserved region 1) and UCR2 of 59 and 79 amino acids, respectively (*Fig. 1.5*). A linker region (LR1) of 24 amino acids separates UCR1 and UCR2, which is the site

spliced to produce truncated proteins lacking UCR1 in the 'short' isoforms. The 'super-short' PDE4 species have an N-terminal truncation within the UCR2 region of the protein and unique N-terminal sequences (structures of PDE4s are reviewed extensively in Houslay, 2001). PDE4 enzymes are specific for the hydrolysis of cAMP with K_m values in the range of 1 to 5 μM . Modulation of PDE4 activity is carried out by post-translational modifications such as phosphorylation, and through interaction with adapter proteins and phospholipids (reviewed in (Houslay, 2001) and see section 1.3.4. for more details). The various PDE4 species have heterogeneous patterns of expression in cells and specific isoform profiles of various cell types and tissues have been determined (reviewed in Houslay, 2001).

1.2.5. The PDE5 family of phosphodiesterases

There is one PDE5 gene that gives rise to 2 alternatively spliced variants, PDE5A1 and PDE5A2 (Loughney et al., 1998). These enzymes exist as a homodimers, which exhibit cGMP specific hydrolytic activity. Each subunit of the holoenzyme contains two high affinity cGMP non-catalytic binding sites (GAF domains) at their N- terminus. Once bound to cGMP phosphorylation of PDE5 by protein kinase-G (PKG) increases the affinity of the catalytic site for cGMP ($K_m = 1 \mu\text{M}$), and elevates cGMP hydrolysis (reviewed in Beavo, 1995). PDE5 mRNA is most highly expressed in aortic smooth muscle cells, heart, placenta, skeletal muscle and pancreas (Stacey et al., 1998). Sildenafil, the PDE5 selective inhibitor, is marketed by Pfizer as ViagraTM and functions as a treatment for penile erection dysfunction which implicates PDE5 in playing a pivotal role in controlling smooth muscle relaxation (reviewed in Cartledge and Eardley, 1999).

1.2.6. The PDE6 family of phosphodiesterases

The PDE6 family constitutes the central effector enzyme in the phototransduction cascade of the rod and cone photoreceptor cells. The enzyme is regulated by direct interaction with the transducin heterotrimeric G-protein $T\alpha$ subunit (Stryer et al., 1983). The PDE6 enzyme is cGMP specific ($K_m = 60 \mu\text{M}$ for cGMP and 2000 μM for cAMP) and exists in a heterotetrameric complex containing one catalytic α (PDE6A), one catalytic β (PDE6B) subunit and two small inhibitory γ subunits. A δ subunit also co-purifies with PDE6 and is involved in the localisation of the complex to the membranous fraction of the cell (Florio et al., 1996). Both PDE6 catalytic subunits contain two high affinity, non-catalytic, cGMP-binding sites (GAF domains) and binding cGMP at these sites increases the $\alpha\beta$ affinity for

the γ subunits in the catalytic pocket of the enzyme (reviewed in Artemyev et al., 1998). Upon light stimulation of the photoreceptor cell, rhodopsin activates the retinal G-protein, transducin, the $T\alpha$ binds in the catalytic pocket of the $\alpha\beta$ complex, displacing the γ subunit and stimulating enzymatic cGMP hydrolysis.

1.2.7. The PDE7 family of phosphodiesterases

The PDE7 protein was originally found by a genetic screening procedure developed in yeast to identify cDNA clones encoding functional, high-affinity cAMP specific PDEs (Michaeli et al., 1993). PDE7 was initially identified as the cAMP specific, IBMX-insensitive PDE isoform which had a K_m value for cAMP of approximately 0.1 μ M. There are two PDE7 genes, PDE7A whose human gene locus has been mapped to chromosome 8q13 (Han et al., 1998) and has at least three different splice variants (Sasaki et al., 2000; Glavas et al., 2001) and PDE7B (Hetman et al., 2000). The PDE7 isoforms have different sub-cellular localisations determined by the nature of their N-terminal domain. The hydrophobic N-terminus of PDE7A2, for example, interacts directly with membranous fractions of the cell (Bloom and Beavo, 1996). The main functional interest concerning PDE7 is due to its specific expression in activated T-lymphocytes, where it is seen to stimulate cell proliferation and induce expression of the interleukin-2 cytokine (Li et al., 1999).

1.2.8. The PDE8 family of phosphodiesterases

The PDE8 cDNA was identified by screening a database of expressed sequence tags (ESTs, Soderling et al., 1998). The homology of the sequence to known PDE sequences identified this protein as belonging to a novel family of PDEs. Two genes encoding PDE8 have now been identified, and the PDE8A is thought to have 5 splice variants (Wang et al., 2001b). PDE8 is specific for the hydrolysis of cAMP, with a K_m of 70 nM. PDE8 has a PAS/PAC (for Per, ARNT and Sim protein where this motif was originally identified) domain, located within the N-terminal regulatory region of the protein. This domain is found in many signal transduction proteins, and is thought to mediate specific homo- and heteromeric protein-protein interactions, although the function in PDE8 is not clear as yet. PDE8A is most highly expressed in mouse testis, in the seminiferous epithelium (Soderling et al., 1998) whereas PDE8B is expressed in the thyroid gland (reviewed in Soderling and Beavo, 2000). Functional analysis of the enzymes has not yet been performed although up-regulation of PDE8A protein levels have been observed upon activation of T cells (Glavas et al., 2001).

1.2.9. The PDE9 family of phosphodiesterases

The PDE9 cDNA was identified by screening a database ESTs, the homology of the sequence to known PDE sequences identified this protein as belonging to a novel family of PDEs. To date one gene encoding PDE9 has been identified which has four alternative splice variants (Guipponi et al., 1998). The PDE9 enzyme family specifically hydrolyses cGMP with very high affinity ($K_m=70$ nM). It is insensitive to many known PDE inhibitors including rolipram, vinpocetine, sildenafil and IBMX, however, it is sensitive to the PDE5 inhibitor zaprinast ($IC_{50}=35$ μ M, reviewed in Soderling and Beavo, 2000). Tissue distribution studies have identified mRNA of all PDE9 splice variants to be expressed in most tissues, except blood (Guipponi et al., 1998), although no physiological function of the enzymes have yet been identified.

1.2.10. The PDE10 family of phosphodiesterases

The PDE10 cDNA was also identified by screening a database of ESTs (Fujishige et al., 1999). To date only one gene encoding PDE10 has been identified which has no known splice variants. PDE10 has the capacity to hydrolyse both cAMP and cGMP with K_m values of 0.26 μ M and 7.2 μ M, respectively (Fujishige et al., 1999), and contains two N-terminally located GAF domains, which are likely to constitute a low-affinity binding site for cGMP. The kinetics of the protein have implicated this enzyme as a cAMP inhibited cGMP specific phosphodiesterase *in vivo* (reviewed in Soderling and Beavo, 2000). PDE10 is sensitive to inhibition by the general PDE inhibitor, IBMX ($IC_{50} =2.6$ μ M). Tissue distribution studies have identified PDE10 mRNA to be expressed in the putamen and caudate nucleus regions of the brain (Fujishige et al., 1999), although no physiological functions of these enzymes have yet been reported.

1.2.11. The PDE11 family of phosphodiesterases

The PDE11 family is the most recently characterised phosphodiesterase family, again identified by screening a database ESTs (Fawcett et al., 2000). There are potentially three members of the family all having a single N-terminal GAF domain, which constitutes a potential allosteric binding site for cGMP or another small ligand, and hydrolyse cAMP and cGMP with K_m values of 1 μ M and 0.5 μ M, respectively. The enzyme kinetics indicate that PDE11A might regulate both cAMP and cGMP hydrolysis under physiological conditions. However, no studies of physiological functions of the isozymes have yet been

undertaken. Tissue distribution studies have determined PDE11 mRNA to be expressed in skeletal muscle, prostate kidney, liver, pituitary and salivary glands (Fawcett et al., 2000).

1.3. Biochemistry of the PDE4 cAMP-specific phosphodiesterases

The mammalian PDE4 family members are homologues of the *Drosophila melanogaster dunce* gene (Davis and Kiger, Jr., 1981). The importance of PDE4 within cells was initially demonstrated when flies deficient in PDE displayed impaired CNS and reproductive functions (Dudai et al., 1976). The disruption of the reproductive function in *Drosophila* was apparent in a defect in egg deposition due to impaired function of both egg and nursing cells (Byers et al., 1981; Bellen et al., 1987). There are currently 18 different mammalian PDE4 isoforms that have been identified. They are encoded by four distinct genes, each giving rise to multiple splice variants, and each gene represents a PDE4 subfamily (*Fig. 1.6.*).

1.3.1. The PDE4A subfamily

The human PDE4A gene, which is located on chromosome 19p13.1, has been cloned and well characterised (reviewed Houslay, 2001). It is currently thought that there are at least four different PDE4A splice variants (*Fig. 1.7.*), of which three are 'long forms'. PDE4A4B was originally named 'pde46' (Huston et al., 1996) and is a homologue of rodent PDE4A5 (McPhee et al., 1995). These variants are localised to the cortical regions in a cell including membrane ruffles and also perinuclear regions (McPhee et al., 1995) via interactions with adaptor proteins containing src homology 3 (SH3) domains (O'Connell et al., 1996). PDE4A10 is also a 'long-form' PDE4 isoform, cloned from a rat olfactory library (Rena et al., 2001). The 'long-form' rat PDE4A8 (also known as rpde39, Bolger et al., 1996), was originally cloned from a rat testis cDNA library and using RNA protection studies has been shown to be exclusively expressed in the testes and in maturing spermatozoa (Naro et al., 1996). A human homologue of PDE4A8 has not yet been identified. The membrane-associated (Shakur et al., 1995; Pooley et al., 1997) PDE4A1 (also referred to as RD1, Sullivan et al., 1998) is a 'super-short' PDE4A isoform, which lacks UCR1 and has an N-terminally truncated UCR2 (*Fig. 1.7.*), whose expression is confined to the brain (Shakur et al., 1995).

Modulation of long-form PDE4A activity occurs via binding of phosphatidic acid (PA) and phosphatidylserine to a region proposed to be located within the UCR1 domain (Nemoz et

al., 1997). Phosphorylation of PDE4A isoforms also affects the activity of the enzymes. For example, p70s6 kinase is believed to specifically phosphorylate and activate PDE4A4/5 isoforms via a PI 3-kinase dependent pathway in 3T3 F442A adipocytes (MacKenzie et al., 1998) and in U937 monocytic cells (MacKenzie and Houslay, 2000).

1.3.2. The PDE4B subfamily

The human PDE4B gene is located on chromosome 1 (reviewed by Houslay, 2001) and it encodes at least four different splice variants (*Fig. 1.8*). There are three long isoforms, PDE4B1, PDE4B3 and PDE4B4, and one short isoform, PDE4B2, all of which have been found associated with both the soluble and particulate fractions of the cell (Huston et al., 1997; Obernolte et al., 1993).

Phosphorylation plays a key role in modulating PDE4B isoform activities. The 'short-form' of PDE4B, PDE4B2, is phosphorylated at Ser⁴⁷⁸ by ERK and this activates the enzyme. However, ERK phosphorylation of the long PDE4B1 form, at the equivalent residue, Ser⁶⁵⁹, inhibits the enzymatic activity of this protein (Baillie et al., 2000). The binding of the phospholipids, phosphatidic acid and phosphatidylserine, at an as yet unidentified site, up regulates PDE4B1 activity, whereas the short form PDE4B2 activity remains unaffected in the presence of these molecules (Nemoz et al., 1997).

1.3.3. The PDE4C subfamily

The human PDE4C gene is located on chromosome 19p13.2 (Sullivan et al., 1999). There are at least three long forms of PDE4C (Obernolte et al., 1997) and no 'short' or 'super-short' PDE4C species have been identified thus far. Although these proteins have not been characterised in any detail, the PDE4C2 protein has been shown to be a substrate for ERK-mediated phosphorylation. The residue targeted for modification is Ser⁵³⁵, the equivalent residue as that phosphorylated by ERK in the PDE4B isoforms. This ERK phosphorylation causes an inhibition of the PDE4C enzymatic activity (Baillie et al., 2000).

1.3.4. The PDE4D subfamily

The human PDE4D gene is located on chromosome 5 (reviewed in Houslay, 2001). Of the five PDE4D splice variants identified to date, three are 'long-forms' (PDE4D3, PDE4D4 and PDE4D5), PDE4D1 is a 'short-form' and PDE4D2 is a 'super-short' form (*Fig. 1.9*). PDE4D1-5 have molecular weights of 68, 72, 95, 119 and 105 kDa, respectively. The *in*

in vivo function of PDE4D has been investigated in knock-out mice models. PDE4D-deficient mice have reduced viability, diminished sensitivity of the granulosa cells to gonadotropins and reduced fertility (Jin et al., 1999). The latter phenotype is caused by impaired ovulation and degeneration of oocytes due to disrupted metaphase (Jin et al., 1999). Deficient mice also display impaired growth with lower than normal weight due to a proportional decrease in muscle and bone mass and internal organ weight. The airways of these transgenic mice are also no longer responsive to cholinergic stimulation due to defective receptor signalling and are no longer protected against allergen-induced airway hyper-reactivity, thus improving asthma symptoms (Hansen et al., 2000). These characteristics suggest that PDE4D plays a non-redundant role in cAMP signalling, with unique and non-overlapping functions.

1.3.4.1. *'Short-form' splice variants of PDE4D*

PDE4D1 and PDE4D2 have K_m values for cAMP of 5 μ M and are found predominantly in the cytoplasm (Jin et al., 1998; Bolger et al., 1997). PDE4D1 and PDE4D2 protein expression levels are up-regulated upon prolonged stimulation of the cAMP/PKA pathway in vascular smooth muscle cells (VSMC, Liu et al., 2000a), L6 myoblasts (Kovala et al., 1994) and in Jurkat T cells (Erdogan and Houslay, 1997). However, simultaneous activation of the ERK signalling mechanism and cAMP elevation attenuates this cAMP induced expression of PDE4D1 and PDE4D2 (Liu et al., 2000a). Expression of PDE4D1 and PDE4D2 is apparent in the early stages of spermatogenesis, with transcript levels diminishing after day 15 of development (Salanova et al., 1999). Up-regulation of both expression and activity of the 'short-form' PDE4D isoforms can also occur in a hormone dependent fashion, in Sertoli cells treated with follicular stimulating hormone (FSH) or thyroid cells treated with thyroid stimulating hormone (TSH, Vicini and Conti, 1997). Post-translational modifications of PDE4D1 also regulates its enzymatic activity, where the ERK mediated phosphorylation of Ser⁴⁹¹ on PDE4D1, the equivalent residue to Ser⁵⁷⁹ on PDE4D3, stimulates enzymatic activity (MacKenzie et al., 2000).

1.3.4.2. *'Long-form' splice variants of PDE4D*

PDE4D3 in over-expressed systems is found in both the cytosolic and particulate fractions of the cell, having K_m values of 1.4 μ M and 0.6 μ M, respectively (Bolger et al., 1997). The localisation of PDE4D3 within the cell to discrete sites is maintained by the formation of complexes with scaffolding/structural proteins (Dodge et al., 2001; Tasken et al., 2001; Verde et al., 2001). The muscle-selective A-kinase anchoring protein (mAKAP) maintains

a signalling module with PKA and PDE4D3 in complex (Dodge et al., 2001). In rat ventriculocytes, induction of mAKAP by treatment of the cells with hypertrophic stimuli induces a redistribution of PDE4D3, moving it from the cytosol to accumulate in the perinuclear region of the cell where mAKAP is localised (Dodge et al., 2001). At the centrosome of Sertoli cells, PDE4D3 co-localises with PKA-RII α and RII β subunits, in a complex co-ordinated by binding to AKAP450 (Tasken et al., 2001). Centrosomal, Golgi and sarcomeric localisation of PDE4D3 is also brought about by the formation of a complex with a novel structural protein called myomegalin (Verde et al., 2001).

There are well-characterised mechanisms by which PDE4D3 activity is modulated by phosphorylation by kinases such as PKA and ERK, and through interactions with phospholipids (see below).

PDE4D4 is found mainly associated with the particulate fraction of cells (Jin et al., 1998). This localisation may be due to the propensity of PDE4D4 to interact with SH3 containing adapter proteins, specifically of the src family of tyrosyl kinases, via the proline rich region in the unique N-terminus of PDE4D4 (Beard et al., 1999). Modulation of activity of PDE4D4 by phosphorylation events is thought to be similar to that exhibited by PDE4D3 as it is also a long isoform containing the equivalent Ser⁵⁴ and Ser⁵⁷⁹ residues for PKA and ERK phosphorylation, respectively.

PDE4D5 exists in both cytosolic and membrane associated pools of the cell (Bolger et al., 1997; Jin et al., 1998). The interaction of PDE4D5 isoform with the scaffolding protein, receptor for activated C kinase (RACK1), via residues in the unique N-terminus of the PDE, determines the localisation of the PDE within the cell but does not effect enzymatic activity (Yarwood et al., 1999). PDE4D5 is inhibited by ERK phosphorylation of the Ser⁶⁵¹ residue, which is the equivalent residue of Ser⁵⁷⁹ in PDE4D3 (Hoffmann et al., 1999). It is also activated by phosphorylation of Ser¹²⁶ by PKA (Sette and Conti, 1996; Hoffmann et al., 1998), which is the equivalent of Ser⁵⁴ in PDE4D3.

1.3.4.3. Regulation of PDE4D by PKA

Expression of 'short-form' PDE4D isoforms are tightly regulated by cAMP concentration and PKA activity in the cell (Erdogan and Houslay, 1997; Kovala et al., 1994; Liu et al., 2000a), whereas the expression of the long isoforms appears to be influenced only to a minor degree (Liu et al., 2000a). Although the absolute levels of protein are important in determining the cellular activity of the PDE4D enzymes, the main mechanism by which

PKA regulates PDE4D activity occurs through direct phosphorylation. As already mentioned, PKA phosphorylates PDE4D3 at Ser¹³ residue in the unique N-terminus of the protein and at Ser⁵⁴ in the UCR1 domain. Activation of recombinant enzyme depends specifically on the phosphorylation of the latter Ser⁵⁴ residue (Sette and Conti, 1996; Hoffmann et al., 1998). The structural changes, which occur upon PKA phosphorylation of PDE4D3, are such that when PDE4D3 is in its basal conformation a sub-domain in the carboxyl terminus of UCR2, interacts strongly with the catalytic domain, inhibiting the binding of cAMP. When Ser⁵⁴ is phosphorylated a conformational change is brought about and the affinity of the amino terminus of UCR1 for UCR2 increases. This therefore relieves the auto-inhibitory action of UCR2 on the catalytic domain, thus increasing enzyme activity (Lim et al., 1999, *Fig.1.10.*).

1.3.4.4. Regulation of PDE4D by ERK

An ERK consensus phosphorylation motif (P-X-S/T-P) has been identified in the carboxyl terminus of the catalytic domain of PDE4D isoforms. The kinase interaction motif (KIM) and an FQF domain, both of which act as docking motifs for ERK2 (MacKenzie et al., 2000), flank this consensus motif, and are required for ERK2 binding and phosphorylation in the PDE4D enzymes (MacKenzie et al., 2000). The Ser⁵⁷⁹ residue (PDE4D3 residue numbering system) is rapidly and specifically targeted for phosphorylation by ERK2 upon stimulation of the epidermal growth factor receptor (EGF-R, Hoffmann et al., 1999). Depending on the nature of the PDE4D isoform, different effects on the regulation of the enzymatic activity by ERK phosphorylation are seen. There is an up-regulation of the 'short-form' PDE4D1 activity, most probably due to the presence of the extreme N-terminal residues of UCR2 as the super-short PDE4D2 isoform, which lacks these residues, is mildly inhibited upon ERK activation (MacKenzie et al., 2000). However, ERK phosphorylation of the same residue in the long PDE4D isoforms (PDE4D3, PDE4D4 and PDE4D5) causes a large reduction in activity. This effect is attributed to the presence of both the UCR1 and UCR2 domains (MacKenzie et al., 2000).

PMA stimulation of cells causes the inhibition of PDE4D5 in an ERK dependent fashion, which in human aortic smooth muscle cells induces the activation of PKA that subsequently leads to an increase in the activation of PDE4D5 (Baillie et al., 2001). These observations exemplify the existence of a cross talk mechanism, which exists between PKA and ERK, that is regulated through the activity of PDE4D isozymes.

1.3.4.5. Regulation of PDE4D by phosphatidic acid

Phosphatidic acid (PA), a phospholipid which is generated in several cell types on stimulation by hormones and growth factors (Exton, 1994), has been implicated in the stimulation of proliferation of fibroblasts and increases the activity of recombinant PDE4D3 protein (Nemoz et al., 1997). PA specifically binds to a region found between residues 31 and 64 in the N-terminus of PDE4D3. The site is rich in basic and hydrophobic residues and is located within the UCR1 region which contains the Ser⁵⁴ residue, phosphorylated by PKA (Grange et al., 2000).

1.4. Cyclic AMP involvement in the cell cycle

The involvement of cAMP in the regulation of cell cycle control mechanisms has been apparent for decades (Pastan et al., 1975). Elevation of intracellular cAMP in cells can stimulate some cell types to proliferate, whereas, in other cell lines it can cause the cells to quiesce. When thyroid cell lines are incubated with TSH the intracellular levels of cAMP are elevated, PKA is activated and redistribution of the catalytic subunits to the nucleus initiates the phosphorylation of transcription factors (Montminy, 1997). This induces the cells to exit G₀ and to re-enter the cell cycle, promoting proliferation (Tramontano et al., 1988). However, the general effect of the elevation of cAMP on cellular proliferation seems to be one of arresting cells at G₀ or at the G₂/M transition (Pastan et al., 1975). Elevation of intracellular cAMP, through the stimulation of adenylyl cyclase, using forskolin, by addition of non-hydrolysable cAMP derivatives, or by the addition of phosphodiesterase inhibitors, inhibits cell proliferation (Pastan et al., 1975) in many cell lines including fibroblasts (L'Allemain et al., 1997), smooth muscle cells (Koyama et al., 2001) and lymphocytes (Banner et al., 2000). Indeed, it has been noted that in quiesced cells the levels of cAMP are naturally elevated, as is the activity of PKA (Grieco et al., 1996). The initial observations of growth retardation, through the elevation of intracellular cAMP, were made in hamster kidney cells by Burk (Burk, 1963).

1.4.1. Cyclic AMP induced inhibition of cell cycle entry

Ordered progression through the cell cycle is governed by the formation of complexes in which cyclin dependent kinase (cdk) act as catalytic subunits and cyclins act as regulatory subunits of the complex (reviewed in Li and Blow, 2001). Cdks are expressed at similar levels throughout the cell cycle whereas the cyclins tend to be expressed and degraded in a cell cycle dependent fashion, therefore eliciting phase specific activation of the kinases.

Quiescent cells are stimulated to enter the cell cycle by the addition of mitogens which, through the activation of the mitogen signalling cascade, initiate the expression of cyclin D (cyclin D1, D2 and D3, Weber et al., 1997). D-type cyclins form complexes with, and activate, cdk 4 and cdk 6 (Sherr, 1993), which phosphorylate the tumour suppressor Retinoblastoma protein, pRb. The phosphorylation of pRb disrupts its interaction with the E2F family of transcription factors thus allowing the co-ordinated transcription of genes whose activities are required for DNA synthesis (Weinberg, 1995, *Fig. 1. 11.*). Cyclin D is an unstable protein and when mitogens are removed from the cells levels of the protein are rapidly reduced, due to its ubiquitin mediated degradation by the proteasome (Sewing et al., 1993). If the cells have not passed the restriction point within G1 prior to mitogen withdrawal, quiescence is induced. If, however, mitogens are present until after the cells have passed the restriction point, the cells are committed to complete one full cell division under autonomous control (Pardee, 1989). Cyclin D therefore provides a link between extracellular mitogenic signals and the cell cycle machinery.

The E2F transcription factor initiates the transcription of the E-type cyclin which is periodically expressed later in G1 (Koff et al., 1992). Cyclin E has a high affinity for cdk2, to which it binds and forms an active complex required for S-phase entry in all mammalian cells (Ohtsubo et al., 1995). After the cyclin D/cdk4 mediated initial phosphorylation of pRb the active cyclin E/cdk2 complex hyper-phosphorylates pRb, on additional sites providing sustained activity of E2F resulting in the expression of proteins required for the G1/S transition (reviewed in Sherr, 1993). Attenuation of the cdk-mediated phosphorylation of pRb causes E2F to reassociate with it leading to a repression of the heterodimeric E2F transcription factor activity and subsequent down regulation of proteins required for the G1/S transition (Stewart et al., 1999).

The activity of the cdk complexes is not only controlled at the level of cyclin expression but is also regulated by association with the INK4 (inhibitors of cdk4) and *cip/kip* families of inhibitor proteins. The latent G1 phase inhibitor p27^{KIP1} binds to both cyclin D/cdk4 and cyclin E/cdk 2 kinase complexes in a 1:1:1 stoichiometry (Blain et al., 1997), but with a higher affinity for cyclin D/cdk4 than cyclin E/cdk2 (Polyak et al., 1994a). The consequences of the interaction of p27^{KIP1} with the cyclin D/cdk4 complex are contested. Some groups have shown that kinase activity is inhibited as p27^{KIP1} prevents the cdk-activating kinase (CAK) from phosphorylating and activating cyclin D/cdk4 *in vitro* (Kato et al., 1994). More recently, however, it has been shown that the p27^{KIP1} bound cyclin D/cdk4 complex maintains kinase activity *in vivo* (Blain et al., 1997; Ravanko et al., 2000) and that this interaction functions more as a sequestering mechanism for p27^{KIP1}. When

levels of p27^{KIP1} exceed those of cyclin D/cdk4 the inhibitor binds to the cyclin E/cdk2 complex where it act as an effective antagonist of the kinase complex activity (Zerfass-Thome et al., 1997; Ravanko et al., 2000) thereby preventing cell cycle progression (Polyak et al., 1994b). Once activated cyclin E/cdk2, is involved in a positive feedback loop, where it phosphorylates p27^{KIP1}, targeting it for ubiquitin mediated degradation thereby facilitating its own activation (Sheaff et al., 1997; Morisaki et al., 1997, *Fig. 1.11.*).

There are several mechanisms by which cAMP elevation and the activation of PKA influences cell cycle progression (L'Allemain et al., 1997). PKA causes an elevation in the levels of the G1 cyclin dependent kinase inhibitor p27^{KIP1} (Kato et al., 1994) and the tumour supressor p53 (Hayashi et al., 2000) and decreases the levels of the G1 cyclins D1 and D3 (L'Allemain et al., 1997; Naderi et al., 2000). Activation of PKA can also negatively regulate the mitogen signalling cascade, by preventing the activation of ERK (Graves et al., 1993).

1.4.1.1. Cyclic AMP mediated elevation of p27^{KIP1} protein levels

The amounts of p27^{KIP1} mRNA remain constant throughout the cell cycle (Morisaki et al., 1997). However, elevation of cAMP and subsequent activation of PKA causes a rapid increase in the levels of p27^{KIP1} protein, through the initiation of translation and also through a reduction in protein degradation (Hengst and Reed, 1996; van Oirschot et al., 2001). The precise mechanism by which PKA increases p27^{KIP1} translation has not yet been elucidated. It has been postulated that PKA phosphorylation of the cAMP response element binding protein (CREB) initiates activation of the CRE promoter found upstream of the p27^{KIP1} gene that increases p27^{KIP1} expression (Kwon et al., 1996). PKA inhibits proteasome-mediated degradation of the p27^{KIP1} protein (L'Allemain et al., 1997; Boucher et al., 2001) by a mechanism that involves either direct phosphorylation of p27^{KIP1} or phosphorylation of some component of the proteasome (Boucher et al., 2001). In any case, the consequence of elevated p27^{KIP1} levels in the cell is that all cyclin D/cdk4 complexes become bound to the inhibitor. The excess p27^{KIP1} then binds to cyclin E/cdk2, where it effectively blocks its kinase activity thus repressing pRb phosphorylation and consequently reducing the amount of cyclin E (reviewed in Sherr, 1993) and cyclin A (Weinberg, 1995; Zerfass-Thome et al., 1997) protein expression. The net result is that cells arrest prior to their passage through the G1 restriction point (Kato et al., 1994; L'Allemain et al., 1997).

1.4.1.2. *Cyclic AMP mediated down regulation of D-type cyclins*

Cellular levels of cyclin D are low during quiescence in the absence of growth factors but then rise upon mitogenic stimulation and remain elevated throughout the rest of the cell cycle (Weber et al., 1997; Sewing et al., 1993; Matsushima et al., 1991). Elevation of cAMP in a cell reduces the protein levels of cyclins D1 (L'Allemain et al., 1997) and D3 (van Oirschot et al., 2001; Naderi et al., 2000), by increasing their proteasome dependent degradation (Diehl et al., 1997); Stewart et al., 1999). Elevation of cAMP also decreases levels of cyclin D by reducing the rates of cyclin D translation (Naderi et al., 2000; Sewing et al., 1993; L'Allemain et al., 1997). The decrease in active cyclin D/cdk4 correlates with a decrease in the phosphorylation of pRb (Boucher et al., 2001) and therefore a decrease in the expression of the proteins required for the G1/S transition (van Oirschot et al., 2001; Naderi et al., 2000). Low levels of the cyclin D/cdk4 complex increases the amount of free p27^{KIP1} protein, which can then redistribute, bind to and inhibit cyclin E/cdk2 (L'Allemain et al., 1997; Naderi et al., 2000).

1.4.1.3. *Cyclic AMP mediated interference of the mitogen activated protein kinase cascade.*

The activation of extracellular signal-regulated protein kinases (ERK) is central to mitogenic signalling in many cell types (Frye, 1992). The major pathway for ERK activation by ligands for receptor tyrosine kinases occurs via Ras dependent stimulation of Raf-1 and mitogen activated protein kinase kinase (MEK), a dual specificity kinase that specifically activates ERKs 1 and 2. Once ERK is activated it targets p90^{s6k} for phosphorylation and both proteins translocate to the nucleus where they activate early response transcription factors such as *c-jun* (Pulverer et al., 1991), *c-myc* (Seth et al., 1991) and *Elk* (reviewed in Davis, 1995). Sustained activation of ERK1 is required for the continued expression of cyclin D1 (Weber et al., 1997), phosphorylation of pRb (Stewart et al., 1999) and down regulation of p27^{KIP1} (Greulich and Erikson, 1998) in G1 to enable S phase entry (Ramakrishnan et al., 1998) and cellular proliferation (reviewed in Roovers and Assoian, 2000). Ras is a member of the small guanine 5'-triphosphate (GTP) binding protein superfamily. It is the product of an oncogene, found to be mutated in 15 % of tumour cell lines (Bos, 1989). Cells can be transformed by a point mutation of ras which leads to uncontrolled cell division due to continual activation of ERK (Bos, 1989). Non-hydrolysable cAMP analogues have been shown to induce growth inhibition of such transformed cells in a manner that is dependent on PKA activity (Noguchi et al., 1998). The attenuation of mitogenic signalling by the activation of PKA occurs in a fashion that is

still not yet completely resolved. The effects of cAMP elevation on cell cycle progression is dependent on the isoforms of the Raf family expressed in the cell and on the growth factor used as a stimulus for proliferation (Cospedal et al., 1999). PKA mediates the inhibition of Raf-1 via different mechanisms (Boucher et al., 2001). Firstly, it can phosphorylate Raf-1 directly (Ramstad et al., 2000), preventing it from binding to Ras and activating the MEK/ERK cascade (Cook and McCormick, 1993; Houslay and Kolch, 2000). Alternatively, Raf-1 activity can be modulated by another small G-protein of the Ras family, Rap1, which itself can be regulated by PKA. The mechanisms involving Rap1 activation and inhibition of cell proliferation are still unclear and the downstream effects appear to be mechanistically and cellularly distinct (reviewed in Bos et al., 2001). Cyclic AMP binds directly to Epac and increases its guanine nucleotide exchange factor activity towards Rap1, thus activating it (Zwartkruis and Bos, 1999; de Rooij et al., 2000; Kawasaki et al., 1998). Rap1 has also been shown to be directly regulated by cAMP in a PKA and Epac independent manner, whereby increases in cAMP inactivate Rap1, which causes the inhibition of ERK and PI3-kinase/PKB activity in glioma cell lines (Wang et al., 2001a). The activation of Rap1 increases its affinity for Raf-1 which might act to trap Raf-1 in an inactive complex (Bos, 1998) and hence antagonise the Ras/Raf-1 interaction in the Ras-Raf-MEK-ERK pathway (Schmitt and Stork, 2001; Koyama et al., 2001). Although mutants of Rap1 inhibit the ERK pathway, no studies have observed the absolute inhibition (or activation) of Raf1 kinase upon extracellular Rap1 activation, suggesting additional pathways are involved in the inactivation of the MEK/ERK signalling pathway (Bos et al., 2001). Conversely, in some cells Rap1 is implicated in activation of the ERK pathway in cells which express the Raf family member, B-raf (Vossler et al., 1997; Houslay and Kolch, 2000; Schmitt and Stork, 2000; Tsygankova et al., 2001).

1.4.1.4. PI3-kinase pathway

The phosphoinositide 3-kinase (PI 3-kinase) pathway is another signalling cascade within cells at which cAMP can elicit its inhibitory effects on cell cycle proliferation (reviewed in Ammit and Panettieri, Jr., 2001). Upon platelet derived growth factor interaction with its cognate GPCR PI 3-kinase is activated by the dissociated $\beta\gamma$ complex (Walker et al., 1998). PI 3-kinase can be equally activated by mitogens interacting with receptor tyrosine kinases (reviewed in Cantrell, 2001). PI 3-kinase then phosphorylates membrane phosphoinositides, in the 3' position of the inositol ring, which function as second messengers and activate downstream effector molecules such as protein dependent kinase (PDK1), which in turn activates PKB, p70s6 kinase and the Rho family of GTPases (reviewed in Cantrell, 2001). PI 3-kinase activates the cyclin D1 promoter and DNA

synthesis via an ERK independent mechanism (Page et al., 2000) and p70s6 kinase activates the 40S ribosomal protein which up-regulates the translation of cyclin D1 mRNA (Scott et al., 1996). PI 3-kinase mediated signalling cascades also regulate the phosphorylation of the pRb causing the release of the E2F transcription factor and increasing the levels of expression of the G1 dependent cyclins (Brennan et al., 1997; Krymskaya et al., 1999). All these mechanisms are capable of initiating proliferation, although the activation of PI 3-kinase alone appears to be insufficient for the initiation of DNA synthesis in T cells (Brennan et al., 1997). With the elevation of cAMP, through the addition of forskolin to cells, G1 progression is inhibited as cAMP interferes with the interaction of the p85 adapter subunit of PI 3-kinase with the tyrosine kinase receptor (Monfar et al., 1995; Scott et al., 1996; Frost et al., 1995).

1.4.2. Cyclic-AMP involvement of M phase transition

Mitosis is the stage in the cell cycle during which cell division takes place. It can be separated into five distinct phases. In prophase the chromosomes condense and nuclear envelope breakdown occurs (Nigg, 2001). In prometaphase the mitotic spindles to which the chromosomes attach are formed. The alignment of chromosomes along the metaphase plate then takes place during metaphase (Leblond and El Alfy, 1998). At the onset of anaphase, the sister chromatid cohesion is reduced, they separate and migrate to the opposite poles of the cell and telophase determines the time at which the daughter cells physically separate by cytokinesis (Leblond and El Alfy, 1998). To maintain the ordered progression through mitosis there are highly regulated intrinsic mechanisms which depend on multiple feedback loops involving an increasing number of kinases and phosphatases. The entry of cells into mitosis is under the control of the maturation-promoting factor (MPF) which is a complex composed of the mitotically expressed cyclin B1 and the kinase subunit cdk1. MPF activity is tightly regulated by post-translational modifications, under the control of checkpoint phosphorylation and dephosphorylation mechanisms. The activation of MPF leads to alterations in spindle dynamics and the architecture of the cell as well as initiating chromosome and centrosome duplication (reviewed in Nigg, 2001; Smits and Medema, 2001; Ohi and Gould, 1999).

Mitotic exit requires chromatid separation, spindle disassembly and cytokinesis, the co-ordination of which is dependent on the ubiquitin-dependent proteolysis of key regulatory proteins (King et al., 1996). The critical step in mitotic protein destruction is mediated by the anaphase promoting complex (APC), or the 20S cyclosome: a multi-subunit complex that functions as a cell cycle dependent ubiquitin ligase (King et al., 1995). Once

ubiquitylation of target proteins has occurred, they are then subjected to degradation by the 26S proteasome, which ensures unidirectional progression through mitosis (Morgan, 1999). Cyclic AMP levels are usually elevated in cells in order to maintain an interphase state and antagonise mitotic entry (Lamb et al., 1991). Cyclic AMP levels are reduced in mitosis (Grieco et al., 1996) leading to activation of the MPF (Hohmann et al., 1993) and the APC (Kotani et al., 1999). The mechanisms by which cAMP levels are reduced and PKA is inactivated during mitosis have not yet been identified *in vivo*.

1.4.2.1. *Cyclic AMP dependent modulation of MPF activity*

The concentration of cAMP oscillates during the cell cycle, thus altering the levels of free PKA catalytic subunit and participating in the temporal regulation of the PKA mediated signalling cascade (Zeilig et al., 1976; Grieco et al., 1994). Cyclic AMP and PKA activity is elevated prior to the entry of cells into mitosis, with the activity then falling rapidly as cells enter mitosis (Kotani et al., 1998; Zeilig et al., 1976). The inactivation of PKA promotes the activation of the MPF at the onset of mitosis (Grieco et al., 1996; Fernandez et al., 1995) as PKA antagonises the activation of MPF (Hohmann et al., 1993; Ohi and Gould, 1999; Grieco et al., 1994). Prolonged PKA activation using temperature sensitive mutants of PKA or cAMP elevating agents gives rise to abnormal mitotic spindle formation, blocks chromosome separation (Ishii et al., 1996) and inhibits nuclear envelope breakdown (Lamb et al., 1991), underlining the importance of this enzyme in these processes.

1.4.2.2. *Cyclic AMP dependent modulation of the anaphase promoting complex activity*

The activity of the anaphase-promoting complex (APC) is regulated by at least four distinct mechanisms: the phosphorylation and dephosphorylation of the ubiquitin ligase subunits and by the binding of positive and negative regulatory factors (reviewed Kotani et al., 1999). However, the precise regulatory mechanism of substrate specific activation of mammalian APC remains to be elucidated.

Elevation of PKA activity prior to the metaphase /anaphase transition inhibits mitotic exit through negative regulation of the APC activity, at least *in vitro* (Kotani et al., 1998; Yamashita et al., 1996; Yanagida et al., 1999). *Saccharomyces cerevisiae* (Anghileri et al., 1999) and *Schizosaccharomyces pombe* (Yamashita et al., 1996; Yanagida et al., 1999) yeast species, in which temperature sensitive mutants of the APC subunits have been

generated, are being used to elucidate mechanisms involved in APC activation and mitotic progression. PKA phosphorylates the Cut4 (mammalian homologue APC1) and cut9 (mammalian homologue APC6) subunits of the APC during interphase (Ishii et al., 1996; Kotani et al., 1998; Yamashita et al., 1996) and this impairs the assembly of an active APC complex (Yamashita et al., 1999; Yanagida et al., 1999). The yeast Cut 20 and mammalian Cdc27 APC subunits have also been identified as targets for PKA phosphorylation (Yamashita et al., 1996; Kotani et al., 1998) and both could be involved in the negative regulation of the APC. Dephosphorylation of the PKA phosphorylated APC subunits by PP1 at metaphase allows assembly of the APC subunits resulting in the formation of an active ubiquitin ligase complex (Ishii et al., 1996).

The temporal control of PKA activity is not the only important mechanism by which it regulates mitotic progression, since the spatial regulation of active PKA is crucial in the determination of the targets for phosphorylation. PKA has been shown, in fibroblasts, to co-localise with MPF at the centrosome (Tournier et al., 1991). The PKA regulatory subunit, RII α , is targeted for phosphorylation by the MPF which causes its redistribution from the centrosome/Golgi, where it is held through an interaction with AKAP75, to the cytosol (Keryer et al., 1998).

1.5. Phosphodiesterases and the cell cycle

Intracellular cAMP degradation, elicited by phosphodiesterases, has been studied in many cell types during the cell cycle. Maintaining a low level of cAMP within cells is associated with continual cell proliferation and is dependable on high PDE activities (Pan et al., 1994; Leitman et al., 1986; Drees et al., 1993; Matousovic et al., 1997). Many disease states that are characterised by excessive cellular proliferation have elevated PDE activity (Savini et al., 1995). In proliferating cultured colon carcinoma cell lines levels of PDE activity are high, maintaining low concentrations of cAMP. As the cells reach confluency the PDE activity decreases, the concentration of cAMP increases and the proliferation rate markedly slows (Savini et al., 1995). High levels of PDE activity have been observed in rat hepatomas (Tsou et al., 1974) and endometrial cancer (Tsou et al., 1986), where continual cellular proliferation is evident. In rat models of mesangialproliferative glomerulonephritis (MSGN), a disease hallmarked by excessive mesangial cell proliferation, nephron cellularity is decreased by treatment with the PDE3 selective inhibitors (Tsuboi et al., 1996). Such treatment of these cells inhibits the mitogenic pathway and MAPK activity, leading to the reduction in cell proliferation (Tsuboi et al., 1996). The PDE4 specific inhibitor, rolipram, however, has no effect on the activation of MAPK in these cells, even

though PDE4 is two times more abundant than PDE3 (Matousovic et al., 1995) indicating the significance of compartmentalisation of the cAMP signalling cascades.

PDE inhibitors have been shown to inhibit the proliferation of endothelial cells (Leitman et al., 1986), melanoma cell lines (Drees et al., 1993) and epithelial cells (Matousovic et al., 1997), arresting them all at the G1/S boundary, prior to the restriction point. Other studies have made implications of differential control of cAMP degradation by PDEs at other stages of the cell cycle. The general PDE inhibitor, IBMX, arrested *Amphidiunium operculatum* cells at G2/M transition as well as at the G1/S boundary (Leighfield and Van Dolah, 2001). In *Actinomyces*, PDE activity has been shown to increase at G2 phase (Lefebvre et al., 1980), and this high level of PDE activity is maintained during mitosis. Furthermore, the inhibition of PDE activity in both budding and fission yeast, through the generation of temperature sensitive mutants, has been shown to block mitotic exit (Yamashita et al., 1996; Kishimoto and Yamashita, 2000).

There have also been studies on the fluctuations of PDE activity in different phases of the cell cycle. The initial observations were made during cell proliferation in the slime mould, *Physarum polycephalum* (Lovely and Threlfall, 1978; Lovely and Threlfall, 1979; Kupetz and Jeter, Jr., 1985). Later studies in *actinomyces* indicated that in the early stages of the cell cycle, during the first stage of protein synthesis and DNA replication, there was a decrease in the specific activity of PDEs. This increased activity post DNA replication as cells entered G2 and M (Lefebvre et al., 1980). Fluctuations of PDE activity have also been noted in germ cell proliferation, in seminiferous epithelium, where rolipram sensitive activity was maximal at the early stages of sperm development (stages II-VI) and minimal at later stages (stages IX-XII, Morena et al., 1995). As fluctuations of cAMP levels have been studied so extensively during the cell cycle and the mechanisms that they influence are now being elucidated and fully characterised.

1.5.1. Phosphodiesterases and T cell proliferation

The human T lymphotropic virus (HTLV-1) is endemic in some Asian, Caribbean and African countries. It is capable of infecting and transforming mature T cells and has been implicated in the adult T cell leukaemia (ATL): a rapidly progressive, usually fatal, mature T cell leukaemia (Greene and Leonard, 1986). MJ cells, a HTLV-1 transformed T cell line, have elevated levels of PDE4 activity compared to untransformed cells (Ekholm et al., 1999), suggesting that cAMP hydrolysis maintains the proliferative ability of the cells.

Additionally, incubation of MJ cells with the PDE4 specific inhibitor, rolipram, reduces cell proliferation (Ekholm et al., 1999).

Inhibition of PDE3 (Giembycz et al., 1996), PDE4 (Essayan et al., 1997) and PDE7 (Li et al., 1999; Mary et al., 1987) have all been shown to attenuate the proliferation of T cell lines. However, the precise cellular mechanisms by which the inhibition of PDEs decrease proliferation are difficult to pinpoint as the full activation of T cells, which leads to their increased proliferation, requires the activation of multiple pathways.

T cells require two distinct extracellular signals in order to be activated, to proliferate and to induce an immune response. An antigen, bound to the major histocompatibility complex (MHC) on the antigen-presenting cell, interacts with the CD3 T cell receptor complex on the surface of T cells (Geppert and Lipsky, 1986) inducing the expression of low levels of the cytokine interleukin 2 (IL-2) and causing cells to pass from quiescence to G1 (Tsoukas et al., 1985). IL-2 acts in an autocrine fashion when bound to its cognate receptor (Smith, 1984), inducing further activation of the T cell by stimulating the protein tyrosine kinase-dependent pathways that activate Ras (reviewed in Izquierdo et al., 1995), the transcription factors Stat3 and Stat5 (Johnston et al., 1995) and PI 3-kinase (Brennan et al., 1997). PI 3-kinase increases the transcriptional activation of E2F, which in turn increases the levels of cyclins D2, D3 and E and decreases the amount of p27^{KIP1} (Modiano et al., 1994) in the T cell (Brennan et al., 1997). Nevertheless, the stimulation of PI 3-kinase through the IL-2 signalling pathway alone is not sufficient to induce DNA synthesis (Brennan et al., 1997).

Expression of IL-2 in primed T cells is enhanced synergistically upon co-stimulation of CD28, an accessory molecule expressed on the surface of the T cell, that is stimulated non-specifically by the antigen-presenting cell (reviewed in Jenkins and Johnson, 1993). The cellular signalling events initiated upon CD3 and CD28 co-stimulation include an increase in PDE activity, leading to decreased levels of cAMP (Skalhegg et al., 1994; Takemoto et al., 1978; Epstein et al., 1980). This decrease in cAMP inactivates PKA, enabling the activation of the MAPK pathway which causes primed T cells to increase their production of IL-2 (Mary et al., 1987) and expression of IL-2 receptors (IL-2R, Toribio et al., 1989; Krause and Deutsch, 1991). All these effects consequently elicit the full activation of the T cell. When T cells are fully activated, DNA synthesis is initiated, the cells make the transition into S phase (Smith, 1984) and clonal expansion of the cell population is prompted, generating an immune response (Giembycz et al., 1996; Lingk et al., 1990). In addition to inducing cell proliferation, the decrease in cAMP levels, upon CD3/CD28 activation also increases the levels of cytokine expression and exocytosis (Shahinian et al.,

1993) from the activated T cells (Borger et al., 1996; Giembycz et al., 1996; Shichijo et al., 1997).

Elevation of cAMP levels in T cells by the addition of catecholamines, prostaglandin 2 (PGE₂, Wacholtz et al., 1991; Baker et al., 1981), forskolin (Lingk et al., 1990; Shichijo et al., 1997), cholera toxin (Wacholtz et al., 1991) and PDE inhibitors (Ekholm et al., 1999) attenuates mitogen stimulated T cell proliferation (Baker et al., 1981; van Oirschot et al., 2001) and IL-2-mediated DNA synthesis (Lingk et al., 1990), suppressing the immune response.

1.5.1.1. PDE4 and T cell proliferation

T cell activation is associated with inflammatory diseases such as atopic dermatitis and asthma (reviewed in Kay, 2000). Mononuclear cells from patients with atopic dermatitis are found to be more sensitive to the anti-proliferative effects of PDE4 inhibitors than non-atopic subjects (Banner et al., 1995), as they appear to express elevated levels of cAMP specific PDEs (Holden et al., 1986). Human T lymphocytes and mononuclear cells, stimulated with the lectin phytohaemagglutinin (PHA), decrease their proliferation upon treatment with PDE4 and PDE3 specific inhibitors (Banner et al., 2000; Banner et al., 1995; Robicsek et al., 1991). This suggests that phosphodiesterases influence the control of cell cycle machinery at least to some extent.

PDE4 inhibition augments the proliferative responses of antigen-driven T helper cell clones (Essayan et al., 1997) and suppresses the production of several cytokines including IL-1 (Giembycz et al., 1994), IL-2 (Giembycz et al., 1996), IL-4 (Robicsek et al., 1991) and IL-13 in human T cells (Shichijo et al., 1997; Essayan et al., 1997; Kanda and Watanabe, 2001), again underlying the importance of this class of enzyme in the regulation of T cell activation.

The effects of PDE inhibition on the modulation of the different T cell responses are not solely dependent on the net increase of cAMP levels in the cell but are also dependent on the localisation of the PDE isoforms. The Barnes group (Giembycz et al., 1996) showed that inhibition of cytosolic PDE4 led to the attenuation of both IL-2 release and proliferation of PHA treated and CD3 induced CD4⁺ and CD8⁺ T lymphocytes, whereas inhibition of the membrane associated PDE3 had no effect on any of these responses. Interestingly, however, inhibition of PDE3 potentiates the anti-proliferative effect of PDE4 inhibitors (Giembycz et al., 1994), indicating cross talk between the classes of

phosphodiesterases. Stimulation of T cells with different mitogens has been demonstrated to determine alternative modes of activation of the cell. When PMA and ionomycin are used as co-mitogens of the CD4⁺ and CD8⁺ lymphocytes inhibition of PDE4 does not affect proliferation, but does suppress IL-2 and interferon γ (IFN γ) release (Giembycz et al., 1996).

1.5.1.2. PDE7 and T cell proliferation

Following inhibition of both PDE4 and PDE3 in T lymphocytes it was noted that there was between 25 – 40 % residual cAMP specific activity in the cytosolic fraction of the T cell (Robicsek et al., 1991; Tenor et al., 1995; Giembycz et al., 1996). This has been attributed to PDE7 and referred to as the cAMP specific, rolipram-insensitive activity in these T cells (Ichimura and Kase, 1993), to which selective inhibitors have only recently being developed (Martinez et al., 2000; Barnes et al., 2001). Both CD4⁺ and CD8⁺ T cells express PDE7 isoforms (Giembycz et al., 1996) at low levels in peripheral T lymphocytes. When the cells are activated by anti-CD3/CD28 stimulation, there is a rapid increase in PDE7A1 and PDE7A3 mRNA and protein levels (Glavas et al., 2001). However, PHA stimulation of the same cells has no effect on PDE7 levels or activity (Kanda and Watanabe, 2001; Bloom and Beavo, 1996). PDE7 activity is associated with the signalling cascades that initiate full activation of the T cells inducing cell proliferation and IL-2 release from the cells (Giembycz et al., 1996). Down-regulation of PDE7 expression, using anti-sense oligonucleotides (Kanda and Watanabe, 2001), decreased the amount of IL-2 expression and inhibited proliferation of activated T cells by 70 - 80 % (Li et al., 1999). With PDE7 contributing significantly to mechanisms involved in the full activation of T cells it could be a potential target for drug design, to inhibit IL-2 production and prevent excessive cellular proliferation without the toxicity associated with PDE4 inhibition (Barnes et al., 2001).

1.5.2. PDEs and smooth muscle cell proliferation

Increased airway smooth muscle mass, caused by increased hypertrophy and hyperplasia (Johnson et al., 2001), is associated with airway hyper-responsiveness in type I, and to a lesser degree, in type II asthmatics (Ebina et al., 1993), which leads to amplification of airway resistance. PI 3-kinase-dependent mechanisms are activated in the mitogenic signalling pathway in human airway smooth muscle cells (ASMCs), particularly acting through the stimulation of p70^{S6k}, which increases protein and DNA synthesis and increases cell proliferation (Scott et al., 1996). In cultured ASMCs, β_2 -adrenergic receptor

agonists decrease the proliferative response in part by a cAMP-mediated mechanism (Tomlinson et al., 1995; Stewart et al., 1999). Smooth muscle cell proliferation can also be inhibited by other agents which cause the elevation of cAMP such as prostaglandin E₁, which can be produced by endothelial cells (Loesberg et al., 1985), forskolin and prostaglandin E₂ (PGE₂, Lee et al., 2001; Stewart et al., 1999; Florio et al., 1994) and inhibition of PDEs with the general inhibitor IBMX or by the addition of the PDE3-selective inhibitor, siguazodan (Billington et al., 1999). These cause cells to arrest within G₁ phase, prior to the entry to S phase (Loesberg et al., 1985; Florio et al., 1994; Tomlinson et al., 1995). However, the selective inhibition of PDE₄, by the addition of rolipram to ASMCs, does not attenuate proliferation, This suggests that the compartmentalisation of cAMP elevation, at least in ASMCs, may be functionally relevant (Billington et al., 1999).

A typical event in the pathogenesis of ischemic heart disease resulting from atherosclerosis is the proliferation of vascular smooth muscle cells (VSMCs). This can be treated using catheter-based techniques such as balloon angioplasty. However this damages the smooth muscle cells inducing the formation of neointima resulting in restenosis (Indolfi et al., 1997; Ip et al., 1990). The proliferation of VSMC, caused by this mechanical damage, can be attenuated by the elevation of cAMP through the inhibition of PDEs (Indolfi et al., 1997). Selective inhibitors of PDE₃, such as cilostamide (Tsuchikane et al., 1999), trequinsin (Osinski and Schror, 2000), amrinone (Indolfi et al., 1997) and CI-930 (Johnson-Mills et al., 1998) have all been shown to attenuate proliferation of cultured VSMC (Johnson-Mills et al., 1998; Pan et al., 1994) and also VSMC from subjects which have undergone balloon angioplasty (Indolfi et al., 1997; Tsuchikane et al., 1999). The effect of selective inhibitors of PDE₄, on the proliferation of vascular smooth muscle cells, on the other hand is debatable. Some studies have shown that, when used independently of PDE₃ inhibitors, rolipram attenuates VSMC proliferation (Pan et al., 1994). Whereas, others suggest there is no decrease in proliferation (Johnson-Mills et al., 1998; Souness et al., 1992; Osinski and Schror, 2000). In either case it does seem clear that when PDE₃ and PDE₄ are inhibited simultaneously, a supra-inhibition of VSMC proliferation is observed (Johnson-Mills et al., 1998; Pan et al., 1994; Souness et al., 1992). This has led to speculation concerning the compartmentalisation of PDE isoforms differentially regulating the cell cycle machinery. VSMC proliferation can also be attenuated by the PDE₅ specific inhibitor, sildenafil, which interferes with the mitogenic signalling pathway (Osinski et al., 2001).

Elevated cAMP in VSMC reduces cyclin D1 protein levels (Lee et al., 2001) by increasing proteasome mediated degradation of the protein (Stewart et al., 1999). The reduction of cyclin D1 levels prevents the phosphorylation of the pRb, thereby attenuating cell cycle progression (Stewart et al., 1999). Increased cAMP concentrations also attenuate ERK stimulated activation of p90^{RSK} and *c-Fos* (Lee et al., 2001). The phase of the cell cycle at which the elevation of cAMP causes inhibition of SMC proliferation is at the G1/S transition (Loesberg et al., 1985), where PKA activation antagonises the mitogen signalling cascade (Osinski and Schror, 2000; Osinski et al., 2001). PKA phosphorylates the cAMP response element binding protein (CREB) which subsequently associates with the cAMP response element (CRE) in the cyclin D1 and cyclin A promoter sequence (Musa et al., 1999), impairing the expression of cyclin D1 and cyclin A mRNA and protein (Kronemann et al., 1999).

Although changes in PDE activity have been noted during different phases of the cell cycle in germ cells (Morena et al., 1995) and in prokaryotes (Leighfield and Van Dolah, 2001; Lefebvre et al., 1980), no studies have been carried out to investigate the fluctuation of specific PDE isoform activities in the somatic cell cycle. A significant down regulation of PKA activity has been identified at the metaphase/anaphase transition (Grieco et al., 1996), and this has since been shown to be of fundamental importance in the progression through M phase in yeast (Yanagida et al., 1999). The relevance of the decreased PKA activity, in mammalian cell lines, is still not clear and the mechanisms by which cAMP levels are reduced at the metaphase/anaphase transition have not yet been elucidated. Given that the functions of PKA and PDE work antagonistically, it seemed likely that PDE isoforms might contribute to the control of cAMP regulation during the cell cycle. Therefore, the main aim of this thesis was to examine phosphodiesterase activities in mammalian somatic cells during the cell cycle.

The initial work, presented in chapter 3, deals with the optimisation of methods for arresting cells at the various stages of the cell cycle. These methods were then used in an analysis of PDE and PKA activities throughout the cell cycle. This work uncovered the interesting observation that PDE4D3 activity was selectively and markedly increased during mitosis. A detailed study of this phenomenon was then undertaken, the results of which are presented in chapter 4. In addition, some preliminary work, investigating a poorly characterised member of the PDE family, PDE7, was carried out and this is the focus of chapter 5.

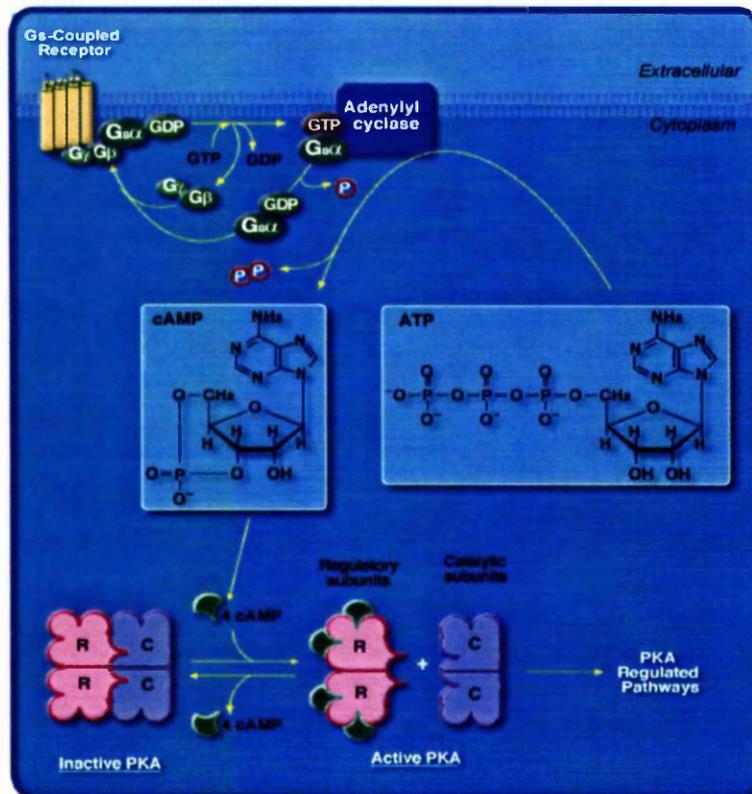


Figure 1.1. G-protein coupled receptor activation of protein kinase A. Upon a ligand binding to its cognate Gs coupled receptor GDP/GTP exchange on the G α subunit occurs and the heterotrimeric G protein dissociates such that the G $\beta\gamma$ complex activates downstream signalling cascades and the G α -GTP interacts with the membrane associated adenylyl cyclase. The active adenylyl cyclase then converts intracellular ATP to cAMP, which diffuses away from the site of production and binds to the regulatory subunits of PKA. This induces a conformational change in the PKA subunits, causing the active catalytic subunits to disassociate and activate PKA regulated pathways. Picture taken from <http://www.biocarta.com/pathfiles/gspathway.asp>.

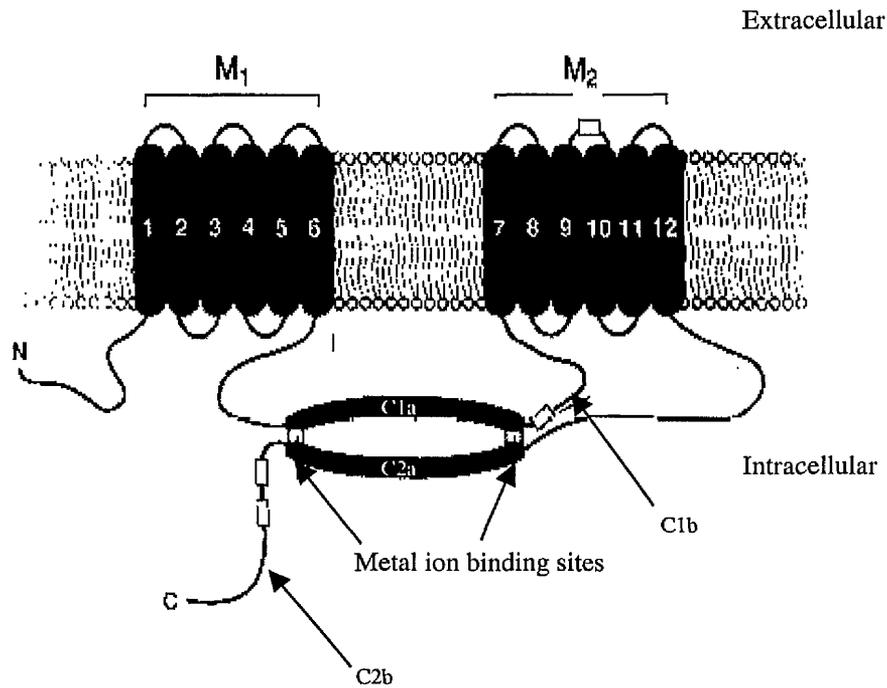
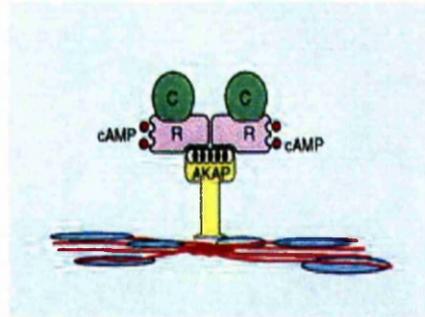


Figure 1.2. The topology of membrane bound adenylate cyclase. The adenylate cyclase enzyme is composed of two sets of six transmembrane helices (M_1 and M_2). These are separated by the first large intracellular loop which is composed of the catalytic C1a domain and the regulatory C1b domain. The long intracellular C-terminal domain is composed of the C2a catalytic domain and the terminal regulatory C2b domain. Divalent metal ions bind at the interface of the two catalytic motifs, holding the catalytic domain together. Both the N- and C- termini of the protein are intracellular. Picture adapted from Houslay & Milligan (1997).

A



B

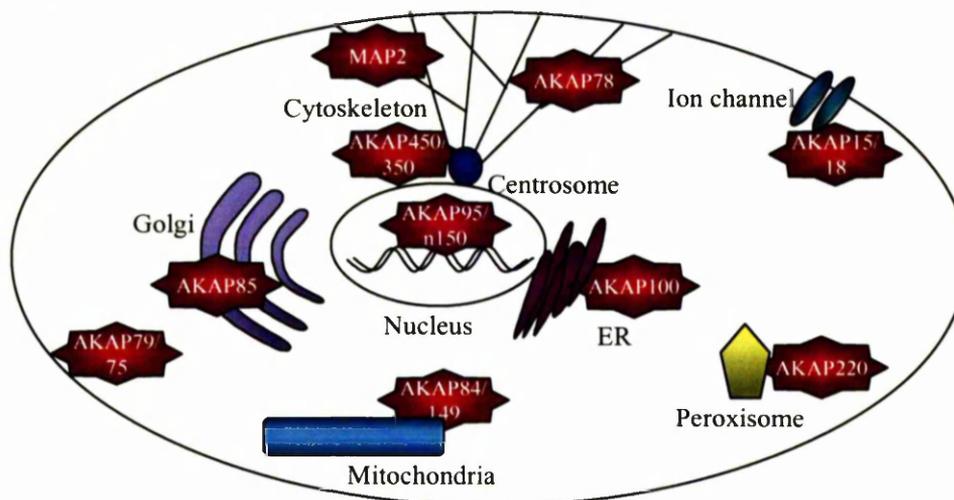
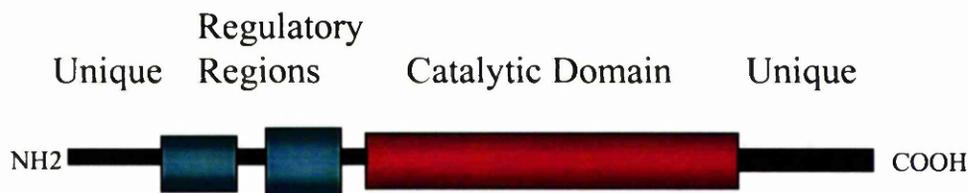


Figure 1.3. Interaction of AKAPs with PKA regulatory domains. *Panel A.* AKAPs interact with the first 30 amino acids of the N-terminus of the PKA RII regulatory subunits. These residues also promote dimerisation of the RII subunits, which is a prerequisite for binding to AKAP. Each regulatory subunit of PKA interacts with a catalytic subunit. Upon binding two molecules of cAMP a conformational change of the regulatory subunit causes dissociation of the catalytic subunits. *Panel B.* The targeting domain of AKAPs determines the localisation at discrete subcellular compartments.



PDE Family	Regulatory Module	Nucleotide Specificity
1	Ca ⁺⁺ /Calmodulin	cAMP/cGMP
2	cGMP/GAF	cAMP/cGMP
3		cAMP
4	UCR1/UCR2	cAMP
5	cGMP/GAF	cGMP
6	cGMP/GAF	cGMP
7		cAMP
8	PAS/PAC	cAMP
9		cGMP
10	GAF	cAMP/cGMP
11	GAF	cAMP/cGMP

Figure 1.4. Mammalian PDE isozyme families. The table summarises the current classification of PDEs into 11 isoenzyme families. This classification is based primarily on sequence homology however different enzyme families often display distinctive pharmacological and biochemical properties such as substrate preference and mode of regulation. The name of the regulatory module is indicated and binding to these areas determines catalytic domain affinity and enzymic activity of the isoform.

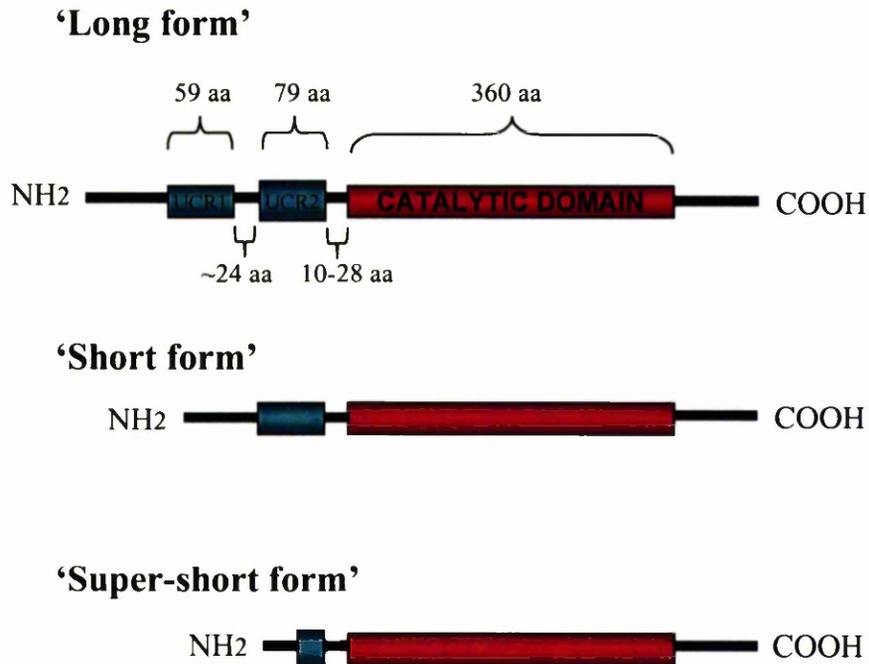


Figure 1.5. Splice variation of PDE4 isoforms. The diversification of a PDE family is brought about by splice variation of the protein. All PDE4 isoforms contain a catalytic domain: a region of approximately 360 amino acids (aa) near the C-terminus. In the ‘long-form’ PDE4 isoforms, this is joined to the 79 aa upstream conserved region 2 (UCR2) through the linker region 2 (LR2), which consists of 10-28 aa depending on the PDE4 family. The UCR2 is joined to the 59 aa of the upstream conserved region 1 (UCR1) by the 24 aa linker region 1 (LR1). The ‘short form’ PDE4 isoforms are spliced within the LR1 region and therefore lack the UCR1. ‘Super-short’ PDE4 isoforms are further truncated and lack the UCR1, LR1 and the N-terminal portion of the UCR2 domain.

1 50
er s...s..... .g.....p khlwrqprtp iriqqrgysd
 A MEPPTVPSEr SLsLSLPGPr EGQATLKPPP QHLWRQPRTp IRIQQRGYSd
 BMKKSR SVMTVMADDN VKDYFECSLS KSYSSSSNTL GIDLWRGRRC
 C .MENLGVGEG AEACSRLSRs RGRHSMTRAP KHLWRQPRRp IRIQQRfYSd
 D

51 100
a.....ar. .d.s.....swp.s. .t...s...
 A SAERAERERQ PhRPIERADA MDTSDRPGLR TTRMSWPSSf HGTGTGSGGA
 B CSGNLQLPPL SQrQSERART PEGDG..... ...ISRPTTL PLTTLPSIAI
 C PDKSAG.....CRE RDLSPRPELR KSRLSWPVS.
 D

UCR1

101 150
 ...S.r.Fdv eNG..pSpGR spLDpqaSpG .Gl.l.A.fp .hSQRRESfL
 A GGGSSRRFEA ENGPTPSPGR SPLDSQASP. .GLVLHAG.A ATsQRRESfL
 B TTVSQECFDV ENG..PSPGR SPLDPQASSS AGLVLHATFP GHSQRRESfL
 C ...SCRRFDL ENGL..SCGR RALDPQSSPG LGRIMQAPVP .HSQRRESfL
 D RRHSWICFDV DNG..TSAGR SPLDPMTSPG SGLILQANF. VHSQRRESfL

UCR1

151 200
 YRSDSDYdLs PKaMSRNSSv aS..Hg.DlI VTPFAQVLAS LR.VR.Nfaa
 A YRSDSDYDMS PKTMSRNSSV TSEAHAEGLI VTPFAQVLAS LRSVRSNFSL
 B YRSDSDYDLS PKAMSRNSSL PSEQHGDDLI VTPFAQVLAS LRSVRNFTI
 C YRSDSDYELS PKAMSRNSSV ASDLHGEDMI VTPFAQVLAS LRTVRSNVAA
 D YRSDSDYDLS PKMSRNSSI ASDIHGDDLI VTPFAQVLAS LRTVRNFAA

LR1

UCR2

201 250
 Ltntlq...sn KrsP.gn.p. vnkatp.Eet yQkLA.ETLe ELDWCLdQLE
 A LTNVpV.PSN KRSPLGgPTP VCKATLSEET CQQLARETLe ELDWCLEQLe
 B LTNLHG.TSN KRSPAASQPP VSRVNPQEEs YQKLAMETLe ELDWCLDQLe
 C LARQQCLGAA KQGPVGNPSS SNQLPPAEDT GQKLALETLD ELDWCLDQLe
 D LTNLQDRAPS KRSPMCNQPS INKATITEEA YQKLASETLe ELDWCLDQLe

UCR2

251 300
 TlQT..SVSe MASnKFKRmL NRELTHLSEm SRSGNQVSEy ISnTFLDkQn
 A TMQTYRSVSE MASHKFKRML NRELTHLSEM SRSGNQVSEY ISTTFLDKQN
 B TIQTYRSVSE MASNKFKRML NRELTHLSEM SRSGNQVSEY ISNTFLDKQN
 C TLQTRHSVGE MASNKFKRIL NRELTHLSET SRSGNQVSEY ISRTFLDQQT
 D TLQTRHSVSE MASNKFKRML NRELTHLSEM SRSGNQVSEf ISNTFLDKQH

LR2

Catalytic

301 350
 eVEiPspTqk erekkk.p..qpMsqIs G.kkLmHsSs
 A EVEIPSPtMK EREKQAPRP RPSQPPPPV PHLQPMSQIT GLKKLMHSNS
 B DVEIPSPtQK DREKkkKQ..QLMTQIS GvKKLMHSSS
 C EVELPKVTAE EAP.....QPMSRIS GLHGLCHSAS
 D EVEIPSPtQK EKEKKKRp..MSQIS GvKKLMHSSS

Catalytic

351 400
 LnnssipRFg Vkt.qE..LA keLEdlNKWG Ln.F.vadys gnRpLTcImy
 A LNNSNIPRFg VKTDQEElla QELenLNkWG LNIFCVSDYA GGRSLTCIMY
 B LNNTSISRfG VNTENEDHLA KELEDLNkWG LNIFNVAGYS HNRPLTCIMY
 C LSSATVPRfG VQTDQEEQla KELEDtNkWG LDVfKVADVS GNRPLTAIf

401 .IFQERDLLK tFrIpvDTli TY..tLEdHY HadVAYHNSl HAADVaQSTH 450
 A MIFQERDLLK KFRIPVDTMV TYMLTLEDHY HADVAYHNSL HAADVlQSTH
 B AIFQERDLLK TFRISSDTFI TYMMTLEDHY HSDVAYHNSL HAADVAQSTH
 C SIFQERDLLK TFQIPADTLA TYLLMLEGHY HANVAYHNSL HAADVAQSTH
 D TIFQERDLLK TFKIPVDTLI TYMLTLEDHY HADVAYHNNI HAADVvQSTH

Catalytic

451 VLL.TPAL.A VFTDLEILAA .FA.AIHdVD HPGVSNQFLI NTNSelALMY 500
 A VLLATPALDA VFTDLEILAA LFAAAIHdVD HPGVSNQFLI NTNSelALMY
 B VLLSTPALDA VFTDLEILAA IFAAAIHDVD HPGVSNQFLI NTNSelALMY
 C VLLATPALEA VFTDLEILAA LFASAIHDVD HPGVSNQFLI NTNSDVALMY
 D VLLSTPALEA VFTDLEILAA IFASAIHDVD HPGVSNQFLI NTNSelALMY

Catalytic

501 NDeSVLENHH LAVGFkLLQe enCDIFqNL. kkQRqsLRkM ViDmVLATDM 550
 A NDeSVLENHH LAVGFkLLQE DNCDIFQNLs KRQRQSLRkM ViDMVLATDM
 B NDeSVLENHH LAVGFkLLQE EHCDIFMNLt KKQRQTLRkM ViDMVLATDM
 C NDASVLENHH LAVGFkLLQA ENCDIFQNLs AKQRSLRRM ViDMVLATDM
 D NDSSVLENHH LAVGFkLLQE ENCDIFQNLt KKQRQSLRkM ViDIVLATDM

Catalytic

551 SKHMnLLADL KTMVETkKVT SsGVLLLDNY sDRIOVL.Nm VHCADLSNPT 600
 A SKHMTLLADL KTMVETkKVT SSGVLLLDNY SDRIOVLRNM VHCADLSNPT
 B SKHMSLLADL KTMVETkKVT SSGVLLLDNY TDRIQVLRNM VHCADLSNPT
 C SKHMnLLADL KTMVETkKVT SLGVLLLDNY SDRIOVLQNL VHCADLSNPT
 D SKHMnLLADL KTMVETkKVT SSGVLLLDNY SDRIOVLQNM VHCADLSNPT

Catalytic

601 KpLeLYRQWT DRIM.EFFqQ GDrERErGme ISPMCDKhtA SVEKSQVGF I 650
 A KPLELYRQWT DRIMAEFFQq GDRERERGME ISPMCDKHTA SVEKSQVGF I
 B KSLELYRQWT DRIMEEFFQq GDKERERGME ISPMCDKHTA SVEKSQVGF I
 C KPLPLYRQWT DRIMAEFFQq GDRERESGLD ISPMCDKHTA SVEKSQVGF I
 D KPLQLYRQWT DRIMEEFFRQ GDRERERGME ISPMCDKHNA SVEKSQVGF I

Catalytic

651 DYIvHPLWET WADLVHPDAQ diLDTLEDNR eWYqS.IpqS PSpppdee.r 700
 A DYIVHPLWET WADLVHPDAQ EILDtLEDNR DWYYSAIRQS PSPPPEEESR
 B DYIVHPLWET WADLVQPDQA DILDtLEDNR NWYQSMIPQS PSPPLDEQNR
 C DYIAHPLWET WADLVHPDAQ DLLDtLEDNR EWYQSKI PRS PSDLTNPERD
 D DYIVHPLWET WADLVHPDAQ DILDtLEDNR EWYQSTIPQS PSPAPDDPEE

Catalytic

701 ..g.qgIp.k FQFELTLee eeed.e.... ..k...e.. 750
 A GPGHPPLPDK FQFELTLeee EEEEISMAQI PCTAQEALTA QGLSGVEEAL
 B ..DCQGLMEK FQFELTLDEE DSEGPE.... ..KEG....
 C G.....PDR FQFELTLeea EEEDEE.... ..EEE
 D ..GRQqTEK FQFELTLeeD GESDTE.... ..KDSGSQV

751 eg...sask .l...d.e.. e..le.d.e. .l.....s. ..a..... 800
 A DATIAWEASP AQESLEVMAQ EASLEAELEA VYLTQQAQST GSAPVAPDEF
 B EGHsYFSSTK TLCVIDPENR DSLGETDID. .IATEDKSP VDT.....
 C EGEETALAKE ALELPDTELL SPEAGDPGD LPLDNQRT..

```

801                                     850
.....
A SSREEFVVAV SHSSPSALAL QSPLLPAWRT LSVSEHAPGL PGLPSTAAEV
B .....
C .....
D PDT.....

      851                                     890
.....
A EAQREHQAAK RACSACAGTF GEDTSALPAP GGGGSGGDPT
B .....
C .....
D .....

```

Figure 1.6. Alignment of the deduced amino acid sequences of cDNAs for the human PDE4 families. The figure shows an alignment, made using the GCG PILEUP multiple alignment software, of the PDE4 isoforms HSPDE4A4, HSPDE4B1, HSPDE4C1 and HSPDE4D3. The regions of sequence coloured in green are regions conserved between all PDE4 isoforms. These are UCR1 (residues 141-200 in HSPDE4A4B), UCR2 (residues 224-302 in HSPDE4A4B) and the catalytic region (residues 332-688 in HSPDE4A4B). The positions of LR1 (residues 201-223 in HSPDE4A4B) and LR2 region (residues 303-331 in HSPDE4A4B) are also shown.

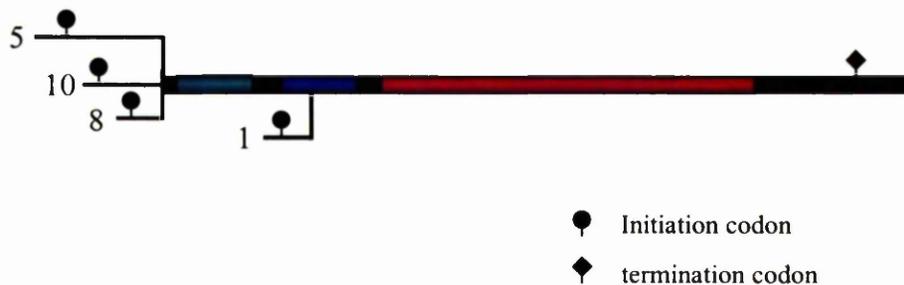


Figure 1.7. Structure of mRNA transcripts from the rat PDE4A gene. The numbers indicate the structure of the following PDE4A mRNA transcripts: 5, PDE4A5; 10, PDE4A10; 8, PDE4A8; 1, PDE4A1. The red bar indicates the catalytic region, the green bar represents upstream conserved region 1 (UCR1) and the blue bar represents upstream conserved region 1 (UCR2) sequences. Regions of alternatively spliced sequence that are unique to each splice variant are shown as thin bars.

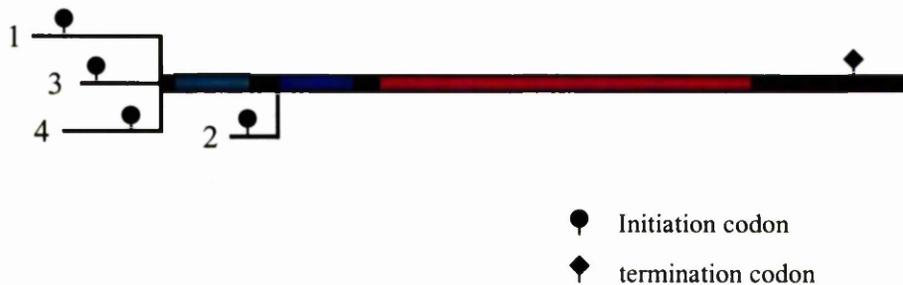


Figure 1.8. Structure of mRNA transcripts from the PDE4B gene. The numbers indicate the structure of the following PDE4B mRNA transcripts: 1, PDE4B1; 2, PDE4B2; 3, PDE4B3; 4, PDE4B4. The red bar indicates the catalytic region, the green bar represents upstream conserved region 1 (UCR1) and the blue bar represents upstream conserved region 2 (UCR2) sequences. Regions of alternatively spliced sequence that are unique to each splice variant are shown as thin bars.

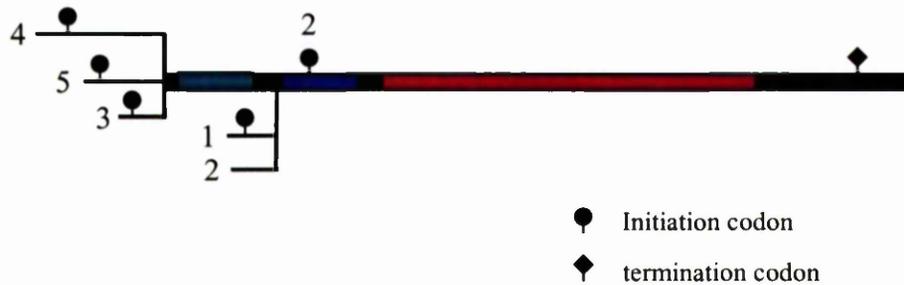


Figure 1.9. Structure of mRNA transcripts from the PDE4D gene. The numbers indicate the structure of the following PDE4D mRNA transcripts: 1, PDE4D1; 2, PDE4D2; 3, PDE4D3; 4, PDE4D4; 5, PDE4D5. The red bar indicates the catalytic region, the green bar represents upstream conserved region 1 (UCR1) and the blue bar represents UCR2. Regions of alternatively spliced sequence that are unique to each splice variant are shown as thin bars.

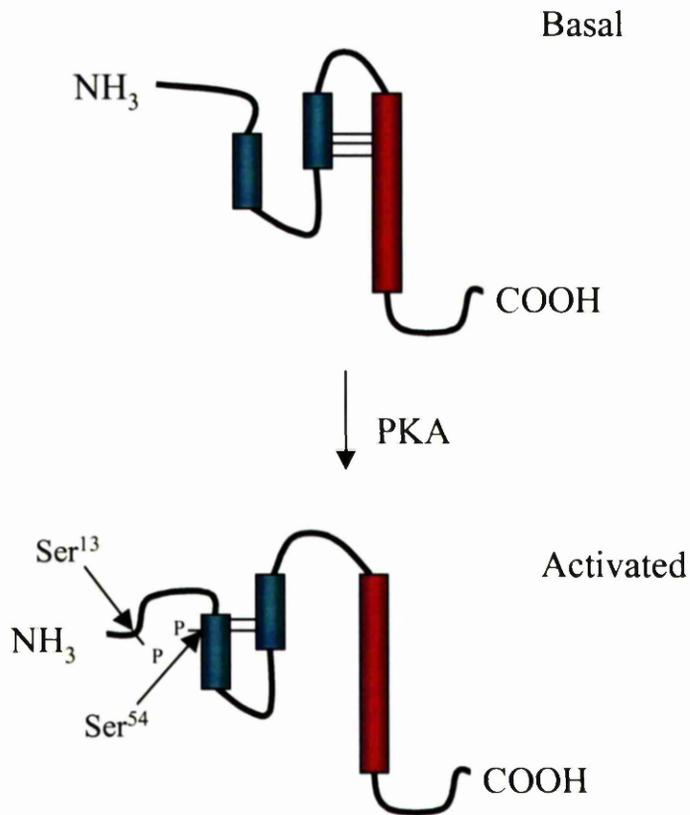


Figure 1.10. Postulated mechanism of 'long form' PDE activation upon PKA phosphorylation. Long form PDE4 isoforms impose inhibition of cAMP specific activity by the interaction of the N-terminus of the UCR2 domain forming weak interactions with the catalytic domain of the protein. Upon PKA phosphorylation of the Ser¹³ and Ser⁵⁴ residues a conformational change of the PDE is induced through an increase in the affinity of the N-terminus of UCR1 for the C-terminus of UCR2. This relieves the UCR2 mediated inhibition on the catalytic domain and PDE activity is increased.

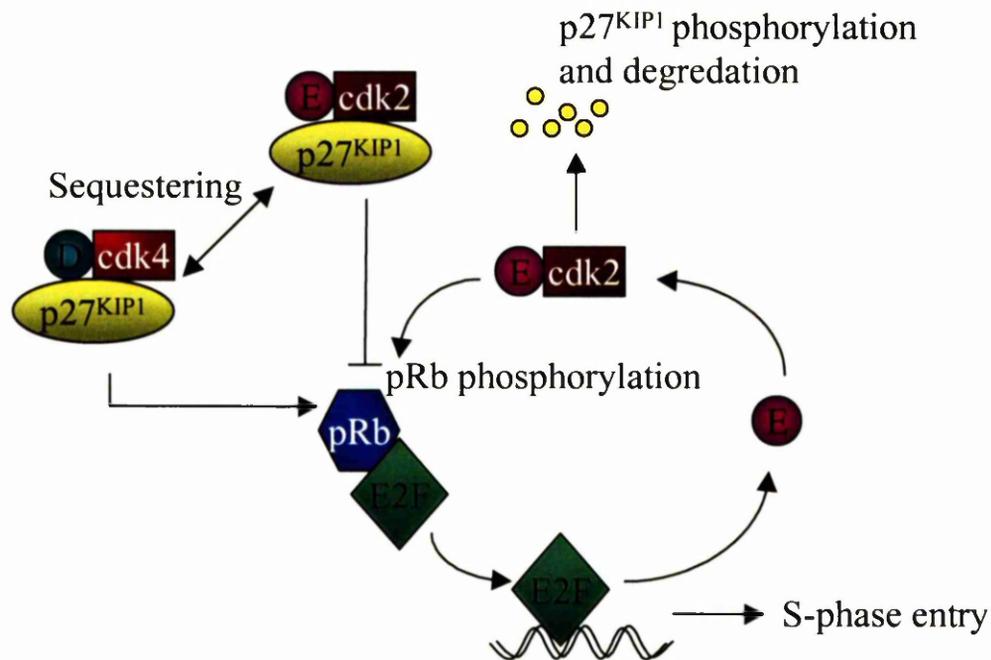


Figure 1.11. Regulation of G1/S transition. Mitogenic signals promote the assembly of the active cyclin D/cdk4 complexes, with p27^{KIP1} at the start of G1 phase. The sequestering of p27^{KIP1} facilitates activation of the cyclin E/cdk2 complex later in G1 phase. Both active complexes phosphorylate pRb, repressing its ability to bind the E2F transcription factors and allowing the initiation of transcription of proteins required for entry into S phase. Cyclin E/cdk2 antagonises the p27^{KIP1} mediated inhibition of the complex by phosphorylating it which targets the inhibitor for proteasome mediated degradation in effect positively regulating its own activity.

Adenylate Cyclase Isoform	Activators	Inhibitors
I	Gs α , forskolin, Ca ²⁺ /Calmodulin	Gi α , G $\beta\gamma$, Adenine nucleoside 3' polyphosphates
II	Gs α , forskolin, G $\beta\gamma$, PKC	Adenine nucleoside 3' polyphosphates
III	Gs α , forskolin, Ca ²⁺ /Calmodulin	CaM kinase II, Adenine nucleoside 3' polyphosphates
IV	Gs α , forskolin, G $\beta\gamma$	Adenine nucleoside 3' polyphosphates
V	Gs α , forskolin, PKC & ζ	Gi α , Ca ²⁺ , PKA, G $\beta\gamma$, Adenine nucleoside 3' polyphosphates
VI	Gs α , forskolin	Gi α , Ca ²⁺ , PKA, PKC, Adenine nucleoside 3' polyphosphates
VII	Gs α , forskolin, G $\beta\gamma$, PKC	Adenine nucleoside 3' polyphosphates
VIII	Gs α , forskolin, Ca ²⁺ /Calmodulin	Adenine nucleoside 3' polyphosphates
IX	Gs α	Calcineurin, Adenine nucleoside 3' polyphosphates

Table 1.1. Effectors which modulate adenylate cyclase isoform activity. The table summarises the modes of regulation of each adenylate cyclase isoform. The abbreviations are PKA; cAMP dependent protein kinase; PKC, protein kinase C and Camkinase II, Calmodulin dependent kinase type II.

Chapter 2

Materials and methods

47
Except where stated biochemicals were obtained either from Fisons or from Sigma-Aldrich and were of analytical grade.

2.1. Mammalian cell culture

2.1.1. Maintenance of cell lines

2.1.1.1. Rat-1 cell line

Rat-1 fibroblasts, a rat embryo fibroblast derived cell line, were maintained in Dulbecco's Modified Eagle's Medium (DMEM, Sigma) supplemented with 2 mM Glutamine, 10 % foetal bovine serum (FBS) and penicillin/streptomycin (100 units/ml) at 37 °C in an atmosphere of 5 % CO₂. Cells were passaged at 90 % confluency, where they were split 1:5. This was done by rinsing the cells with pre-warmed phosphate buffered saline (PBS), to which 1 -2 ml 0.25 % trypsin/0.03 % EDTA solution was added. The flasks were incubated at room temperature until the cells detached. 10 ml fresh culture medium was added and the cells were collected by centrifugation at 1000 rpm for 3 min in the MSE Mistral 1000 swinging bucket centrifuge. The cells were then resuspended in fresh culture media and dispensed into new culture flasks at approximately 10⁵ cells/ml final volume.

2.1.1.2. HeLa cell line

The HeLa cell line (ATCC CCL 2), a cervical carcinoma cell line with epithelial like morphology (Puck et al., 1972), was maintained in Minimum Essential Media (MEM, Sigma) supplemented with 10 % FBS at 37 °C in an atmosphere of 5 % CO₂. The HeLa cells were passaged as the Rat-1 fibroblasts.

2.1.1.3. SK-N-SH cell line

The SK-N-SH cell line (ATCC HTB 11), a human neuroblastoma derived cell line, with neuroblast or epithelial morphology (Biedler et al., 1973), were maintained and passaged in the same manner as the Rat-1 fibroblasts.

2.1.1.4. COS-1 and COS-7 cell lines

The COS-1 and COS-7 cells lines (ATCC CRL 1650 and CRL 1651 respectively, (Gluzman, 1981), are both African green monkey kidney derived cell lines, transformed

with the SV40 virus, which have a fibroblast morphology. The cells were maintained and passaged as the Rat-1 fibroblast cell line.

2.1.1.5. *HuT-78, Molt-3 and Jurkat J6 cell lines*

The cutaneous lymphoma T-cell line, HuT-78 (ATCC TIB 161) and the human leukaemic T cell lines: Jurkat J6 (ATCC BS TCL 110, Kaplan et al., 1988) and Molt-3 (ECACC 90021901, Minowada et al., 1972) were grown in suspension, maintained in RPMI 1640 media, supplemented with 10 % FBS, 2 mM Glutamine and penicillin/streptomycin (100 units/ml) at 37 °C in an atmosphere of 5 % CO₂. The T cell lines were maintained at a cell density between 1 x 10⁶ and 5 x 10⁷ cells/ml. The cells were collected by centrifugation at 1000 rpm for 3 min (MSE mistral 1000 swinging bucket centrifuge) and resuspended in fresh culture media. Cells at a concentration of 10⁵ cells/ml were used to seed fresh culture flasks.

2.1.1.6 *HEK-293, U118 MG, FTC113 and U937 cell lines*

The human embryonic kidney cell line, HEK-293 (ATCC CRL 1573, Harrison et al., 1977), which has an epithelial cell morphology and the U-118 MG cells (ATCC Number: HTB-15), which are a human glioblastoma cell line, were maintained and sub-cultured as the Rat-1 cells. The human follicular thyroid carcinoma cell lines FTC133 (Wright et al., 1991) and the U937 human monocyte-like cells derived from a lymphoma (ATCC Number: CRL-1593.2, Sundstrom and Nilsson, 1976) were maintained and cultured in RPMI 1640 supplemented with 10 % FBS, 2 mM Glutamine and penicillin/streptomycin (100 units/ml), as the T cell lines (see section 2.1.1.5).

2.1.2. *DEAE-Dextran transient transfection*

Cells were passaged the day prior to transfection and allowed to grow to 50 -70 % confluency. 10 µg plasmid DNA was diluted to 250 µl with sterile Tris-EDTA (TE) buffer (1 mM Ethylenediaminetetra-acetic acid (EDTA), 10 mM Tris/HCl, pH7.5) in a sterile 15 ml centrifuge tube, to which 200 µl sterile DEAE Dextran (10 mg/ml in PBS) was added, mixed and incubated at room temperature for 15 min. 10 ml of DMEM cell culture media, supplemented with 10 % Newborn Calf Serum (NCS) and 2 mM Glutamine penicillin/streptomycin (100 units/ml) was added to the DNA along with 10 µl filter sterilised 100 mM chloroquine. The solution was mixed and added to the monolayer of cells which were then incubated at 37 °C in an atmosphere of 5 % CO₂ for 3 -4 h before

the media was removed and replaced with 10 ml sterile PBS supplemented with 10 % DMSO. This was incubated on the cells at room temperature for 2 -3 min, the cells were then washed twice with PBS and fresh cell culture media was added back to the cells. The transfected cells were incubated at 37 °C in an atmosphere of 5 % CO₂ for 24 -48 h prior to harvest of the expressed recombinant protein.

2.1.3. LipofectAMINE™ transfection of HeLa cells

Transfection of HeLa cells was carried out utilising lipofectAMINE™ reagent (GibcoBRL). Cells were passaged the day prior to transfection into 100 mm dishes, and grown to approximately 50 % confluency. 7.5 µg plasmid DNA was diluted to a total volume of 300 µl with Optimem I media (Gibco BRL) in a sterile 15 ml centrifuge tube and mixed. Into a fresh 15 ml centrifuge tube 30 µl lipofectAMINE™ was diluted with 270 µl Optimem I media and this solution was mixed and added, in a dropwise fashion, to the DNA solution whilst the tube was agitated. Once all the lipofectAMINE™ solution had been added to the DNA containing solution the tube was incubated at room temperature for 30 min. Prior to the addition of the DNA/lipofectAMINE™ solution to the monolayer of cells they were washed twice in 5 ml Optimem I media. 3.4 ml Optimem I media was added to the DNA/lipofectAMINE™ solution, which was mixed and transferred to the washed cell monolayer. The cells were harvested 18 -24 h post-transfection.

2.1.4. Cell cycle arrest

To isolate Rat-1 fibroblast cells at different specific phases of the cell cycle cells the cells were subject to several different treatments. The optimisation of isolation of cells in specific phases of the cell cycle is explained in detail in section 3.3.2.

2.1.4.1. Asynchronous cell isolation

Rat-1 cells were seeded into 100 mm dishes at a density of 10⁶ cells/ml and incubated overnight in 10 ml cell culture media (DMEM, 10 % FBS, 2 mM glutamine, penicillin/streptomycin (100 units/ml)) and maintained at 37 °C in an atmosphere of 5 % CO₂. The cells, after 24 h growth, were asynchronous and either manipulated further or harvested.

2.1.4.2. G0 phase arrest

Cells were seeded and incubated overnight as in 2.1.4.1., and then washed twice in PBS. The cell culture media was replaced with 10 ml serum free media (DMEM, 2 % Glutamine, penicillin/streptomycin (100 units/ml)) and the cells were incubated at 37 °C in an atmosphere of 5 % CO₂ for 48 h, prior to their harvest.

2.1.4.3. G1/ S phase arrest

Cells were seeded and incubated overnight as in 2.1.4.1., after which 2 mM thymidine, dissolved in DMSO, was added to the media for a 16 h incubation at 37 °C in an atmosphere of 5 % CO₂. The cells were then washed twice with PBS and fresh media without thymidine was added to the cells for 14 h incubation. A further thymidine block was then carried out by the addition of 2 mM thymidine to the cells for a 16 h incubation, prior to their harvest.

2.1.4.4. S / G2 phase arrest

Cells were seeded and incubated overnight as in 2.1.4.1., after which time 2.5 mg/ml aphidicolin, dissolved in DMSO, was added to the culture media for a 24 h incubation at 37 °C in an atmosphere of 5 % CO₂. The cells were then either harvested after the 24 h to obtain cells isolated in early S phase or, alternatively, the S phase arrested cells were washed twice with pre-warmed PBS and fresh culture media added for a 4 h incubation at 37 °C in an atmosphere of 5 % CO₂ to isolate cells in early G2 phase.

2.1.4.5 Mitotic arrest

Cells were seeded and incubated overnight as in 2.1.4.1., after which time 50 ng/ml nocodazole, dissolved in DMSO, was added to the media for a 14 h incubation at 37 °C in an atmosphere of 5 % CO₂. The cells harvested after this time were isolated in M phase. Alternatively, after nocodazole incubation cells were washed twice with pre-warmed PBS and fresh cell culture media added for up to two hours to isolate cells moving through the latter phases of mitosis into G1.

2.2. Analysis of cells in the cell cycle

2.2.1. Propidium iodide (PI) double stranded DNA staining

Cells, once isolated at specific cell cycle phases (section 2.1.4), were washed with 5 ml PBS and removed from the plate by incubation with 1 ml 0.2 % Trypsin / 0.03 % EDTA solution for 2 min. The plates were agitated to dislodge all cells, which were then suspended in 5 ml culture media prior to collection by centrifugation at 1000 g for 3 minutes (MSE Mistral 1000 swinging bucket centrifuge). The cells were then washed with 5 ml ice-cold PBS and after collection were re-suspended in 5 ml ice-cold 0.1 % Saponin / 0.5 % BSA in PBS (Eylar et al., 1994), collected by centrifugation and drained before being re-suspended in 0.5 ml Propidium Iodide (100 µg/ml)/100 U/ml RNase A (Gibco). The cells were transferred to 10 cm² FACs analysis tube, wrapped in foil for protection against light and incubated at 37 °C for 30 minutes, after which time they were analysed by flow cytometry on the Becton Dickinson FACScan.

2.2.2. FACs analysis of PI stained cells

The settings of the FACscan were controlled using the CELLQuest software package on the Apple Macintosh computer attached to the Becton Dickinson FACScan. Forward scatter (FSC) was left on the default setting (E00), Side scatter (SSC) adjusted to 288 volts, FL2-H (Propidium iodide detection channel) set to about 535 volts, and all other settings left as default. 20000 cells were collected for analysis and analysis settings on the FL2-H channel altered to maintain a peak of G1 cells at 200 -300 amps and G2/M peak at 400 - 600 amps on a histogram of FL2-H vs counts (*Fig. 2.1.*).

2.2.3. Labelling cells for dual PI and bromo-deoxyuridine (BrdU) DNA analysis

2.2.3.1. Incorporating BrdU to proliferating cells

Cells were seeded into 75 cm² flasks at a density of 10⁵ cells/ml in 15 ml cell culture media and grown for at least 24 h at 37 °C in an atmosphere of 5 % CO₂, to enable asynchronous cell populations to establish. The flasks were wrapped in silver foil to prevent light exposure to the cells prior to the addition of 15 µl of 10 mM bromo-deoxyuridine (BrdU) dissolved in DMSO. BrdU is photogenically unstable, causing mutations in the cellular DNA which leads to S phase arrest, therefore any manipulations of cells after BrdU

addition were carried out in reduced lighting conditions. The cells were incubated in the presence of BrdU at 37 °C in an atmosphere of 5 % CO₂ for 30 min, they were then washed three times with pre-warmed PBS. Fresh cell culture media was added to the cells, which were treated as required prior to harvesting.

2.2.3.2. Fixing BrdU labelled cells

Cells, after the incorporation of BrdU as described in 2.2.3.1., were harvested by incubation with 0.25 % Trypsin/ 0.03 % EDTA until they detached from the flask. The cells were suspended in cell culture media and collected by centrifugation at 1000 rpm for 3 min (MSE Mistral 1000 swinging bucket centrifuge), they were then washed once with ice-cold PBS and collected by centrifugation. The cells were fixed by resuspending the cell pellet in 100 µl PBS, to which 1 ml ice-cold 70 % ethanol was added in a dropwise fashion, whilst vortexing. The cells were kept on ice for at least 1 hour to fix or at 4 °C for longer periods prior to further staining.

2.2.3.3. Staining BrdU labelled cells with FITC conjugated antibody and propidium iodide

After fixing the BrdU labelled cells were collected by centrifugation at 1000 g for 3 min (MSE Mistral 1000 swinging bucket centrifuge) and the ethanol aspirated from them. The cells were resuspended in 500 µl 0.5 M NaCl, to which 500 µl 4 N HCl was added whilst vortexing. The cells were incubated at room temperature for 15 min, after which time the cells were collected by centrifugation, and then washed three times in 1 ml PBT (0.5 % BSA/ 0.1 % Tween-20 in PBS) to remove the acid. The cells were then resuspended in 100 µl PBT, to which 20 µl anti-BrdU-FITC conjugated antibody (Becton Dickinson) was added and incubated for 30 min, protected from light, at room temperature. 1 ml PBT was added to the cells whilst vortexing and the cells were then collected by centrifugation, 1000 rpm for 3 min. The cell pellet was resuspended in 500 µl 5 ng/ml PI and incubated at 4 °C for at least 30 min prior to FACs analysis.

2.2.4. FACs analysis of BrdU-FITC and PI stained cells

The Becton Dickinson FACScalibur was used for the analysis of the BrdU-FITC/PI stained cells, using the CELLQuest software on the attached Apple Macintosh computer. FACs analysis enabled a quantitative measurement of the parameters of interest to be carried out. The PI which intercalated with the double stranded DNA was detected in the second

channel (FL2-H) at around 600 volts and cells labelled with the FITC conjugated anti-BrdU antibody were excited and detected in the first channel (FL1-H) at around 500 volts. 20000 cells were collected for analysis.

2.2.4.1. FACScalibur acquisition settings

A histogram of FL2-H vs counts was drawn that gave a normal DNA distribution enabling the determination of G0/1, S and G2/M phase cells. The FL2 amps were balanced so the peak of G0 cells was around 300 -400 on the linear scale for FL2-H (*Fig. 2.1.*). Doublet discrimination was carried out to verify that all the cells being analysed were single cells. This was done by gating out any aneuploid cells, which had increased or decreased fluorescence pulse width, which is measured as the length of time the cell breaks the laser beam as it passes through. On a density plot of FL2-H vs FL2-W the clumps of cells were those which fell outside the G2/M population, which was 600 -800 on the FL2-H channel. Similarly apoptotic cells and cell debris were removed from analysis on the same density plot by gating out particles with a small pulse width, typically those less than 300-400 on the FL2-H (*Fig. 2.2.*). A histogram of FL1-H vs counts enabled the FL1 amps to be balanced to maintain a peak of cells at 10^1 , which correspond to the G1 peak of cells. A shoulder on this G1 peak corresponded to cells in G2/M and the peak at 10^2 related to S phase cells (*Fig. 2.3.*).

2.2.4.2. FACs data analysis

Once acquired the cell distribution data was analysed further using the MODfit™ analysis software package. This works by breaking down the acquisition plots and using compensation for over lapping peaks of cellular distribution in the phases of the cell cycle, detected by flow cytometry, enabling a better approximation of the number of cells in each phase of the cell cycle. To carry out this analysis in MODfit™ the plot of FL2-W vs FL2-H was gated around the diploid cell population. This gated population was then analysed on an FL2-H vs FL1-H plot and the cells in S-phase gated (*Fig. 2.4. Panel A*). The computer then required the sample model of the cells being analysed to be stipulated (fresh, diploid cells with a distinct G2/M and no clumps of cells) and the peaks on the histogram relating to the G1 and G2/M population estimated and highlighted (*Fig. 2.4. Panel B*). The MODfit™ package then calculates the number of cells in each phase of the cell cycle as a percentage of the total number of single cells detected.

2.2.5. Apoptotic analysis of cells

2.2.5.1. Labelling cells for apoptotic analysis

Control cells were seeded into 2 flasks, one was maintained as asynchronous and one was treated with the apoptosis inducing agent, staurosporine, for 24 h (Fraker et al., 1995). All cells were harvested by the addition of 0.25 % trypsin/ 0.03 % EDTA solution and once detached from the cell culture flask they were suspended in 5 ml cell culture media and collected by centrifugation at 1000 rpm for 3 min (MSE Mistral 1000 swinging bucket centrifuge). The cells were washed twice in ice-cold PBS, drained well and resuspended in 500 μ l binding buffer (10 mM HEPES, pH7.4, 140 mM NaCl, 2.5 mM CaCl₂). 100 μ l of the cell suspension was transferred to a 10 cm² FACs tube wrapped in foil. The asynchronous control cells were treated in the following manner: To one tube 10 μ l 50 μ g/ml PI was added, to one tube 5 μ l fluorescein conjugated annexin V (annexin V-FITC) antibody was added and to the final tube nothing was added. All cells for apoptotic analysis were double stained with 10 μ l annexin V-FITC antibody and 10 μ l 50 μ g/ml PI, the staurosporine treated cells provided a positive control for apoptosis.

2.2.5.2. FACs analysis of apoptotic cells

The settings of the FL1-H and FL2-H channels were determined in each experiment by analysing the distribution of the control cells on an acquisition FL2-H vs FL1-H dot-plot. 20000 cells were collected in each analysis and the cells should fall in the following quadrants of the dot blot:

FL1-H	UL	UR
	LL	LR
	FL2-H	

For the control cells the unstained cells were found only in the lower left (LL) quadrant and the PI only stained cells were found in the LL & lower right (LR) quadrants. The FL2-H amps were altered to isolate cells exclusively in these areas with LR representing the apoptotic cells. The annexin V-FITC conjugated stained cells were found in the LL and upper left (UL) quadrants, with the FL1-H amps altered to isolate cells exclusively in these areas, the cells in the UL were apoptotic. The staurosporine treated dual labelled cells were isolated in the upper right (UR) quadrant, by alterations in FL1-H and FL2-H amps, as all these cells are apoptotic. All cells analysed for apoptosis were found within LL and UR

quadrants, determining the proportion of cells that are non-apoptotic and apoptotic in the population.

2.3. Protein analysis

2.3.1. Harvesting cell lysate

2.3.1.1. Whole cell lysate production

Cells were harvested at reduced temperatures to minimise the effect of protein degradation and enzyme inactivation caused by the disruption of the cell. The cell culture dishes were maintained on ice and all buffers used in the procedures were chilled. The cell culture media was removed from cells, which were washed twice with 5 ml ice-cold PBS. The cells were then drained thoroughly and 200 µl/100 mm dish 3T3-lysis buffer (20 mM N-2-Hydroxyethylpiperazine-N'-2-ethanesulfonic acid (HEPES), pH7.4, 50 mM NaCl, 50 mM NaF, 10 % glycerol, 1 % triton X-100, 10 mM Ethyleneglycol-bis(P-aminoethylether)-N,N,N',N'-Tetra-acetic acid (EGTA), 30 mM sodium pyrophosphate, proteases inhibitor cocktail) was added. The cells were scraped from the plate, placed into a 1.5 ml eppendorf and subjected to a 20 min incubation at 4 °C with end-over-end rotation. The cell lysate was clarified by centrifugation at 10000 g at 4 °C (Heraeus bench-top centrifuge) for 5 min, the supernatant was removed, aliquoted and snap frozen and stored at -80 °C until required.

2.3.1.2. Crude sub-cellular fractionation by differential centrifugation

Cells were harvested at reduced temperatures to minimise the effect of protein degradation and inactivation caused by the disruption of the cell. The cell culture dishes were maintained on ice and all buffers used in the procedures were chilled. The cell culture media was removed from cells which were washed once with 5 ml ice-cold PBS and then drained well. The cells were then incubated with 500 µl/100 mm dish ice-cold cKHEM (50 mM HEPES KOH, pH7.4, 50 mM KCl, 10 mM EGTA, 1.92 mM MgCl₂ supplemented with 1 mM dithiothreitol (DTT) and protease inhibitors) on ice for 5 min. The cells were drained thoroughly and scraped into a 1.5 ml eppendorf and diluted to a known volume with cKHEM. The cells were drawn through a 13 gauge needle 30 times whilst on ice and the unbroken cells and nuclei removed (P1 fraction) by centrifugation at 2000 g, 4 °C for 7 minutes (Heraeus refrigerated bench-top centrifuge). The supernatant was maintained and the resultant pellet was washed twice in cKHEM and resuspended in the same volume of

cKHEM as the supernatant. The supernatant was centrifuged at 75000 g, 4 °C for 45 min (Beckman TL-100 ultracentrifuge) producing the supernatant fraction (S fraction), enriched in cytosolic proteins, and the remaining pellet (P2 fraction), enriched in plasma membrane, vesicles formed from the Golgi apparatus and the endoplasmic reticulum, lysosomes and endosomes. The P2 was washed with cKHEM to remove any contaminating cytosolic proteins and resuspended in the same volume of cKHEM as the P1 and S fraction. Each fraction was aliquoted, snap frozen and stored at –80 °C for later use.

2.2.1.3. *Refined sub-cellular fractionation by differential centrifugation*

Cells were harvested after appropriate treatment at reduced temperatures to minimise the effect of protein degradation and inactivation caused by the disruption of the cell. The cell culture dishes were maintained on ice and all buffers used in the procedures were chilled. The cell culture media was removed from cells that were washed twice with 5 ml ice-cold sucrose solution (250 mM Sucrose, 10 mM triethanolamine-acetic acid, pH7.6, 1 mM EDTA, supplemented with protease inhibitors) and then drained well. The cells were scraped from the plate and transferred to a tight fitting douce homogeniser and the pestle raised and lowered 10 times. The unbroken cells, large sheets of plasma membrane and nuclei were collected by centrifugation at 1000 rpm at 4 °C for 10 min (Heraeus refrigerated bench-top centrifuge, N fraction). The pellet was washed twice in the sucrose buffer and the supernatant retained. The supernatant was subject to centrifugation at 13000 rpm at 4 °C for 15 min (Heraeus refrigerated bench-top centrifuge) in order to isolate the membranous fractions containing large cell organelles (M fraction) from the homogenate. The M fraction pellet was washed twice with the sucrose buffer and the supernatant retained for isolation of the microsomes- small vesicles and fragments of organelles. The supernatant was centrifuged at 75000 rpm at 4 °C for 60 min (Beckman TL-100 ultracentrifuge). The resultant microsome pellet was washed twice with the sucrose buffer and the supernatant enriched in cytosolic proteins was retained. Each fraction was aliquoted, snap frozen and stored at –80 °C until further use

2.3.2. *Quantification of protein (Bradford assay)*

Protein assays were carried out in 96 well microtitre plates. A spectrophotometric standard curve of protein concentration was produced using 0-5 µg bovine serum albumin (BSA), which was dissolved in 50 µl distilled water. The protein quantification of cell lysate was carried out by taking 10 µl of diluted lysate sample and placing in wells on the 96 well

microtitre plate to which 40 μ l distilled water was added, each sample was analysed in triplicate. Bio-Rad Bradford Assay reagent was diluted 1/5 with distilled water and 200 μ l added to each well occupied with protein samples. The 96 -well plate was then analysed using the Revelation package on the computer, connected to an MRX microtitre plate reader, which read absorbance at a wavelength of 590 nm. Protein concentrations were determined by plotting the standard curve and using least squared regression analysis to obtain the line of best fit. The equation of the line was used to determine the protein concentration of the samples.

2.3.3. Enzyme-linked immunosorbent assay

Concentration of specific protein within a cell lysate sample was quantified using enzyme-linked immunosorbent assay (ELISA) carried out in a 96 well microtitre plate (Huston et al., 1996). Lysates taken from cells were quantified for total protein concentration and between 0.4 and 50 μ g protein loaded into wells, in triplicate for each lysate. The samples were diluted to 100 μ l with bicarbonate buffer, pH 9.6 and incubated overnight at 4 °C. The wells were washed 3 times with TBS-tween20 (137 mM NaCl, 20 mM Tris/HCl pH7.4, 0.05 % Tween20) and blocked at room temperature for 2 h with 200 μ l 5 % skimmed milk powder/TBS-tween20. The wells were washed 3 times with TBS-tween20 and all residual solution removed, the primary antibody was diluted 1:2000 in 0.1 % skimmed milk powder /TBS-tween20 and 100 μ l added to each sample containing well for a 2 h incubation at room temperature. The plate was washed 3 times in TBS-tween20 and all residual solution removed. The secondary alkaline phosphatase conjugated anti-immunoglobulin (IgG) antibody raised against the primary antibody was diluted 1:30000 in 0.1 % skimmed milk powder/TBS-tween20 and 100 μ l added to each sample containing well for a 1 h incubation at room temperature. The wells were then washed a further 6 times in TBS-tween20 before the addition of substrate solution. Equal volumes of solution A and B of the BCIP Microwell phosphatase substrate system (Kirkegaard & Perry Laboratories) solutions were mixed and 100 μ l of the solution added to each well for a 30 - 60 min incubation at room temperature. To arrest the alkaline phosphatase catalysed reaction 100 μ l 2 % EDTA solution was added to each well and the absorbances of the solutions at a wavelength of 620 nm were measured by the Revelation software on the computer, connected to an MRX microtitre plate reader. The absorbances were then compared for each sample to determine changes in expression levels of the protein between them.

2.3.4. Lactate Dehydrogenase (LDH) assays

Sub-cellular fractionations were assayed for the lactate dehydrogenase (LDH) activity by the reverse reaction; Pyruvate + NADH \rightarrow Lactate + NAD. This kinetic enzymatic assay was carried out in 96 well microtitre plates and the conversion of NADH to NAD was measured spectrophotometrically using the MRX microtiter plate reader (Dynex Technologies), set at a wavelength of 340 nm. For each sample two sets of wells were set up in triplicate, the first set, measuring the free LDH, contained 186 μ l 150 mM Tris/HCl, pH7.4, 7 μ l 10 mM Na pyruvate and 7 μ l sample. To the second set of wells, used to measure occluded LDH, was added 172 μ l 150 mM Tris/HCl, pH7.4, 7 μ l 10 mM Na pyruvate, 14 μ l 30 % triton and 7 μ l sample. The reaction was started by the addition of 10 μ l 2 mM β -NADH and readings of the absorbance were taken at 20 sec intervals for 10 min. The initial rate of decrease in the absorbance at 340 nm was taken to be directly proportional to the LDH activity present in the sample.

2.3.5. SDS-poly-acrylamide gel electrophoresis (SDS-PAGE)

2.3.5.1. Sample preparation

Lysate obtained from cells were assayed for protein concentration and 25 –100 μ g protein diluted 1/5 with 5 x laemmli sample buffer (260 mM Tris/HCl (pH6.7), 55.5 % Glycerol, 8.8 % SDS, 0.007 % Bromophenol blue, 11.1 % 2-mercaptopethanol, Laemmli et al., 1970), which was made up to 150 μ l with 1x laemmli's sample buffer. The sample was boiled for 5-10 min to allow denaturation and reduction of the protein

2.3.5.2. Casting and running a tris-glycine gel

All gels were run on Bio-Rad Protean II xi cell unless otherwise stated. The apparatus was assembled according to the manufacturer's instructions. A resolving gel containing the appropriate percentage of acrylamide (determined by the molecular weight of the protein of interest), usually 8 % unless otherwise stated, was cast between the two plates of the gel apparatus (8 % 29:1 acrylamide:N,N'-methylenebisacrylamide mix, 375 mM Tris/HCl (pH8.8), 0.1 % SDS, 0.1 % Ammonium persulphate, 0.06 % N,N,N',N'-tetramethylethylenediamine (TEMED)). This was overlaid with 1 ml water and allowed to polymerise at room temperature, the water was then removed, a comb placed between the plates and the resolving gel overlaid with stacking gel (5 % 29 :1 acrylamide:N,N'-methylenebisacrylamide mix, 125 mM Tris/HCl (pH6.8), 0.1 % SDS, 0.1 % Ammonium

persulphate, 0.1 % TEMED). The gel was left for 30 min to polymerise, the comb was removed and the wells were washed out with tris-glycine running buffer (192 mM Glycine, 25 mM Tris, 0.15 % SDS) to remove un-polymerised acrylamide. The gels were then assembled onto the central running stand according to the manufacturer's instructions and placed into the running tank containing tris-glycine running buffer. The pre-boiled samples were loaded into each well and a standard lane was loaded with 10 µl Bio-Rad prestained broad range precision protein markers to determine protein migration weight by gel electrophoresis. The top reservoir of the gel running tank was filled with running buffer and run for approximately 5 h at 35 milliamps per gel or 16 h at 8 milliamps per gel, until the dye front reached the bottom of the gel.

2.3.6. Visualising protein by coomassie staining

Proteins were separated by gel electrophoresis as in 2.3.5., the gel was removed from the plates and washed with distilled water. The gel was placed in Coomassie stain (0.025 % Coomassie Brilliant Blue R250, 40 % methanol, 7 % acetic acid) with gentle shaking at room temperature for 30 min and then placed in destain (40 % methanol, 7 % acetic acid) overnight, to remove all background staining of the gel. The Coomassie stain remained bound to proteins to enable visualisation.

2.3.7. Visualising protein by silver staining

Greater sensitivity of detection of proteins on acrylamide gels than Coomassie staining was achieved by silver staining, the detection limit for which is 2-5 ng protein. The silver stain plus kit from Bio-Rad was used according to the manufacturer's instructions, briefly: The fixative enhancer solution (50 % methanol, 10 % acetic acid, 10 % fixative enhancer concentrate, 30 % dH₂O) was added to the gel and incubated for 20 min at room temperature with agitation. The gel was washed in dH₂O and then added to staining solution (10 % Silver complex solution, 10 % Reduction Moderator solution, 10 % image development reagent in water. Prior to addition to gel an equal volume of development Accelerator Solution was added for a 20 min incubation at room temperature with agitation. After the desired staining was reached the gel was transferred to 5 % acetic acid solution to stop the reaction.

2.3.8. Western immuno-blotting

Proteins were separated by gel electrophoresis as in 2.3.5., after which the protein was transferred to nitrocellulose before being detected with specific antibody.

2.3.8.1. Transfer of protein from acrylamide gel to nitrocellulose

Under transfer buffer (192 mM Glycine, 25 mM Tris, 20 % Methanol) in a transfer cassette a piece of foam soaked in transfer buffer, was overlaid with a piece of Whatmann 3 MM paper. Onto this was placed the SDS gel and overlaid with a piece of nitrocellulose paper (Schleicher & Schuell), ensuring that all air bubbles were excluded from between all layers. The nitrocellulose was in turn covered by another piece of Whatmann 3 MM paper and a piece of foam. The outer cassette was used to close and hold the apparatus which was placed with the nitrocellulose to the positive electrode in the Hoefer TE series transphor electrophoresis unit, filled with transfer buffer. The proteins were transferred with an applied current of 0.7 amps for 90-120 min or 0.05 amps overnight.

2.3.8.2. Immunoblotting nitrocellulose

Once the proteins had been transferred onto the nitrocellulose as in section 2.3.8.3. it was washed with distilled water followed by visualisation of the transferred proteins with ponceau S stain (0.1 % Ponceau S, 3 % Trichloroacetic acid). The ponceau S stain was added to the nitrocellulose for a few minutes until the protein became stained, the nitrocellulose membrane was then washed with 30 ml Tris-buffered saline (TBS-tween 20) (137 mM NaCl, 20 mM Tris/HCl (pH7.6), 0.1 % tween20) before immunological detection of protein. The unoccupied protein binding sites on the nitrocellulose were blocked with 5 % skimmed milk powder in TBS-tween20 for 1 h at room temperature with agitation. After blocking the membrane was washed several times in TBS-tween20 and the appropriate primary antibody added to the membrane diluted 1:10000 in 1 % skimmed milk powder in TBS-tween20. This incubation was carried out for 2 h with vigorous agitation, after which time the nitrocellulose was washed several times in TBS-tween20 before having the secondary antibody added to the membrane. The secondary antibody was a horse-radish peroxidase (HRP) conjugated anti-immunoglobulin (IgG) antibody, directed against the primary antibody, diluted 1:5000 in 1 % skimmed milk powder in TBS-tween20. This was incubated with the nitrocellulose membrane for 1 h with vigorous agitation, after which the nitrocellulose was washed several times in TBS-tween20 and then incubated with ECL reagents (Amersham), according to the manufacturers instructions. A piece of x-ray film

(Kodak) was exposed to the membrane in a darkroom for several minutes and then developed using a Kodak X-omat.

2.3.9. Phosphodiesterase-4 activity assay

Phosphodiesterase activity was measured in a cAMP hydrolysis assay. This used a modification of the two step procedure of Thomson and Appleman (Thompson and Appleman, 1971), as described previously by Marchmont and Houslay (Marchmont and Houslay, 1980). ^3H -cyclic nucleotide (8 position of the adenine or guanine ring) was hydrolysed to form labelled nucleotide mono-phosphate. The nucleotide mono-phosphate ring was converted to the corresponding labelled nucleoside by incubation with snake venom, which has 5'-nucleotidase activity. The conditions were such that complete conversion takes place within the incubation time. Unhydrolysed cyclic nucleotide was separated from the nucleoside by batch binding of the mixture to Dowex-1-chloride. This removes the charged nucleotides but not the uncharged nucleosides.

2.3.9.1. Activation of dowex 1X8-400 anion exchange resin

To activate the Dowex 1 X8 -400, 4 l of 1 M NaOH was added to 400 g of the resin, the mixture was incubated for 15 min at room temperature with gentle mixing. The resin was allowed to settle by gravity and the supernatant removed. The resin was then extensively washed with 4 l distilled water (30 washes). After its last wash the resin was resuspended in 4 l 1 M HCl and incubated for 15 min at room temperature with gentle mixing before being allowed to settle by gravity. The resin was then washed 3 times with 4 l distilled water, until the supernatant had a pH of 3. The activated resin was stored at 4 °C as a 1:1 slurry with distilled water until required.

2.3.9.2. Assay tube preparation

Into 1.5 ml eppendorf tubes an appropriate amount of cell lysate was placed (0.1 -50 μg protein depending on the activity of the sample) and made up to a volume of 25 μl with PDE assay diluting buffer (20 mM Tris/HCl, pH7.4), each sample tube was repeated in triplicate. All tubes were set up on ice, and remained on ice until all components for the assay had been added. To every tube 50 μl 2 μM cAMP containing 3 μCi [^3H]cAMP in 20 mM Tris/HCl /10 mM MgCl_2 pH7.4 was added, the tubes vortexed and incubated at 30 °C for 10 min. After this time the tubes were boiled for 2 min to inactivate any PDE present and then cooled on ice. 25 μg snake venom (either *Ophiophagus Hannah* or *Crotalus atrox*

venom) in 25 μ l 20 mM Tris/HCl, pH 7.4 was added to each tube, mixed by vortexing and incubated at 30 °C for 10 min. The tubes were then held on ice and 400 μ l Dowex/ethanol/water, in a 1 :1 :1 ratio was added to the tubes, mixed and incubated on ice for at least 20 min. The tubes were vortexed, the dowex removed by centrifugation at 13000 rpm for 2 min (Heraeus bench top centrifuge) and 150 μ l of the clear supernatant added to 1 ml Opti-scint scintillation fluid and counted on a Wallac 1409 liquid scintillation counter.

2.3.9.3. Determination of PDE3 and PDE4 activity

The PDE3 family is specifically inhibited by the drug cilostamide (Hidaka et al., 1979) and the PDE4 family by rolipram (Wachtel, 1982). PDE inhibitors were dissolved in 100 % DMSO as 10 mM stocks and diluted in PDE assay dilution buffer for use in assay. The residual levels of DMSO do not affect PDE activity at the concentrations used (Spence et al., 1995). Measurement of PDE activity with and without cilostamide (10 μ M) and with and without rolipram (10 μ M) present gave the contribution of PDE3 and PDE4 respectively.

2.3.10. Immunoprecipitation

2.3.10.1. Pre-clearing agarose beads

Protein G beads were used when the target protein was immuno-precipitated with a monoclonal antibody or a polyclonal antibody raised in a sheep and protein A beads were used when the target protein was immuno-precipitated with any other polyclonal antibodies. 25 μ l of the appropriate beads were washed in 200 μ l 3T3-Lysis buffer and recovered by centrifugation at 13000 rpm for 2 min at 4 °C in a refrigerated bench-top centrifuge. 300 μ g of protein from cell lysate, diluted to a total of 500 μ l with lysis buffer supplemented with protease inhibitors, was added to the washed beads and incubated with end-over-end rotation at 4 °C, for 30 min.

2.3.10.2. Binding target protein to antibody

After pre-clearing the beads were collected by centrifugation at 13000 rpm at 4 °C for 2 min (Heraeus refrigerated bench-top centrifuge), the supernatant was removed and placed into a fresh eppendorf tube. To this fresh tube 7 μ l of the polyclonal antibody or 3 μ l monoclonal antibody was added and the tube rotated end-over-end at 4 °C for at least 2 h,

to enable the protein and antibody to bind. The solution was then transferred into a tube containing 60 μl pre-washed protein beads (A or G as required) and rotated end-over-end for at least one hour at 4 $^{\circ}\text{C}$. The beads were isolated from solution by centrifugation at 13000 rpm at 4 $^{\circ}\text{C}$ for 2 min (Heraeus refrigerated bench-top centrifuge) and washed to remove any non-specifically bound protein. The beads were washed firstly in lysis buffer supplemented with 500 mM NaCl, secondly with lysis buffer supplemented with 0.1 % SDS and then washed with 0.1 % NP-40 in 10 mM Tris pH 7.4. A final wash of the beads was carried out with PBS if the isolated protein was to be used in SDS-PAGE. Otherwise the final wash was carried out in 20 mM Tris (pH 7.4), when the protein was used in a PDE assay, or in kinase assay buffer if the protein was to be subject to *in vitro* phosphorylation.

2.4. Kinase assays

2.4.1. PKA assay

2.4.1.1. Cell lysate extraction for PKA assay

Mammalian cells were grown and treated as required, after which time the cell media was removed, the cells washed with PBS and drained thoroughly. The monolayer of cells were scraped into 500 μl extraction buffer (5 mM EDTA, 50 mM Tris, pH 7.5) and homogenized by drawing through a 13 gauge needle 10 times. The cell debris was then removed by centrifugation for 2 mins at 13000 rpm at 4 $^{\circ}\text{C}$ (Heraeus refrigerated bench-top centrifuge) and the supernatant was used for a PKA assay.

2.4.1.2. PKA assay tube pre-incubation

For each cell lysate the following were set up on ice in 1.5 ml eppendorf tubes, adding the cell extract last and incubating on ice for 20 min, to allow the inhibitor to bind PKA. N.B- due to time restrictions during the assay a maximum of 9 different lysates can be analysed at any one time:

Tube	Cell Extract	Diluent	4x PKA Inhibitor	4x PKA Activator
A	10 μl	20 μl	0 μl	0 μl
B	10 μl	10 μl	10 μl	0 μl
C	10 μl	10 μl	0 μl	10 μl
D	10 μl	0 μl	10 μl	10 μl

Diluent – 50 mM Tris, pH7.5.

4 xPKA Inhibitor- 4 μ M PKI(6 -22) amide, 50 mM Tris, pH7.5.

4 xPKA Activator- 40 μ M cAMP, 50 mM Tris, pH7.5).

2.4.1.3. PKA assay reaction

To 1 ml of the 4 x PKA substrate (200 μ M Kemptide, 400 μ M ATP, 40 mM $MgCl_2$, 1 mg/ml BSA, 50 mM Tris, pH7.5) 6000 μ Ci/mmol of [γ - ^{32}P]ATP was added whilst maintained on ice. To the first assay tube (1A) 10 μ l of radioactive 4 x PKA substrate solution was added, the contents were mixed gently before being placed in a rack within a waterbath at 30 °C for 10 min. 15 seconds after substrate addition to the first tube 10 μ l of the radioactive substrate was added to the next tube (1B), which was then mixed and incubated. This method of addition of substrate to tubes every 15 seconds continued until all the tubes with substrate were incubating at 30 °C. After the 10 min incubation of the first tube 20 μ l of the reaction mix was removed and spotted onto a pre-marked piece of ion exchange phosphocellulose paper P81 (Whatman). This was carried out for each tube after they had each undergone the 10 min incubation with the substrate. The phosphocellulose pieces were then placed into a large beaker containing 1 %(v/v) phosphoric acid (H_3PO_4) and washed for 3 min with slight agitation. The waste acid was removed and the acid wash repeated. The phosphocellulose was then washed twice in dH_2O before being placed in 1.5 ml eppendorf tubes, to which 1 ml scintillation fluid was added. The ^{32}P incorporated into the peptide bound to the phosphocellulose was counted on the Wallac 1409 liquid scintillation counter. To two separate vials 10 μ l of the radioactive 4 x PKA substrate was added to scintillation fluid, to enable the determination of the total counts from the substrate solution.

2.4.1.4. Calculations for PKA assay data

Step 1.

$$\frac{\text{Total counts}}{4\text{nmolATP}} \times \frac{1\text{nmol}}{1000\text{pmol}} = \text{cpm/pmol phosphate}$$

Step 2.

$$\frac{(cpm/phosphocellulose) \times 2}{STEP1} = \text{total pmol peptide - incorporated phosphate}$$

Step 3.

$$\frac{STEP 2}{10 \text{ min}} = \text{pmol/ min /assay tube}$$

Step 4.

$$\frac{STEP 3}{0.01ml \text{ extract}} = \text{pmol/ min /ml}$$

Step 5.

$$\text{Tube A} - \text{Tube B} = \text{pmol/min activated PKA}$$

$$\text{Tube C} - \text{Tube D} = \text{pmol/min total PKA}$$

Step 6.

$$\frac{\text{pmol/ min activated PKA}}{\text{pmol/ min total PKA}} \times 100 = \% \text{ activated PKA}$$

2.4.2. Alkaline phosphatase treatment of protein

Protein was immunoprecipitated from cell lysate as described in 2.3.10. with the final wash of the protein bound beads carried out in 10 mM Tris, pH8, plus protease inhibitors (PI). The isolated beads were resuspended in 70 μ l 10 mM Tris, pH8, plus PI, to which 10 μ l 10 x Calf intestinal alkaline phosphatase (CIAP) buffer (Promega) was added. This reaction mix was split into two fresh eppendorfs, to one 10 μ l CIAP (10 units) was added, to the other 10 μ l 10 mM Tris, pH8 was added. The tubes were incubated at 30 °C for 30 min, after which time to the CIAP containing tube another 10 units of CIAP was added, and a further incubation for 30 min at 30 °C was carried out. The beads were then isolated by centrifugation at 13000 rpm for 2 min at 4 °C (Heraeus refrigerated bench-top centrifuge)

and either boiled in 35 μ l 2 x Laemmli sample buffer to be separated by SDS-PAGE or else washed in 20 mM Tris prior to a PDE assay.

2.4.3. MBP fusion protein production

2.4.3.1. Induction of *E.Coli* cells transformed with a recombinant protein-containing construct

A 50 ml sterile centrifuge tube containing 25 ml rich growth media (170 mM NaCl, 0.5 % (w/v) BactoYeast Extract, 1 % (w/v) Bacto-Tryptone pH7.5, 0.2 % glucose) supplemented with 100 mg/ml ampicillin was seeded with *E.Coli* (JM109) transformed with a recombinant protein construct, fused to maltose binding protein (MBP), and incubated at 37 °C with agitation overnight. The cells from the overnight culture were used to inoculate a 2 l flask containing 400 ml rich growth media, supplemented with 100 mg/ml ampicillin which was incubated at 37 °C with agitation until the absorbance of the culture at 600 nm was between 0.6 -1. Once growth of the cultures to the desired density had occurred addition of 400 μ l of 100 mM isopropyl- β -D-thiogalactopyranoside (IPTG, Boehringer Mannheim) to induce fusion protein expression was carried out and the culture incubated at 30 °C with agitation for a further 3.5 h. Samples of cells before and after induction of recombinant protein expression were taken, separated by gel electrophoresis and visualised by Coomassie stain of the gel to ensure of protein expression. The induced cells were harvested by centrifugation at 5000 rpm for 10 min at 4 °C in the Beckman centrifuge, and frozen at -80 °C until required.

2.4.3.2. Isolation of recombinant MBP fusion protein from *E.Coli* cells

The frozen *E.Coli* cells (2.4.3.1.) were defrosted on ice and resuspended in 10 ml ice-cold PBS, per original 400 ml culture, supplemented with 1mM DTT and protease inhibitors. The cell suspension was separated into 2x 6ml bijou bottles and sonicated on ice at 40 volts for 3x 1 min periods with 1 min intervals. The cell debris was removed by centrifugation at 9000 g for 30 min at 4 °C and the supernatant containing the recombinant protein retained. Amylose resin (1 ml) was washed twice in 20 ml PBS and a final wash in PBS supplemented with 1 mM DTT and protease inhibitors in a 50 ml centrifuge tube. The supernatant containing the recombinant protein was then added to the resin, which was rotated at 4 °C for 1 h to enable binding of the protein, the resin was then collected by centrifugation at 3000 rpm for 1 min and the supernatant discarded. The resin was washed

twice for 15 min at 4 °C, with rotation, with 20 ml PBS supplemented with 1 mM DTT and protease inhibitors and then once for 15 min at 4 °C with PBS alone. The protein could then be used bound directly to the resin or could be eluted from it.

2.4.3.3. Elution of recombinant MBP fusion protein from amylose resin

After the recombinant protein bound to the amylose resin had been washed it was resuspended in 1 ml PBS and transferred to 2 eppendorf tubes, the resin was collected by pulse spinning (Heraeus refrigerated bench-top centrifuge) and the supernatant was discarded. 500 µl of 10 mM maltose was added to each eppendorf and incubated at 4 °C with rotation for 30 min. The eluate was retained and 500 µl of 10 mM maltose was added for another incubation at 4 °C with rotation for 30 min, the eluates were pooled and protein concentration measured.

2.4.3.4. TEV cleavage of MBP fused recombinant protein from amylose resin

The amylose resin bound to the recombinant protein prepared as in 2.4.3.3. was washed in 20 x rTEV Buffer (1 M Tris/HCl, pH8, 10 mM EDTA). The resin was collected and resuspended in 15 µl 20 x rTEV Buffer, 3 µl 100 mM DTT, 20 units of recombinant TEV Protease and 100 µl dH₂O. The reaction mix was incubated at 16 °C for 16 hr, the digested protein was then isolated in the supernatant.

2.4.4. In vivo phosphorylation of protein

Cells were seeded at a concentration of 10⁶ cells/ml into 100 mm dishes the day prior to incubation of the cells with phosphate free media for whole cell labelling. Cells were washed twice with pre-warmed phosphate free media (Sigma) and then incubated for 1h with 5 ml phosphate free media at 37 °C in an atmosphere of 5 % CO₂ prior to the addition of ³²P orthophosphate. 300 µCi/ml ³²P orthophosphate or ³³P orthophosphate was added to the cells for a 2-4 h incubation at 37 °C in an atmosphere of 5 % CO₂. The cells were then washed in PBS and lysed in 3T3-lysis buffer as described in 2.3.1.1. The target protein was isolated by immunoprecipitation from the lysate as described in 2.3.10., separated from other proteins by gel electrophoresis and transferred onto nitrocellulose as described in 2.3.8.1.. The radiolabelled isolated protein was visualised by exposing the nitrocellulose to a phosphorimage plate (Kodak) for up to one week. The phosphorimage was detected

using the Bio-Rad Molecular Imager® FX phosphorimager on the Quantity One software (BIO-Rad).

2.4.5. In vitro phosphorylation of protein

2.4.5.1. Phosphorylation of a target protein from mammalian cells using a purified kinase

The protein for phosphorylation by a purified kinase was immunoprecipitate from mammalian cell lysate as described in 2.3.10., the final wash of the protein beads was in kinase assay buffer (KAB) (80 mM β -glycerophosphate, pH7.2, 40 mM NaF, 0.2 mM $\text{MgCl}_2 \cdot 6 \text{H}_2\text{O}$). The beads were then resuspended in 100 μl full KAB (KAB + 10 μM okadaic acid 1 mM ATP, 1 μCi $[\gamma\text{-}^{32}\text{P}]\text{ATP}$). 1 μl (1 unit) of recombinant kinase was added to all tubes except one, which serves as a negative control for the experiment. One of the kinase containing tubes also had 0.4 μM of the kinase inhibitor added to it to block the phosphorylation event, again acting as a control for the experiment. The solutions were mixed and incubated for 30 min at 30 °C, shaking occasionally to mix the settling protein beads. After incubation the beads were isolated by centrifugation for 2 min at 13000 rpm at 4 °C (Heraeus refrigerated bench-top centrifuge) and the supernatant removed. The beads were washed twice in KAB to remove any residual $[\gamma\text{-}^{32}\text{P}]\text{ATP}$ and then boiled for 10 min in 70 μl 2 x laemmli sample buffer.

2.4.5.2. Phosphorylation of recombinant target protein from E.Coli. using cellular lysate

Recombinant protein overexpressed in bacterial cell systems can be subject to phosphorylation by kinases present in cellular lysate. Recombinant protein from bacterial cells was purified as described in 2.4.3. and, once bound to the amylose resin, the final wash of the resin was in KAB. Two 1000 mm dishes of asynchronous cells or cells arrested in mitosis (as described in 2.1.4.5.) were washed twice with 5 ml breaking buffer (EBS) (100 mM Sucrose, 80 mM β -glycerophosphate, pH7.2, 20 mM EGTA, 15 mM $\text{MgCl}_2 \cdot 6 \text{H}_2\text{O}$, before use add 1 mM DTT, 2 mM ATP and 1 mM PMSF and 1 μM okadaic acid with mitotic lysate). The cells were then drained well and scraped into 2 x 1.5 ml eppendorf tubes. The cells were disrupted by passing them through a 13 gauge needle 10 - 30 times and the lysate isolated by centrifugation of the homogenate for 15 min at 13000 rpm at 4 °C (Heraeus refrigerated bench-top centrifuge). To increase the concentration of

proteins within the isolated cellular lysate 1 ml of the lysate was centrifuged in a centricon YM10 devise (Millipore) at 5000 rpm in a Beckman fixed angle centrifuge rotor at 4 °C for 45 minutes. The concentrated lysate was collected from the centricon devise by inverting the concentrating column and placing the opening in a collection tube. The apparatus was then centrifuged for 10 min at 1000 rpm at 4 °C in the Beckman fixed angle centrifuge.

100 µl amylose resin bound recombinant protein was placed in a fresh 1.5 ml eppendorf tube to which 100 µl concentrated cell lysate was added, which was supplemented with 1 mM ATP and 1 µCi of [γ -³²P] ATP. The tubes were mixed and incubated at 30 °C for 30 min to enable phosphorylation of the protein. The resin was washed twice in KAB to remove any residual [γ -³²P] ATP and then boiled for 10 min in 70 µl 2 x laemmli sample buffer.

2.4.5.3. Phosphorylation using an isolated kinase

Cells isolated in mitosis or interphase were harvested as described in 2.4.5.2., in EBS buffer. The kinase of interest was immunoprecipitated from the lysate using a specific monoclonal antibody as described in 2.3.10. The beads were washed finally in KAB and placed in a fresh 1.5ml eppendorf tube, to which 100 µl eluted recombinant protein from *E.Coli* was added, produced as described in 2.4.3. Each tube was also supplemented with 1 mM ATP and 1 µCi of [γ -³²P]ATP and incubated at 30 °C for 30 min to enable phosphorylation of the protein. To the tube 15 µl 5 x laemmli sample buffer was added and the tube boiled for 10 min to reduce and denature the proteins.

2.4.5.4. Radiolabelled analysis of protein

An 8 % tris-glycine gel was produced as described in 2.3.5. and the labelled proteins loaded into the wells of the gel a standard lane was loaded with 8 µl of Rainbow [¹⁴C] methylated protein molecular weight markers (Amersham Pharmacia Biotech). The molecular weights of the protein standards were: Myosin, 220 kDa, Phosphorylase b 97 kDa and 66 kDa, Ovalbumin 45 kDa, Carbonic anhydrase 30 kDa, trypsin inhibitor 20.1 kDa and lysozyme 14.3 kDa. The gel was allowed to run as described in 2.3.5. after which the proteins were transferred onto nitrocellulose as described in 2.3.8.1. The nitrocellulose was then placed into a phosphor-imaging cassette with a pre-blanked phosphorimaging plate (Kodak). The radiolabelled proteins were visualised using the Quantity One software

(BIO-Rad) on the computer connected to the Bio-Rad Molecular Imager ® FX phosphorimaging system.

2.4.5.5. 'Cold' in vitro phosphorylation of proteins

Proteins phosphorylated for the analysis of activity changes were treated in the same manner as the reactions described in 2.4.5.1. omitting the [γ - 32 P]ATP from the reaction mix. Activity changes of the protein were analysed via the PDE assay as described in 2.3.9. with the protein bound to beads being washed in 20 mM Tris, pH7.4, prior to the assay. Visualisation of the cold phosphorylated protein was carried out by immunoblotting as described in 2.3.8..

2.4.6. Tryptically digested phosphopeptide analysis by 2D TLC

Recombinantly expressed target protein was isolated from *E.Coli* cells as described in 2.4.3. The protein was then subject to a hot phosphorylation reaction in the presence of either mitotic or interphase isolated concentrated cell lysate, as described in 2.4.5.2. The phosphorylated protein bound to the amylose resin was washed twice in Tev cleavage buffer and was then subject to Tev cleavage as described in 2.4.3.4. The phosphorylated proteins were separated by gel electrophoresis, transferred to nitrocellulose and visualised as described in 2.4.5.4.

2.4.6.1. Tryptic cleavage of phosphorylated protein

The area of nitrocellulose to which the radiolabelled protein of interest bound was cut out and placed into a 1.5 ml eppendorf. The nitrocellulose was blocked with 0.5 % PVP-40 in 100 mM acetic acid incubated at 37 °C for 30 min and was then washed 5 times in dH₂O and twice in 50 mM NH₄HCO₃. 200 μ l fresh 50 mM NH₄HCO₃ was added to the nitrocellulose to which 10 μ g sequencing grade trypsin (Promega) was added. This was incubated for 2 h at 37 °C, then another 10 μ g sequencing grade trypsin was added for an 8 h incubation at 37 °C. 300 μ l dH₂O was added to the digest, the supernatant removed and placed in a fresh 1.5 ml eppendorf, with a pierced lid. The solution was snap frozen and dried under vacuum.

2.4.6.2. *Isolation of tryptically cleaved peptides*

Fresh performic acid (1 volume 30 % H₂O₂ added to 9 volume formic acid incubated at room temperature for 1 h) was cooled on ice and 50 µl added to the dried down peptides. The resuspended peptides were incubated on ice for 2 h then 1 ml dH₂O added and the solution snap frozen and dried under vacuum.

2.4.6.3. *Loading plates for 2D TLC separation of phosphopeptides*

An electrophoresis buffer with a pH of 1.9, composed of 50 ml formic acid (88 % w/v), 156 ml glacial acetic acid and 1794 ml deionised water was used for the first dimension separation of the phosphopeptides. The electrophoresis buffer of pH1.9 was used as at this pH value most peptides are soluble and streak maps are obtained less often (Van Der Geer et al., 1993). The phosphopeptides were dissolved in 20 µl electrophoresis buffer, the tubes containing the peptides were Çerenkov counted to ensure all of the radiolabelled phosphopeptide had been removed. The samples were loaded 1 µl at a time to the TLC plate (*Fig. 2.5.*), with air-drying between applications to ensure minimal dispersal of the sample. The 10 µl of the marker dye mixture, ε-dinitrophenyl-lysine- which migrates with a charge of 0 at pH1.9 - and xylene cyanol blue FF- which migrates with a charge of -1 at pH 1.9 (Hardie et al., 1993), was loaded at the indicated position (*Fig. 2.5.*), in the same manner as the sample.

2.4.6.4. *First dimension thin-layer electrophoresis*

The TLC plate was soaked with electrophoresis buffer, using blotting paper placed over the plates with holes cut out where the sample and marker loading points were. The buffer was brushed onto the blotting paper and was allowed to absorb into the sample and marker wells to concentrate the samples at these points. The plate was not wetted excessively and any pools of buffer were removed with blotting paper. The plate was then placed in the electrophoresis tank and two wicks measuring 20 x10 cm were wetted with the electrophoresis buffer and placed on the edges of the TLC plate into the buffer containing wells of the tank. The water cooling system on the running tank was engaged and a current of 1000 V applied to the plate until there is good separation of the marker dyes. The time for electrophoresis was variable for each plate but was usually carried out for 35 min in the first instance. The plate was then removed from the electrophoresis apparatus and allowed to air-dry for 2 h.

2.4.6.5. *Second dimension thin-layer chromatography*

The buffer used for chromatography was composed of 750 ml *n*-butanol, 500 ml pyridine, 150 ml glacial acetic acid and 600 ml deionized water. This buffer was selected as it is hydrophilic so would separate out the phosphopeptides, preventing them from binding to the stationary phase (Van Der Geer et al., 1993). A piece of blotting paper soaked in the chromatography buffer was used to line the chromatography tank, enough chromatography buffer to fill the first centimetre of the tank was added and the lid placed on the tank about 1 h prior to adding the TLC plate. This enabled equilibration of the solvents in the tank, to allow uniform migration of the phosphopeptides. The TLC plates were placed in the tank and chromatography was carried out until the solvent front was 2 cm from the top of the TLC plate.

2.4.6.6. *Identification radiolabelled phosphopeptides*

The TLC plate, once chromatography had been carried out was air-dried for 2 h, to enable evaporation of the solvents, and was then subject to a week long exposure to a phosphorimage plate. The phosphopeptides were detected from the phosphorimage plate using the BioRad Quantity One package (see section 2.4.5.4.).

2.4.7. *Tryptically digested phosphopeptide analysis by HPLC*

Protein was subjected to *in vitro* phosphorylation using concentrated asynchronous or mitotic lysate. The reaction was stopped by rinsing the beads twice with kinase assay buffer and then adding 80 μ l of 10 mM DTT and 1 % SDS solution. The samples were boiled for 5 min and then cooled prior to the addition of 0.5 % (v/v) 4-vinylpyridine. The samples were then shaken at 30 °C for 30 min, then 20 μ l 4 x novex sample buffer was added and the proteins that were consequently separated by gel electrophoresis on a 4-12 % gradient gel (Novex). The gel was then sealed in plastic and exposed to high performance autoradiography film (amersham pharmacia biotech) for 10 min. The phosphorylated protein was cut from the gel and the gel pieces subjected to scintillation counting on the Wallac 1409 liquid scintillation counter to calculate levels of 32 P incorporated into the protein.

2.4.7.1. *In gel tryptic digest of phosphorylated protein*

The gel preparation for tryptic digestion was carried out in a keratin free environment in a laminar flow hood. The gel, from 2.4.7., was washed sequentially in 1 ml H₂O for 15 min, 1 ml 50 % acetonitrile for 15 min, 1 ml 0.1 M ammonium bicarbonate for 15 min and finally 0.1 M in 50 % acetonitrile for 15 min. The solution was removed and the pieces of gel were crushed into fine pieces with a small spatula. The gel pieces were then washed with 100 % acetonitrile for 10 min, after which time the acetonitrile was removed and the gel pieces were dried by rotary evaporation for 10 -20 min. To the dried gel pieces 2 µg trypsin, diluted in 200 µl 50 mM ammonium bicarbonate and 0.05 % (w/v) zwittergent 3 -16, was added and incubated at room temperature for 30 min. After the initial incubation a further 200 µl 50 mM ammonium bicarbonate and 0.05 % (w/v) zwittergent 3 -16 was added and left to incubate with shaking at 30 °C overnight. The supernatant from the digest was removed and 0.2 % trifluoroacetic acid (TFA, by volume) added and the samples were loaded analysed by HPLC.

2.4.7.2. *HPLC analysis of phosphopeptides*

The tryptically digested protein samples from 2.4.7.1. were loaded onto a Vydac C₁₈ (Separation group) column which had been equilibrated in 0.1 % (v/v) TFA in H₂O. The column was developed with a linear acetonitrile gradient at a flow rate of 0.8 ml/min and 0.4 ml eluates were collected. The levels of ³²P incorporated into peptides were then measured on a Wallac scintillation counter. The eluates containing high levels of incorporated ³²P were dried down and subjected to either mass spectrometric analysis and cycle burst Edman degradation sequencing or retained for phosphoamino acid analysis.

2.4.7. *Protein binding assay*

Protein labelled with ³⁵S was synthesised using the TNT® Quick Coupled Transcription/ Translation Systems (Promega), according to the manufacturer's instructions. Briefly, 40 µl TNT® T7 Quick master mix, 2 µl 10mCi/ml [³⁵S] methionine, 1 µl T7 TNT® PCR and 5 µl purified vector DNA were mixed in a 0.5 µl eppendorf and incubated at 30 °C for 90 min. 5 µl of this synthesised protein was diluted in 500 µl cKHEM, to which 10 µg of the *E. Coli* expressed protein GST fusion protein of interest was added. This was placed on an end over end rotor at 4 °C for 2 h after which time 60 µl of pre-washed Glutathione (GSH) beads were added and rotated for 30 min at 4 °C. The GSH beads were isolated by

14
centrifugation 13000 rpm for 1 min at 4 °C and washed 3 times with cKHEM. The beads were boiled for 10 min in 1 x laemillis sample buffer before being run on an 8 % Tris-Glycine SDS-PAGE gel. The proteins were then transferred onto nitrocellulose and exposed to a phosphorimage plate overnight, the proteins were visualised using the BioRad Quantity one package (see section 2.4.5.4.).

2.5. Molecular Biology

All molecular biology techniques were carried out with sterilised equipment and buffers, to prevent contamination of solutions used.

2.5.1. Large scale production of plasmid DNA

500 ml LB growth media (170 mM NaCl, 0.5 % (w/v) BactoYeast Extract, 1 % (w/v) Bacto-Tryptone pH7.5) supplemented with 100 mg/ml ampicillin in a 2 l flask was spiked with a pipette tip from a glycerol stock of transformed cells containing the DNA of interest. The culture was incubated at 37 °C overnight with agitation and harvested the next day by centrifugation at 6000 g for 15 min using the JA-14 rotor in the Beckman refrigerated centrifuge. The DNA was extracted from the cell pellet using the Qiagen Maxiprep kit, according to the manufacturer's instructions, briefly: The bacterial pellet was resuspended in 10 ml Buffer P1 (resuspension buffer), to which 10 ml Buffer P2 (lysis buffer) was added, the solutions were mixed and incubated at room temperature for 5 min. 10ml of chilled buffer P3 (neutralisation buffer) was then mixed with the lysed cells which was incubated on ice for 20 min. The cell lysate was clarified by centrifugation of the solution at 10000 g for 30 min at 4 °C. Meanwhile the QIAGEN-tip 500 was equilibrated with 10 ml Buffer QBT which was allowed to flow through by gravity. The supernatant from the lysed cells was passed through muslin into the equilibrated column, which was then washed twice with 30 ml Buffer QC. The DNA, which had bound to the resin in the QIAGEN-tip 500, was eluted by the addition of 15 ml buffer QF.

2.5.1.1. Ethanol precipitation of DNA

DNA was precipitated from the eluted solution (section 2.5.1.) by the addition of 0.7 volumes room temperature isopropanol. The solutions were mixed and centrifuged at 15000 g for 30 min at 4 °C. The DNA pellet was washed with 5 ml room temperature 70 % ethanol and air-dried for 5 -10 min before being resuspended in 500 µl dH₂O.

2.5.1.2. Quantification of DNA

DNA was quantified spectrophotometrically; 5 μ l DNA was diluted to 1 ml with distilled water and absorbance measurements were taken at 260 nm and 280 nm using a Shimadzu UV-1201 UV-VS spectrophotometer blanked with distilled water. The concentration of nucleic acid was then calculated using the following approximations:

An absorbance reading of 1 at 260 nm corresponds to;

50 μ g/ml double stranded DNA

37 μ g/ml single stranded DNA

The ratio between the absorbance measurements at 260 nm and 280 nm provided an indication of the purity of the nucleic acid. In solution, pure DNA typically has $A_{260} : A_{280}$ ratios of 1.8. If the absorbance ratio is significantly less than this it indicates that the nucleic acid may be contaminated.

2.5.2. Small scale production of plasmid DNA

5 ml LB growth media supplemented with 100 mg/ml ampicillin in a sterile 25 ml universal tube was spiked with a pipette tip from a glycerol stock of transformed cells containing the DNA of interest. The culture was incubated at 37 °C overnight with agitation and the cells harvested the next day by centrifugation at 3000 rpm for 5 min (Heraeus bench-top refrigerated centrifuge). The DNA was extracted from the cells using the QIAprep spin miniprep kit according to the manufacturer's instructions, briefly: The bacterial pellet was resuspended in 250 μ l Buffer P1 (resuspension buffer), to which 250 μ l Buffer P2 (lysis buffer) was added, the solutions were mixed and incubated at room temperature for 5 min. 350 μ l of Buffer N3 (neutralisation buffer) was then mixed with the lysed cells and the solution was centrifuged for 10 min at 13000 rpm. The supernatant was added to the QIAprep spin column, which was centrifuged at 13000 rpm for 1 min, the flow through was discarded and the column washed with 750 μ l Buffer PE. The column was centrifuged for 1 min prior to the elution of the bound DNA. 50 μ l dH₂O was placed onto the resin in the column and incubated for 1 min, the DNA was eluted from the column by centrifugation for 1 min at 13000 rpm (Heraeus bench-top refrigerated centrifuge).

2.5.3. Analysis of plasmid DNA

2.5.3.1. DNA restriction digest

The restriction enzyme and the optimum restriction buffer used in the reaction depended on the site of digestion of the DNA for subsequent manipulations. If two restriction enzymes were used and the optimum restriction buffers were not compatible ethanol precipitation of the DNA between restriction digests was carried out. Each digest was carried out on 300 ng DNA in a total volume of 10 μ l per restriction enzyme used in the reaction. 1 unit of restriction enzyme was used and the appropriate volume of 10 x restriction added to the mix. The digests were carried out for 1-2 h at the optimal temperature for the enzyme, usually 37 °C.

2.5.3.2. Agarose gel analysis of DNA

DNA was visualised using agarose gel electrophoresis, the percentage of agarose used in the gel was dependent on the size of DNA fragment to be identified. For a 1 % agarose gel 1 % agarose was dissolved in 1 x TAE (40 mM Tris/HCl, 1 mM EDTA, 0.114 % glacial acetic acid) by heating until the agarose dissolved. To this 0.01 % ethidium bromide was added, which enabled visualisation of the DNA under a UV light source. The molten agar was poured into the gel apparatus, set up according to the manufacturer's instructions and allowed to set completely. The comb and end stoppers were removed, the gel tank filled with 1x TAE and the samples loaded into the lanes. All DNA samples were diluted 6:1 in 6x sample buffer (0.25 % Bromophenol Blue, 0.25 % xylene cyanol blue, 30 % glycerol in H₂O). In one lane 5 μ l standard 1 kb DNA ladder markers (Roche) were add to enable prediction of the size of DNA fragments run on the gel. The gel was run at 50 V until the dye front had migrated along the gel and the fragments of DNA were separated, the gel was removed from the tank and the DNA observed under UV light. The range of separation of linear DNA molecules according to agarose concentration;

Percentage Gel	Size of Fragment (kb)
0.9	0.5 -7
1.2	0.4 -6
1.5	0.2 -3
2	0.1 -2

2.5.3.3. Gel purification of digested DNA

The DNA once isolated by agarose gel electrophoresis was cleaved from the agarose gel and purified using the QIAquick Gel Extraction kit according to the manufacturer's instructions for using the spin columns, briefly: The gel slice containing the target DNA was weighed in an eppendorf tube and 3 volumes of buffer QG was added per one volume of gel. This was incubated at 50 °C for 10 min until the gel had dissolved. One gel volume of isopropanol was then added to the sample and mixed, the solution was then added to a QIAquick column and centrifuged for 1 min at 13000 rpm (Heraeus benchtop centrifuge). The column was washed with 750 µl Buffer PE, which was centrifuged through the column at 13000 rpm for 1 min, a further centrifugation for 1 min at 13000 rpm was carried out to remove excess solution prior to elution of the DNA. The DNA was eluted from the column by the addition of 50 µl dH₂O to the resin of the column which was incubated for 1 min and the DNA was then collected by centrifugation for 1 min at 13000 rpm.

2.5.4. Ligation of dsDNA

For the ligation of DNA 100 ng of restriction digested vector DNA was added to a 0.5 ml eppendorf, to which 50 ng of dsDNA with cohesive ends was added. 1 µl 10 x ligase buffer (30 mM Tris/HCl, pH7.8, 100 mM MgCl₂, 100 mM DTT, 10 mM ATP) and 1 µl T4 DNA-ligase (Promega) was added to the DNA mix and the volume made up to 10 µl with sterile distilled water. The contents of the tube were mixed thoroughly and incubated at 22 °C for 3 h.

2.5.5. Production of Competent Cells

For Competent cell production aseptic techniques were used at all times. Either DH5α or XL1-Blue cells were spiked from a glycerol stock into 5 ml LB media and incubated overnight at 37 °C with agitation. 500 µl of the overnight culture was used to seed 50 ml LB growth medium which was incubated at 37 °C with agitation until the OD₆₀₀ = 0.2. The cells were harvested by centrifugation at 4000 rpm for 10 min at 4 °C (Beckman refrigerated centrifuge) and resuspended in 25 mls ice-cold 100 mM CaCl₂. Incubation of the cell suspension on ice was carried out for 20 min and the cells were then collected by centrifugation, 4000 rpm for 10 min at 4 °C. The cell pellet was resuspended in 2.5 ml ice-

cold 100 mM CaCl₂ and glycerol was added to a final concentration of 10 %, the cells were then aliquotted and snap frozen in liquid N₂ and stored at –80 °C until required.

2.5.6. Transformation of Competent Cells with Target DNA

Transformation of competent cells was carried out with either 10ng of purified plasmid DNA, or 1 µl ligation product produced in 2.5.4. The DNA was placed in the bottom of a pre-chilled transformation tube (Falcon) to which 50 µl competent cells produced in 2.5.5. were added. The DNA and cells were incubated for 30 min on ice and then heat shocked at 42 °C for 45 sec. To the transformed cells 1 ml LB media was added and the cells were recovered at 37 °C for 1 h with agitation. 50 -100 µl of cell suspension was plated onto LB-amp agar plates (170 mM NaCl, 0.5 % (w/v) BactoYeast Extract, 1 % (w/v) Bacto-Tryptone pH7.5, 1 % agar, supplemented with 100 mg/ml ampicillin) using aseptic techniques, which were allowed to dry for 10 min before being inverted and incubated at 37 °C overnight.

2.5.7. Glycerol Stock Production

A 500 µl sample from an overnight culture of transformed cells was taken aseptically and placed into a sterile screw top cryovial to which 500 µl sterile 80 % glycerol was added. The sample was mixed well and stored at –80 °C for further use.

2.5.8. DNA Sequencing

The DNA sequencing reaction was carried out using the BigDye termination kit and the resulting PCR product was sequenced by the University Sequencing Service. In a sterile 0.5 ml PCR tube the reaction mix for the PCR reaction was set up as follows: 500 ng DNA, 3.2 pmol primer, 8 µl Big Dye Sequencing mix, dH₂O, to a final volume of 20 µl. The tubes were then mixed and subject to the following PCR reaction cycles:

96 °C	30 seconds	} 25 cycles
50 °C (variable depending on T _m)	15 seconds	
60 °C	4 minutes	
4 °C	Hold	

The DNA product was precipitated from the reaction mix by the addition of 2 µl 3 M NaOAc, pH4.8 and 50 µl EtOH to the solution, this was mixed and incubated on ice for 10

min. The precipitated DNA was isolated by centrifugation at 13000 rpm for 30 min at 4 °C. The pellet was washed once with 70 % ethanol and dried completely by heating in the PCR machine for 3 min at 80 °C.

2.5.9. Site directed mutagenesis of DNA using the QuickChange™ kit

Site directed mutagenesis of DNA was performed using the QuickChange™ site directed mutagenesis kit (Stratagene) using primers designed to incorporate the mutation of the DNA required, flanked by unmodified nucleotide sequence. The mutagenesis was carried out according to the manufacturer's instructions, briefly: The reaction was set up in a 0.5 ml sterile PCR tube with 5-50 ng dsDNA template, 125 ng primer 1, 125 ng primer 2, 5 µl 10 x reaction buffer (100 mM KCl, 100 mM (NH₄)₂SO₄, 200 mM Tris/HCl, pH8.8, 20 mM MgSO₄, 1 % Triton X-100, 1 mg/ml BSA), 1 µl dNTP mix and ddH₂O to a final volume of 50 µl. To this 2.5 units *PfuTurbo*DNA polymerase was added, mixed and subject to the following PCR reaction cycles:

95 °C	30 seconds	} 12-18 cycles depending on type of mutation
96 °C	30 seconds	
55 °C	1 minute	
68 °C	2 minutes/kb plasmid length	
4 °C	Hold	

2.5.9.1. Isolation and transformation of mutated DNA

To each amplification reaction from 2.5.9. 10 units of *DpnI* restriction enzyme was added and incubated at 37 °C for 1 h. *E.Coli* XL-1 Blue supercompetent cells were thawed on ice and 50 µl added to a chilled transformation tube (falcon) to which 1 µl of the *DpnI* treated DNA was added. The DNA and cells were mixed and incubated on ice for 30 min then heat pulsed for 45 sec at 42 °C. The cells were left on ice for 2 min before the addition of 500 µl pre-warmed NZY⁺ broth (1 % (w/v) NZ amine (casein hydrolysate), 0.5 % (w/v) NaCl, pH7.5, 12.5 mM MgCl₂, 12.5 mM MgSO₄ and 20 mM glucose). The cells were incubated at 37 °C with shaking for 1 h and then plated into LB-amp agar plates. The plates were inverted and incubated overnight at 37 °C.

2.5.10. Reverse transcription PCR (RT-PCR)

2.5.10.1 RNA isolation

Total RNA was isolated from cells using the RNeasy kit from Promega, according to the manufacturers instructions. Briefly, cells were aspirated of all growth media and the cells were lysed into 600 μ l buffer RLT, the cells were scraped into an eppendorf tube and homogenised by passing the supernatant 5 times through a 20 gauge needle connected to a syringe. 600 μ l 70 % ethanol was added to the homogenate and mixed by pipetting. The sample was applied to an RNeasy minispin column which was centrifuged for 15 sec at 8000 g (Hereaus benchtop centrifuge). The RNA bound to the column was washed initially with 700 μ l buffer RW1, which was incubated for 5 min at room temperature and then centrifuged at 8000 g for 15 sec. The column was washed a further two times by the addition of 500 μ l buffer RPE, this was removed by centrifugation for 15 sec at 8000 g initially with a final drying centrifugation at 13000 g for 2 min. The RNA was eluted from the column in 30 μ l RNase-free water by centrifugation at 8000 g for 1 min.

2.5.10.2. First strand complementary DNA (cDNA) synthesis

First strand cDNA was synthesised using the Pharmacia First-strand cDNA Synthesis Kit according the manufacturers instructions. Briefly 5 μ g of total RNA was made up to 20 μ l with DEPC treated distilled water. This was heated to 65 °C in a thermal cycler for 10 min then immediately chilled on ice. The "Bulk 1st strand cDNA mix" (supplied with the kit) was gently mixed by being pipetted up and down several times and was then collected with a brief centrifugation. The cDNA synthesis reaction mixture was assembled in a sterile 0.5 ml Eppendorf tube that was chilled on ice. The cDNA synthesis reaction was then incubated at 37 °C for 1 h.

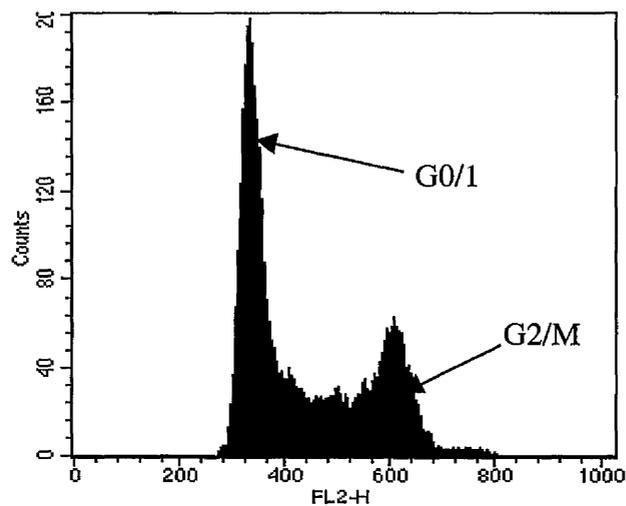


Figure 2.1. FL2-H distribution of cells labeled with propidium iodide. Rat-1 cells were arrested at specific phases of the cell cycle (*see section 2.1.4.1. - 2.1.4.5.*), harvested and stained with propidium iodide (*as described in section 2.2.1.*). 20000 cells were acquired for analysis by flow cytometry and utilising the acquisition setting on the CELLQuest package the amps of the FL2 channel were adjusted to place the peaks of G0/1 cells between 300-400 and the G2/M cells between 600-800, as indicated on the diagram.

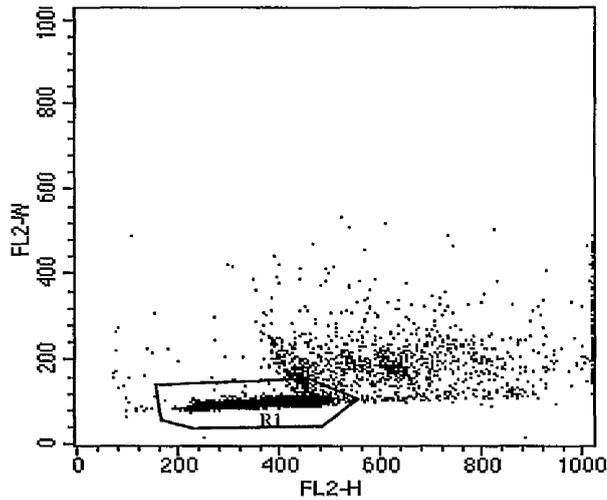


Figure 2.2. Doublet discrimination of a Rat-1 cell population. Rat-1 cells when arrested at specific stages of the cell cycle (*as described in section 2.1.4.1. - 2.1.4.5.*) were then harvested and labeled with BrdU-FITC and propidium iodide (*as described in section 2.2.3.3.*). 20000 labeled cells were then collected and analysed by flow cytometry, using the CELLQuest acquisition package.. A density plot of FL2-H vs FL2-W from these collected cells was produced (the cells are represented by the black dots on the density plot) and the cells were gated (thin black line) to remove clumps of cells, apoptotic cells and cell debris, leaving the single diploid cells (R1) for further analysis.

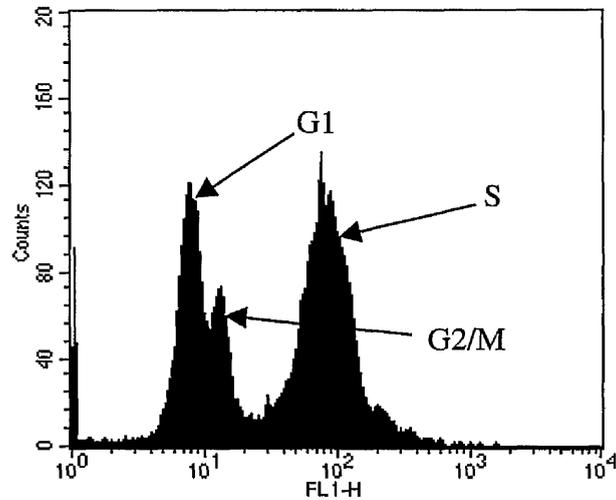


Figure 2.3. Normal FL1-H distribution of cells from an asynchronous population. Asynchronous Rat-1 cells were harvested and stained with BrdU-FITC and propidium iodide (*as described in section 2.2.3.3.*). 20000 labeled cells were collected by FACs and analysed using the CELLQuest acquisition package. A histogram of FL1-H vs counts was generated and the amps in the FL1 channel were adjusted to place the G1 peak of cells at $<10^1$, the G2/M peak as a shoulder on the G1 peak and the S cells peak at 10^2 , as indicated on the diagram.

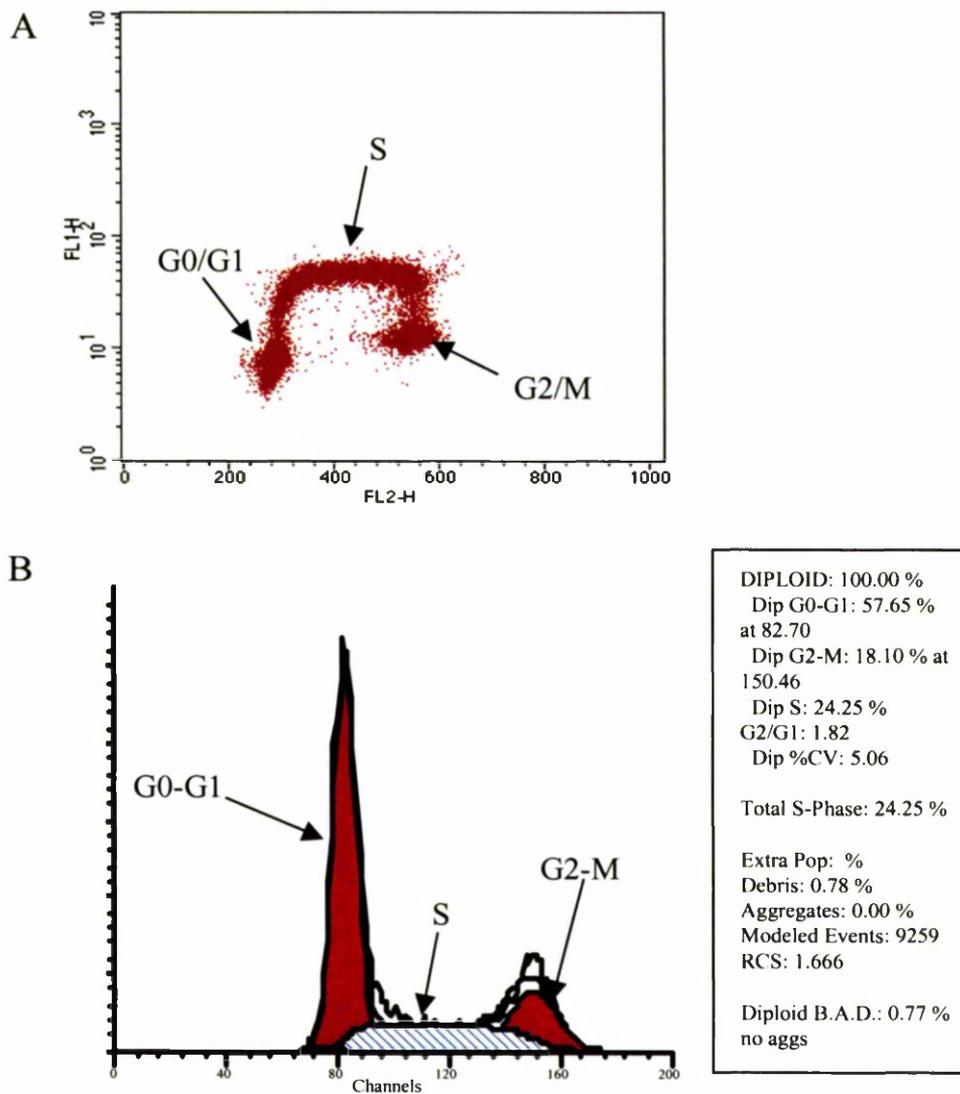


Figure 2.4. MODfit™ analysis of BrdU-FITC and propidium iodide labelled cells. Rat-1 cells which had been stained with BrdU-FITC and propidium iodide (as described in section 2.2.3.3.) were acquired by FACs using the CELLQuest package (as described in section 2.2.4.1.) and then quantified using the MODfit™ analysis package. *Panel A.* The distribution of the labelled population of cells was acquired on a FL2-H vs FL1-H density plot and the cells within the G0/G1, S and G2/M phases of the cell cycle, as indicated on the diagram, were identified. The S phase cells were gated and quantified as a proportion of the total cell distribution *Panel B.* Quantification of the cells distributed within G0/G1, S and G2/M phase by the MODfit™ analysis package displayed the number of cells in each phase as a percentage of the number of diploid cells analysed. The analysis also displays the percentage debris in the population, the percentage aggregated cells and the number of cells analysed (Modelled Events).

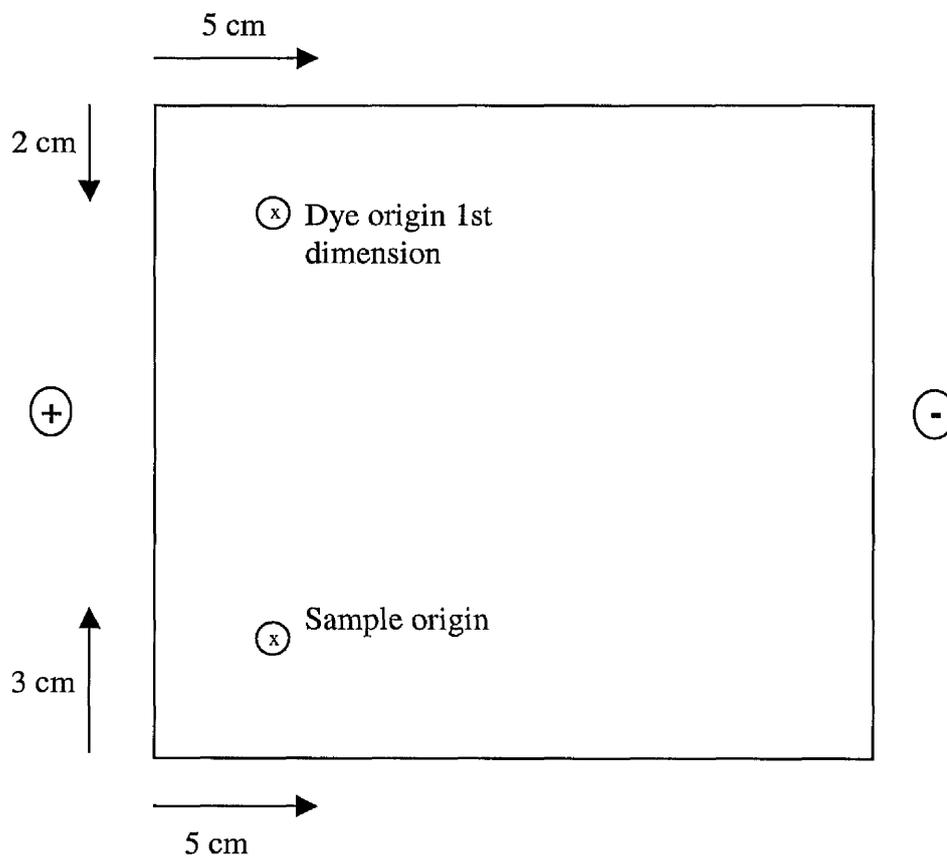


Figure 2.5. Locations of sample and dye origins for two-dimensional separation of phosphopeptides on 20 x 20 TLC plates. The figure indicates the locations of the application points for the sample and dye for electrophoresis at pH 1.9 on a TLC plate, as described in section 2.4.6.3. Also indicated are the orientations of the charges that are applied to the TLC plate upon first dimension separation of peptides.

Chapter 3

Phosphodiesterases and the cell cycle

3.1. Introduction

3.1.1. *The cell cycle; a brief overview*

The identification of the cell cycle began with the discovery of the mechanisms which lead to cell division, where the generation of two cells from one was termed mitosis. With the invention of high powered microscopes the observation was made that DNA replicated in a restricted part of interphase and this part of the cell cycle was termed S phase (Howard and Pelc, 1953). Mitosis and S phase are separated by two gap phases, G₁ occurring between M and S phase and G₂ occurring between S and M phase (Mitchinson, 1971, *Fig. 3.1.*). During G₁ phase cells are under the influence of extra-cellular mitogenic stimuli. If deprived of these mitogens the cells enter G₀ phase, or quiescence (Ammit and Panettieri, Jr., 2001; Lee et al., 2001). Mitogens have to be present until the cells have passed the restriction point within G₁, after which time the cell is committed to complete one full cell division under autonomous control (Pardee, 1989). The cell cycle is a complicated process and S and M phases are rigorously ordered to allow correct duplication of the cell. Checkpoint mechanisms exist during the cell cycle, which are regulated by the coordinated action of proteases and cyclin dependent kinases (cdk). The control mechanisms are specifically activated at the G₁/S boundary, during S phase and during the G₂/M transition (Nurse, 2000) and enable analysis of DNA damage and incomplete DNA replication as well as the misalignment of chromosomes on spindle bodies (Ford and Pardee, 1998). Mitosis is a complex cell cycle phase, which is separated into distinct stages. In prophase, spindle formation occurs and the chromosomes condense. In prometaphase they then attach to the spindles by their centromere, and during metaphase, they start aligning on the spindle fibres. During anaphase the chromatids segregate and migrate to the opposite poles of the cell. Cytokinesis then takes place during telophase, resulting in the production of two identical daughter cells (*Fig. 3.2.*, Leblond and El Alfy, 1998).

3.1.2. *Cyclic AMP control of the cell cycle*

The involvement of cAMP in the regulation of cell cycle control mechanisms has been apparent for decades (Pastan et al., 1975). Initial observations of the retardation of proliferation by the elevation of intracellular cAMP were made in hamster kidney cells by Burk (Burk, 1968). It has since been exemplified in many cell lines, through increasing intracellular cAMP, by either forskolin-stimulation of adenylyl cyclase, by the addition of non-hydrolysable cAMP derivatives, or by addition of phosphodiesterase inhibitors. All methods seemingly serve to inhibit cell proliferation (Pastan et al., 1975). It has been

noted, however, that the elevation of intracellular cAMP can actually stimulate cell division in certain cell types, specifically the thyroid and pituitary (Felicciello et al., 2000). However, these appear to be distinct cases and thus the inhibitory effect of cAMP on proliferation will be primarily considered here.

3.1.2.1. *Elevated cAMP induces cell quiescence*

Elevation of cAMP activates the cAMP dependent protein kinase (PKA), which blocks proliferation of cells through an array of different intracellular signalling mechanisms. PKA causes the down regulation in expression of the G1 specific cdk regulatory subunit proteins, cyclin D1 (L'Allemain et al., 1997; Koyama et al., 2001) and cyclin D3 (Naderi et al., 2000; van Oirschot et al., 2001) at the level of transcription and translation, respectively (Musa et al., 1999). The decrease in cyclin D1 protein levels, and its associated activity, cause dephosphorylation of the tumour suppressor, Retinoblastoma (Rb) protein which, in turn, binds to and inactivates the E2F transcription factor. This prevents DNA synthesis and G1/S phase transition (Tomlinson et al., 1995; Naderi et al., 2000; Christoffersen et al., 1994; Blomhoff et al., 1988). High levels of cAMP also increase the levels of expression of the G1 specific cdk inhibitor, p27^{KIP1}. This inhibitor binds to active cdk complexes causing their inactivation, blocking the cell cycle prior to passage through the G1 restriction point (Kato et al., 1994; L'Allemain et al., 1997). A rise in cAMP concentration causes a respective inhibition of the Mitogen Activated Protein Kinase (MAPK) signalling cascade required for G1/S progression through the activation of PKA which antagonises the Ras/Raf-1 interaction in the Ras-Raf-MEK-ERK pathway (Koyama et al., 2001; Schmitt and Stork, 2001, *Fig.3.3.*).

3.1.2.2. *Cyclic AMP controls cells in interphase and mitosis*

Cyclic AMP-mediated control of the cell cycle is evident during the transition of cells from S to G2. Elevated levels of cAMP decrease the stability of the mitosis-specific cdk complex, MPF, which causes a decrease in the rate of passage of cells into and through G2 phase, thus acting as a checkpoint mechanism (Kato et al., 1994; Kurokawa and Kato, 1998). A decrease in cAMP levels is crucial for the passage of cells into mitosis, as inhibition of PKA is required in order to allow formation and activation of the mitotically-regulated ubiquitin ligase, the anaphase promoting complex (APC) (Grieco et al., 1996; Yamashita et al., 1996; Kotani et al., 1998; Kishimoto and Yamashita, 2000). High levels of cAMP during mitosis have been seen to give abnormal mitotic spindle formation, block chromosome separation and prevent telophase exit (Anghileri et al., 1999).

3.1.3. Phosphodiesterases inhibit cell cycle progression

Phosphodiesterase (PDE) elicited intracellular cAMP degradation, during the cell cycle has been studied in many cell types and fluctuations in PDE activity have been observed during cell proliferation in the slime mould, *Physarum polycephalum* (Kupetz and Jeter, Jr., 1985). Indeed, high levels of PDE activity have been associated with the proliferation of colon carcinoma cells, with a consequently decrease in PDE activity as the cells reached confluency (Savini et al., 1995). The effect of PDE inhibition on the cell cycle has been extensively studied in T cell proliferation, as cellular proliferation is fundamental to progression of diseases such as asthma (reviewed in Kay, 2000). In virally-transformed T cells PDE4 dependent cAMP-specific PDE activity has been shown to be functionally up-regulated and such T cells appear to arrest in G1 phase upon the addition of the PDE4 selective inhibitor rolipram (Ekholm et al., 1999). PDE4 inhibitors specifically down-regulate antigen driven proliferation of T helper cell clones (Essayan et al., 1997) and PHA-stimulated mononuclear cell division (Banner et al., 2000; Banner et al., 1995). Non-selective PDE inhibitors have also been shown to inhibit proliferation of smooth muscle cells (Pan et al., 1994; Souness et al., 1992), endothelial cells (Leitman et al., 1986), melanoma cell lines (Drees et al., 1993) and epithelial cells (Matousovic et al., 1997), arresting them all on G1/S boundary, prior to passing the restriction point. Other studies have implied that differential control of cAMP degradation by PDEs is important at other stages of the cell cycle. The non-selective PDE inhibitor, IBMX arrests *Amphidiunium operculatum* cells at G2/M transition as well as at the G1/S boundary (Leighfield and Van Dolah, 2001). In actinomycetes PDE activity has been shown to increase at G2 phase and is maintained during mitosis (Lefebvre et al., 1980). The inhibition of PDE activity in both budding and fission yeast, through the generation of temperature sensitive mutants, has been shown to block mitotic exit (Yamashita et al., 1996; Kishimoto and Yamashita, 2000).

I have undertaken a study to investigate the involvement of PDEs in the control of the cell cycle so as to establish whether specific PDE isoforms are implicated in the cell cycle checkpoint regulatory mechanisms that are under the control of intracellular cAMP. An endogenous cellular system was used for observing changes in PDE activity profiles during phases of the cell cycle. The model cell line of choice was the Rat-1 fibroblasts which were originally isolated from rat embryos (for details see Materials and methods 2.1.1.1.). Rat-1 fibroblasts were used for initial cell cycle isolation work and in the elucidation of the PDE profiles and intracellular signalling mechanisms at different phases of the cell cycle. Signalling mechanisms of Rat-1 cell lines have been well characterised and they have

previously been used extensively in studies of the cell cycle (Prouty et al., 1993; Crossen et al., 1986; Knudsen et al., 1998).

Results

3.2. Characterisation of Rat-1 fibroblast PDE4 profile

In order to define the profile of PDE4 isoforms expressed in the Rat-1 cells a western blot analysis approach, as described in section 2.3.8., was undertaken using rat PDE4A, PDE4B, PDE4C and PDE4D carboxy-terminal specific antibodies to probe cellular lysate from asynchronous cells.

3.2.1. Western blot analysis of PDE4A splice variants

Immunoblots (Materials and methods 2.3.8.) of whole cell lysate from asynchronous Rat-1 cells identified no PDE4A species that co-migrated specifically with any of the recombinant protein PDE4A standards. This suggested that either there was no PDE4A expression or that the level of expression of the PDE4A isoforms in the Rat-1 cells was too low to be detected by immunoblotting whole cell lysates with the PDE4A specific antibody. Thus, in order to concentrate PDE4A for blotting I set out to immunoprecipitate PDE4A (Materials and methods 2.3.10) using the Genosys '270' polyclonal antibody, raised in rabbits against a GST fusion protein containing the TPGRWGSGGDPA peptide, corresponding to the extreme C-terminal residues present in all rat PDE4A isoforms. The immunoprecipitated PDE4A protein was then immunoblotted with the same antibody. Using these a single PDE4A isoform was identified in the Rat-1 cells. This appeared to be the 109 kDa PDE4A5 protein (Genbank accession L27057, *Fig. 3.4., Panel A*). However, the PDE4A5 appeared to run with a higher mobility than the standard recombinant protein, an observation made repeatedly in the laboratory (personal communication, E. Huston). Therefore the immunoprecipitated protein was immunoblotted with the PDE4A5 N-terminal specific '24' antibody. This antibody was raised in rabbit to a GST fused peptide that corresponded to the unique sequence within the N-terminus of PDE4A5. This clearly identified a PDE4A5 species which had a slightly lower apparent molecular weight than the standard PDE4A5 proteins (*Fig 3.4., Panel B*).

3.2.1.1. RT-PCR analysis of PDE4A isoforms found in Rat-1 fibroblast

To confirm by a further independent means that the PDE4A protein expressed in Rat-1 cells was the PDE4A5 isoform RT-PCR analysis was carried out on total RNA isolated from the cells (Materials and methods 2.5.10.). The primers used for the RT-PCR were confirmed as being unique to particular isoforms by analysis using the BLASTn program

(Altschuler et al, 1991), against the non-redundant database (*Fig. 3.5.*). RT-PCR analysis of total cellular RNA extracted from Rat-1 cells, using generic PDE4A primers confirmed expression of the PDE4A gene in these cells (*Fig. 3.6.*). However, the expression of the PDE4A5 isoform could not be specifically shown in this way.

3.2.2. Western blot analysis of PDE4B splice variants

To determine whether PDE4B isoforms were expressed in Rat-1 fibroblasts, cell lysate from an asynchronous population of cells were immunoblotted with a polyclonal antibody (Materials and methods 2.3.8.) raised against a GST protein fused to the sequence DPENRDSLGETDIDIATED, which corresponds to the extreme C-termini of all known rat PDE4B isoforms. This detected a single PDE4B splice variant that co-migrated with PDE4B2 (Genbank accession L27058) standard recombinant protein, at 80 kDa, on an SDS-PAGE gel (*Fig. 3.7.*).

3.2.2.1. RT-PCR analysis of PDE4B isoforms found in Rat-1 fibroblasts

As the PDE4B2 protein appeared to migrate with a slightly different molecular weight to the recombinant protein standards by SDS-PAGE further confirmation that the PDE4B protein expressed in Rat-1 cells was the PDE4B2 isoform was carried out using RT-PCR analysis of total RNA isolated from the cells (see section 2.5.10.). The primers used for the RT-PCR were again designed to unique nucleotide sequences within the individual isoforms, which were confirmed as being unique using the BLASTn program against the non-redundant database (*Fig. 3.8.*). The RT-PCR analysis of total cellular RNA extracted from Rat-1 cells confirmed the expression of the PDE4B2 isoform (*Fig. 3.9.*).

3.2.3. Western blot analysis of PDE4C isoforms

Asynchronous cellular lysate from the Rat-1 fibroblasts was probed with the Genosys '232' C-terminal PDE4C specific polyclonal antibody (Materials and methods 2.3.8.). This had been raised in rabbits against the a GST protein fused to the peptide sequence KEALELPDTELLSPEAGPDPGD, which corresponds to a peptide located in the extreme C-termini of all known PDE4C isoforms. The expression levels of the PDE4C protein were too low to be detected directly from cellular lysate, therefore immunoprecipitation of the PDE4C protein with the same polyclonal antibody was carried out to concentrate the protein (Materials and methods 2.3.10.). The isolated PDE4C species were then immunoblotted with the same antibody and a protein that co-migrated with recombinant

PDE4C2 at 80 kDa was identified (*Fig. 3.10.*, Genbank accession L27061, M25347 and M28410, all of which are partial sequences).

3.2.4. Western blot analysis of PDE4D isoforms

To assess whether PDE4D isoforms were expressed in Rat-1 cells, immunoblot analysis (Materials and methods 2.3.8.) was performed using a SAPU PDE4D specific polyclonal antibody, which was raised in sheep to a peptide corresponding to the sequence QVEEDTSCSDSKTLCTQDSESTEPLDEQVEEEAVGEEEEESQPEACVIDDRSPDT, located at the extreme C-termini of all rat PDE4D isoforms. This revealed the only major PDE4D splice variant expressed endogenously within the cells was the 95 kDa, PDE4D3 (*Fig. 3.11., Panel A*, Genbank accession U09457). Immunoprecipitation of the Rat-1 cell lysate (Materials and methods 2.3.10.) was carried out using the same PDE4D specific antibody and immunoprobings of the isolated protein was done with the ICOS PDE4D monoclonal antibody (Bolger et al., 1997). This mouse monoclonal antibody was raised against the TDQSESTEPLDEQVEE peptide, also present near the extreme C-termini of PDE4D isoforms and revealed no PDE4D isoforms were expressed in the Rat-1 cells in addition to the PDE4D3 (*Fig. 3.11., Panel B*).

3.3. Cell cycle analysis in Rat-1 fibroblasts

In order to study the changes in PDE isozyme activities during the cell cycle it was necessary, initially, to characterise the distribution of an asynchronous population of Rat-1 cells through the cell cycle. Then determination of rates at which the cells pass through the different cell cycle phases was made. Once these observations had been made populations of cells were isolated at specific phases of the cell cycle in order to ascertain whether there were alterations in specific PDE activities during the cell cycle.

3.3.1. Determination of the rates of proliferation of Rat-1 fibroblasts

Asynchronous Rat-1 cells were analysed by flow cytometry (Materials and methods 2.2.4.), indicating a mixed distribution of the population through the cell cycle, with approximately 57 % of the cells in G1, 18 % in S and 25 % in G2/M (*Fig. 3.12.*).

To decipher the length of time it took Rat-1 cells to move through phases of the cell cycle, and the time it took the cells to complete one cell division, BrdU-labelled cells (see section 2.2.3.) were analysed by FACs (see section 2.2.4.). The time taken by the cells to move

from the start of one S phase to the beginning of the next consecutive S phase was determined as the duration of one complete cell cycle. For Rat-1 cells this was found to be approximately 16 h (*Fig. 3.13.*).

In an attempt to isolate a large population of cells at different phases of the cell cycle, cells were deprived of serum for 48 h. The re-addition of serum to the cells caused them to re-enter the cell cycle, although synchrony was lost within 6 h (data not shown). Therefore alternative methods of isolation of synchronous populations of cells within distinct phases of the cell cycle were required.

3.3.2. Method development for the isolation of Rat-1 cells in specific phases of the cell cycle

Highly synchronous cell populations were required for the analysis of PDE activities in specific cell cycle phases, thus a strategy for isolating cells at checkpoints within the cell cycle by chemical means was utilised. Although well described, these methods have been previously employed for cell types other than Rat-1 cells (Zeilig et al., 1976; Cordeiro-Stone and Kaufman, 1985; Crossen et al., 1986; Jordan et al., 1992; Keryer et al., 1998). These I had to optimise to achieve cell cycle arrest in Rat-1 cells.

3.3.3. Arresting Cells in G0 phase

As evidenced by FACs analysis cells were completely arrested in G0 phase of the cell cycle through serum deprivation for 48 h (*Fig. 3.14.*). Some cells lines undergo apoptosis after such prolonged serum withdrawal (Helbing et al., 1998). However, clear cell synchrony was only obtained in the Rat-1 fibroblasts after such extensive periods of serum starvation. Furthermore, only a small proportion of these cells appeared to have entered apoptosis after this time (data not shown).

3.3.4. Arresting Cells in G1/S

To inhibit cells at G1/S, the double thymidine block method was utilised (Materials and methods 2.1.4.3. Cho et al., 2001). As evidenced by FACs analysis, the thymidine feedback inhibition of DNA synthesis blocked cells already undergoing S-phase (*Fig. 3.15.*) so it was necessary to carry out a double blocking mechanism to collect all cells at the G1/S boundary. Several thymidine block release times were investigated, including 8 h, 14 h and 20 h. A 14 h release was found to be sufficient to almost completely synchronise

cells at the G1/S checkpoint upon the re-application of 2.5 mM thymidine for 16 h, post release (*Fig. 3.15.*), whereas other release times arrested too many cells in S phase.

3.3.4.1. Alternative means of G1 arrest

Another means of G1/S synchronisation was investigated utilising the cyclin-dependent kinase inhibitor, olomucine (Abraham et al., 1995). However, as evidenced by FACs analysis, it was found that cells were being blocked at both the G1/S checkpoint and the S/G2 checkpoint, utilising olomucine. This method of cell cycle inhibition was not efficient enough for isolation of individual populations of cells (*Fig. 3.16.*).

3.3.5. Inhibition of cells in S-phase

Aphidicolin is a tetracyclin diterpene antibiotic that acts as an inhibitor of DNA polymerase α and δ , causing cell cycle arrest at S-phase (Spadari et al., 1985). In previous studies for the isolation of cells at S phase prior synchronisation of cells using the double thymidine block has been implemented (Keryer et al., 1998). I undertook an investigation to assess whether prior synchronisation of Rat-1 cells was required for optimal S phase isolation of the cells. I found that the addition of aphidicolin to an asynchronous population of Rat-1 cells caused their arrest directly in S phase without the need for prior treatment (*Fig. 3.17. Panel A*). Release of the cells from an aphidicolin induced block, by washing them twice with PBS and incubating with fresh media for 3 h prior to cell harvest, allowed the isolation of 88 % of cells in S/G2 (*Fig. 3.17. Panel B*).

3.3.5.1. Alternative means of S phase arrest

The plant amino acid L-mimosine, which inhibits the eIF5-A transcription factor (Hanuske-Abel et al., 1994; Frost et al., 1995), has been reported to arrest cells in S phase (Krude, 1999). However, it was found to be ineffective at arresting Rat-1 fibroblasts in S phase as many cells proceeded to enter G2/M following incubation with the cells (*Fig. 3.18.*).

3.3.6. Inhibition of cells in M-phase

Mitotic arrest can be brought about through several different mechanisms, one method is through the inhibition of cells in S-phase, by the addition of hydroxyurea, which is then removed and cells are released and harvested once they have moved into M phase. This

method of isolating requires exact knowledge of the length of time it takes the cells to pass from S phase, through G2 phase and into mitosis. A more precise mechanism of M-phase arrest uses nocodazole which has a highly specific antimicrotubular activity, promoting tubulin depolymerisation (Mikhailov and Gundersen, 1998; Jordan et al., 1992; Verdoodt et al., 1999). This prevents the cell from establishing a bipolarised state and blocks cell division midway through mitosis at the metaphase/anaphase transition point.

3.3.6.1. *Microtubule disruption agents and M-phase arrest*

The inhibition of mitosis in the Rat-1 cells, as evidenced by FACs analysis (see section 2.2.4.), was apparent upon addition of nocodazole for 14 h (*Fig. 3.19.*). However, nocodazole has also been shown to induce apoptosis in certain cells, including thymocytes (Bumbasirevic et al., 1995), lymphocytes (Verdoodt et al., 1999) and Rat-1 (Kook et al., 2000) cells. Nevertheless, at the concentration of nocodazole used here to achieve mitotic arrest (50 ng/ml), in Rat-1 cells, it was shown not to induce apoptosis (*Table 3.1.*), as evidenced by FACs analysis (Materials and methods 2.2.5.). Nocodazole-induced mitotic arrest was reversible as upon removal of nocodazole from Rat-1 cells re-entry into the next cell cycle was observed (*Fig. 3.20.*).

3.3.6.2. *Alternative antimicrotubular agents for M-phase arrest*

Studies using a different antimicrotubular agent, colcemid, were carried out to confirm the action of nocodazole in causing M-phase arrest. Colcemid also induced mitotic arrest in the Rat-1 fibroblasts. However, nocodazole is used widely as a mitotic inhibitor (Hayne et al., 2000; Mikhailov and Gundersen, 1998; Tsuiki et al., 2001) and was the preferred means of inducing mitotic arrest.

3.3.7. *Expression of marker proteins to determine the isolation of Rat-1 cells in cell cycle phases*

I wished to provide independent confirmation of the observations obtained by FACs analysis on the isolation of the Rat-1 cells in the various phases of the cell cycle, using the different cell cycle inhibitors (see section 2.1.4.). To do this I analysed the presence of cell cycle markers in lysates from the treated cells.

3.3.7.1. *Detection of Cyclin E in cells isolated at different phases of the cell cycle*

Cyclin E during the cell cycle exhibits differential levels of expression and is required for the transition of cells from G1 to S phase (Ohtsubo et al., 1995; Koff et al., 1992; Nakayama et al., 2001; Sheaff et al., 1997). I thus used cyclin E as a marker to confirm the FACs analysis data. Cell lysates isolated from Rat-1 fibroblasts arrested at different phases of the cell cycle (Materials and methods 2.1.4.) were immunoblotted, as outlined in section 2.3.8., with a cyclin E antibody (Santa Cruz Laboratories). The antibody was raised in rabbit against an epitope mapping to the carboxy terminus of cyclin E of rat origin. The levels of cyclin E were elevated in cells isolated at the G1/S point upon treatment with the double thymidine block (Materials and methods 2.1.4.3.), decreasing in the cells subjected to the aphidicolin treatments (S phase) and reaching a minimal level in cells incubated with nocodazole (*Fig. 3.21., Panel A.*).

3.3.7.2. *Detection of Cyclin B in cells isolated at different phases of the cell cycle*

Cyclin B1-dependent activation of cdk1 is required for the transition of cells from G2 to mitosis (Nigg, 2001; Ito, 2000; Grieco et al., 1996) and cyclin B1 exhibits differential levels of expression during the cell cycle (Piaggio et al., 1995; Pines and Hunter, 1989; Smits and Medema, 2001). I thus used cyclin B1 as a further marker to confirm the FACs analysis data, for determination of stage specific isolation of cells upon inhibitor addition (Materials and methods 2.1.4.). Cell lysates isolated from Rat-1 fibroblasts arrested at different phases of the cell cycle (Materials and methods 2.1.4.) were immunoprobed, as outlined in section 2.3.8., with a cyclin B antibody (Pharmingen). There were no detectable levels of cyclin B expressed in cells isolated in G0 or G1/S. However, in cells isolated after either aphidicolin block and release (Materials and methods 2.1.4.4.) or upon nocodazole treatment (Materials and methods 2.1.4.5.) then cyclin B immunoreactivity was evidenced (*Fig. 3.21., Panel B.*). This confirms these treatments arrested cells within G2 and mitosis, as in agreement with the FACs analysis data (*see Figs. 3.17. & 3.19.*).

3.3.7.3. *Detection of phospho-ERK in cells isolated at different phases of the cell cycle*

ERK has been shown to exhibit different levels of activation during the cell cycle (Roovers and Assoian, 2000; Wright et al., 1999; Black et al., 2000; Hayne et al., 2000; Laird et al., 1999). I thus also used this as a marker to confirm the FACs analysis data, for determination of stage specific isolation of cells upon inhibitor addition (Materials and methods 2.1.4.). The activation status of ERK was determined by analysis of the phosphorylation of the TEY motif, detected using a phospho-ERK antibody. Cell lysates isolated from Rat-1 fibroblasts, arrested at different phases of the cell cycle (Materials and methods 2.1.4.), were immunoprobed, as outlined in section 2.3.8., with a phospho-ERK antibody (Upstate Biotechnology). The antibody was raised in mouse against a phosphopeptide specific for dually-phosphorylated ERK1 and ERK2. There were high levels of immunoreactive phospho-ERK detected during serum deprivation, the levels decreased in thymidine treated cells (Materials and methods 2.1.4.3.), recovering again in cells subjected to aphidicolin treatments (Materials and methods 2.1.4.4.). The levels of phosphorylated ERK were reduced in cells isolated in mitosis, upon incubation with nocodazole. (*Fig. 3.21., Panel C.*)

3.3.7.4. *Detection of phospho-MEK in cells isolated at different phases of the cell cycle*

MEK directly activates ERK by phosphorylation of the TEY motif (Crews and Erikson, 1992; Crews et al., 1992). MEK also exhibits differential activation during the cell cycle, paralleling the activity profile of ERK (Roovers and Assoian, 2000; Wright et al., 1999; Hayne et al., 2000; Laird et al., 1999). MEK was therefore also used as a marker to confirm the FACs analysis and phospho-ERK data, for determination of stage specific isolation of cells upon inhibitor addition (Materials and methods 2.1.4). Activation of MEK was determined by analysis of the phosphorylation status of residues Ser²¹⁸ and Ser²²², as detected using a phospho-MEK antibody. Cell lysates isolated from Rat-1 fibroblasts arrested at different phases of the cell cycle (Materials and methods 2.1.4.) were immunoprobed, as outlined in section 2.3.8., with the phospho-MEK antibody (Upstate Biotechnology). The antibody was raised in goat against a phosphopeptide specific for dually-phosphorylated MEK1 of human origin. There were high levels of immunoreactive phospho-MEK detected after serum deprivation, the levels were decreased in double thymidine-blocked cells, isolated at the G1/S transition and increased again in cells

subjected to aphidicolin treatment. The levels of phosphorylated MEK were also low in cells isolated in mitosis, upon incubation with nocodazole (*Fig. 3.21., Panel D*).

3.4. Analysing the changes in cAMP phosphodiesterase activity in the cell cycle

Once I established that populations of Rat-1 cells could be isolated at specific phases of the cell cycle in sufficient amounts to perform biochemical analysis. I thus set out to see if alterations in PDE isozyme activities occurred on the progression of the cells through the cell cycle.

3.4.1. Determination of cAMP PDE activity in Rat-1 cells isolated at different stages of the cell cycle

The profile of total PDE enzymatic activity (Materials and methods 2.3.9.) changed in lysates obtained from Rat-1 cells arrested at specific stages of the cell cycle (*Fig. 3.22., Panel A*). There appeared to be a general increase in the total PDE activity of cells that had been serum starved for 48 h. This activity then decreased in cells arrested at the G1/S transition and then decreased further as cells passed through S phase and entered G2. However, when cells were arrested within mitosis an elevated total PDE activity was seen, which decreased as the cells were released into the latter phases of mitosis and the next cell cycle.

Cyclic AMP hydrolysis in cells can be achieved through the action of various different PDE isozymes. Thus the activities of the major cAMP hydrolytic enzymes, PDE3 and PDE4, were examined in the Rat-1 cells in order to assess their relative contributions.

3.4.1.1. PDE4 activity in Rat-1 cells isolated at different stages of the cell cycle

In order to monitor cAMP specific hydrolysis catalysed by PDE4, PDE enzymatic activity of cell lysates was assayed in the presence of 10 μ M of the PDE4-specific inhibitor, rolipram (Materials and methods 2.3.9.). It was found that the rolipram-sensitive PDE4 activity provided a major fraction of the total cAMP-specific hydrolytic activity in these cells when they were left asynchronous (~ 75 %, *Fig 3.22., Panel B*). Whilst little change in the profile of PDE4 activity occurred during different stages of the cell cycle, a slight increase in PDE4 activity was seen in cells arrested in mitosis. This elevation in PDE4

activity decreased as cells passed through mitosis, reaching 'basal' levels as the cells entered the next G1.

3.4.1.2. PDE3 activity in Rat-1 cells isolated at different stages of the cell cycle

In order to elucidate possible changes in PDE3 activity in cells arrested at specific phases of the cell cycle, PDE assays were done in the presence of 10 μ M of the PDE3-specific inhibitor, cilostomide. Almost all of the residual cAMP-specific PDE activity, after PDE4 inhibition, was found to be attributable to PDE3 (*Fig. 3.22.*). The profile of PDE3 activity did not appear to change through the cell cycle and thus further studies were focused on the cell cycle dependent changes in PDE4 activity.

3.4.2. Analysis of PDE4 isoform activity changes in cells isolated at different stages of the cell cycle

With PDE4 identified as the most active class of cAMP hydrolysing PDE within Rat-1 fibroblasts a more detailed analysis of the enzymatic activity of the individual PDE4 isoforms in lysates isolated at different phases of cell cycle was carried out. Specific PDE4 isoforms were immunoprecipitated from the cell lysates using PDE4 sub-family specific antiserum (see section 3.2.). It has previously been confirmed that antibody binding to the PDE4 isoforms during immunoprecipitation does not affect their activity (Baillie et al., 2000). This provides an effective means of assessing individual PDE4 isoform activity. Indeed, it is the only way currently available because, as yet, there are no PDE4 isoform-specific inhibitors.

3.4.2.1. Changes in PDE4A and PDE4C isoform activity in cells isolated at different stages of the cell cycle

PDE4A and PDE4C proteins from Rat-1 cell lysates were successfully immunoprecipitated (for examples see *Figs. 3.4. & 3.10.*). However, the activities they exhibited showed little discernible change when isolated from Rat-1 cells arrested in specific phases of the cell cycle (*Fig. 3.23., Panels A and C*).

3.4.2.2. *Changes in PDE4B activity in cells isolated at different stages of the cell cycle*

Depending on which particular stage of the cell cycle the cells had been arrested, between 15-40 % of the total PDE4 activity in Rat-1 cells was attributable to the PDE4B isoform (*Fig. 3.23.*). The PDE4B specific activity was constant in lysates from cells isolated at all phases of the cell cycle apart from those cells subjected to aphidicolin block release. This arrested cells at S/G2, where PDE4B activity was increased by 0.5-fold. However, isolation of cells in mitosis showed no such increase in PDE4B activity (*Fig. 3.23., Panel B*).

3.4.2.3. *Changes in PDE4D activity in cells isolated at different stages of the cell cycle*

PDE4D was the most active species of the PDE4 subfamilies contributing to the cAMP hydrolytic activity in the Rat-1 cells (*Fig. 3.23.*). From immunoblotting studies of the Rat-1 cell lysates it was evident that the only species of PDE4D present was PDE4D3 (*see Fig. 3.11.*). There was very little change in activity of PDE4D observed in lysates isolated in the G0, G1, S and early G2 cell cycle phases. However, in cells arrested in mitosis there was a 1.7-fold increase in PDE4D activity (*Fig. 3.23., Panel D*).

3.4.2.4. *Changes in PDE4D protein expression in cells isolated at different stages of the cell cycle*

I set out to determine whether the increase in PDE4D cAMP-specific hydrolytic activity seen in cells arrested in mitosis was due to an activity change or whether it was the result of an increase in PDE4D3 protein expression. I thus analysed the expression levels of PDE4D3 in cell lysates isolated at different stages of the cell cycle. This was carried out by enzyme linked immuno-absorbent assay (ELISA, Materials and methods 2.3.3.), using the C-terminal PDE4D specific antibody. In mitotically extracted lysates the level of PDE4D protein expression was similar to that found in cells lysates from all other phases of the cell cycle (*Table 3.2.*). Thus suggesting that the increase in PDE4D activity in mitosis was not caused by up regulation of PDE4D3 protein or the up-regulation of any other PDE4D isoform, but was due to a change in the specific activity of PDE4D3.

3.4.3. Subcellular localisation of PDE4D protein in cells isolated at different stages of the cell cycle

Changes in the subcellular distribution of PKA RII α subunit has been noted in during mitosis (Keryer et al., 1998). Therefore I set out to determine whether there was a change in the subcellular localisation of PDE4D3 in cells isolated at different phases of the cell cycle. When cells isolated in different phases of the cell cycle (Materials and methods 2.1.4.) were fractionated by differential centrifugation (Materials and methods 2.1.3.2.) it was found that there was no change in the distribution of PDE4D protein between the subcellular fractions (*Figures 3.24a & 3.24b.*).

3.5. Analysis of the changes in PKA activity in the cell cycle

The changes observed in PDE4 activity during the cell cycle in Rat-1 cells may provide an important contribution in determining the intracellular concentrations of cAMP by mediating its degradation. If increased cAMP hydrolysis should lead to lower the cAMP concentration in the cells this, in turn, may lead to the inactivation of PKA, so terminating the PKA signalling cascade activation. In order to determine the importance of the variation in PDE4 activities in Rat-1 cells, and any relationship it has to the changes in PKA activity, I set out to observe if alterations in PKA activity occurred in cells isolated at different stages of the cell cycle.

3.5.1. Determination of PKA activity in cells isolated at different stages of the cell cycle

Work has been carried out by several groups on the activity of PKA during the cell cycle in cell types as diverse as *Xenopus* oocytes and *Saccharomyces cerevisiae* (Felicciello et al., 2000; Grieco et al., 1996; Anghileri et al., 1999). In order to establish the fluctuations of PKA activity in Rat-1 fibroblasts, cells were isolated at specific stages of the cell cycle and then analysed for PKA activity (Materials and methods 2.4.1.).

3.5.1.1. Changes in PKA activity in the cell cycle

PKA activity peaked in lysates isolated at G0 phase of the cell cycle (*Fig. 3.25.*). However, the activity of PKA was lower in lysates obtained from cells isolated at other phases of the cell cycle, with the lowest activity observed during nocodazole-induced, metaphase arrest.

PKA activity increased again as the cells were released from the mitotic block and passed through the end of mitosis into G1 of the next cell cycle (*Fig. 3.25.*).

3.5.1.2. Detection of phospho-CREB in cell lysates isolated at different phases of the cell cycle

In addition to measuring PKA activity directly, as above, the phosphorylation of the cyclic-AMP response element binding protein (CREB) was used as a marker of PKA activity. Rat-1 cell lysates were immunoprobed with a phospho-CREB antibody (Upstate biotechnology). The antibody has been raised in rabbits to a synthetic phosphopeptide corresponding to residues KRREILSRPpSYRK, which specifically detects PKA phosphorylated CREB (Bito et al., 1996). In agreement with the PKA activity data, the cell lysates isolated at specific phases of the cell cycle indicated that CREB was highly phosphorylated in cells arrested in G0 and the levels of CREB phosphorylation decreased in cells isolated at different stages of S phase, reaching a minimum in cells isolated in mitosis (*Fig. 3.26.*).

3.5.1.3. Levels of PKA activity controlled specifically by PDE4 dependent mechanisms in Rat-1 cells

To assess the contribution of PDE4 enzymes in the control of intracellular PKA activation, Rat-1 cells arrested in different phases of the cell cycle were treated with the PDE4 specific inhibitor rolipram for 15 min prior to harvesting for the PKA activity assay. It was observed that, upon the addition of rolipram to asynchronous cells and cells isolated in quiescence, there was no change in PKA activity. However, in cells isolated during S phase and mitosis the rolipram-mediated inhibition of PDE4 induced an elevation in PKA activity, increasing the percentage of active PKA in the cells back to basal levels observed in cells deprived of serum for 48 h (*Fig. 3.27.*).

3.6. The effects of the inhibition of PDE isoforms on cell proliferation

In order to study the significance of PDE activity on the control of cell cycle transition, the inhibition of the various cAMP-specific PDE isoforms, within the Rat-1 cells, was carried out. It has previously been shown that growing bovine aortic endothelial cells in the presence of the non-selective PDE inhibitor, IBMX, inhibits growth of the cells by 60 - 80 % (Leitman et al., 1986). The inhibition of PDE4 specifically has been demonstrated to

inhibit the proliferation of such cells as umbilical cord blood mononuclear cells (Banner et al., 2000), vascular smooth muscle cells (Pan et al., 1994) and in MJ cells, an HTLV-1 transformed T cell line (Ekholm et al., 1999).

3.6.1. Inhibition of PDE4 reduces Rat-1 cell proliferation

I set out to examine the effect of PDE4 inhibition on the rate of cell cycle phase transition and proliferation. I analysed the distribution of Rat-1 cells, within the cell cycle, in the presence and absence of the PDE4 specific inhibitor, rolipram, by FACs analysis (see section 2.2.4.). Sub-confluent, proliferating Rat-1 cells were pulse-labelled with BrdU for 30 min, then incubated with 10 μ M rolipram for up to 18 h. Cells were removed at 3 h intervals during this treatment and their distribution within the cell cycle were determined.

3.6.1.1. Inhibition of PDE4 alters the distribution of Rat-1 cells within the cell cycle

Upon inhibition of PDE4 in Rat-1 cells there was a decrease in the proportion of cells isolated in S phase when the distribution of the cells within the cell cycle was compared to untreated cells. This change in cell cycle phase distribution was due, within the first 9 h of cell isolation, to an increase in the proportion of cells entering G2 /M (*Fig. 3.28.*). In the later stages of the study, from 12 h to 18 h, there was also a decrease in the amount of cells isolated in S phase. This was due to the elevation of cells in the G1 / G0 phases of the cell cycle. Thus the rolipram-mediated inhibition of PDE4 presumably increased cAMP concentration in these cells and reduced the rate of G1/S transition.

3.6.2. Inhibition of PDE3 does not alter the rate of Rat-1 cell proliferation

To examine the effect of PDE3 inhibition on the rate of cell cycle phase transition and proliferation cell cycle, the distribution of Rat-1 cells was determined by FACs analysis (see section 2.2.4.), in the presence and absence of the PDE3 specific inhibitor, cilostomide. Sub-confluent proliferating Rat-1 cells were pulse-labelled with BrdU for 30 min, then incubated with 10 μ M cilostomide for up to 18 h. Cells were removed at 3 h intervals during this treatment and their distribution within the cell cycle was determined.

3.6.2.1. Inhibition of PDE3 does not alter the distribution of Rat-1 cells within the cell cycle

Upon incubation of cells with cilostomide the distribution of cells through the phases of the cell cycle did not alter throughout the 18 h analysis period when compared cells treated with vehicle only. There was a slight initial decrease in the proportion of cells in S phase, with 3 h cilostomide treatment, which was concurrent with an increase in the proportion of cells detected in G2 /M phase (*Fig. 3.29.*). Unlike rolipram treatment of the Rat-1 fibroblasts there was no accumulation of cells within the G1 /G0 phases after a 12 –18 h incubation with cilostomide.

3.7. Discussion and conclusions

Every cell type appears to express a unique profile of PDE isoforms (for some examples see Conti et al., 1998; Juilfs et al., 1997; Bloom and Beavo, 1996; Erdogan and Houslay, 1997). These presumably enable differential control of hydrolysis of cyclic nucleotides so as to elicit specific functional consequences within the cell. The major cyclic nucleotide phosphodiesterases that specifically hydrolysed cAMP in Rat-1 fibroblasts were shown to be of the PDE3 and PDE4 families. The PDE4 isozymes contributed the majority (~72 %) of the total cAMP specific enzymatic activity within these cells, assessed at 2 μ M cAMP. The elucidation of the PDE4 isoform profile showed conclusively that the PDE4B2, PDE4C2 and PDE4D3 isoforms were expressed. Although the profile of expressed PDE4A isoforms was not conclusively established it was presumed, from observations made in this study and from those made previously by other lab members (personal communication, E. Huston) that the PDE4A5 isoform was also expressed.

Increased PDE activity is associated with cells that have elevated proliferation rates (Tsou et al., 1974; Tsou et al., 1986). This, presumably, acts to reduce levels of cAMP and maintain low levels of the G1 cyclin dependent kinase (cdk) inhibitor, p27^{KIP1} (Hengst and Reed, 1996; van Oirschot et al., 2001). As high levels of the active cdk complexes, cdk4/cyclin D and cdk2/cyclin E, are required for G1/S transition (L'Allemain et al., 1997; van Oirschot et al., 2001; Naderi et al., 2000) this may provide a major means whereby cAMP regulates the cell cycle. During progression through the cell cycle changes in the profiles of activities of PDE families have been noted within *Actinomyces* (Lefebvre et al., 1980) and *Physarum polycephalum* (Lovely and Threlfall, 1978; Lovely and Threlfall, 1979; Kupetz and Jeter, Jr., 1985). Similarly, alterations in the activities of specific PDE isoforms during the cell cycle have been observed within germ cells (Morena et al., 1995). However, no attempts have been made to identify changes in specific PDE isoform activities in somatic cell lines.

In order to study activities of PDE isoforms at specific phases of the cell cycle in a somatic cell line it is necessary to isolate sufficiently large populations of cells at these phases to allow for biochemical analysis. Although many studies have been able to maintain an asynchronous population of cells by the re-addition of growth factors to serum deprived cells, this was found not to be a means by which Rat-1 cells retained synchrony.

There are well-characterised methods for the isolation of various cell types at different phases of the cell cycle, using chemical means (Fantès and Brooks, 1993). In this study

these methods were optimised for Rat-1 fibroblasts and cell cycle distribution was determined utilising FACs analysis. These observations were confirmed by immunoblot analysis of cell lysate for cyclins that undergo differential expression (Sauer and Lehner, 1995; Nakayama et al., 2001; Piaggio et al., 1995; Pines and Hunter, 1989; Smits and Medema, 2001) and enzymes which are subjected to differential activation (Roovers and Assoian, 2000; Wright et al., 1999; Black et al., 2000; Hayne et al., 2000; Laird et al., 1999) through the cell cycle.

Once methods of isolation of Rat-1 cell populations at specific stages of the cell cycle were established I undertook investigations into the fluctuation of cAMP-specific PDE activity in these cells. No clear alterations in total PDE activity in Rat-1 cells was evident in cells isolated at different stages of the cell cycle. However, a slight elevation in total PDE activity was noted in cells isolated in both G0 and mitosis (*Fig. 3.22., Panel A*). As both PDE3 and PDE4 represent the major fraction of the total cAMP PDE activity, in cells assayed at 2 μ M cAMP, I then analysed the rolipram-inhibited PDE4 activity. This allowed me to identify a slight increase in PDE4 activity in cells arrested in mitosis. Similarly, PDE4 activity represents the action of multiple isoforms. I thus determine that in the mitotic cell population the activity of PDE4D3 contributed to approximately 67 % of the PDE4 activity, PDE4B2 contributed to approximately 17 %, PDE4C2 approximately 8 % and PDE4A5 approximately 7 %. Meanwhile, cilostomide-inhibited, PDE3 activity showed no change in activity between lysates isolated at any stage of the cell cycle.

This study of the changes of PDE4 isoform activity profiles in the cell cycle made evident the fact that there was a 1.7 fold elevation in the levels of PDE4D3 activity within cell lysates isolated during mitosis (*Fig. 3.23, Panel D*), whereas no other isoforms demonstrated any major fluctuations in activity. Given that the absolute levels of PDE4D3 protein appeared unchanged throughout the cell cycle a likely explanation for this increased activity was that PDE4D3 was being modified in some way, so as to activate it. One possibility is that this modification and activation occurs through phosphorylation, another is that an inhibitory protein could be released from the phosphodiesterase when the cells are arrested in mitosis, again elevating activity. However, phosphorylation of PDE4D3 by PKA and ERK is known to regulate its enzymatic activity (Sette and Conti, 1996; Hoffmann et al., 1999), as is the binding of phospholipids (Grange et al., 2000; Nemoz et al., 1997). Of the phosphorylation processes, PKA phosphorylation of Ser⁵⁴ in UCR1 of PDE4D3 causes it to be activated (Lim et al., 1999) and in contrast ERK phosphorylation of Ser⁵⁷⁹ in the catalytic unit causes its inhibition (Hoffmann et al., 1999).

As I observed activation of PDE4D3 in mitosis I set out to see if PKA was activated during mitosis.

Fluctuations in the levels of active PKA during the cell cycle have been shown in oocytes (Grieco et al., 1996) and cells from budding and fission yeast (Yamashita et al., 1996; Grieco et al., 1996; Kotani et al., 1998). The proportion of active PKA in Rat-1 fibroblasts was shown to be maximal in quiesced cells, which had been deprived of serum for 48 h, confirming previously documented observations of the increase in active PKA in quiesced cells (Pastan et al., 1975; Grieco et al., 1996). Cells arrested through the stages of S phase had a decreasing proportion of active PKA, and those cells arrested in mitosis contained the lowest detected proportion of active PKA. These alterations in PKA activity were confirmed by immunoblot analysis of the amount of CREB in the cell that had been phosphorylated by PKA.

A decrease in PKA activity can be brought about either by the inactivation of adenylate cyclases or by the activation of phosphodiesterases (Houslay and Milligan, 1997). A decrease in PKA activity during mitosis has been noted before by others in *xenopus* oocytes (Grieco et al., 1996; Fernandez et al., 1995), budding yeast (Anghileri et al., 1999), in fission yeast (Yamashita et al., 1996; Yanagida et al., 1999), in lymphoid precursor Reh cells (Blomhoff et al., 1988; Christoffersen et al., 1994) and in fibroblasts (Lamb et al., 1991; Hohmann et al., 1993; Kotani et al., 1998; Kotani et al., 1999; Oh et al., 1996; Zeilig et al., 1976). However, the underlying mechanism of PKA inactivation at mitotic onset has not been elucidated, although in yeast the deletion of phosphodiesterases prevents mitotic exit (Anghileri et al., 1999; Yanagida et al., 1999). The mitotic elevation of PDE4, and more specifically the increase in PDE4D3 activity, coincides with this observed down-regulation in PKA activity. This raises the intriguing possibility that the elevated PDE4D3 activity in mitotic cells decreases the levels of cAMP, causing the inactivation of PKA. To investigate the involvement of PDE4 isoforms in the control of PKA activity in cells isolated at different phases of the cell cycle I thus set out to specifically inhibit PDE4 activity, using rolipram, in order to define the consequential changes in PKA activity. This showed that rolipram inhibition of PDE4 activity appeared to cause an increase in PKA activity in cells isolated in S phase and mitosis. This is consistent with the suggestion that PDE4 is playing a role in the control of PKA activity during mitosis.

Studies by other groups have suggested that PDE4 inhibition causes a reduction in the rates of proliferation in several cell types, including umbilical cord and peripheral blood mononuclear cells (Banner et al., 2000; Banner et al., 1995), T helper cell clones (Essayan

et al., 1997), aortic endothelial cells (Leitman et al., 1986), melanoma and mammary carcinoma cells (Drees et al., 1993). Indeed, inhibition of PDE4 has also been shown to specifically inhibit cell cycle progression at the G1/S transition (Matousovic et al., 1997 133 /id; Drees et al., 1993). However, negligible alterations in proliferation of Rat-1 cells were seen here upon the incubation of Rat-1 cells with rolipram (*Fig. 3.28.*), Indeed, there appeared only to be a small proportion of the cells arresting prior to the G1/S transition. However, there was a slight redistribution of the Rat-1 cells within the cell cycle upon incubation with rolipram, presumably due to a reduction of cells in S phase. This coincided with an increase in the amount of cells in G2/M and a decrease in the number of cells moving from G1 (*Fig. 3.28.*). Although the incubation of Rat-1 cells with rolipram appeared only to give a slight change in cell cycle distribution there was no change in the distribution of Rat-1 cells incubated with the PDE3 inhibitor cilostamide. The simultaneous inhibition of PDE3 and PDE4 might be an interesting area to look into here, as it has been shown that simultaneous inhibition of the phosphodiesterases potentiates the inhibition of smooth muscle cell proliferation (Johnson-Mills et al., 1998; Pan et al., 1994; Souness et al., 1992).

In this chapter I have presented work showing the optimisation of conditions for accurately arresting Rat-1 fibroblasts at various stages of the cell cycle. This was then used for analysis of PKA and PDE activities in these various phases. Such studies uncovered the novel and particularly interesting observation that PDE4D3 enzymatic activity was increased during mitosis, a phase where PKA is least active. Rolipram mediated inhibition of PDE4 activity was shown to activate PKA at G1/S, S, G2 and M phases of the cell cycle. There is also a suggestion that there is a slight redistribution of cells from S phase to the G2/M and G1 phases of the cell cycle upon incubation with rolipram. The next chapter aims to build on these observations and in particular to focus on and further characterise the cell cycle-dependent alterations in PDE4D3 activity.

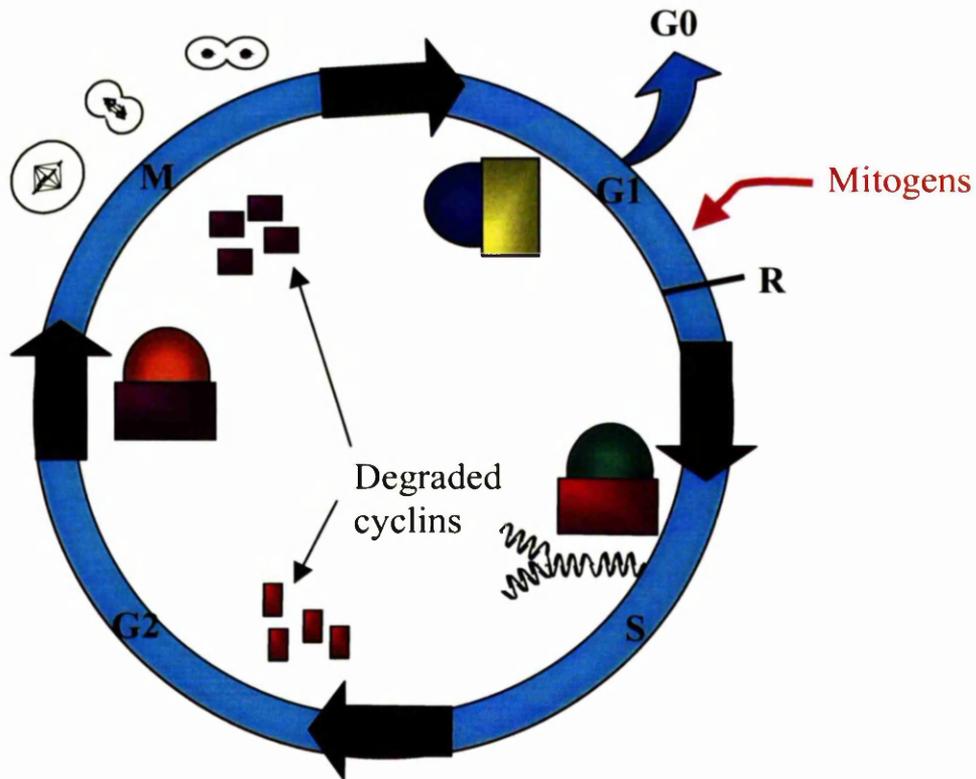


Figure 3.1. Stages of the cell cycle. A schematic representation of the phases of the cell cycle indicates that mitogen stimulation of cells in G1 induces the expression of protein required for G1/S transition. If mitogens are removed prior to the passage of cell through the restriction point (R) they leave the cell cycle and quiesce (G0). Once passed R, however, cells are committed to complete one cell cycle under autonomous control. DNA is replicated during S phase and checkpoint mechanisms allow cyclin degradation and allow progression into the second gap phase (G2). Mitotic progression (M) is under strict control mechanisms which rely on the degradation of cyclins to enable cell division to take place.

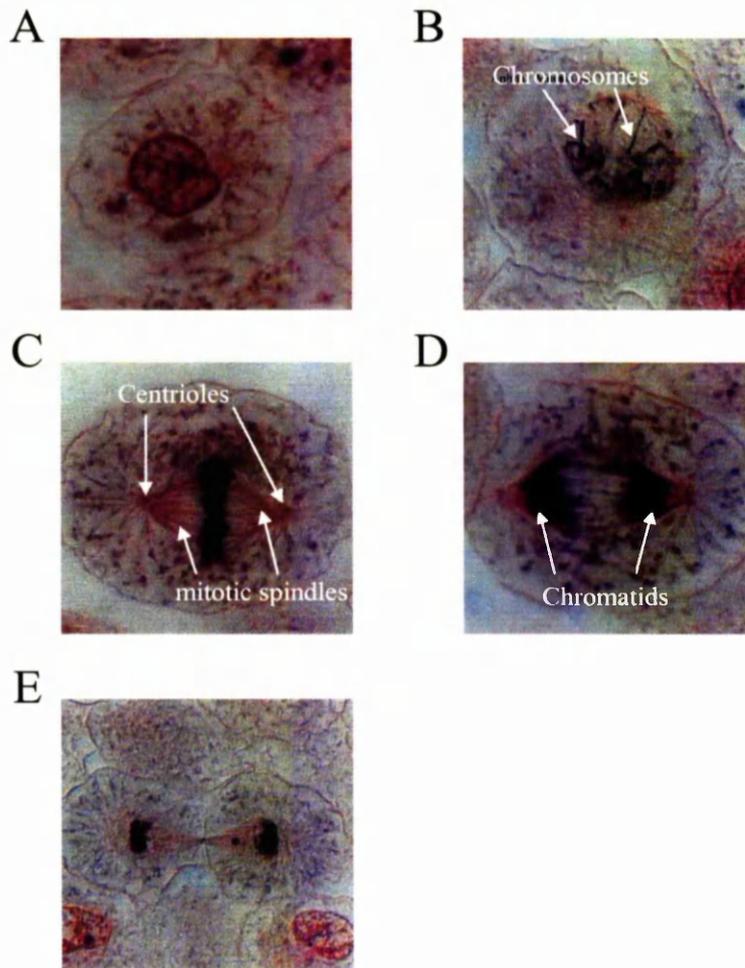


Figure 3.2. The changes in chromosome morphology during the different phases of mitosis. Upon transition of the cells from interphase (A) to prophase (B) the chromosomes condense and become visible. Chromosomes then attach to the mitotic spindles, which are generated between the centrioles, during metaphase (C). The chromatids segregate and migrate to opposite poles of the cell in anaphase (D) and the cells finally divide by cytokinesis during telophase (E). Pictures taken from <http://www.bioweb.uncc.edu/biol1110/Stages.htm>

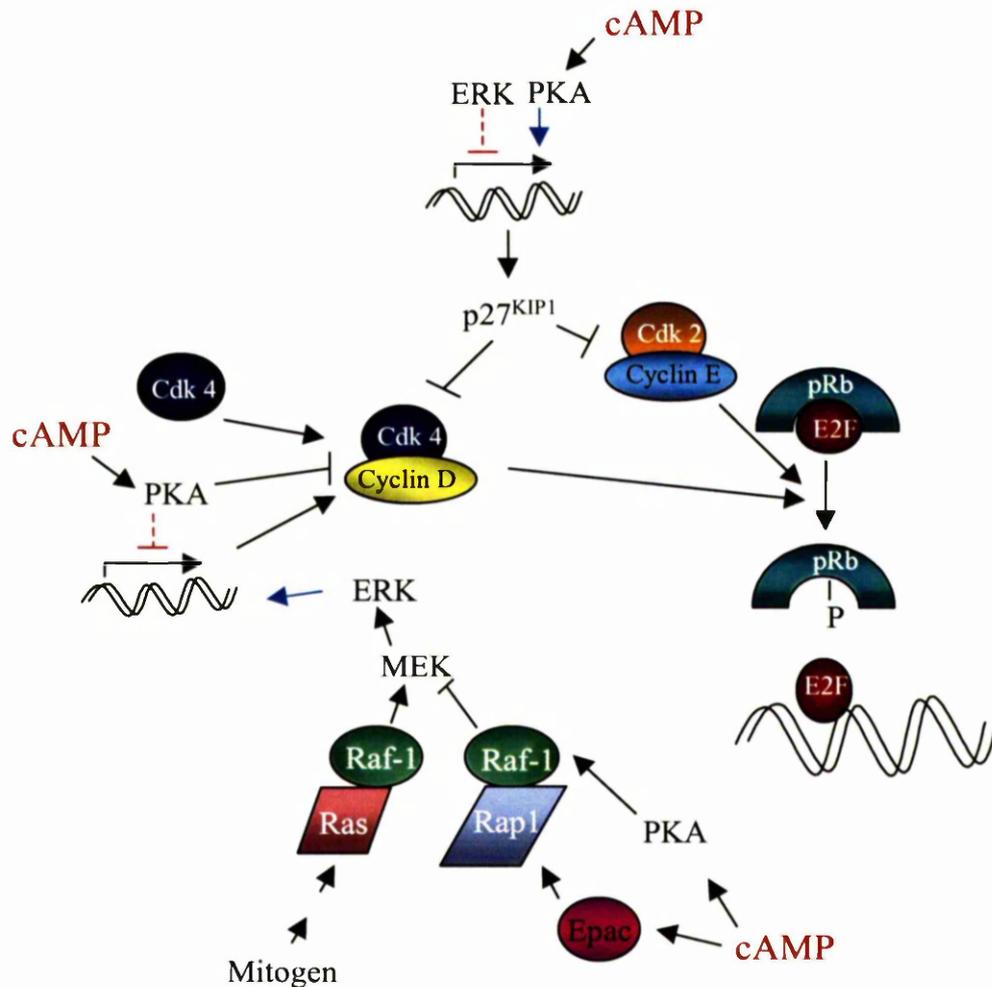


Figure 3.3. Effects of cAMP elevation and PKA activation on G1/S arrest. Cyclic AMP elevation acts on several signalling mechanisms in order to bring about arrest of cells prior to the G1/S transition. Activation of PKA, by cAMP, leads to down regulation of the expression of the G1 dependent D-type cyclins. PKA increases the expression of p27^{KIP1}, the cdk inhibitor molecule which binds to the active cdk complexes, cyclin D/cdk4 and cyclin E/cdk2. By decreasing the levels of active cyclin complexes the phosphorylation of the tumour suppressor retinoblastoma protein (pRb) is blocked. This then sequesters the E2F transcription factor and prevents expression of proteins required for G1/S transition. PKA activation interferes with the activation of the ERK signalling cascade as PKA phosphorylation of Raf-1 prevents it from forming an active complex with Ras and thus interferes with the activation of MEK. Cyclic AMP can also activate Epac, which causes activation of Rap-1. The affinity of Rap-1 for Raf-1 increases which in turn inactivates the MEK-ERK mediated mitogen signalling cascade.

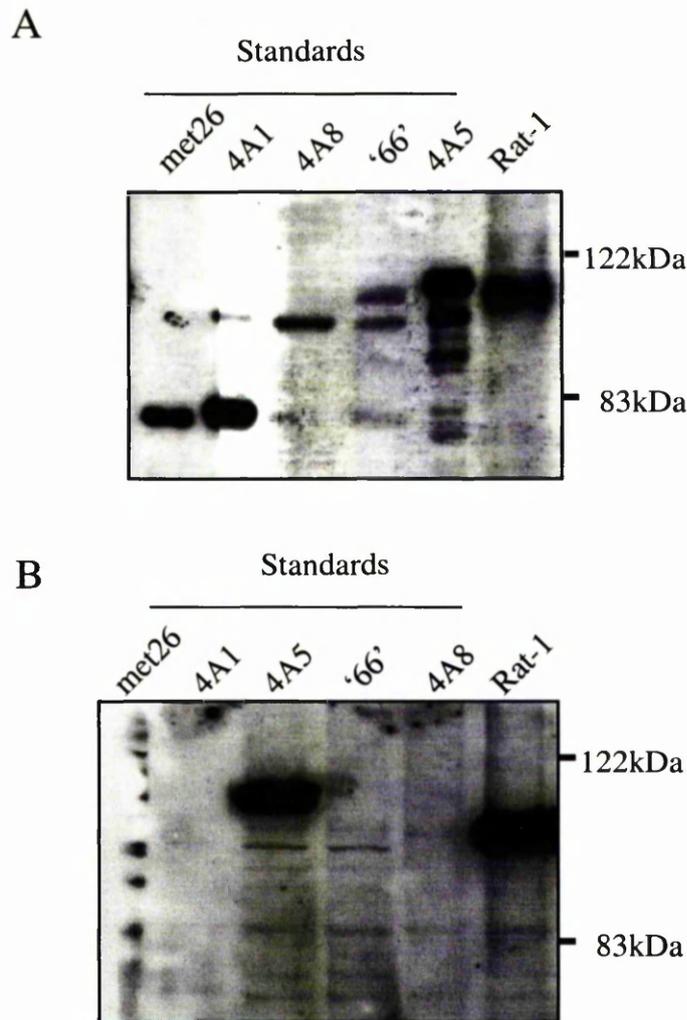


Figure 3.4. Western blot analysis of PDE4A isoforms expressed in Rat-1 cells. *Panel A*, Rat-1 cells were harvested in 3T3 lysis buffer and PDE4A was isolated from 1 mg of Rat-1 lysate using a specific antibody directed against the C-terminus of PDE4A, as described in section 3.2.1.. The isolated protein (Rat-1) was subjected to SDS-PAGE on an 8 % gel alongside 25 μ g recombinant protein of PDE4A splice variants PDE4Amet26 (met26, an N-terminally truncated species of PDE4A1, 76 kDa), PDE4A1 (4A1, 79 kDa), PDE4A8 (4A8, 98 kDa), rpde66 ('66', a rat PDE4A splice variant that has since been found to be an artefact) and PDE4A5 (4A5, 109 kDa), as indicated. The proteins were transferred to nitrocellulose which was then immunoblotted with the same PDE4A specific antibody. The positions of molecular weight markers are indicated. *Panel B*, The same immunoprecipitated protein and protein standards were immunoprobed with a PDE4A5 specific antibody directed against the N-terminus of PDE4A5, as described in section 3.2.1., the molecular weight markers are indicated.

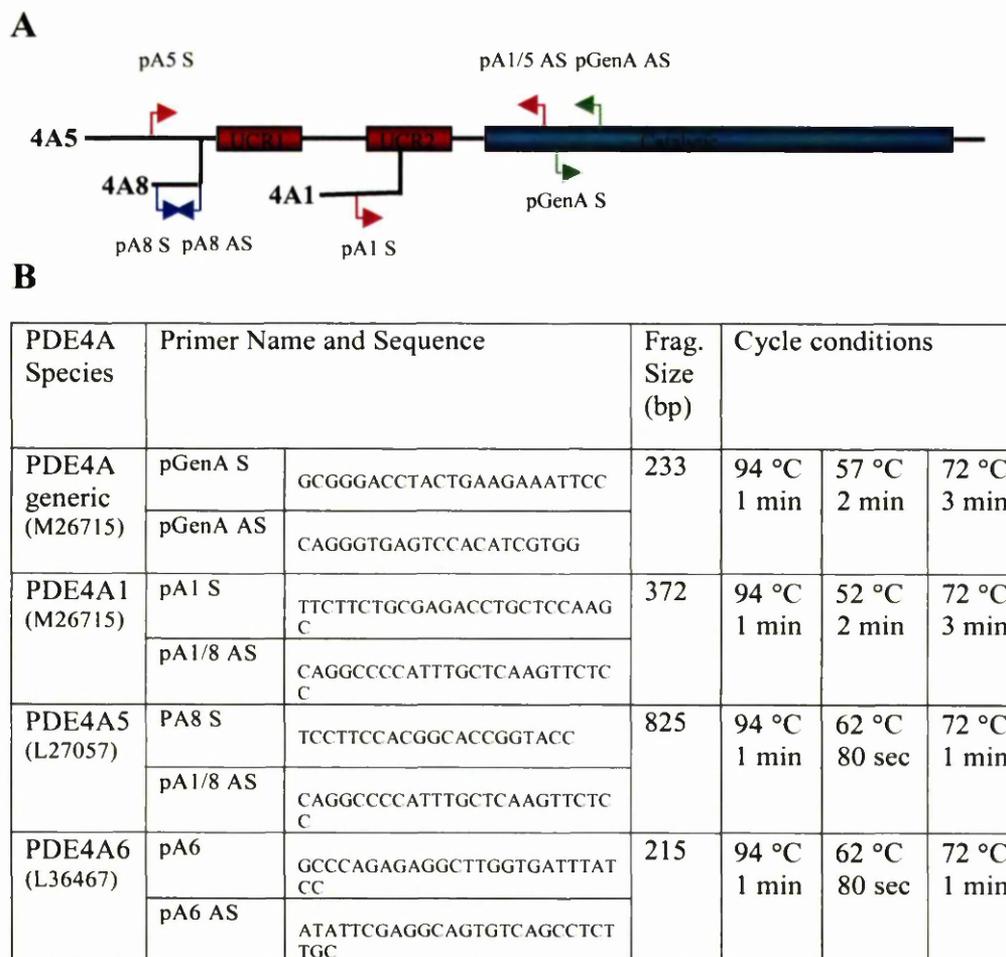


Figure 3.5. Annealing positions of primers and primer sequences for RT-PCR analysis of rat PDE4A splice variants. *Panel A*, a schematic representation of the annealing positions for the RT-PCR primers on mRNA transcripts of rat PDE4A splice variants, RNPDE4A1A, RNPDE4A5A and RNPDE4A8. The primer pairs used in each reaction are highlighted in the same colours, with all sense primers indicated by arrows to the right and antisense primers indicated by arrows to the left. *Panel B*, a table defining specificity of each primer, the primer nomenclature, the primer sequence, the expected size of each amplified fragment and the PCR cycling conditions. Each RT-PCR reaction was subjected to an initial 15 min incubation at 95 °C followed by 40 cycles, specified for each primer pair.

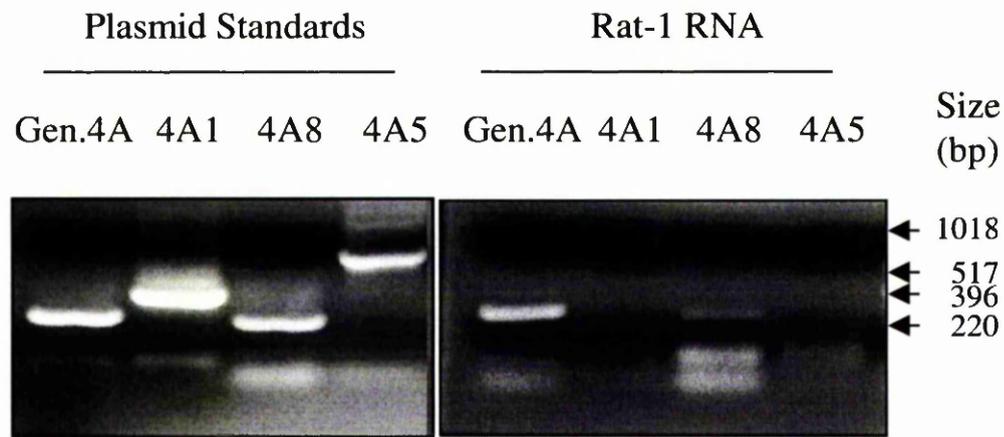


Figure 3.6. RT-PCR analysis of Rat-1 cell total RNA using PDE4A specific primers. RNA isolated from Rat-1 cells was subjected to first strand cDNA synthesis followed by RT-PCR (*see section 2.5.10.*), using primers designed specifically to regions found within the generic PDE4A sequence (Gen 4A), to PDE4A1 specific sequence (4A1), PDE4A5 specific sequence (4A5) and PDE4A8 specific sequence (4A8) (*see Fig. 3.5.*). As controls plasmids encoding the relevant PDE4A isoform, as indicated, were subjected to the same PCR reactions. The PCR products were separated on a 2 % agarose gel and the PDE4A products from the Rat-1 RNA (right hand panel) were compared to the produces from PCR of the plasmid standards (left hand panel, for product sizes see *Fig. 3.5.*). The size of the standard DNA markers are indicated in base pairs (bp).

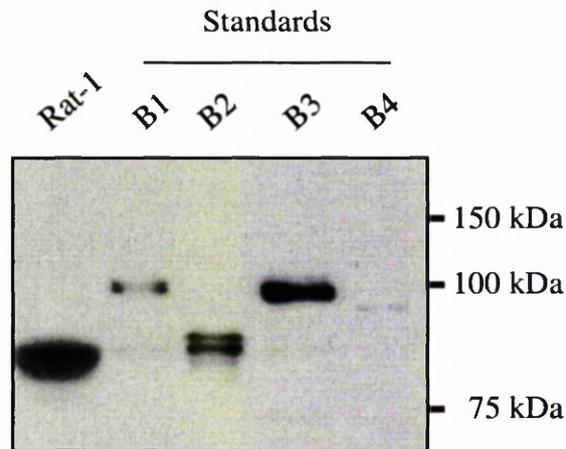
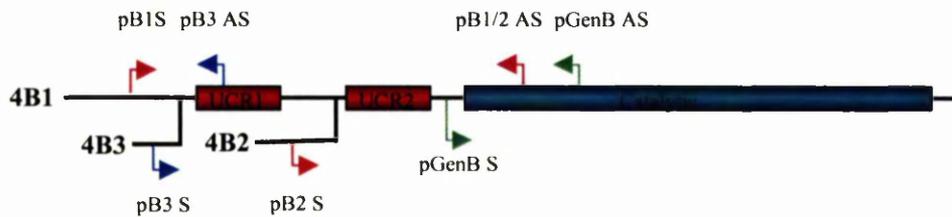


Figure 3.7. Western blot analysis of PDE4B isoforms expressed in Rat-1 cells. Rat-1 cells were harvested in 3T3 lysis buffer and 100 μ g protein from the cell lysate (Rat-1) was subjected to SDS-PAGE on an 8 % gel alongside 25 μ g recombinant PDE4B isoform standards of PDE4B1 (B1, 104 kDa), PDE4B2 (B2, 80 kDa), PDE4B3 (B3, 103 kDa) and PDE4B4 (B4, 90kDa). The proteins were transferred to nitrocellulose and immunoblotted with a polyclonal PDE4B specific antibody, as described in section 3.2.2.. The positions and sizes of molecular weight markers are indicated on the right hand side.

A



B

PDE4A Species	Primer Name and Sequence		Frag. Size (bp)	Cycle conditions		
	Primer Name	Sequence		94°C	55°C	72°C
PDE4B generic (J04563)	pGenB S	CAGCTCATGACCCAGATA AGTGG	786	94°C 1min	55°C 2min	72°C 3min
	pGenB AS	GTCTGCACAATGTACCAT GTTGCG				
PDE4B1 (J04563)	pB1 S	GGAGAGGCAGAAGGTGCT GT	929	94°C 1min	58°C 80sec	72°C 70sec
	pB1/2 AS	GCCACGTTGAAGATGTTA AGGCC				
PDE4B2 (L27059)	pB2 S	GGTAGATCACTGACACCT CATCC	667	94°C 1min	58°C 80sec	72°C 70sec
	pB1/2 AS	GCCACGTTGAAGATGTTA AGGCC				
PDE4B3 (U85048)	pB3 S	CTCCACGCAGTTCACCAA GGAAT	598	95°C 1min	63°C 2min	72°C 3min
	pB3 AS	TGTGTCAGCTCCCGGTTCA GC				

Figure 3.8. Annealing positions of primers and primer sequences for RT-PCR analysis of rat PDE4B splice variants. *Panel A*, a schematic representation of the annealing positions for the RT-PCR primers on mRNA transcripts of rat PDE4B splice variants, PDE4B1, PDE4B2 and PDE4B3. The primer pairs used in each reaction are highlighted in the same colours, with all sense primers indicated by arrows to the right and antisense primers indicated by arrows to the left. *Panel B*, a table defining specificity of each primer, the primer nomenclature, the primer sequence, the expected size of each amplified fragment and the PCR cycling conditions. Each RT-PCR reaction was subjected to an initial 15 min incubation at 95°C followed by 40 cycles, specified for each primer pair.

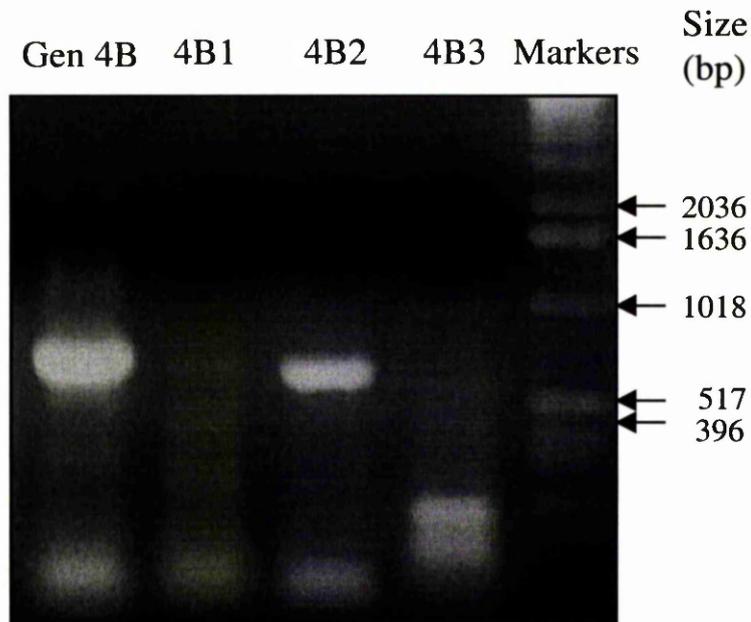


Figure 3.9. RT-PCR analysis of Rat-1 cell total RNA using PDE4B specific primers. RNA isolated from Rat-1 cells was subjected to first strand cDNA synthesis followed by PCR (*see section 2.5.10.*), using primers designed specifically to regions found within the generic PDE4B sequence (Gen 4B, expected product size 786 bp), to PDE4B1 specific sequence (4B1, expected product size 929 bp), PDE4B2 specific sequence (4B2, expected product size 667 bp) and PDE4B3 specific sequence (4B3, expected product size 598 bp) (*as shown in figure 3.8.*). The PCR products were separated on a 2 % agarose gel the positions and sizes (in base pairs) of the standard DNA markers are shown on the right hand side.

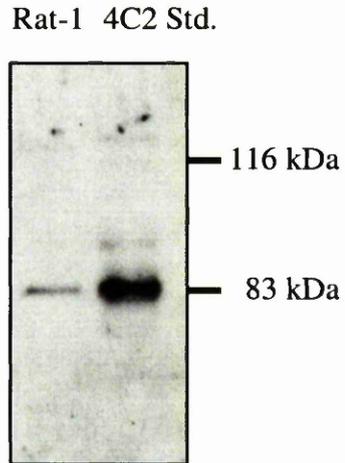


Figure 3.10. Western blot analysis of PDE4C isoforms expressed in Rat-1 cells. Rat-1 cells were harvested in 3T3 lysis buffer and PDE4C isoforms were isolated by immunoprecipitation using the PDE4C specific antibody, as described in section 3.2.3., from 1 mg cell lysate. The isolated protein (Rat-1) was subjected to SDS-PAGE on an 8 % gel alongside 25 μ g recombinant PDE4C2 protein standard (4C2 Std., 80 kDa). The proteins were transferred to nitrocellulose and immunoprobed with the PDE4C specific antibody. The positions and sizes of molecular weight markers are indicated on the right.

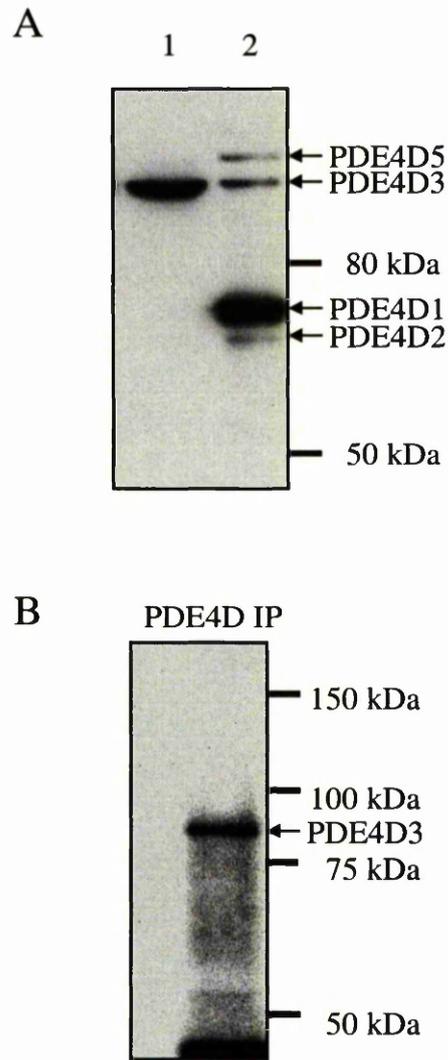


Figure 3.11. Western blot analysis of PDE4D isoforms expressed in Rat-1 cells. *Panel A*, 25 μ g recombinant protein of the PDE4D splice variants (lane 2) were subjected to SDS-PAGE on an 8 % gel alongside 100 μ g of Rat-1 lysate, harvested in 3T3 lysis buffer. The proteins were transferred to nitrocellulose and immunoblotted using a PDE4D specific polyclonal antibody directed against the C-terminus of PDE4D, as described in sections 3.2.4 and 2.3.8.. The recombinant PDE4D protein species of PDE4D1 (68 kDa), PDE4D2 (67 kDa), PDE4D3 (95 kDa) and PDE4D5 (105 kDa) and the positions of molecular weight markers are indicated. *Panel B*, PDE4D was immunoprecipitated from 1 mg Rat-1 cell lysate, using the PDE4D specific polyclonal antibody, as described in materials and methods. The isolated proteins (PDE4D IP) were subjected to SDS-PAGE on an 8 % gel and were transferred to nitrocellulose which was immunoblotted using a PDE4D specific monoclonal antibody (*see section 3.2.4.*). The isolated PDE4D isoform (~95 kDa) and the position of the molecular weight markers are indicated.

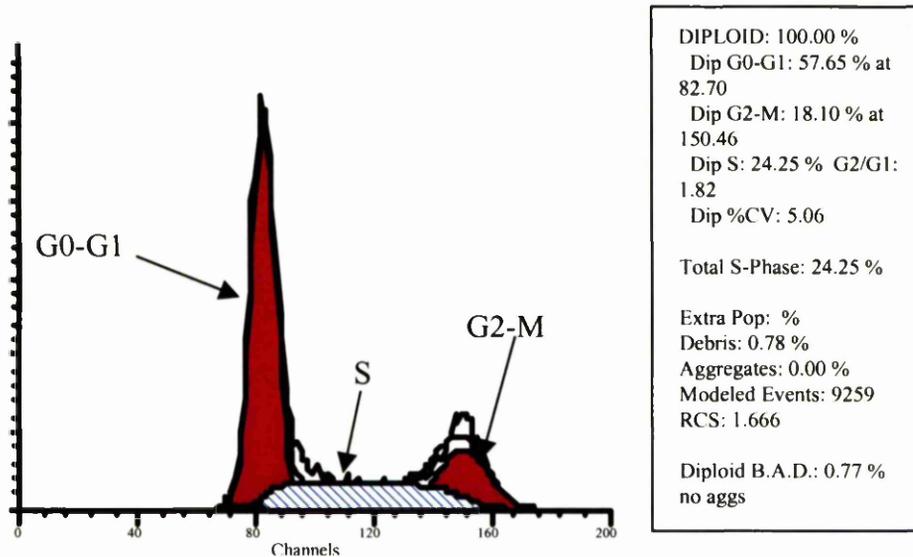


Figure 3.12. Analysis of cell cycle distribution in an asynchronous population of Rat-1 cells. An asynchronous population of Rat-1 cells was dual labelled with BrdU-FITC and propidium iodide (*see section 2.2.3.*), harvested and the distribution of 20000 cells in the phases of the cell cycle was analysed by flow cytometry (*see section 2.2.4.*). The cell cycle distribution acquired by the CELLQuest acquisition programme is indicated on the histogram, with the peaks of cells laying in G0/G1, S and G2/M phases indicated. Quantification of the cell cycle distribution was carried out using the MODfit™ analysis package. Calculations of the distribution of cells within the phases of the cell cycle are displayed as a percentage of the analysed events in the accompanying table.

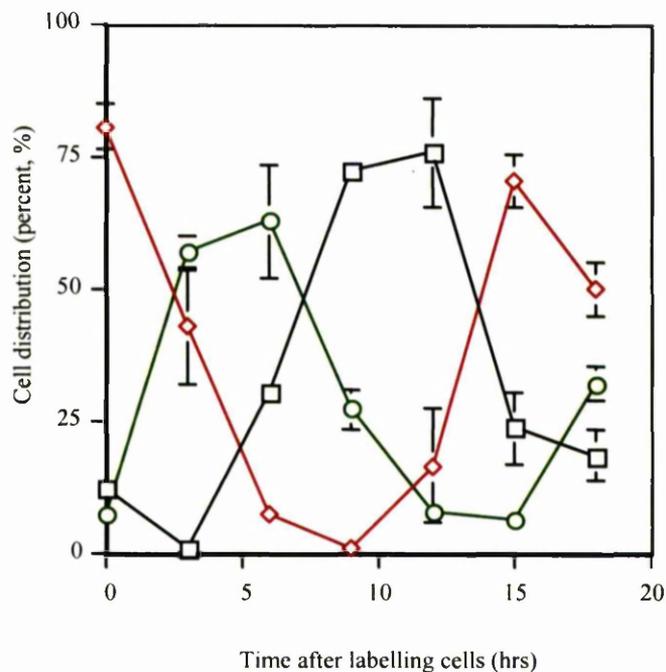


Figure 3.13. Determination of the duration of a complete cell cycle in Rat-1 cells. Asynchronous Rat-1 cells were harvested at 3 h intervals, as indicated, and dual labelled with BrdU-FITC/PI (*see section 2.2.3.*). The distribution of 20000 of the sampled cells within the phases of the cell cycle was determined by flow cytometry (*see section 2.2.4.*). The distribution of cells within G1 (\square), S (\diamond) and G2/M (\circ) are expressed as a percentage of all the cells analysed at that time point. The shown data are the means \pm S.E. of 5 independent experiments.

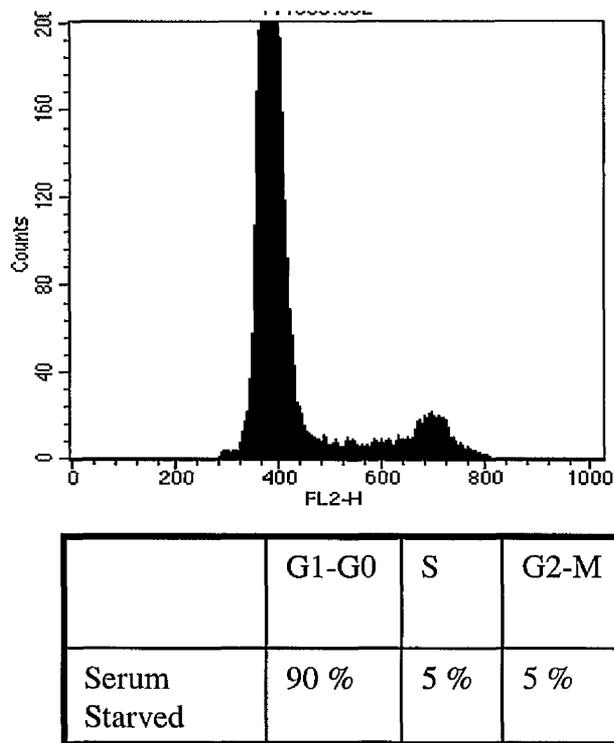


Figure 3.14. Arrest of Rat-1 cells in G0 upon 48 h serum starvation. Rat-1 cells were incubated in serum-free cell culture media for a period of 48 h. Cells were harvested, dual labeled with BrdU-FITC and propidium iodide, and 20000 were analysed by flow cytometry (*see sections 2.2.3. and 2.2.4.*). The histogram denoting cellular DNA content of the sampled population was generated by the CELLQuest acquisition programme, and quantification was carried out using the MODfit™ analysis package. The calculation of cell cycle phase distribution of the population is displayed as a percentage of the analysed events in the accompanying table. These figures are representative of three independent experiments.

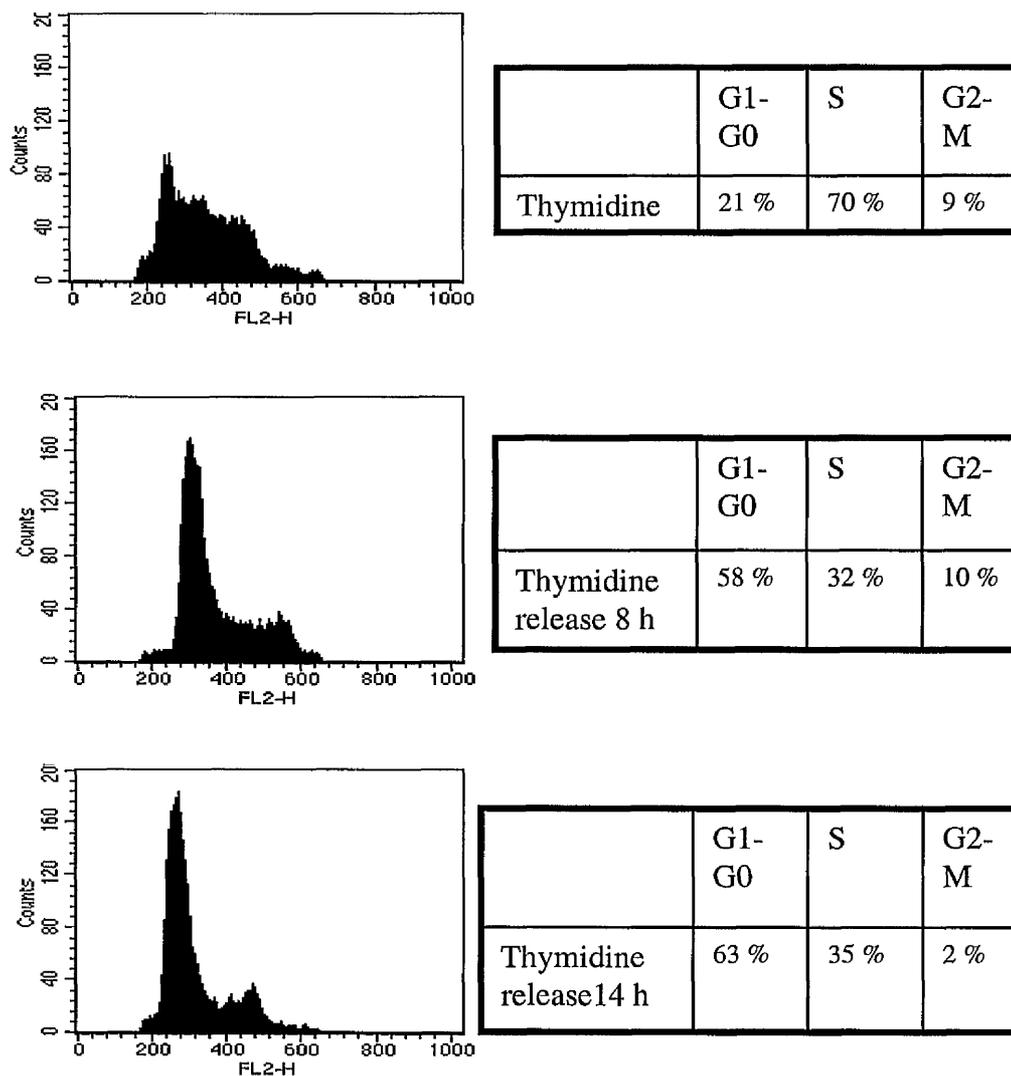
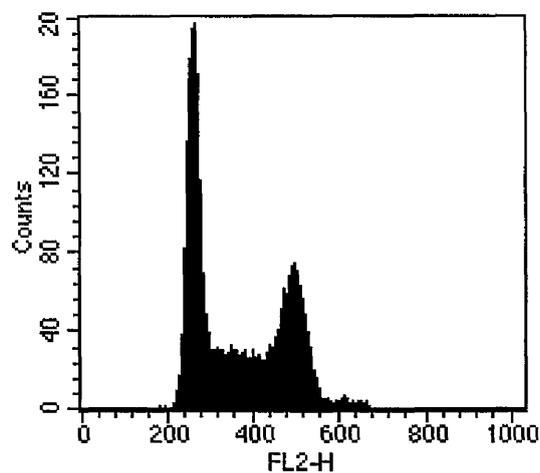


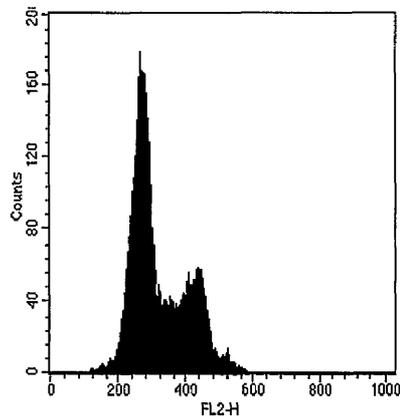
Figure 3.15. Arrest of Rat-1 cells at G1/S upon a double thymidine block. Rat-1 cells were treated with 2.5 mM thymidine for 16 h (*top panel*), or with 2.5 mM thymidine for 16 h, released for 8 h prior to readdition of 2.5 mM thymidine overnight (*middle panel*) or with 2.5 mM thymidine for 16 h then released for 14 h prior to readdition of 2.5 mM thymidine overnight (*bottom panel*), prior to cell harvest. The cells were dual labeled with BrdU-FITC/PI (*see section 2.2.3.*) and the distribution of 20000 of the treated cells within the cell cycle was analysed by flow cytometry (*see section 2.2.4.*). The histograms showing the cellular DNA content of the population were generated by the CELLQuest acquisition program, and quantification of the distribution of cells within the phases of cell cycle was carried out using the MODfit™ analysis package. The results are displayed in the accompanying tables as a percentage of the total cells analysed. These figures are representative of three independent experiments.



	G1-G0	S	G2-M
Olomucine	52 %	26 %	22 %

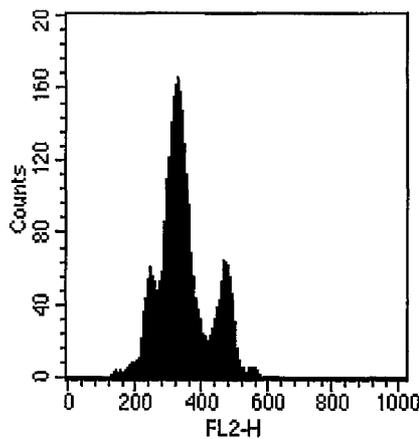
Figure 3.16. Treatment of Rat-1 cells with olomucine. Rat-1 cells were treated with the 10 μM cyclin dependent kinase inhibitor olomucine for 24 h. The cells were then harvested and dual labeled with BrdU-FITC/PI (*see section 2.2.3.*) and 20000 cells were analysed by flow cytometry (*see section 2.2.4.*). The histogram denoting cellular DNA content was generated by the CELLQuest acquisition programme, and quantification of the distribution of the population within the phases of the cell cycle was carried out using the MODfit™ analysis package. The distribution of cells within the phases of the cell cycle are displayed as a percentage of the total events analysed in the accompanying table. These figures are representative of two independent experiments.

A



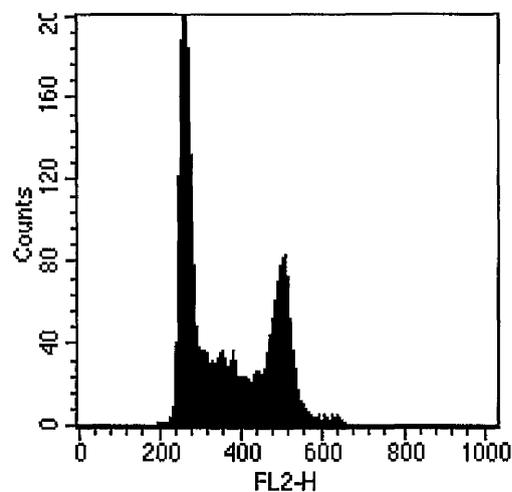
	G1-G0	S	G2-M
Aphidicolin	9 %	77 %	14 %

B



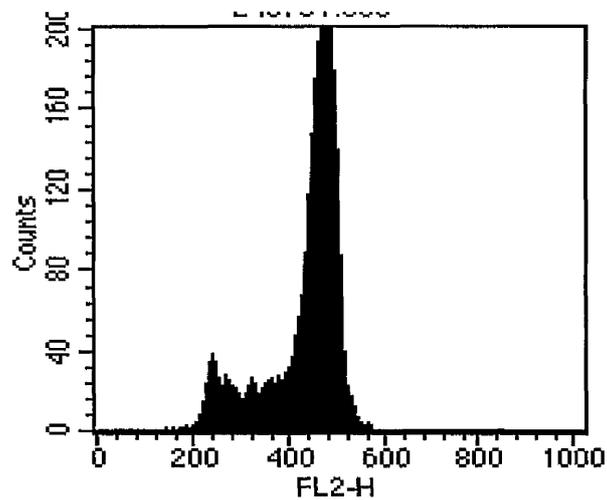
	G1-G0	S	G2-M
Aphidicolin release 3hrs	12 %	54 %	34 %

Figure 3.17. Arrest of Rat-1 cells in S and S/G2 upon incubation with aphidicolin. Aphidicolin was added cell culture media (2.5 mg/ml) which was incubated on Rat-1 cells for a 24 h prior to cells being harvested (*Panel A*) or for 24 h with a 3 h release from the block prior to the cells being harvested (*Panel B*). Cells were dual labeled with BrdU-FITC/PI (*see section 2.2.3.*) and 20000 cells were analysed by flow cytometry (*see section 2.2.4.*). The histogram denoting cellular DNA content was generated by the CellQuest acquisition programme, and quantification was carried out using the MODfit™ analysis package. The calculation of cell cycle phase distribution is displayed as a percentage of the analysed events in the accompanying table. These figures are representative of three independent experiments.



	G1-G0	S	G2-M
L-Mimosine	53 %	33 %	13 %

Figure 3.18. Treatment of Rat-1 cells with L-mimosine for 24 h. L-mimosine was added to Rat-1 cells for 24 h. The cells were harvested and then dual labeled with BrdU-FITC/PI (*see section 2.2.3.*). 20000 cells were then analysed by flow cytometry (*see section 2.2.4.*). The histogram denoting cellular DNA content was generated by the CELLQuest acquisition programme, and quantification of the cell cycle distribution was carried out using the MODfit™ analysis package. The distribution of cells within the phases of the cell cycle are displayed in the accompanying table as a percentage of the total events analysed. These figures are representative of three independent experiments.



	G1-G0	S	G2-M
Nocodazole	0 %	4 %	96 %

Figure 3.19. Arrest of Rat-1 cells in M phase upon 14 h incubation with nocodazole. Nocodazole was added to the cell culture media (50 ng/ml) which was incubated on Rat-1 cells for a period of 14 h. Cells were harvested and dual labeled with BrdU-FITC/PI (*see section 2.2.3.*) and 20000 cells were analysed by flow cytometry (*see section 2.2.4.*). The histogram denoting cellular DNA content was generated by the CELLQuest acquisition programme, and quantification was carried out using the MODfit™ analysis package. The distribution of the sampled population within the phases of the cell cycle is displayed as a percentage of the analysed events in the accompanying table. These figures are representative of two independent experiments.

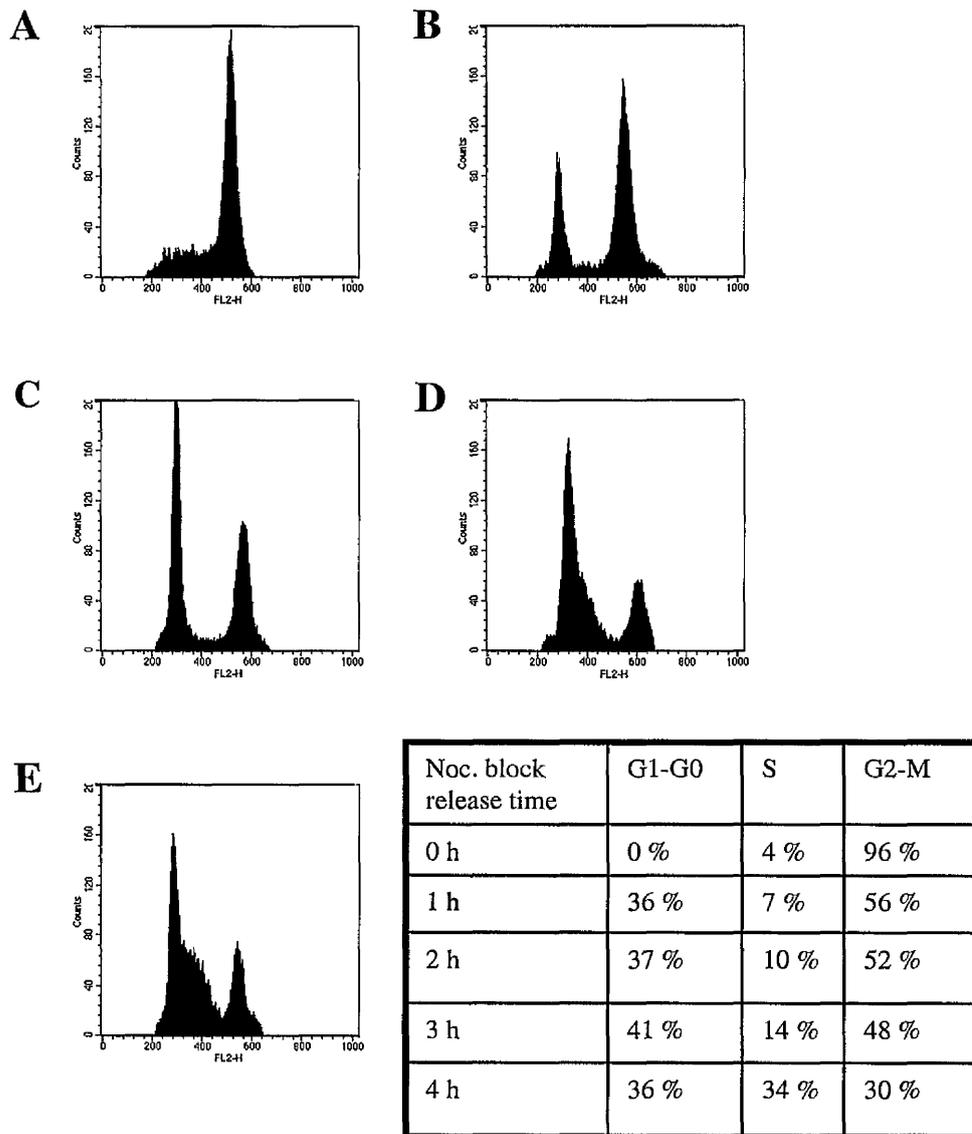


Figure 3.20. Redistribution of Rat-1 cells within the cell cycle upon release of nocodazole block. Rat-1 cells were released from the 14 h incubation with 50 ng/ml media nocodazole (A) for 1 h (B), 2 h (C), 3 h (D) and 4 h (E) prior to harvesting. Cells were dual labeled with BrdU-FITC/PI (see section 2.2.3.) and 20000 cells were analysed by flow cytometry (see section 2.2.4.). The histogram denoting cellular DNA content was generated by the CELLQuest acquisition programme, and quantification was carried out using the MODfit™ analysis package. The calculation the distribution of the sampled population within the phases of the cell cycle is displayed as a percentage of the analysed events in the accompanying table. These figures are representative of three independent experiments.

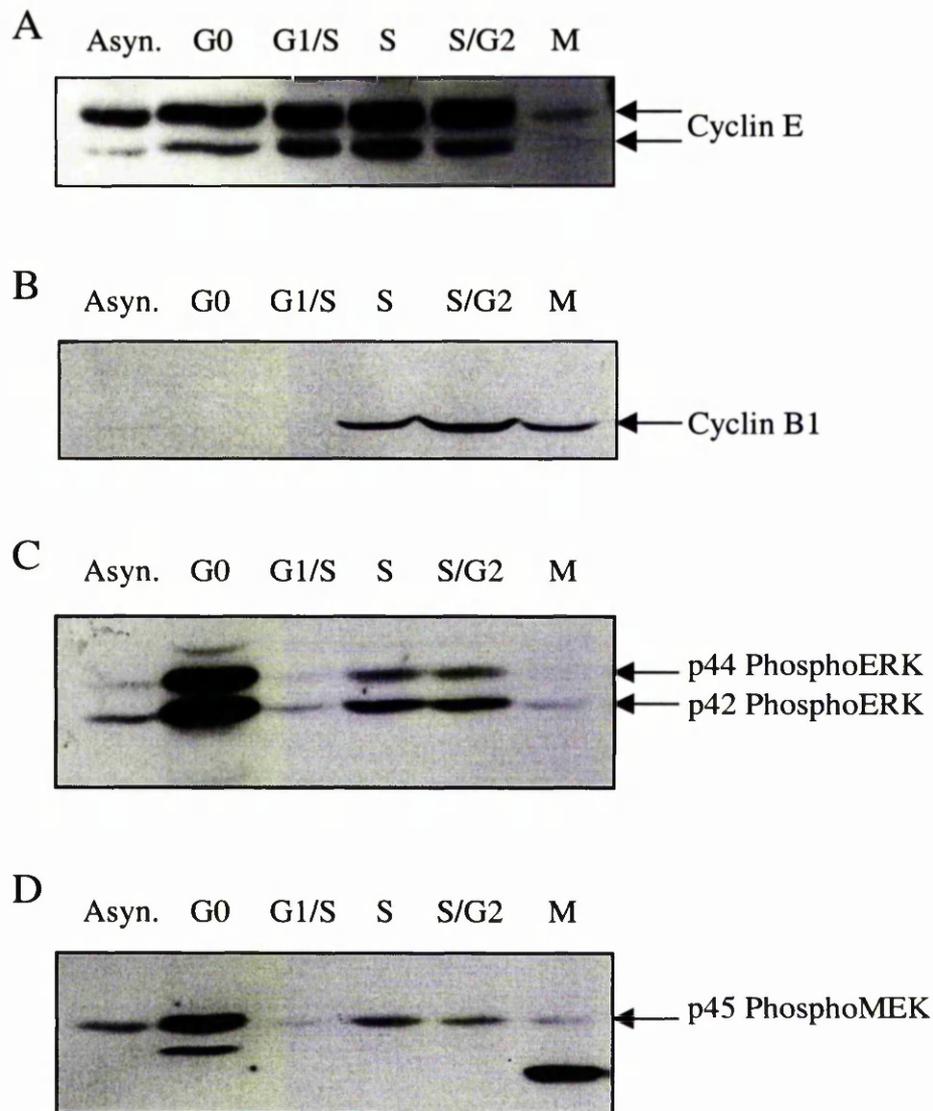


Figure 3.21. Differential expression and phosphorylation of marker proteins in Rat-1 cells isolated at different phases of the cell cycle. Rat-1 cells were arrested in the indicated stages of the cell cycle (see sections 2.1.4.1. – 2.1.4.5.). The cells were harvested in 3T3 lysis buffer and 100 μ g of protein from these cell lysates were subjected to SDS-PAGE on an 8 % gel. Proteins were then transferred to nitrocellulose and immunoblotted with specific antibodies raised against cyclin E (Panel A, 52 kDa), cyclin B1 (Panel B, 58 kDa), phospho-ERK (Panel C, 42 and 44 kDa) and phosphoMEK (Panel D, 45 and 46 kDa), as described in section 3.4.7.. The migratory positions of the proteins are indicated.

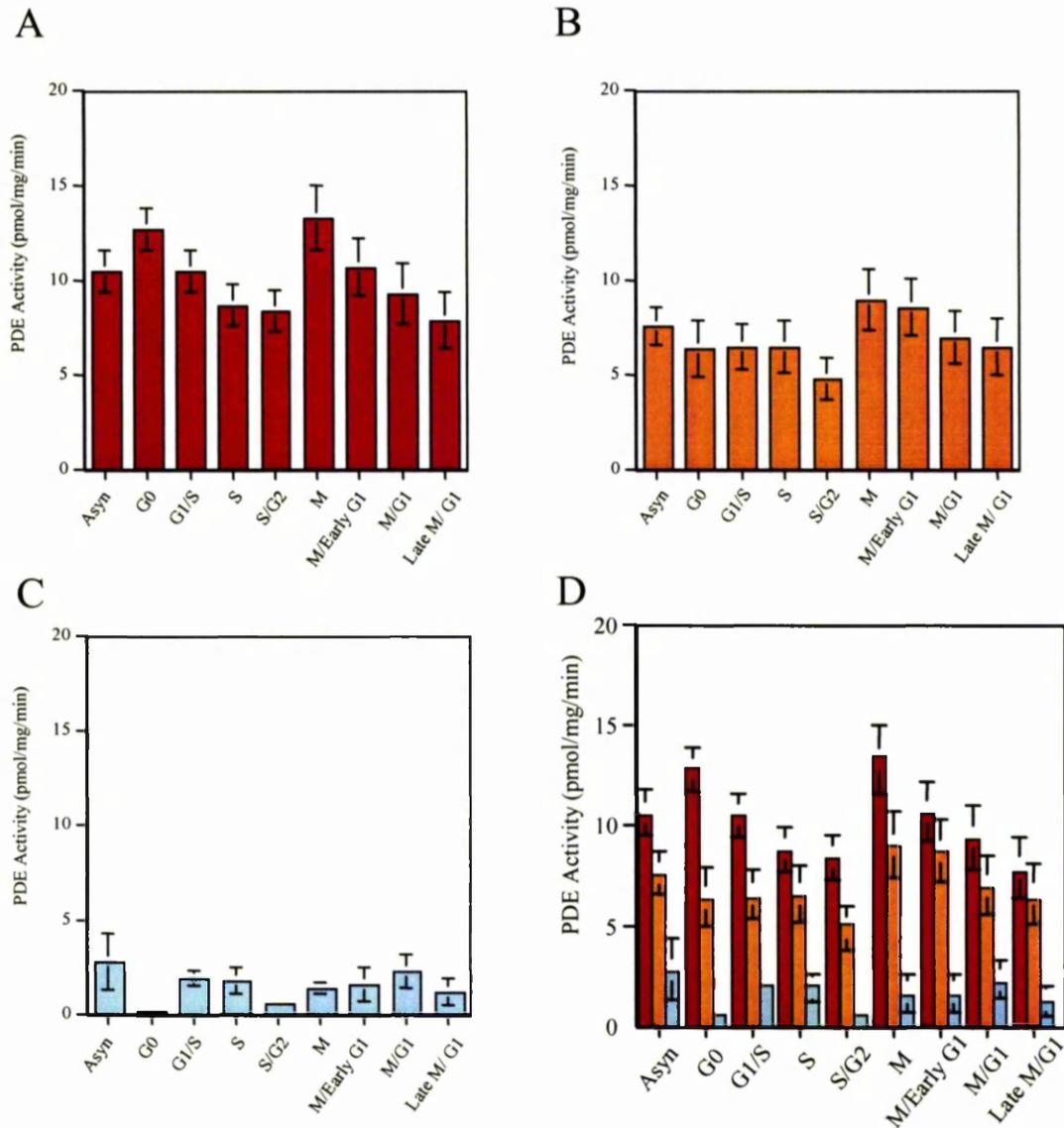


Figure 3.22. Change in cAMP specific PDE activities in Rat-1 cell lysates isolated at different stages of the cell cycle. Rat-1 cells were isolated at specific stages of the cell cycle, as indicated (*see sections 2.1.4.1 – 2.1.4.5*). The cells were harvested in 3T3 lysis buffer and the lysates were assayed for; *Panel A* total cAMP-specific PDE activity (■), *Panel B* PDE4 enzymatic activity (▣), determined as the rolipram-sensitive fraction of the cell lysate and *Panel C* PDE3 (▣) enzymatic activity, determined as the cilostamide-sensitive fraction of the cell lysate (*see section 2.3.9*). These activities are compared directly to one another in *Panel D*. The changes in enzymatic activities of the different cell cycle phases are shown as the means \pm S.E. of between four and eleven independent experiments.

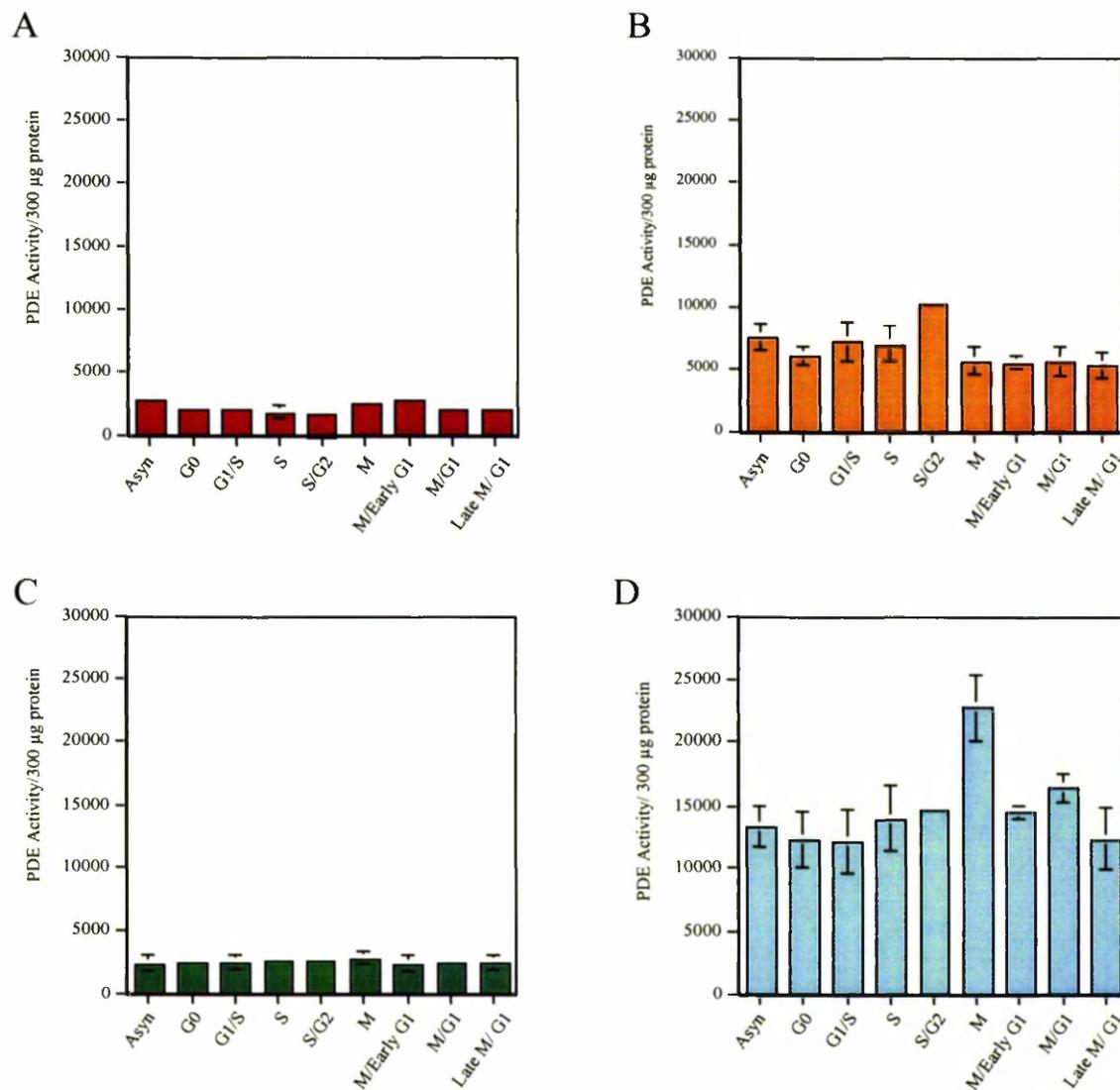


Figure 3.23. Change in specific PDE4 isoform activities in Rat-1 cell lysates isolated at different stages of the cell cycle. Rat-1 cells were isolated at specific stages of the cell cycle, as indicated, (see sections 2.1.4.1 – 2.1.4.5.) and harvested in 3T3 lysis buffer. The PDE isoforms were immunoprecipitated from 300 µg of these cell lysates, using specific antibodies raised to the C-termini of the individual PDE4 subfamilies, PDE4A (■, Panel A), PDE4B (■, Panel B), PDE4C (■, Panel C) and PDE4D (■, Panel D) (see section 2.3.10.). The enzymatic activities of the isolated proteins were monitored by PDE assay (see section 2.3.9.). The changes in activities of the isoforms in the different phases of the cell cycle are shown as the means \pm S.E. of between three and seven independent experiments.

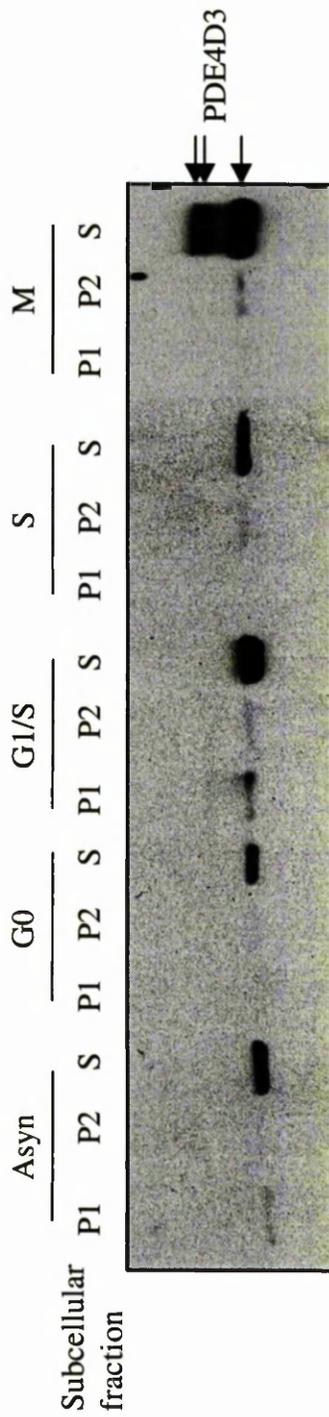


Figure 3.24a. Analysis of subcellular distribution of PDE4D protein in Rat-1 cells isolated at different phases of the cell cycle. Rat-1 cells were arrested at the specified phases of the cell cycle, as indicated (*see sections 2.1.4.1. - 2.1.4.5.*), and the cells were harvested in kHEM buffer. The cells were homogenised through a 13 gauge needle and the low speed cell pellet (P1) was collected by centrifugation at 2000 g for 15 min. The high speed cell pellet (P2) was collected at 75000 g for 45 min and the residual supernatant fraction (S) was retained (*described in detail in section 2.3.1.2.*). 100 μ l of each cellular fraction was separated by SDS-PAGE on an 8 % gel, the proteins were transferred to nitrocellulose and immunoblotted using a PDE4D specific antibody. The migration of the PDE4D3 protein in each fraction is indicated.

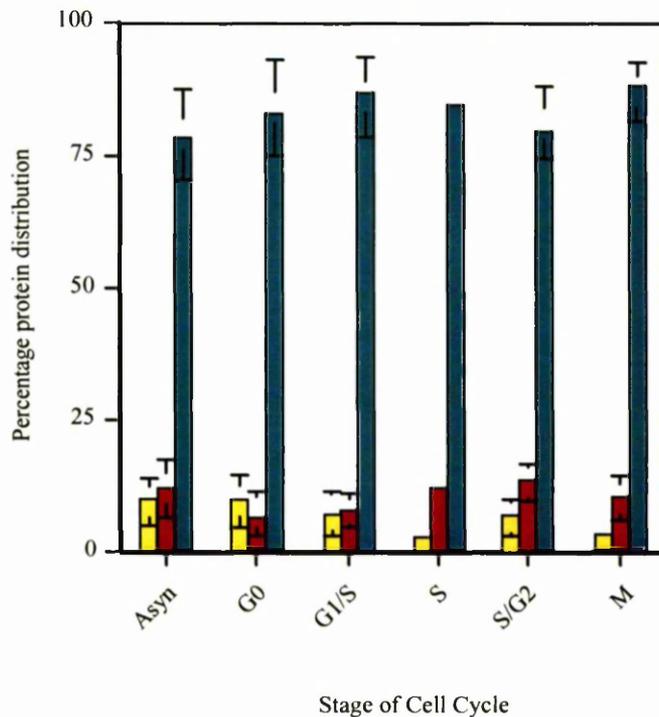


Figure 3.24b. Quantification of changes in subcellular localisation of PDE4D protein in Rat-1 cells isolated at different phases of the cell cycle. Rat-1 cells were arrested at specified phases of the cell cycle and the lysates were subjected to crude fractionation by differential centrifugation. 100 μ l of the P1 (■), P2 (■) and S (■) fraction were separated by SDS-PAGE the proteins were transferred to nitrocellulose and then immunoblotted using a PDE4D specific antiserum (*see Fig. 3.24a.*). The protein was then quantified by densitometric scanning of the immunoblots. The amount of PDE4D3 protein in each fraction is expressed as a percentage of the total PDE4D3 protein in the cell, the results are shown as the mean \pm S.E. of four independent experiments.

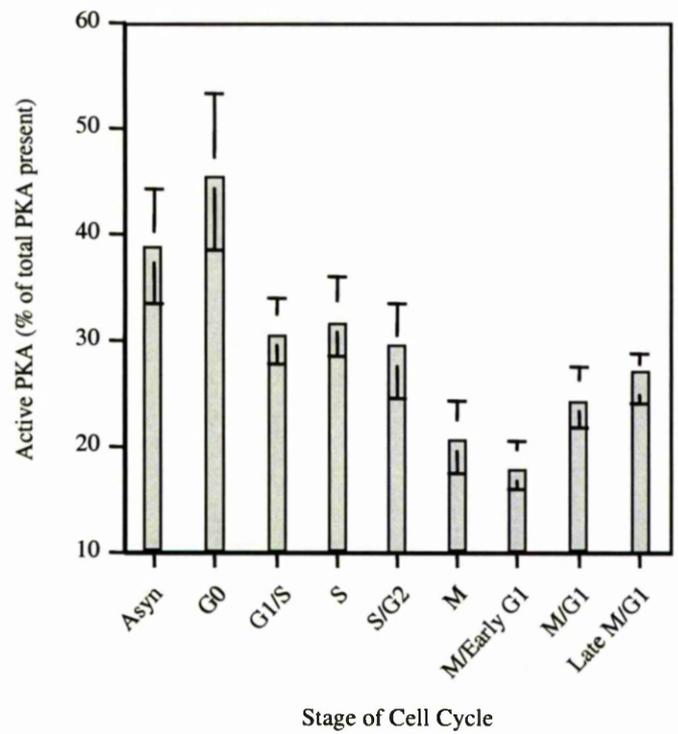


Figure 3.25. Analysis of PKA activity in Rat-1 cell lysates isolated at different phases of the cell cycle. Rat-1 cells were arrested at specific phases of the cell cycle, as indicated (*see sections 2.1.4.1. – 2.1.4.5.*), and harvested in extraction buffer (*see section 2.4.1.1.*). The lysates were assayed for active PKA as outlined in section 2.4.1. and the results are expressed as a percentage of the total PKA present in the cell lysate that could be stimulated by exogenously added excess cAMP. The values are shown as the means \pm S.E. of between three and five independent experiments assayed for active PKA.

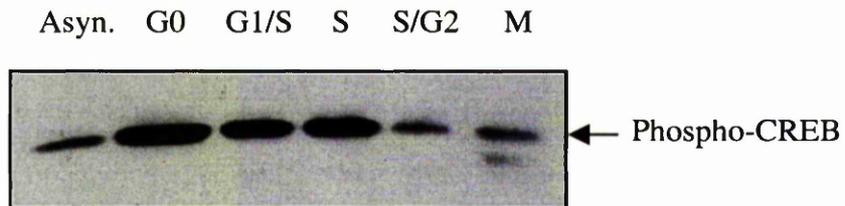


Figure 3.26. Analysis of CREB phosphorylation in Rat-1 cell lysates isolated at different phases of the cell cycle. Rat-1 cells were arrested in the indicated stages of the cell cycle (*see sections 2.1.4.1.- 2.4.1.5.*) and harvested in 3T3 lysis buffer. 100 μg of protein from the cell lysates were subjected to SDS-PAGE on an 10 % gel, transferred to nitrocellulose and immunoblotted with a specific antibody raised against PKA phosphorylated CREB. The migration of phospho-CREB (43 kDa) is indicated.

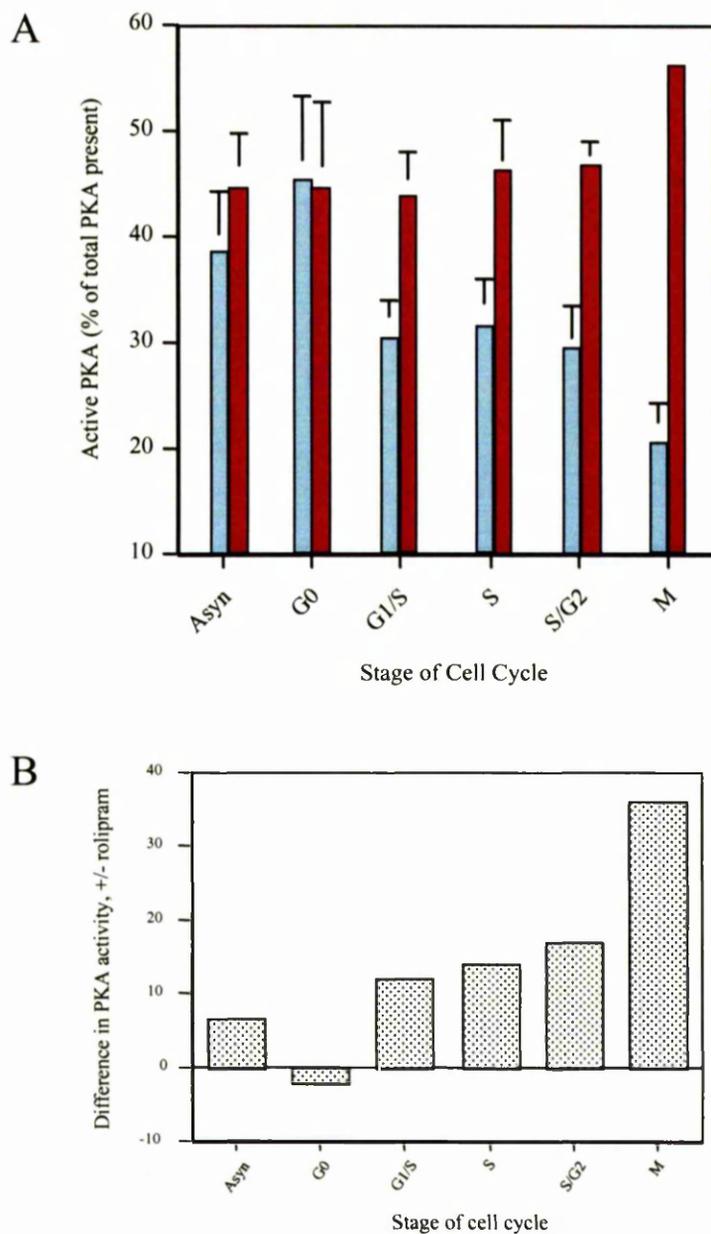


Figure 3.27. The effect of PDE4 inhibition on the percentage active PKA in Rat-1 cells isolated at different phases of the cell cycle. *Panel A* Rat-1 cells were arrested at specific phases of the cell cycle, as indicated (*see sections 2.1.4.1.- 2.4.1.5.*), in the presence (■) or absence (□) of 10 μ M of the PDE4 specific inhibitor, rolipram. The cells were harvested in extraction buffer (*see section 2.4.1.1.*) and the lysates were assayed for active PKA (*see section 2.4.1.*). The results are expressed as a percentage of the total PKA present in the cell lysate that could be stimulated by exogenously added cAMP. The values are shown as the means \pm S.E. of between three and five independent experiments. *Panel B.* A graph which highlights the approximate differences between the amount of active PKA in cells with and without treatment with 10 μ M rolipram.

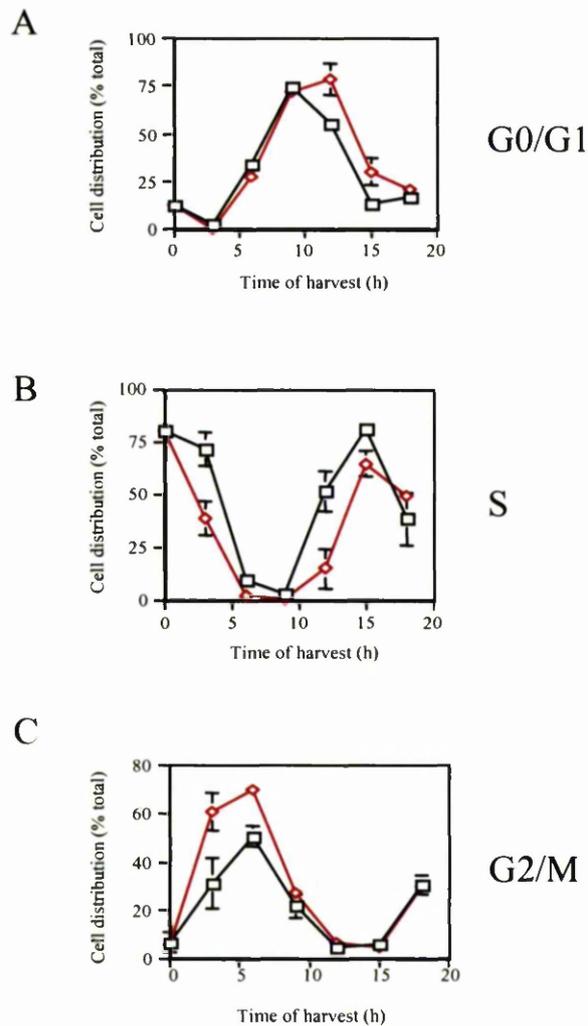


Figure 3.28. Changes in cell cycle distribution of Rat-1 cells upon incubation with rolipram. Rat-1 cells incubated with (\diamond) and without (\square) $10 \mu\text{M}$ of the PDE4 specific inhibitor, rolipram were removed at 3 h time intervals over an 18 h period. The cells were dual labelled with BrdU-FITC/PI (see section 2.2.3.). The distribution of 20000 cells within G1 (Panel A), S (Panel B) and G2/M (Panel C) were measured by flow cytometry (see section 2.2.4.). The distribution of the cells in each phase is expressed as a percentage of all cells analysed at that time point. These data are shown as the mean \pm S.E. of five independent experiments.

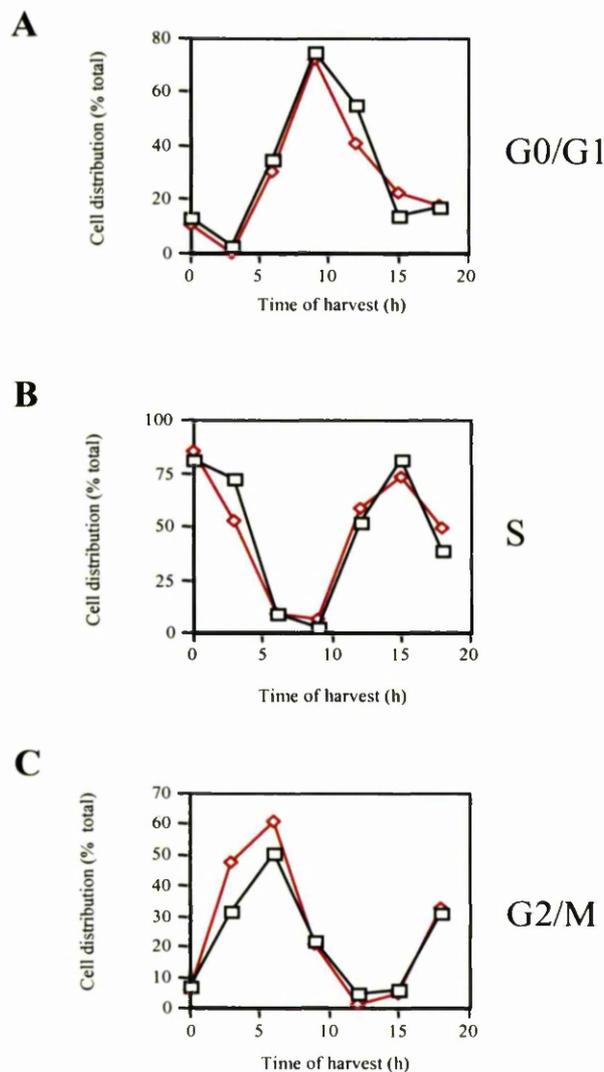


Figure 3.29. Changes in cell cycle distribution of Rat-1 cells upon incubation with cilostomide. Rat-1 cells incubated with (\diamond) and without (\square) 10 μ M of the PDE3 specific inhibitor, cilostomide were removed at 3 h time intervals over an 18 h period. The cells were dual labelled with BrdU/PI (see section 2.2.3.) and the distribution of 20000 cells within G1 (Panel A), S (Panel B) and G2/M (Panel C) were measured by flow cytometry (see section 2.2.4.). The distribution of the cells in each phase is expressed as a percentage of all cells analysed at that time point. These data are representative of four independent experiments.

Quadrant location	Cell No. (percentage of total cells analysed)	
	Asynchronous	Mitotic
Lower Left (LL)	63 %	73 %
Lower Right (LR)	4 %	5 %
Upper Left (UL)	3 %	8 %
Upper Right (UR)	29 %	14 %

Table 3.1. Quantification of the proportion of apoptotic Rat-1 cells on an FL1-H vs FL2-H density plot when treated with nocodazole. Rat-1 cells were subjected to nocodazole-induced mitotic arrest (*see section 2.1.4.5.*) and were then harvested and stained with Annexin V-FITC and propidium iodide (*see section 2.2.5.1.*). The labelled cells were collected by FACs and analysed using the CELLQuest acquisition package, on a density plot of FL1-H vs FL2-H (*see section 2.2.5.2.*). The distribution of cells within the four quadrants of the density plot are indicated, which corresponds to the amount of dual labelled apoptotic cells (UR) and intact cells (LL) and the single labelled population (LR and UL).

Cell Cycle Phase	Fold change in PDE4D3 expression (per 25 μ g cell lysate)
Asynchronous	1 \pm 0
G0	0.8 \pm 0.25
G1/S	0.93 \pm 0.16
S	1.02 \pm 0.06
S/G2	0.9 \pm 0.01
M	1.05 \pm 0.05

Table 3.2. Assessment of PDE4D3 protein expression in Rat-1 cells isolated at different phases of the cell cycle. Rat-1 cells were arrested at different phases of the cell cycle (*see sections 2.1.4.1 – 2.1.4.5.*, as indicated) and the concentration of PDE4D protein within 25 μ g cell lysate were determined by ELISA (*see section 2.3.3.*). The changes in PDE4D protein concentrations are expressed as the fold change in comparison to levels expressed in asynchronously isolated cells. The results are shown as mean \pm S.E. of three independent experiments.

Chapter 4

Investigation of PDE4D3 in mitosis

4.1. Introduction

Mitosis is the stage in the cell cycle at which cell division takes place. It can be separated into five distinct phases. In prophase the chromosomes condense and nuclear envelope breakdown occurs (Nigg, 2001). In prometaphase the mitotic spindles are formed to which the chromosomes attach, and the alignment of chromosomes along the metaphase plate then takes place during metaphase (Leblond and El Alfy, 1998). At the onset of anaphase the sister chromatid cohesion is reduced, they separate and migrate to the opposite poles of the cell and telophase determines the time at which the cell physically separates by cytokinesis, producing two daughter cells (Leblond and El Alfy, 1998, *see Fig. 3.2.*). To maintain the ordered progression through mitosis, highly regulated intrinsic mechanisms, which depend on multiple feedback loops, have evolved. Our understanding of the control of mitotic progression is a rapidly evolving, with an increasing number of kinases and phosphatases being identified in achieving the regulation of mitosis.

4.1.1. PKA and mitotic regulation

The onset of mitosis, which involves the condensation of chromosomes and the breakdown of the nuclear envelope, is controlled by the formation and activation of the maturation-promoting factor (MPF). The MPF is an active kinase complex formed between the cyclin expressed in mitosis, cyclin B, and the kinase unit, cdk1 (also known as p34 cdc2). Exit from mitosis requires the activation of the anaphase promoting complex (APC) or 20S cyclosome, a multi-subunit complex that functions as a cell cycle dependent ubiquitin ligase, targeting cyclins for proteolysis by the 26S proteasome (Morgan, 1999).

Down-regulation of PKA activity appears to be essential for the induction of mitosis (Lamb et al., 1991) as it regulates the mechanisms that lead to mitotic spindle formation (Browne et al., 1990) and nuclear envelope breakdown (Lamb et al., 1991). Elevation of cAMP prior to metaphase inhibits mitotic progression as active PKA compromises the activity of the MPF (Fernandez et al., 1995; Hohmann et al., 1993; Oh et al., 1996) and thus the nuclear envelope persists (Lamb et al., 1991). Cellular PKA activity is minimal at metaphase (Zeilig et al., 1976), but increases as the cells pass from metaphase through to anaphase and reaches a peak at the M/G1 transition (Grieco et al., 1996). This reactivation of PKA is required for the reformation of the nuclear envelope at M/G1 transition (Steen et al., 2000). Thus elevating levels of cAMP after metaphase increases the rate of cells transition through mitosis (Zeilig et al., 1976).

The spatial regulation of PKA-mediated signalling cascades during the cell cycle appears to be very important. PKA, in fibroblasts, co-localises with MPF at the centrosome (Tournier et al., 1991) where it is held through an interaction with AKAP75 (Keryer et al., 1998). The PKA regulatory subunit, RII α , is targeted for phosphorylation by the active MPF, during the early stages of mitosis, which causes its redistribution from the centrosome/golgi to the cytosol (Keryer et al., 1998).

Formation of the active APC, at the onset of anaphase, is regulated by several mechanisms including cell cycle specific phosphorylation and dephosphorylation of its component subunits (Yanagida et al., 1999; Ishii et al., 1996). The specificity of the targets for APC-dependent ubiquitinylation is determined by the interaction of the APC with WD-repeat proteins (Anghileri et al., 1999). The formation and activation of the APC complex is inhibited at the onset of mitosis by dominant PKA phosphorylations of the Cut4, Cut9 (mammalian homologue, Cdc7) and Cut20 (mammalian homologue, Tsg24) subunits (Kotani et al., 1998; Yamashita et al., 1996). Only when PKA activity is down-regulated at metaphase (Kotani et al., 1998) by an as yet unidentified mechanism and only when these subunits are dephosphorylated by protein phosphatase-1 (Yanagida et al., 1999) is the APC formed and activated (*Fig. 4.1.*). Once activated, mitotic cyclins are targeted for degradation and the cells progress through the M/G1 transition.

4.1.2. PDE4D3 function, localisation and modification

In order to establish spatio-temporal signalling cascades within cells, defined cAMP concentration gradients exist. PDE4 isoforms have specific subcellular localisations, due to their ability to interact with membranes and scaffolding proteins (Shakur et al., 1995; Dodge et al., 2001). As such their reactivities may underpin the creation, stabilisation and shaping of such gradients of cAMP and hence PKA activity in cells. PDE4D3 maintains specific subcellular localisations through its ability to complex with the scaffolding/structural A-kinase anchoring proteins (AKAPs) (Dodge et al., 2001; Tasken et al., 2001; Verde et al., 2001). The muscle selective AKAP (mAkap) co-ordinates the formation of a complex between PKA and PDE4D3 which maintains a cAMP signalling module that establishes a negative feedback loop to maintain basal cAMP levels (Dodge et al., 2001). PDE4D3 can also co-localise with the PKA RII α and RII β regulatory subunits at the centrosome of Sertoli cells in a complex co-ordinated by AKAP450 (Tasken et al., 2001). Centrosomal and Golgi localisation of PDE4D3 has also been associated with its ability to form a complex with a novel structural protein called myomegalin (Verde et al., 2001).

PDE4D3 activity is modified post-translationally by phosphorylations mediated by both PKA and ERK (Sette and Conti, 1996; Hoffmann et al., 1999). PKA phosphorylates PDE4D3 at Ser¹³ and Ser⁵⁴ residues. The phosphorylation of Ser⁵⁴ induces a conformational change that disrupts the interaction between UCR2 and the catalytic region of the protein causing an increase in the V_{max} of the enzyme (Sette and Conti, 1996) (Hoffmann et al., 1998; Lim et al., 1999). It is unclear what the physiological relevance of the Ser¹³ phosphorylation might be.

Phosphorylation of PDE4D3 by ERK occurs at Ser⁵⁷⁹ within the catalytic unit and this leads to a marked reduction of PDE4D3 activity (Hoffmann et al., 1999; MacKenzie et al., 2000). This inhibitory effect of ERK phosphorylation is orchestrated by the regulatory UCR1 and UCR2 domains found in PDE4D3, as ERK phosphorylation of the 'naked' PDE4D catalytic unit has little effect on activity (Baillie et al., 2000). ERK inhibition of PDE4D3 can be expected to increase cAMP levels and activate PKA. Indeed, this provides a unique feedback system as the activated PKA can phosphorylate PDE4D3 on Ser⁵⁴. This serves to negate the inhibitory effect of ERK phosphorylation (Baillie et al., 2001).

Phosphatidic acid, a phospholipid which has been implicated in the stimulation of proliferation of fibroblasts, can also increase the activity of recombinant PDE4D3 protein (Nemoz et al., 1997). Phosphatidic acid has been shown to interact directly with PDE4D3 at a site which has been mapped to the N-terminus of the UCR1 domain, within the same region as the Ser⁵⁴ PKA phosphorylation motif (Grange et al., 2000).

In this chapter I set out to characterise the modification which led to the activation of PDE4D3 during mitosis, as shown previously in chapter 3. This was done in an attempt to identify the control mechanisms that could link the activation of PDE4D3 to the decrease in PKA activity that also takes place upon entry of cells into mitosis.

Results

4.2 Characterisation of PDE4D3 in nocodazole-induced mitosis

In Chapter 3, I showed the specific activity of PDE4D markedly increased in Rat-1 cells isolated in mitosis, when compared to the PDE4D activity in asynchronous cells. The Rat-1 fibroblasts only express the long PDE4D3 isoform, so this isoform was further studied during mitosis with a view to understanding the nature of the modification responsible for its increased activity.

4.2.1. Changes in PDE4D electrophoretic mobility during mitosis

To determine whether the increase in PDE4D3 activity coincided with a change in the electrophoretic mobility of PDE4D3, Rat-1 cell lysates from cells arrested at different stages of the cell cycle (Materials and methods 2.1.4) were immunoblotted with the PDE4D C-terminal specific antiserum. The lysate from the Rat-1 cells isolated in mitosis showed a change in electrophoretic mobility of PDE4D3, with about 35 % of the PDE4D3 protein migrating with a reduced electrophoretic mobility compared to the native PDE4D3 protein (*Fig 4.2.*). The PDE4D3 migrated as two electrophoretically shifted species, with a lower and hyper-shifted band, now referred to as *stage 1* (which migrates with an apparent molecular weight of approximately 100 kDa) and *stage 2* (which migrates with an apparent molecular weight of 102 kDa) respectively (*Fig. 4.2.*).

4.2.1.1. Identification of electrophoretically retarded PDE4D species in Rat-1 cells

To confirm that the proteins migrating at *stage 1* and *stage 2* in mitosis were in fact modified PDE4D3 protein and not PDE4D5, a long form PDE4D that migrates with a higher molecular weight of 105 kDa, lysates from Rat-1 cells arrested in mitosis were immunoblotted with the Genosys '224' antibody. This is a PDE4D5 specific antibody that has been raised in sheep to the peptide MAQQTSPDTLTVPEVDNPHC, which corresponds to residues within the unique N-terminal region of PDE4D5. No PDE4D5 immunoreactivity was detected in either the asynchronous or mitotic Rat-1 cell lysates (*Fig. 4.3.*).

4.2.2. Subcellular distribution of PDE4D3 protein in mitosis

PDE4D3 is associated with the both the cytosolic and particulate fraction of the cell, with approximately 17 % of the protein present in the 100000 g pellet upon subcellular fractionation of VSMCs (Bolger et al., 1997). A similar amount of particulate associated PDE4D3 was seen in Rat-1 cells and the majority of the PDE4D3 was found to remain within the cytosol at all phases of the cell cycle (*see Figures 3.24a. & 3.24b.*). To determine in which subcellular fraction the modified PDE4D3 was associated in mitotic cells, fractionation of Rat-1 cells was done by two methods of differential centrifugation were carried out (Materials and methods 2.3.1.2. and 2.3.1.3.). The resulting subcellular fractions were then immunoblotted using the PDE4D specific antiserum. The electrophoretically shifted species of the PDE4D3 were found to be predominantly associated with the cytosolic fraction of the cells. There was also a very small amount of the *stage 1* shifted PDE4D3 protein associated with the P2, microsome fraction (*Figs. 4.4a. & 4.4b.*).

4.2.3. Modification of PDE4D3 as cells accumulate in mitosis

In order to investigate the increase in PDE4D activity, and the coincidental decrease in the PDE4D3 electrophoretic mobility in cells isolated in mitosis, the addition of nocodazole to asynchronous Rat-1 cells over a 24 h period was carried out. The accumulation of cells in mitosis and the alterations in PDE4D3 activity and electrophoretic mobility were then analysed.

4.2.3.1. Nocodazole induced modification of PDE4D3 is not brought about by disruption of microtubule dynamics

High concentrations of nocodazole (200 nM-10 μ M) cause the disruption of microtubular dynamics (Mikhailov and Gundersen, 1998). This disruption is a rapid process with the microtubules showing disorder within 1-2 h of nocodazole treatment. At lower concentrations (1 nM), and over longer time-courses, nocodazole induces cell cycle arrest at mitosis by interfering with the microtubule dynamics (Jordan et al., 1992). To ascertain whether the modification(s) of PDE4D3, which caused a decrease in its electrophoretic mobility, were specifically due to a mitotic event or as a cause of microtubule disruption *per se*, asynchronous cells were treated with a range of concentrations of nocodazole, from 50 ng/ml to 5 μ g/ml, for 2 h (*Fig. 4.5.*). There was no change in the electrophoretic

mobility or activity of PDE4D3 with the incubation of the various concentrations of nocodazole on cells over this 2 h time course.

4.2.3.2. *Accumulation of Rat-1 cells in mitosis with nocodazole treatment*

To determine the rate of accumulation of Rat-1 cells in mitosis asynchronous cells were incubated with 50 ng/ml nocodazole over 7 h and samples removed at 1 h time intervals. The distribution of each sample of cells within the phases of the cell cycle was then analysed by flow cytometry (Materials and methods 2.2.). After a 4 h incubation of the cells with nocodazole approximately 54 % cells were isolated in the G2/M-phases of the cell cycle and by 6 -7 h, 90 -95 % of the labelled cells in the analysed population were in the G2/M-phases (*Fig. 4.6.*).

4.2.3.3. *Electrophoretic mobility of PDE4D3 is reduced as cells accumulate in mitosis*

I set out to determine the time-course of generation of the electrophoretically shifted species of PDE4D3. This was detected by immunoblot analysis over a 14 h time course, subsequent to incubation of the asynchronous cells with 50 ng/ml nocodazole. PDE4D3 species with reduced electrophoretic mobilities were detected after 4 h incubation of cells with nocodazole (*Fig. 4.7.*). The amount of PDE4D3 protein, migrating at *stage 1* and *stage 2*, increased over the time course of nocodazole incubation, reaching a maximal level after 14 h.

4.2.3.4. *Activity of PDE4D increases as cells accumulate in mitosis*

I then set out to analyse the time-course for the increase in PDE4D3 specific activity in Rat-1 cells upon nocodazole-induced mitosis. Thus, asynchronous cells were treated with 50 ng/ml nocodazole and collected every 1 h or 2 h over a 24 h time course for PDE assay (Materials and methods 2.3.9.). The enzymatic activity of PDE4D increased steadily over the first 7 h of nocodazole addition and then declined slightly after 8 h, only to increase again, reaching a peak at 14 h after the start of incubation with nocodazole (*Fig. 4.8.*). After a 14 h nocodazole incubation the activity of PDE4D decreased slightly, then plateaued and remained constant after 16 h.

4.2.4. Modification of PDE4D3 as cells leave mitosis

In order to investigate the inactivation of PDE4D3 and the increase in electrophoretic mobility of PDE4D3 as cells leave mitosis, characterisation of PDE4D3 when cells were released from nocodazole-induced mitotic arrest was carried out.

4.2.4.1. Cell cycle analysis of Rat-1 cells released from nocodazole block

Rat-1 cells were released from nocodazole-induced mitosis and harvested at 30 min intervals for analysis of the distribution of the cells within the cell cycle by flow cytometry (Materials and methods 2.2.). It was found that after a 30 min release no cells had started to move into G1 phase (*Fig. 4.9.*). After 1 h release there was an increase in the population of cells in G1 and after 2 h some 62 % of cells had moved from mitosis and into the next cell cycle.

4.2.4.2. Electrophoretic mobility of PDE4D3 is increased as Rat-1 cells leave mitosis

To ascertain when the increase in the electrophoretic mobility of PDE4D3 occurs as cells leave mitosis, Rat-1 cells were released from nocodazole-induced mitosis and harvested at 30 min intervals post-release. The electrophoretic mobility of PDE4D3 was analysed by SDS-PAGE and immunoblotting (Materials and methods, 2.3.8.). It was found that as the cells were released from the mitotic block then the electrophoretic mobility of the PDE4D3 increased (*Fig. 4.10.*). After 30 min release, there was a 4 % decrease in the amount of protein migrating in *stage 2*. The amount of protein migrating in *stage 1* only decreased after 1.5 – 2 h after release from mitosis, when all PDE4D3 protein migrated at the same mobility as the native species.

4.2.4.3. Activity of PDE4D decreases as Rat-1 cells leave mitosis

To determine whether there was a change in the activity of PDE4D as cells were released from the mitotic block, Rat-1 cells were arrested in mitosis by incubation with nocodazole, then released and harvested at 30 min intervals. The PDE4D3 protein was isolated from cells by selective immunoprecipitation, and the enzymatic activity was determined by PDE assay (Materials and methods 2.3.10.). There was an almost 2-fold decrease in PDE4D3 activity 30 min after cells were released from the mitotic block (*Fig. 4.11.*). After 1 h

release the activity of PDE4D3 increased slightly and subsequently decreased again after 1.5 -2 h until it returned to the level of activity observed in asynchronous cells.

4.3. Identification of the PDE4D3 mitotic modification

Modifications of PDE4 isoforms, which have led to alterations in the activity of the enzymes include the direct phosphorylation by PKA (Sette and Conti, 1996), the direct phosphorylation by ERK (Hoffmann et al., 1999) and phosphorylation via a PI 3-kinase dependent mechanism, possibly acting through p70s6 kinase (MacKenzie et al., 1998). Interaction with lipids, such as phosphatidic acid (Grange et al., 2000), and interactions with AKAPs (Dodge et al., 2001) also modulated the activity of PDE4 enzymes. I undertook studies to identify the cause of the modification of PDE4D3 in mitotically isolated Rat-1 cells, which lead to the increase in the enzymatic activity and coincided with the shift in the electrophoretic migration of the protein by SDS-PAGE.

4.3.1. Mitotically isolated PDE4D3 is not ubiquitinated

Ubiquitinylation of a protein occurs through the recognition of phosphorylated PEST motifs or phosphorylated destruction box motifs (R-(A/T)-(A)-L-(G)-X-(I/V)-(G/T)-(N)) found on cell cycle regulatory proteins (Ciechanover et al., 2000). Many proteins are targeted for ubiquitinylation during mitosis and such a modification could decrease the electrophoretic mobility of a protein. There are two potential PEST motifs located within the extreme C-terminus of PDE4D3, from residues 569-590 and 633-668. To investigate whether ubiquitination modifies PDE4D3 during mitosis, PDE4D3 was isolated by immunoprecipitation from mitotic cells and immuno-probed with an anti-ubiquitin antibody, raised in rabbit to ubiquitin conjugated to keyhole limpet haemocyanin using glutaraldehyde (Haas and Bright, 1985). No ubiquitinylation of PDE4D3 was observed (Fig. 4.12.).

4.3.2. In vivo phosphorylation of PDE4D3 with ³²P orthophosphate

To determine whether the mitotic modification of PDE4D3 was due to a phosphorylation event, cells were arrested in mitosis, by treatment with 50 ng/ml nocodazole, prior to being labelled *in vivo* with [³²P]-orthophosphate (Materials and methods 2.4.4.). Once the cells were labelled PDE4D3 was isolated by immunopurification (Materials and methods 2.3.10) and analysed for incorporated ³²P by phosphorimage analysis (Materials and methods 2.4.4.). The immuno-isolated PDE4D3 protein was found to be phosphorylated in

151
asynchronous cells, and when analysed by densitometry 1.3 -fold more ^{23}P was incorporated in PDE4D3 in the mitotic cells (*Fig. 4.13.*). However, the electrophoretically retarded *stage 1* and *stage 2* species of PDE4D3, observed by immunoblotting whole cell lysate from mitotic cells (*Fig. 4.13.*), was not detected on the phosphorimage of the ^{32}P labelled PDE4D3.

4.3.3. The mitotic modifications of PDE4D can be maintained by phosphatase inhibition

Although the shifted species of PDE4D3 could not be detected by *in vivo* phosphorylation, the phosphorylation the protein was subjected to further investigations. Firstly, an attempt was made to maintain the activated and shifted species of PDE4D3, by inhibiting phosphatases, as the cells were released from the mitotic block.

4.3.3.1 Electrophoretically shifted species of PDE4D3 are maintained upon addition of okadaic acid to mitotically released cells

Okadaic acid (OA) inhibits of protein phosphatase 1 (PP1) at concentrations of 10 -15 nM but can selectively inhibit protein phosphatase 2 A (PP2A) at the much lower concentrations of 0.1 nM (Cohen et al., 1990). To investigate whether phosphatase inhibition could facilitate an increase in the electrophoretic mobility of PDE4D3 as cells leave mitosis, Rat-1 cells were released from nocodazole-induced mitotic arrest for 2 h in the presence of a range of OA concentrations. The loss of the PDE4D3 forms of reduced electrophoretic mobility (*stage 1* and *stage 2*) seen as Rat-1 cells leave mitosis (*Fig. 4. 10.*) was inhibited by OA in a concentration dependent fashion (*Fig. 4.14.*). With 19 % of PDE4D3 migrating as a shifted species at 200 nM OA, 33 % of PDE4D3 migrating with the shifted PDE4D3 species at 500 nM OA and 37 % PDE4D3 migrating with the shifted species at 1000 nM.

4.3.3.2. Elevated PDE4D activity is maintained with Okadaic acid addition to mitotically released cells

As the shifted *stage 1* and *stage 2* species of PDE4D3 were maintained with OA incubation on cells released from mitosis (see section 4.3.3.1.) the effect that this same incubation with OA had on the activity of PDE4D3 was assessed. Rat-1 cells were thus released from nocodazole-induced mitotic arrest over a period of 2 h in the presence of a range of OA concentrations. As above, PDE4D3 was immunopurified from the lysate and

its activity determined. The decrease in PDE4D3 activity observed over a 2 h release period from mitosis was blocked by OA in a concentration dependent fashion (*Fig. 4.15.*). With PDE4D3 maintaining a 1.1 -fold increase in activity in the presence of 100 – 200 nM OA, a 1.3 -fold increase with 500 nM OA and a 1.8 –fold increase in the presence of 1000 nM OA.

4.3.4. Phosphatase treatment of mitotic PDE4D3

I further investigated the phosphorylation-state of PDE4D3 during mitosis by treating mitotic PDE4D3 with phosphatase to determine the effect of dephosphorylation of the protein on its activity and electrophoretic mobility. Lysate extracted from Rat-1 cells arrested in mitosis was treated with calf intestinal alkaline phosphatase (CIAP) to remove all phosphate groups from the protein (Materials and methods 2.4.2.). Such phosphatase treatment of PDE4D3 caused the *stage 1* and *stage 2* forms seen in mitosis, to disappear and a single form migrated at the same molecular weight as the native form of the protein (~95 kDa), when analysed by SDS-PAGE (*Fig. 4.16.*).

The activity of the PDE4D3, after CIAP treatment of mitotic lysate, was also analysed. This showed that the removal of phosphate by CIAP caused a 3 –fold decrease in the activity of the protein thus activity of mitotic PDE4D3 returned to levels found in asynchronous cells (*Fig. 4.17.*).

4.3.5. Utilisation of staurosporine to identify the nature of the mitotic modification of PDE4D3

The elevation of PDE4D3 activity and the change in the electrophoretic migration of PDE4D3 protein in Rat-1 cells arrested in mitosis appeared to be due to a phosphorylation event. Indeed, phosphatase inhibition by OA served to maintain the activity and the shifted species of PDE4D3 and the treatment of PDE4D3 with CIAP reduced activity and removed the *stage 1* and *stage 2* species of PDE4D3 with lowered electrophoretic mobility. A study was therefore undertaken to try to identify the kinase that was targeting PDE4D3 for phosphorylation during mitosis.

The general kinase inhibitor staurosporine has specificity for PKA ($IC_{50} = 7$ nM), PKC ($IC_{50} = 0.7$ nM), CaM kinase ($IC_{50} = 20$ nM), myosin light chain kinase ($IC_{50} = 1.3$ nM), PKG ($IC_{50} = 8.5$ nM), cdk2 ($IC_{50} = 0.07$ nM), Chk1 ($IC_{50} = 20$ nM) and Janus kinase (JAK2, $IC_{50} = 100$ nM). Staurosporine is also known to inhibit many kinases at higher

concentrations due to the similarities of its structure to the adenosine group on ATP (Toledo and Lydon, 1997). This was used initially to decrease the activity of a number of kinases that could be active in the mitotic cells, in an attempt to eliminate the bandshift and activity increase of PDE4D3.

4.3.5.1. *Staurosporine increases the electrophoretic mobility of mitotically modified PDE4D3*

A range of staurosporine concentrations were incubated on Rat-1 cells arrested in mitosis for 2 h in an attempt to identify potential kinases and eliminate other candidate kinases that could be targeting PDE4D3 during mitosis. The electrophoretic mobility of PDE4D3 from mitotic cells treated with staurosporine was analysed by SDS-PAGE and immunoblotting (Fig. 4.18.) and it was determined that migration of the shifted species of PDE4D3 protein was ablated when staurosporine at concentrations above 10 nM were incubated with the mitotic cells (Fig. 4.18.). However, at lower staurosporine concentrations, no alteration in PDE4D3 electrophoretic mobility were observed (Fig. 4.18.).

To ascertain the rate at which staurosporine ablates the PDE4D3 modification a time course of staurosporine incubation on mitotic cells was carried out. Staurosporine (100 nM) was incubated with mitotically arrested cells for up to 2 h and cells were harvested at various time points. The electrophoretic mobility of the PDE4D3 protein was analysed by SDS-PAGE and it was found that 100 nM staurosporine inhibited the phosphorylation of PDE4D3 in a time dependent fashion (Fig. 4.19.). All of the *stage 2* migrating species of PDE4D3 was lost after 10 min incubation with staurosporine, increasing the amount of immunoreactive protein that migrated at *stage 1*. There was a 6 % decrease in the amount of PDE4D3 migrating with the *stage 1* species of PDE4D3 after 20 min and all of the PDE4D3 protein migrated the same as the native, unmodified PDE4D3 (~95 kDa) after a 60 min incubation of mitotic cells with staurosporine (Fig. 4.19.).

4.3.5.2. *Staurosporine decreases the activity of mitotically modified PDE4D*

As incubation of mitotic cells with staurosporine led to loss of the *stage 1* and *stage 2* forms of PDE4D3, an investigation as to whether there was an accompanying down regulation of PDE4D3 activity was undertaken. Rat-1 cells were arrested in mitosis and then incubated with 100 nM staurosporine over a 2 h time course. During this time cells were removed at intervals and PDE4D3 isolated by immunopurification so that its cAMP-PDE activity could be determined. After a 10 min period with 100 nM staurosporine there

was no change in PDE4D3 activity (*Fig. 4.20.*). After 20 min there was a 0.25 -fold decrease in PDE4D3 activity, after 30 min there was a 0.35 -fold decrease in activity and after 60 min staurosporine incubation with mitotic cells there was a 0.5 fold decrease in PDE4D3 activity. After 60 mins no further decrease in the PDE4D3 activity was observed.

4.3.5.3. *Staurosporine does not induce premature exit of Rat-1 cells from mitosis*

Staurosporine has been shown to induce premature exit of cells from mitosis, by bypassing cytokinesis to produce hyperloid cells in yeast and glioma cell lines (Tsuiki et al., 2001). Staurosporine also increases the rate at which cells leave mitosis when added to mitotically-released HeLa cell lines (Ling et al., 1998). To check that the changes in activity and electrophoretic migration of PDE4D3 upon staurosporine incubation on the mitotic Rat-1 cells was not due to their premature exit from mitosis, cells were analysed by flow cytometry for their distribution within the cell cycle (Materials and methods 2.2.). There was no premature exit of the cells from mitosis and there was no increase in hyperloid cells upon staurosporine treatment (*Fig. 4.21.*).

4.3.6. *Use of specific kinase inhibitors to identify the kinase which targets PDE4D3 in mitosis*

Kinase inhibitors act by binding to the ATP site of the enzyme, as in the case of the cyclin dependent kinase inhibitor, olomucine (Abraham et al., 1995), or by binding competitively to the same site of the kinase as the target protein, as occurs with the PKC selective inhibitor chelerythrine chloride (Herbert et al., 1990). Both mechanisms prevent the transfer of the phosphate group of ATP to the target protein. Specific kinase inhibitors were utilised as a tool in a study to attempt to identify the kinase that modifies PDE4D3 in cells arrested in mitosis by nocodazole.

4.3.6.1. *Protein kinase C inhibitors do not affect the mitotic modification of PDE4D3*

Staurosporine was initially recognised as a PKC specific inhibitor (Tamaoki et al., 1986). Therefore, as the mitotic modification of PDE4D3 was inhibited by staurosporine more selective PKC inhibitors were investigated to determine whether they too ablated the *stage 1* and *stage 2* mobility shifted forms of PDE4D3 and decreased the activity of PDE4D3 in mitosis. Bisindolylmaleimide II and chelerythrine chloride, both highly specific inhibitors

of PKC were incubated on mitotic Rat-1 cells for up to 2 h. The electrophoretic shift and the change in PDE4D activity seen in Rat-1 cells arrested in mitosis was not affected by these inhibitors (*The effects of Bisindolylmaleimide are shown in Figs. 4.22. & 4.23. and the data for chelerythrine chloride are not shown*).

4.3.6.2. Many commercially available specific kinase inhibitors do not affect the mitotic modification of PDE4D3

With the PKC inhibitors having no effect on the modifications of PDE4D3 which occur in nocodazole induced mitosis, a panel of specific kinase inhibitors were incubated with mitotic cells for time courses up to 2 h. The inhibitors used included U0126 (10 μ M), H89 (10 μ M), genistein (10 μ M), 5,6-Dichloro-1- β -D-ribofuranosylbenzimidazole (DRB, 10 μ M), Wortmannin (1 mM), LY294002 (10 μ M), Olomucine (20 μ M), PD98059 (10 μ M), ML-7 (5 μ M). They target multiple intracellular signalling cascades, full details of which are shown in Table 4.1. The activity of PDE4D3 and the electrophoretic mobility of the PDE4D3 protein by gel electrophoresis after incubation of inhibitors on cells arrested in mitosis was analysed, none of these inhibitors decreased PDE4D3 activity or ablated the formation of *stage1* and *stage 2* forms of PDE4D3 (*Figs. 4.22. & 4.23.*).

4.4. The effect of PKA activation on PDE4D3 in mitotic cells

The PKA inhibitor H89 had no effect on decreasing the activity of PDE4D or ablating the bandshifted species of PDE4D3 when incubated on Rat-1 cells isolated in mitosis (4.3.6.2.). However, PKA is a kinase which targets PDE4D3 for phosphorylation, a modification which increases the activity of the protein (Lim et al., 1999) and inhibits PDE4D3 electrophoretic migration by SDS-PAGE (Sette and Conti, 1996). A study was therefore undertaken to investigate the effect of activating PKA in mitotic cells on the modifications of PDE4D3, to determine whether it could enhance activation or increase the amount of PDE4D3 protein migrating with decreased electrophoretic mobility.

4.4.1. Forskolin increases the amount of 'mitotic' PDE4D3 showing retarded electrophoretic migration

Forskolin is an agonist for adenylate cyclase and, when incubated with cells, increases the concentration of cAMP enough to stimulate the PKA mediated phosphorylation of PDE4D3 (Liu and Maurice, 1999; Lim et al., 1999; Liu et al., 2000a; Sette and Conti, 1996). Asynchronous cells and cells in nocodazole-induced mitosis were treated with 100

150
 μM forskolin for 15 min and the electrophoretic mobility of PDE4D3 on SDS-PAGE was analysed. In the mitotic population there was an increase of 17 % in the proportion of PDE4D3 that migrated with the *stage 1* and an increase of 14 % in the proportion of PDE4D3 that migrated with the *stage 2* form of PDE4D3 which was accompanied by a 31 % loss of the faster migrating 'native' PDE4D3. In fact, virtually all the PDE4D3 protein was migrating as the bandshifted *stage 1* and *stage 2* species (~70 % immunoreactive PDE4D3). In the asynchronous population of cells, treated with forskolin, there was also about 70 % of PDE4D3 that migrated with a reduced electrophoretic mobility, however it only migrated as a single shifted species (*Fig. 4.24.*).

4.4.1.1. *Forskolin retarded PDE4D3 is insensitive to H89*

H89 was initially identified as a specific inhibitor for PKA (Chijiwa et al., 1990; Geilen et al., 1992) although, subsequently, it has been found to inhibit other kinases at higher concentrations. The IC_{50} values of H89 for known kinases are; PKA (48 nM), Calmodulin kinase II (29.7 μM), casein kinase I (38.3 μM), myosin light chain kinase (28.3 μM), PKC (31.7 μM) (Calbiochem catalogue). H89, at a concentration of 10 μM , has been shown to ablate the PKA mediated phosphorylation of Ser⁵⁴ on PDE4D3 (Liu and Maurice, 1999). An investigation to see whether the forskolin-mediated increase in the proportion of PDE4D3 migrating with the retarded electrophoretic mobility was due to a PKA-specific phosphorylation event was carried out. Asynchronous and nocodazole arrested mitotic cells were pre-treated with 10 μM H89 for 10 min prior to the addition of 100 μM forskolin for 15 min. The electrophoretic mobility of PDE4D3 was then analysed by SDS-PAGE and immunoblotting. The pre-incubation of asynchronous cells with H89 ablated the forskolin-stimulated formation of the 'bandshifted' species of PDE4D3 (*Fig. 4.24.*). The pre-incubation of mitotic cells with H89 did not, however, completely abolish the forskolin-stimulated modification of PDE4D3 (*Fig. 4.25.*). There was a 10 % decrease in the amount of protein that comigrated with the *stage 1* shifted PDE4D3 protein. However, there seemed to be only a 2 % decrease in the amount of PDE4D3 that migrated with the *stage 2* form of PDE4D3 (*Fig. 4.24.*).

4.4.2. *Forskolin increases the activity of mitotic PDE4D*

Forskolin is known to activate PKA, which targets PDE4D3 for phosphorylation and leads to an increase in the activity of the protein (Sette and Conti, 1996). In order to ascertain whether stimulation of PKA could further enhance the activity of PDE4D3 in mitotic cells,

the effects of forskolin-treatment on PDE4D3 in both asynchronous and mitotic cells was studied. Nocodazole-treated mitotic cells and asynchronous cells were thus treated with 100 μ M forskolin for 15 min and PDE4D3 was isolated by immunopurification. The enzymatic activity of the isolated PDE4D3 protein was analysed and found to have increased approximately 2.5-fold in asynchronous cells stimulated with forskolin. However, the activity of PDE4D3 in forskolin-stimulated mitotic cells was only increased by approximately 33%, when compared to the unstimulated cells. The forskolin-stimulated activation of PDE4D3 in mitotic cells did not increase to levels any higher than those in the forskolin-treated asynchronous cells (*Fig. 4.25.*).

4.4.2.1. Forskolin-stimulated PDE4D3 activity is insensitive to H89

To determine whether the forskolin stimulated increase in PDE4D3 activity from asynchronous and mitotic cells was brought about by a PKA mediated phosphorylation the PKA inhibitor H89 was incubated with asynchronous and mitotic cells for 20 min prior to forskolin stimulation. The enzymatic activity of isolated PDE4D3 was analysed and it was found that the forskolin-induced increase of PDE4D3 activity seen in asynchronous cells was reduced by 35 % when the cells were pre-treated with H89 (*Fig. 4.25.*). In contrast, the forskolin-induced increase of PDE4D3 activity seen in nocodazole-induced mitotic cells did not appear to decrease when the cells were pre-incubated with H89.

4.5. Identification of the potential phosphorylation sites in PDE4D3

The kinase(s) responsible for the modifications of PDE4D3 during mitosis, causing increases in PDE4D enzymatic activity and causing the PDE4D3 protein to decrease its electrophoretic mobility, could not be identified by inhibition of kinases using several commercially available inhibitors. An alternative approach to identify the kinase(s) was therefore taken to try to ascertain the residues or peptide fragments of PDE4D3 that were being phosphorylated during mitosis and thus to use the motifs within these as a starting point for identifying the candidate kinase(s). Several analysis packages were used to investigate the potential phosphorylation motifs in PDE4D3 and then mutational analysis of potentially phosphorylated residues was carried out.

4.5.1. Analysis packages used for identification of target sequence motifs in PDE4D3

There are several packages accessible over the Internet that can be utilised to predict the sites on a protein that could be phosphorylated by commonly studied kinases. NetPhos 2.0 Prediction Server, at the Center for Biological Sequence Analysis, produces neural network predictions for serine, threonine and tyrosine phosphorylation sites in eukaryotic proteins with a sensitivity in the range from 69 to 96 %. PhosphoBase v2.0, a database of phosphorylation sites provided by the Center for Biological Sequence Analysis (Kreegipuu et al., 1999) is a service which implements a prediction algorithm based on substrate consensus sequences of some more common protein kinases. The results for these predicted protein phosphorylation sequence sites have to be interpreted with caution however, as many sequences that do not correspond to a consensus sequence can be phosphorylated and not all consensus phosphorylation sequences are indeed phosphorylated *in vivo*. The sites identified by these services were therefore only used as a guideline for the potential phosphorylation sites of the protein.

4.5.1.1. Predicted serine, threonine and tyrosine phosphorylation sites of PDE4D3

The amino acid sequence for the rat PDE4D3 isoform (*Fig. 4.26.*) was submitted for phosphorylation sequence prediction via the web at either the NetPhos prediction server (<http://www.cbs.dtu.dk/services/NetPhos/>) or at the PhosphoBase prediction server (<http://www.cbd.dtu.dk/database/Phosphobase/predict/predform.html>). The residues predicted to be phosphorylated and their calculated probabilities are shown in Tables 4.2 and 4.3..

4.6. Mutational analysis of the modification of PDE4D3 during mitosis in alternative cell lines

PDE4D3 (accession number U50159.1) is a 'long' PDE4D isoform, which has a unique 15 amino acid sequence at the extreme N-terminus, all other residues of the protein are common to other long-form PDE4D isoforms (Bolger et al., 1997). In an attempt to identify the residue(s) of PDE4D3 targeted for modification during mitosis, truncated PDE4D constructs and PDE4D constructs containing mutants of specific serine and threonine residue were studied.

Rat-1 cells do not have a high transfection efficiency (personal observations and Bonfoco et al., 2001). Therefore an alternative cell line, HeLa cells (Materials and methods 2.1.1.2.), which have a high level of transfection efficiency, were utilised to enable the study of modifications of the mutated PDE4D3 constructs.

4.6.1. Endogenous PDE4D3/5 in HeLa cells arrested in mitosis have reduced electrophoretic mobillities

HeLa cells have been extensively characterised and used as a model for cell cycle studies by many different groups (for examples see Stephen et al., 1990; Molinari, 2000) and was a suitable cell line in which to study heterologously expressed mutant PDE4D3 constructs.

HeLa cells endogenously express both PDE4D3 and PDE4D5 isoforms at similar levels (*Fig. 4.27.*) and when the cells were blocked in mitosis a change in the electrophoretic mobility of both the PDE4D3 and PDE4D5 isoforms was observed when analysed by SDS-PAGE and immunoblotting with a PDE4D specific antiserum (*Fig. 4.27.*). The PDE4D3 protein from cells arrested in mitosis appeared to migrate as a single shifted species, although a second shifted species could have co-migrate with the native PDE4D5 protein. The PDE4D5 protein from HeLa cells arrested in mitosis appeared to migrate as two shifted species, similar to the pattern of migration observed for the PDE4D3 protein in mitotic lysates of Rat-1 cells (*Fig. 4.27.*).

4.6.2. Serine and threonine mutants of PDE4D3 are modified during mitosis

Mutant constructs of human PDE4D3, previously engineered in this laboratory (Hoffmann et al., 1998), were employed in an attempt to identify the residues phosphorylated by kinases in mitotic cell lysates.

4.6.2.1. Electrophoretic mobility of mutants of the PKA phosphorylated sites in PDE4D3 during mitosis

PDE4D3 and PDE4D5 both appear to undergo the same modification in cells arrested in mitosis as evidenced by bandshifts (*Fig. 4.27.*). Therefore, it might be concluded that a similar modification occurs in both proteins during mitosis so the sites modified might well be within the common PDE4D 'long-form' sequence.

I set out firstly to analyse whether Ser¹³, the PKA phosphorylation site located in the unique N-terminal 15 amino acids of PDE4D3, was responsible for the changes in motility and activity seen in PDE4D3 to occur in mitosis. The construct used encoded PDE4D3 with the Ser¹³ residue mutated to alanine, it also had a VSV epitope tag at the C-terminus so that it could be selectively isolated from the endogenous PDE4D3 (Hoffmann et al., 1998). The S13A-PDE4D3-VSV construct was transfected into HeLa cells (Materials and methods 2.1.3.) and the cells arrested in mitosis through incubation with nocodazole (Materials and methods 2.1.4.5). Under these conditions the Ser13Ala mutant migrated at the same molecular weight as PDE4D3 on an SDS-PAGE gel and crucially, both the *stage 1* and *stage 2* species of PDE4D3 were apparent (*Figs. 4.28 and 4.29.*). Furthermore, the *stage 1* and *stage 2* forms of PDE4D3 were no longer apparent after a 2 h incubation of the mitotic cells with 100 nM staurosporine (*Fig. 4.28.*), as was the case with wild-type PDE4D3, seen previously.

4.6.2.2. *Analysis of the activity of Ser13Ala and Ser54Ala PDE4D3 mutants in mitosis*

PKA phosphorylates PDE4D3 at both Ser¹³ and Ser⁵⁴. However, activation is attributable to phosphorylation of Ser⁵⁴ in UCR1 (Sette and Conti, 1996). Given that the mitotic modification of PDE4D3 coincided with an increase in the enzymatic activity it was decided to analyse whether the two known PKA phosphorylation sites, Ser¹³ and Ser⁵⁴ were involved in this activation event. To analyse this VSV-tagged mutants of PDE4D3, in which either Ser¹³ or Ser⁵⁴ had been mutated to alanine, were expressed in HeLa cells. These transfected cells were arrested in mitosis and the PDE activities of the cells lysates were measured. There was a slight increase in the activity of wild-type PDE4D3, but no conclusive change in the activity of the mutant proteins was observed (*shown within Fig. 4.30.*).

4.6.2.3. *The electrophoretic mobility of truncated PDE4D mutants in mitosis*

A mutant PDE4D 'long-form' construct has previously been engineered which is truncated at the common splice junction of the PDE4D3, PDE4D5 and PDE4D4 'long' isoforms. It, therefore, lacks the unique N-terminal regions of each of these species (*Fig. 4.31.*). A shorter truncated mutant of PDE4D, which lacks the UCR1 and the LR1 domains, has also been generated (*Fig. 4.31.*). Both mutants were transfected into HeLa cells (Materials and methods 2.1.3.), which were subsequently arrested in mitosis or left asynchronous (Materials and methods 2.1.4.5), and the electrophoretic mobilities of the N-terminally

truncated PDE4D proteins determined by SDS-PAGE and immunoblotting. The PDE4D protein truncated at the common 'long form' splice region behaved as the wild-type species, with decreased electrophoretic mobility observed when the cells were arrested in mitosis (*Fig. 4.29.*). The shorter truncate lacking the UCR1 and LR1 regions, however, showed no change in electrophoretic mobility when the HeLa cells were arrested in mitosis (*Fig. 4.29.*).

4.6.2.4. Analysis of the activity and electrophoretic mobility of other PDE4D3 mutants in mitosis

In an attempt to identify the involvement of putative phosphorylation targets in the residues between the PDE4D common 'long-form' splice junction and the beginning of UCR1 these serine and threonine residues were mutated to alanine (*Fig. 4.31.*). All these mutants of PDE4D3 had altered electrophoretic mobility when the transfected cells were arrested in mitosis (*Fig. 4.29.*). However, when the activities of these PDE4D3 mutants were examined, from asynchronous or mitotic cells, there was no conclusive change in enzymatic activity of the protein (*Fig. 4.30.*).

4.7. In vitro phosphorylation of PDE4D3

4.7.1. UCR1 Is phosphorylated in vitro by mitotic kinases

In order to establish whether the UCR1 region of PDE4D3 is targeted for phosphorylation by mitotic kinases, recombinant GST fusion proteins containing the UCR1 region alone, the UCR2 region alone or the combined UCR1 and UCR2 regions (*Fig. 4.32.*) were subjected to an *in vitro* phosphorylation with mitotic lysate from Rat-1 cells (Material and methods 2.4.5.2.). As a control for the reaction, the purified PKA catalytic subunit was used to try and phosphorylate the same recombinant proteins, as PKA is known to phosphorylate Ser⁵⁴ in UCR1 (Sette and Conti, 1996). The UCR1 domain and the combined UCR1 and UCR2 domains were shown to become phosphorylated by kinases present in mitotic lysates, whereas the UCR2 domain, when subjected to the same reaction conditions, remained unphosphorylated (*Fig. 4.33.*). The UCR1 domain was phosphorylated by the isolated PKA catalytic subunit, as expected, whilst the UCR2 domain remained unphosphorylated when subjected to the same reaction conditions (*Fig. 4.33.*).

4.7.2. Phosphorylation of PDE4D3 by mitotic kinases is within a different peptide to that targeted by PKA

It has previously been reported that when recombinant PDE4D3 protein that has been phosphorylated by the purified PKA catalytic subunit is then cleaved by cyanogen bromide it gives two peptides that incorporate ^{32}P . These peptides were found to contain either the Ser¹³ or Ser⁵⁴ residue (Sette and Conti, 1996). In an attempt to identify the PDE4D3 peptide phosphorylated by kinases present in mitotic or asynchronous cell lysate, a similar strategy of cyanogen bromide cleavage was employed, using full-length PDE4D3 phosphorylated with either cell lysates or PKA catalytic subunit.

4.7.2.1. Cyanogen bromide cleavage of phosphopeptides

Cyanogen bromide (CnBr) reacts specifically with methionine residues in proteins and, under acidic conditions, leads to the cleavage of the peptide bond at the carboxy terminus of the amino acid. Methionine residues are generally in low abundance in proteins and cyanogen bromide cleavage, therefore, generally generates large peptides that can be analysed by SDS-PAGE (Van Der Geer et al., 1993). The peptides generated by cyanogen bromide cleavage of PDE4D3 (*Table 4.4*), which had been phosphorylated by kinases from either asynchronous or mitotic lysate from Rat-1 cells or purified PKA, were separated by SDS-PAGE. I identified two peptides of PDE4D3 phosphorylated by PKA and these migrated at molecular weights of 3.5 kDa and 6 kDa (Sette and Conti, 1996, *Fig. 4.34.*). The kinases present in asynchronous and mitotic lysates appeared to phosphorylate several PDE4D3 peptides. These species migrated with molecular weights of between 3.5 – 6 kDa, 14 kDa, around 20 kDa and a large peptide that migrated at approximately 27 kDa. These four peptides appeared to be distinct from the two peptides phosphorylated by PKA. The kinases present in mitotic lysate from Rat-1 cells appears to phosphorylate PDE4D3 to a greater extent than the kinases in the asynchronous lysate as indicated by densitometric analysis (*Fig. 4.34.*).

4.7.3. 2D analysis of PDE4D3 peptides phosphorylated with mitotic lysate

To further analyse PDE4D3 phosphopeptides phosphorylated by kinases in mitotic cell lysate *E. Coli* expressed recombinant PDE4D3 protein was subjected to *in vitro* phosphorylation, using either lysate from asynchronous cells or cells isolated in mitosis. Isolated PDE4D3 was then digested, using trypsin, to generate peptides for 2D separation.

Trypsin hydrolyses peptide bonds at the carboxy terminal side of arginine (Arg) and lysine (Lys) residues (Cunningham, 1954), so might be expected to generate more peptides from PDE4D3 than cyanogen bromide mediated cleavage (section 4.7.2.).

The trypsin-generated peptides were separated by 2D electrophoresis on thin layer cellulose plates (materials and methods 2.4.6.). In four independent experiments three phospho-peptides from PDE4D3 appeared to be phosphorylated to a higher degree by kinases present in the mitotic lysate compared to the same peptides phosphorylated by kinases in the asynchronous lysate (*Fig 4.35.*).

4.7.4. HPLC identification of PDE4D3 peptides phosphorylated with mitotic lysate

It was initially intended to extract the PDE4D3 phosphopeptides from the cellulose plates and to sequence them. However, cellulose plates contain contaminants that interfere with sequencing (Tavare and Issad, 2001) and to purify the peptides away from these contaminants would result in further loss of phosphorylated protein. As approximately 1 picomole of peptide is required for sequencing, high performance liquid chromatography (HPLC) was employed in order to try and isolate PDE4D3 peptides phosphorylated during mitosis.

E.Coli expressed recombinant PDE4D3 protein was phosphorylated *in vitro* using lysate from asynchronous and mitotic cells in the presence of ^{32}P -ATP. The PDE4D3 protein was then digested, using trypsin, and the phosphorylated peptides isolated by HPLC (Materials and methods 2.4.7.). There were four peaks of radioactivity eluted that had been phosphorylated by kinases from asynchronous cell lysate and eleven radioactive peaks from PDE4D3 phosphorylated using mitotic cell lysate (*Fig. 4.36.*). The four radioactive peaks produced using asynchronous lysate were also present in the peptides phosphorylated by mitotic kinases. However, approximately 4-5 fold higher amounts of ^{32}P were incorporated into these peptides when subjected to mitotic lysate phosphorylation. Having isolated the PDE4D3 peptides associated with the radioactive peaks (Materials and methods 2.4.7.2.), their identification could then be carried out by mass spectrometry analysis.

4.7.4.1. *Mass spectrometry identification of PDE4D3 peptides phosphorylated by mitotic kinases*

The four PDE4D3 peptides, referred to as A, B, C and D, that appeared to be highly phosphorylated by kinases from mitotic cells were submitted to the 'FingerPrints' proteomics facility at the University of Dundee, where identification and sequencing of the peptides was carried out. The smallest peptide phosphorylated by kinases in mitotic lysate, peptide A, corresponded to residues 59-68 and mapped to a region within the N terminus of the UCR1 domain of PDE4D3 (*Fig. 4.37.*). Another larger peptide from UCR1, peptide C, which corresponded to residues 73-98 of PDE4D3 was also phosphorylated by the mitotic kinases. There was one peptide, peptide B, from PDE4D3 that mapped to residues 232/233 to 246 that was located to a region within the N terminal portion of the catalytic domain and another, very large peptide, peptide D, that mapped to residues 534 to 591 in the C terminal portion of the catalytic domain. This large peptide from the catalytic domain was hydrolysed further by the proteomics facility to enable sequencing and identification of the phosphorylated residue within.

4.7.4.2. *Cycle burst identification of residues phosphorylated in mitosis*

The PDE4D3 peptides phosphorylated to a high level by kinases in mitotic lysate were sequenced using Cycle Burst and Edman degradation ('FingerPrints' Proteomics Facility, University of Dundee). This enabled the phosphorylated residues within the PDE4D3 phosphopeptides to be identified. The results from this analysis are summarised in *Figures 4.38a.- 4.38d.*

4.7.5. ***The activity of PDE4D3 is increased by in vitro phosphorylation using kinases present in mitotic lysates***

To determine whether the *in vitro* phosphorylation of PDE4D3 led to a similar increase in enzyme activity as that seen *in vivo*, PDE4D3 protein, immunopurified from a HEK-293 cell line over-expressing PDE4D3, was subjected to 'cold' *in vitro* phosphorylation using kinases in both asynchronous and mitotic cell lysates (Materials and methods 2.4.5.5.). The enzymatic activity of PDE4D3 was then assayed. I found that PDE4D3 treated with the mitotic lysate under phosphorylating conditions had a higher level of activity compared to PDE4D3 treated under similar conditions with asynchronous lysate (*Fig. 4.39.*).

4.8. The effects of the mitotic increase in PDE4D activity on mitotic processes

I set out to determine whether the increase in PDE4D3 activity could influence processes related to mitosis. To do this, cells subjected to nocodazole-induced mitotic arrest were analysed for changes in PKA activity and mitotic progression upon the inhibition of PDE4 activity, using the PDE4 selective inhibitor, rolipram.

4.8.1. Rolipram causes an elevation of PKA activity in mitotic cells

Rat-1 cells that had been arrested in mitosis, where PDE4D3 is activated, were treated with 10 μ M rolipram for up to 2 h. Cells were then harvested at set intervals, lysed and the PKA activity of these samples determined using the standard PKA assay (materials and methods 2.4.1). The activity of PKA in mitotic cells increased 1.5 fold after a 10 min incubation with rolipram (*Fig. 4.40.*). This increase of PKA activity was maintained throughout the 2 h time course of rolipram incubation. Note that I have shown previously (Chapter 3) that rolipram exerts but a small stimulatory effect on PKA activity in asynchronous cells but a profound effect in mitotic cells, where PDE4D3 activity is high.

4.8.2. Rolipram increases the rate of M/G1 transition

PKA activity is down-regulated in cells as they enter mitosis, enabling the activation of the maturation promoting factor (MPF, Fernandez et al., 1995; Oh et al., 1996) and nuclear envelope disassembly (Lamb et al., 1991). Inactivation of PKA prevents cells from completing mitosis by blocking them at metaphase (Grieco et al., 1996). Reactivation of PKA at the metaphase/anaphase transition (Zeilig et al., 1976) is required for the reformation of the nuclear envelope (Steen et al., 2000) and the exit of cells from mitosis (Grieco et al., 1996). I therefore undertook a study to investigate the effects of the inhibition of PDE4 activity on both mitotic progression and on the rate at which cells leave mitosis. Rat-1 cells arrested in nocodazole-induced mitosis were released from this block in the presence of 10 μ M rolipram and the progression of the cells into the next G1 phase was monitored by FACs analysis. The Rat-1 cells incubated with rolipram progressed into the next G1 stage of the cell cycle at a quicker rate than the Rat-1 cells released from the mitotic block in the absence of a PDE inhibitor (*Fig. 4.41.*).

4.9. Discussion

The PDE4D3 isoform is modified in Rat-1 cells and HeLa cells that are subjected to nocodazole-induced mitosis. This modification causes the 1.7 fold activation of PDE4D3. In addition, up to 35 % of PDE4D3 appears to be converted into species that migrate with reduced electrophoretic mobilities when analysed by SDS-PAGE. One of the 'bandshifted' PDE4D3 species has been called here *stage 1*, which has a slightly reduced electrophoretic mobility compared to the native PDE4D3 and appears to migrate with a molecular weight of approximately 100 kDa. The second was called *stage 2*, which exhibits a further reduction in electrophoretic mobility and appears to migrate with a molecular weight of approximately 102 kDa.

It is unclear as to the basis of the observation that only a proportion of PDE4D3 has an altered electrophoretic mobility. It could be, for example, that mitosis brings about a 'redistribution' of only a small proportion of PDE4D3 to a subcellular location where it can be targeted for modification. However, in Rat-1 cells, the bandshifted PDE4D3 protein is found primarily in the cytosolic fraction, with a small amount associated with the microsomal and nuclear fractions. There was no apparent translocation of PDE4D3 in cells isolated at different phases of the cell cycle, thus the cytosolic distribution of PDE4D3 suggests that if there are factors which limit accessibility of the protein to the modifying enzyme(s) they might be due to the formation of complexes with cytosolic proteins. Alternatively, modification of only a fraction of PDE4D3 could reflect a steady state level of modification by specific kinases and phosphatases whose balance is altered in the mitotic cells, compared to the asynchronous ones.

The modifications of PDE4D3, which led to its altered electrophoretic mobility and activity, appear to be specifically related to mitosis. It is only when Rat-1 cells treated with nocodazole accumulate in mitosis that the immunoreactive *stage 1* and *stage 2* forms of PDE4D3 were detected. The accumulation of cells in mitosis also led to a time dependent increase in PDE4D3 enzymatic activity. Incubating cells with nocodazole causes inhibition of microtubule assembly (Thyberg and Moskalewski, 1989). However, it does not appear to be the disregulation of microtubule dynamics *per se* that causes modification of PDE4D3 since short-term incubation with this drug did not affect the electrophoretic mobility or activity of PDE4D3, whilst it did cause disruption of microtubular cytoskeleton.

Confirmation that the 'bandshifts' and the increase in PDE4D3 activity were due to a reversible mitotic event(s) was also indicated using Rat-1 cells released from nocodazole-induced mitosis. Cells rapidly leave mitosis when they are released from a nocodazole block (Hamilton and Snyder, 1982) and, as they pass through the latter phases of mitosis they enter G1. In doing this the species of PDE4D3 with reduced electrophoretic mobilities disappeared and the total PDE4D3 activity progressively decreased back to levels seen in asynchronous cells. These effects were inhibited by incubation of cells released from the mitotic block with high concentrations of the phosphatase inhibitor okadaic acid (OA, >200 nM). This suggests that the dephosphorylation of PDE4D3 leads both to a loss of species with lowered electrophoretic mobility and a restoration of lowered PDE4D3 activity. The identification of the candidate phosphatase for this dephosphorylation of PDE4D3 upon mitotic exit was not ultimately proved. However, it was unlikely to be protein phosphatase 2A, as this species is sensitive to sub-nanomolar concentrations of OA (Cohen et al., 1990), as are the less common protein phosphatases (PP) such as PP3 (Honkanen et al., 1991), PP4 (Brewis et al., 1993) and PP5 (Chen et al., 1994). Other potential candidate protein phosphatases, such as PP2B (Klee and Krinks, 1978) and Cdc25, the cell cycle-dependent phosphatase which has been shown to have high activity during mitosis (Kishimoto and Yamashita, 2000; Honda et al., 1993; Gordon, 1991) are both insensitive to OA. It is thus possible that PP1 may serve to dephosphorylate PDE4D3 upon mitotic exit. However, further studies are needed to confirm this and to exclude any role of PP2B, Cdc25 and any other less common phosphatases, such as PP7, in dephosphorylating PDE4D3 upon mitotic exit. Indeed, further confirmation that PP1 specifically dephosphorylated PDE4D3 is also required.

Dephosphorylation of PDE4D3, by treatment of mitotic lysate with calf intestinal alkaline phosphatase, also led to both the disappearance of the *stage 1* and *stage 2* forms of PDE4D3 and to reduce, by 2.5-fold, PDE4D3 activity. Upon inhibition of kinase activities in mitotic cells it was shown that the general kinase inhibitor staurosporine ablated the appearance of the bandshifted species of PDE4D3. It also caused an approximate 2-fold reduction in the activity of PDE4D3 in mitotic cells, lowering it to a level comparable to that seen in asynchronous cells. Collectively, these results provide more evidence that PDE4D3 was specifically phosphorylated during mitosis and that such events served to both retard the electrophoretic mobility of a portion of total PDE4D3 and to increase PDE4D3 activity approximately 2-fold in mitosis.

I was, however, seemingly unable to detect the *stage 1* and *stage 2* forms of PDE4D3 by *in vivo* labelling of the mitotic cells with ^{32}P orthophosphate, despite these species being

evident on the immunoblot of the same nitrocellulose. This may be due to the fact that only ~30 % of total PDE4D3 had such a reduced electrophoretic mobility in mitotic cells. Thus, if proteins had been exposed to the phosphorimage screen for a longer period the *stage 1* and *stage 2* forms of PDE4D3 might have been detected. Nevertheless, the incorporation of higher levels of ^{32}P into PDE4D3 migrating with the 'native' protein in mitotic cells suggests that the phosphorylation inducing the 'bandshift' and that increasing PDE4D3 activity are two independent events.

Stimulation of mitotic cells with forskolin highlights the fact that the phosphorylation that causes activation of PDE4D3 occurs independently of the phosphorylation which alters the electrophoretic mobility of PDE4D3. When adenylate cyclase was activated; by forskolin, there was a 2-fold increase in the proportion of PDE4D3 protein that migrated with the *stage 1* and *stage 2* forms on SDS-PAGE, which coincided with only a 1.2-fold increase in PDE4D3 activity. If these two events were linked by the same phosphorylation then a proportional increase in activation of PDE4D3 would be expected to accompany the decrease in PDE4D3 electrophoretic mobility. Intriguingly, the increase in the proportion of PDE4D3 which migrated at the *stage 2* position was insensitive to H89, as was the increase in activity of PDE4D3 in the forskolin stimulated mitotic cells. These observations suggest that the enzyme(s) modifying PDE4D3 in this situation was not PKA, but was activated in a cAMP-dependent fashion. This might suggest that either Epac or Rap1 stimulate unidentified kinases to achieve this. Thus multiple phosphorylations of PDE4D3 in mitotic cells might be mediated by the action of multiple proteins.

PDE4 enzymes are known to be phosphorylated in cells by PKA (Sette and Conti, 1996) and ERK (MacKenzie et al., 2000). In an attempt to identify the specific kinase targeting PDE4D3 for modification in nocodazole-induced mitosis, several commercially available kinase inhibitors were incubated with mitotic cells. Unlike staurosporine, none of the specific kinase inhibitors employed either decreased the amount of protein migrating with the *stage 1* and *stage 2* shifted species of PDE4D3 or reduced the activity of PDE4D3. The fact that specific inhibitors of PKA and ERK were among these implies that the kinase targeting PDE4D3 in mitotic cells is one that has not been shown previously to phosphorylate PDE4 isoforms.

There are multiple mitotic kinases for which there are yet no known commercially available inhibitors. These include the members of the Polo-like kinase (Plk) family (Clay et al., 1993), the Aurora kinases (Adams et al., 2001) and mammalian homologues of NIMA (never in mitosis A) family of kinases (Kandli et al., 2000). All of these kinases are

activated at the onset or during mitosis, so may serve as potential candidates for phosphorylating PDE4D3 at the metaphase/anaphase transition. Plk isoforms, for instance, are activated during mitosis (Kotani et al., 1998; Gallant et al., 1995) and are known to target multiple substrates required for spindle formation (Lane and Nigg, 1996), ordered mitotic progression (Nigg et al., 1996) and cell division (reviewed in Donaldson et al., 2001). Aurora kinases are activated in mitosis and are associated with the segregation of chromosomes (Kimura et al., 1997; Hannak et al., 2001). Potential targets for this kinase are continually being discovered and no details regarding the phosphorylation motif are known, so Aurora family of kinases may provide yet more candidate kinases that could target PDE4D3 during mitosis. The NIMA related kinases are thought to regulate multiple events associated with mitosis, such as assembly and maintenance of the centrosome and displays dynamic behaviour within cell localisations through the different stages of interphase and mitosis (Ha et al., 2002). As there are no inhibitors for these kinases, studies will have to be carried out using purified recombinant kinases in an attempt to determine whether they have the potential to phosphorylate PDE4D3 in mitosis and if they do phosphorylate PDE4D3 which sites they target.

Since the identification of the kinase(s) that modifies PDE4D3 during mitosis was not possible through treatment of cells with kinase inhibitors, analysis of potential phosphorylation motifs within the PDE4D3 protein sequence was performed. Some identified sites within the unique 'long-form' N-terminal region of PDE4D isoforms were then mutated in an attempt to ablate the bandshift of PDE4D3 and the concomitant increase in its activity in mitotic cells. Whilst no changes in these properties were observed with a range of point mutations in this region, a truncated mutant of PDE4D3 that lacked the UCR1 and LR1 domains did not 'bandshift' when the cells were arrested in mitosis. This suggests that residues phosphorylated during mitosis might lie within UCR1. It is known that modifications of the UCR1 domain, either through phosphorylation by PKA (Sette and Conti, 1996; Hoffmann et al., 1998) or by interaction with phosphatidic acid (Grange et al., 2000) can increase the activity of PDE4D3. These various data suggest that a phosphorylation of UCR1 might be key to activation of PDE4D3 in mitosis. Further studies, using the isolated UCR1 domain of PDE4D3, established that UCR1 was indeed phosphorylated by kinases in mitotic cell lysates, whereas the UCR2 was not. These observations are entirely consistent with the model of activation of PDE4D3 proposed by both Lim et al. (1999) and Beard et al. (2000) using independent methods. These envisage that phosphorylation of UCR1 induces a conformational change of the protein, thus relieving an inhibitory interaction between the UCR2 and the catalytic domain.

Phosphorylation of full-length PDE4D3 protein and phosphopeptide mapping by 2D electrophoresis identified at least three peptides that were more highly phosphorylated by mitotic than asynchronous lysate. Separation of these peptides by reverse phase HPLC identified four peptides that were more highly phosphorylated by kinases present in mitotic lysate. Two of the identified peptides mapped to the UCR1 domain, both of these incorporated approximately 1 pmole ^{32}P in the *in vitro* kinase reaction using mitotic lysate. One of these peptides mapped to the N-terminus of UCR1 and was phosphorylated at Ser⁶¹, another longer peptide, at the C-terminus of UCR1, was phosphorylated at Ser⁷⁵. Both of these reflect novel phosphorylations of the UCR1 domain. Ser⁶¹ is proximal to residues 31-59, which have been identified as being crucial for the interaction with phosphatidic acid (Grange et al., 2000) and also to the PKA target residue Ser⁵⁴ (Sette and Conti, 1996). In the PhosphoBase prediction Ser⁶¹ had the potential to be phosphorylated by Calmodulin dependent kinase II (CaMII) and PKA. It has been shown in this study that PKA is unlikely to play a role in the activation of PDE4D3 or alteration in PDE4D3 electrophoretic mobility, when analysed by SDS-PAGE. Additionally, mutational analysis (Sette and Conti, 1996) have shown PKA only phosphorylates Ser¹³ and Ser⁵⁴ in PDE4D3. However, calcium oscillations appear to be a property of mitotic progression (reviewed in Whitaker, 1997). CaMII has been shown to be required for metaphase/anaphase transition in HeLa and endothelial cells (Petzelt et al., 2001), and is thought to facilitate activation of Cdc25, the phosphatase activated upon mitotic onset (Patel et al., 1999). Therefore, CaMII could potentially be the kinase phosphorylating Ser⁶¹ in mitosis.

The Ser⁷⁵ residue was predicted to have the potential of being phosphorylated by casein kinase I (CKI). As the CK1 inhibitor, DRB, showed no effect on either the activity or the 'bandshift' of PDE4D3 it is unlikely that CKI is the candidate kinase phosphorylating the Ser⁷⁵ site. However, to confirm this observation the efficacy of the DRB inhibitor compound, on CKI activity would need to be determined. However, Ser⁷⁵ does lie within a consensus motif for the checkpoint dependent protein kinase (Chk1) (ϕ -X- β -X-X-(S/T), where ϕ is hydrophobic (M>I>L>V) and β is a basic amino acid (R>K) and X is any residue Hutchins et al., 2000). Chk1 is a kinase expressed and activated in cells in response to DNA damage (Walworth, 2001). Chk1 then phosphorylates the Cdc25 protein phosphatase which causes Cdc25 to bind to 14-3-3 proteins and prevents its translocation to the nucleus to activate the Cdc2/cyclinB1 kinase. These effects lead to G2/M checkpoint arrest (Yang et al., 1999). Chk1 activity is detectable in cells subjected to nocodazole-induced mitotic arrest (Liu et al., 2000b) and, as the Ser⁷⁵ residue lies within a Chk1 site this suggests that Chk1 could be a candidate kinase for PDE4D3 phosphorylation at Ser⁷⁵.

Two further phosphopeptides arising in PDE4D3 during mitosis that were identified by HPLC/mass spectrometry analysis, were phosphorylated at Ser²³⁹ and Ser⁵⁷⁹. These sites incorporate between 2 -3 pmol more ³²P than the previously detailed serine residues, phosphorylated by kinases active in mitosis. The Ser²³⁹ and Ser⁵⁷⁹ residues map to the catalytic domain of PDE4D3.

Phosphorylation of the Ser²³⁹ residue is potentially interesting as not only is it located within the catalytic domain but it is also found within the N-terminus of the catalytic domain, a region that has been proposed to interact with the inhibitory sub-domain of UCR2 (Lim et al., 1999). With the PhosphoBase prediction glycogen synthase kinase -3 (GSK-3) was identified as a kinase which could phosphorylate this site. However, GSK-3 requires that the serine/threonine four residues upstream of the phosphorylated site is phosphorylated, to act as a priming phosphorylation. The Ser²⁴² in the PDE4D3 was not shown to be phosphorylated, therefore, it is unlikely that GSK-3 phosphorylates this site in mitosis.

Phosphorylation of Ser⁵⁷⁹ has already been shown by our laboratory to be mediated by ERK (Hoffmann et al., 1999). However, this leads to inhibition rather than activation of PDE4D3. The question raised here, however, is why PDE4D3 is phosphorylated by ERK during mitosis as this is the stage in the cell cycle at which the levels of ERK activity and phospho-ERK are lowest (Wright et al., 1999; Hayne et al., 2000, *see section 3.3.7.3.*). It could be that the small proportion of active ERK in the cells at this time is co-localised with PDE4D3 and therefore able to target it for phosphorylation. However, further studies are required to confirm an interaction between PDE4D3 and ERK during mitosis. Why should Ser⁵⁷⁹ be phosphorylated during mitosis when ERK phosphorylation of this site inhibits the enzymatic activity of long-form PDE4 isoforms (Baillie et al., 2000)? However, it has been shown that the increase in PDE4D3 enzymatic activity caused by PKA phosphorylation is a dominant effect over inhibitory ERK phosphorylation of PDE4D3 (Baillie et al., 2000). A similar relationship could exist between the novel mitotic phosphorylations of PDE4D3 and the ERK phosphorylation. Consistent with this, inhibition of ERK in mitotic cells did not affect the activity of PDE4D3 (*see section 4.3.6.2.*). Nevertheless, further studies should be carried out to investigate the significance of the ERK phosphorylation of PDE4D3 in mitotic cells.

Further studies with recombinant kinases are required for absolute identification of the candidate mitotic kinase(s) that phosphorylate PDE4D3 during mitosis. The novel phosphorylation sites should also be mutated individually and in combination and the

resulting PDE4D3 mutants analysed for bandshifts, PDE activity and also for their effects on PKA activity and cell cycle progression. Current speculation of how phosphorylation of the Ser⁶¹, Ser⁷⁵, Ser²³⁹ and Ser⁵⁷⁹ residues of PDE4D3 might be linked to its activation and how they might also alter the electrophoretic mobility of PDE4D3 when observed by SDS-PAGE are discussed further in Chapter 6.

The effect of PDE4 inhibition on processes that occur during mitotic progression indicate that down-regulation of PKA activity in cells entering mitosis, which continues until the metaphase/ anaphase transition (Fernandez et al., 1995; Kotani et al., 1998), is caused by PDE4 dependent hydrolysis of cAMP. It is also clear that release of cells from the mitotic arrest in the presence of rolipram causes cells to progress into the next G1 stage at a quicker rate than untreated cells. These findings confirm observations by other groups that PKA activation is required for mitotic exit (Grieco et al., 1996).

In summary, by relating the changes of PDE4D3 activity to the control of mitotic progression, the results within this chapter suggest that the elevation of PDE4D3 activity upon mitotic entry, is caused by phosphorylation of the enzyme by a staurosporine-sensitive kinase. This phosphorylation occurs at any one or more of the four target residues and serves to increase cAMP hydrolysis and inhibit PKA. The inactivation of PKA is required to allow nuclear envelope breakdown (Lamb et al., 1991), MPF activation (Oh et al., 1996) and chromatin condensation (Fernandez et al., 1995). When the metaphase/anaphase transition is made, PDE4D3 is inactivated by dephosphorylation of the target residues through the action of a phosphatase that is sensitive to high levels of okadaic acid. This initiates the reactivation of PKA, which causes chromatin to decondense (Fernandez et al., 1995) and allows the nuclear envelope to reform (Steen et al., 2000; Lamb et al., 1991). Further studies need to be carried so we can determine conclusively what direct effect PDE4D3 has on PKA activity and the breakdown and formation of the nuclear envelope and chromatin condensation during mitotic progression.

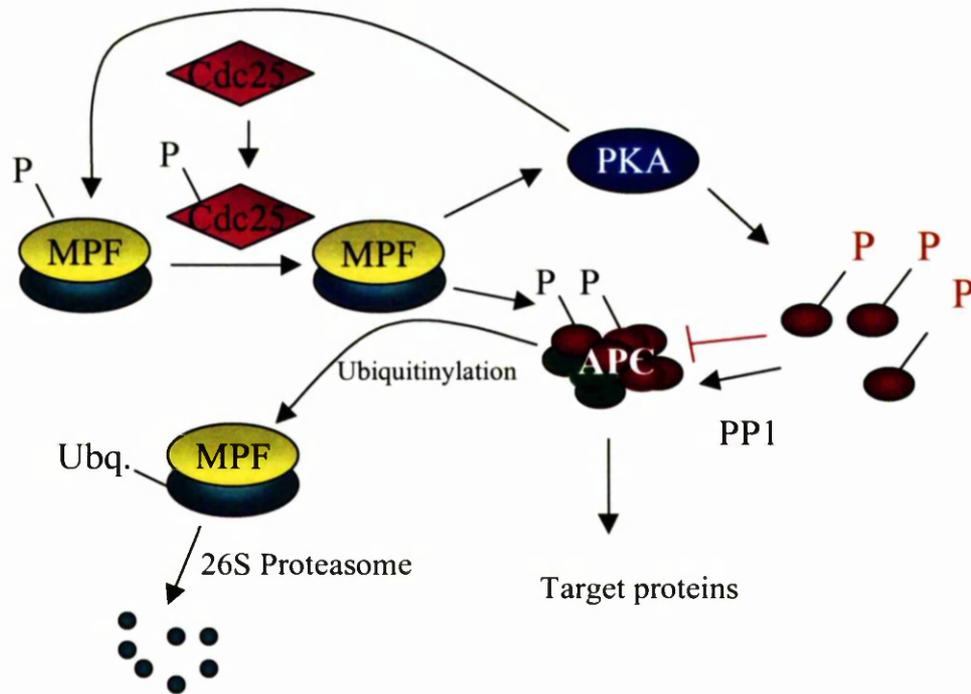


Figure 4.1. PKA activity and mitotic transition. The transition of cells through mitosis is a highly regulated mechanism, entry into mitosis brings about a down regulation of PKA activity. The inhibitory phosphorylation of the maturation promoting factor (MPF) that PKA catalyses, is removed by the Cdc25 phosphatase and the MPF is activated. Down regulation of PKA activity also enables the inhibitory phosphorylations on the anaphase promoting complex (APC) subunits to be removed by protein phosphatase 1 (PP1). This allows assembly of the active APC that acts as a ubiquitin ligase, targeting multiple proteins for ubiquitinylation (ubq.), which marks them for proteolysis by the 26S proteasome. MPF phosphorylates PKA reactivating it after the metaphase/ anaphase transition enabling the exit of cells from mitosis.

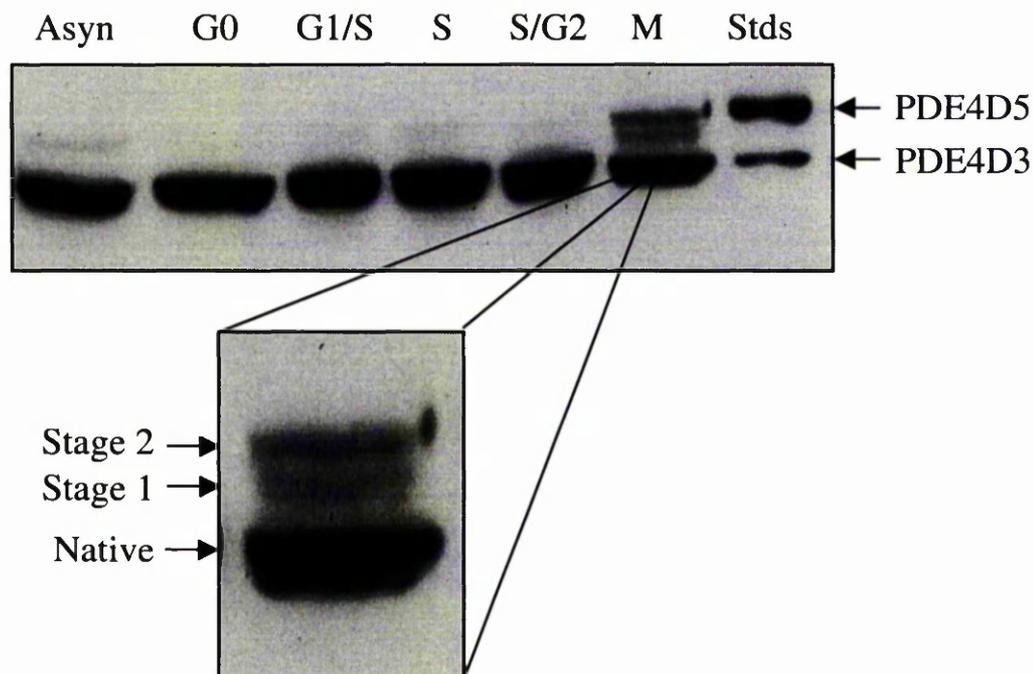


Figure 4.2. Change of PDE4D3 electrophoretic mobility during mitosis. Rat-1 cells were arrested in specific stages of the cell cycle as indicated (*see sections 2.1.4.1. - 2.1.4.5.*, Asyn - M) and harvested in 3T3 lysis buffer. 100 μ g of protein from each cell lysate and 20 μ g recombinant protein standards (Stds) were separated by SDS-PAGE on an 8 % gel. The proteins were transferred to nitrocellulose and immunoblotted with PDE4D C-terminal specific antiserum. The migration of PDE4D3 (95 kDa) and PDE4D5 (109 kDa) proteins are indicated. Cells arrested in mitosis (M) had species of PDE4D3 with reduced electrophoretic mobilities. The enlarged image of PDE4D3 proteins in mitosis is denoted with the nomenclature used for the different species of PDE4D3 (*explained in section 4.2.1.*). The *stage 1* form of PDE4D3 migrates with an apparent molecular weight of 100 kDa and *stage 2* form migrates with an apparent molecular weight of 102 kDa, both are calculated by plotting the Rf values of markers run on the same gel.

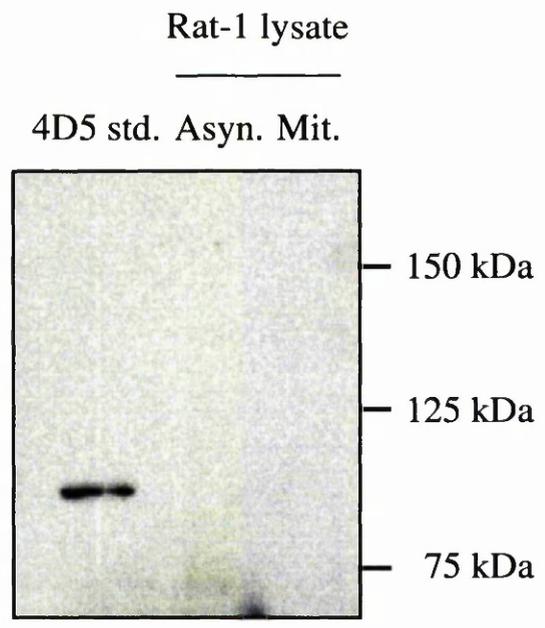


Figure 4.3. PDE4D5 is not expressed in Rat-1 cells. Asynchronous Rat-1 cells (Asyn.) or Rat-1 cells arrested in mitosis (Mit.) were harvested in 3T3 lysis buffer and 100 μ g of proteins from these lysates as well as 20 μ g PDE4D5 recombinant protein (4D5 std., 109 kDa) were separated by SDS-PAGE on an 8 % gel. The proteins were transferred to nitrocellulose and were immunoblotted with a PDE4D5 N-terminal specific antibody (*see section 4.2.1.1.*). The molecular weights of the protein standards are indicated.

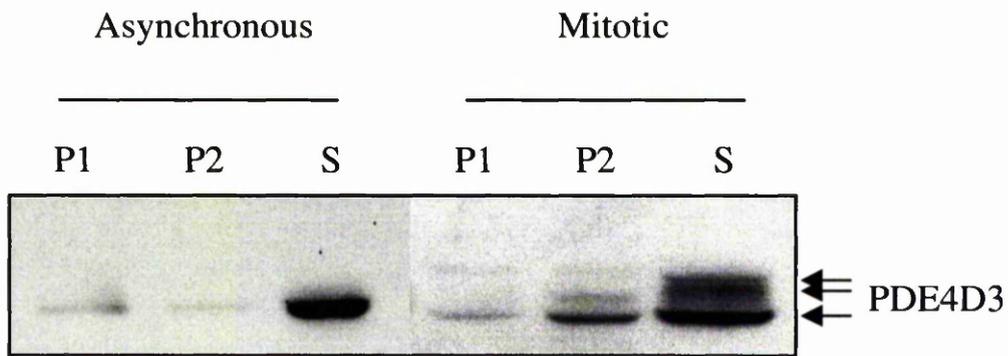


Figure 4.4a. Sub-cellular localisation of PDE4D3 in asynchronous Rat-1 cells and cells isolated in mitosis, determined by crude fractionation. Asynchronous Rat-1 cells or cells arrested in mitosis were homogenised in cKHEM and subject to crude subcellular fractionation (*see section 2.2.1.2.*). The low speed cell fraction (P1) was collected at 2000 g for 10 min in a fixed rotor centrifuge. The high speed fraction (P2) was collected at 75000 g for 30 min in an ultracentrifuge, leaving the residual cytosolic fraction (S). 100 μ l of the proteins from each fraction were separated by SDS-PAGE on an 8 % gel, transferred to nitrocellulose and immunoblotted with a PDE4D specific antibody. The migration of all species of PDE4D3 protein is indicated. The *stage 1* migrates at ~100 kDa, *stage 2* migrates at ~102 kDa and native PDE4D3 migrates at 95 kDa when calculated by plotting the Rf values of markers run on the same gel.

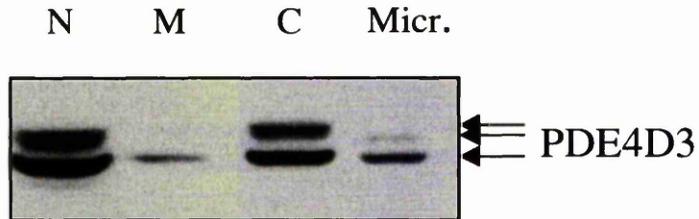


Figure 4.4b. Subcellular localisation of PDE4D3 in Rat-1 cells isolated in mitosis, determined by refined fractionation. Rat-1 cells arrested in mitosis were homogenised in sucrose buffer and subjected to a refined subcellular fractionation (*see section 2.2.1.3.*). The nuclear pellet (N) was collected at 1000 g for 10 min in a fixed angle centrifuge. The membranous fraction (M) was collected at 13000 g for 15 min in a fixed angle centrifuge and the microsomes (Micr.) were collected at 75000 g for 60 min in an ultracentrifuge, leaving the residual cytosolic fraction (C). 100 μ l proteins from each fraction were separated by SDS-PAGE on an 8 % gel, transferred to nitrocellulose and immunoblotted with a PDE4D specific antibody. The migration of all species of PDE4D3 protein are indicated.

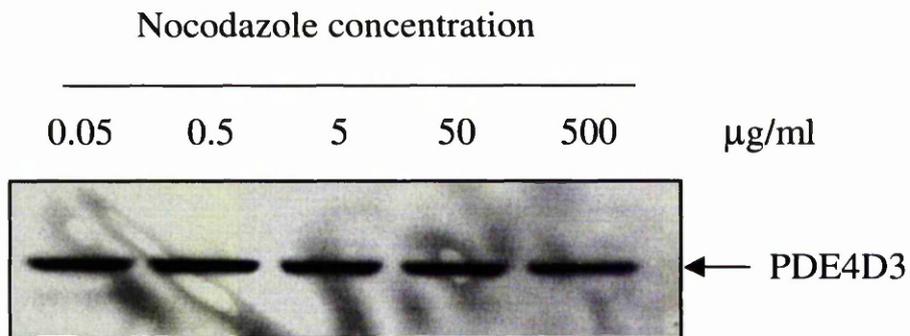


Fig 4.5. The effect of short-term incubation of increasing concentrations of on PDE4D3 modification. Increasing concentrations of nocodazole (0.05 μg -500 μg per ml of growth media, as indicated) were added to asynchronous Rat-1 cells for 2 h, cells were then lysed in 3T3 lysis buffer and 100 μg protein separated by SDS-PAGE on an 8 % gel. The proteins were transferred to nitrocellulose and immunoprobed with a PDE4D specific antiserum. The migration of the PDE4D3 protein (95 kDa) from each cell lysate is indicated.

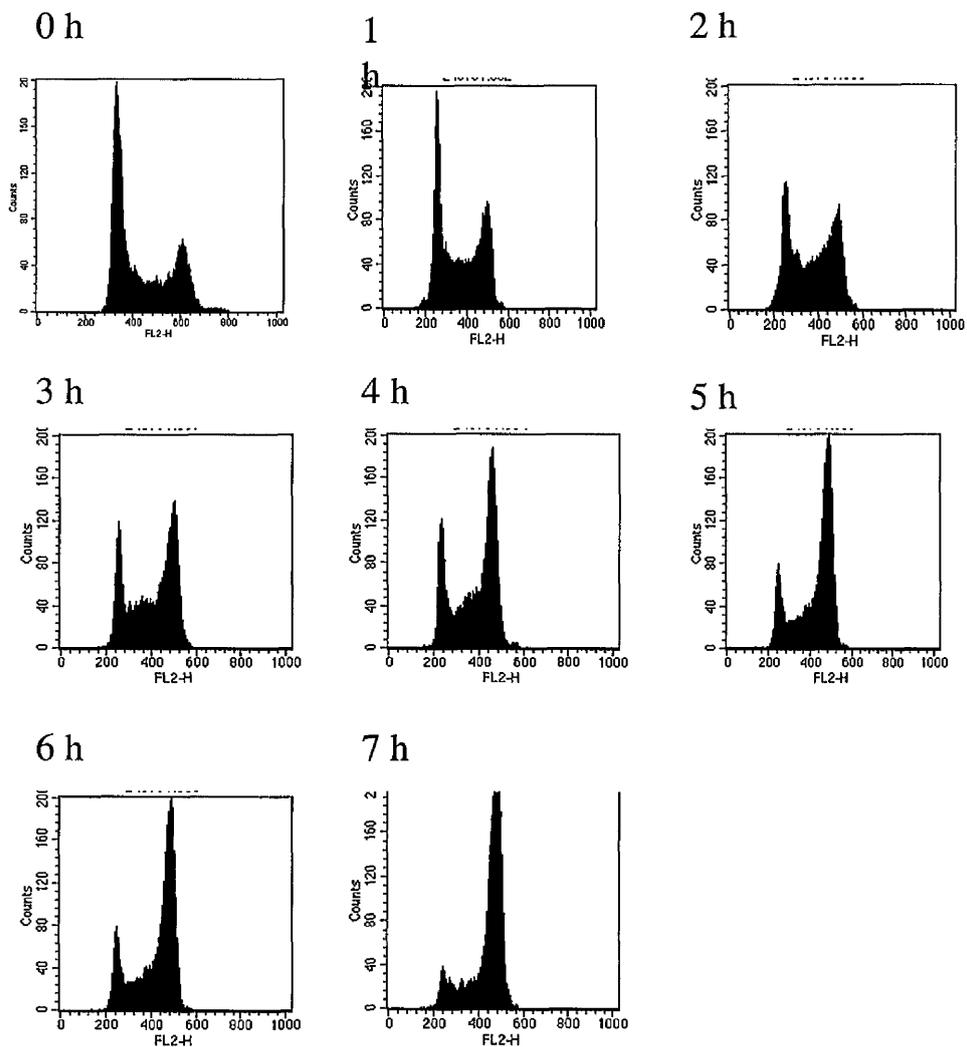


Figure 4.6. Change in Rat-1 cell cycle distribution with the addition of nocodazole. Asynchronous Rat-1 cells were treated with 50 ng/ml media nocodazole for up to 7 h, as indicated. Cells were harvested at 1 h intervals (see section 2.2.1.), as indicated, labelled with propidium iodide and 20000 cells were analysed by flow cytometry for distribution within the cell cycle (see section 2.2.2.). The histograms determine the DNA content of these cells over this time course.

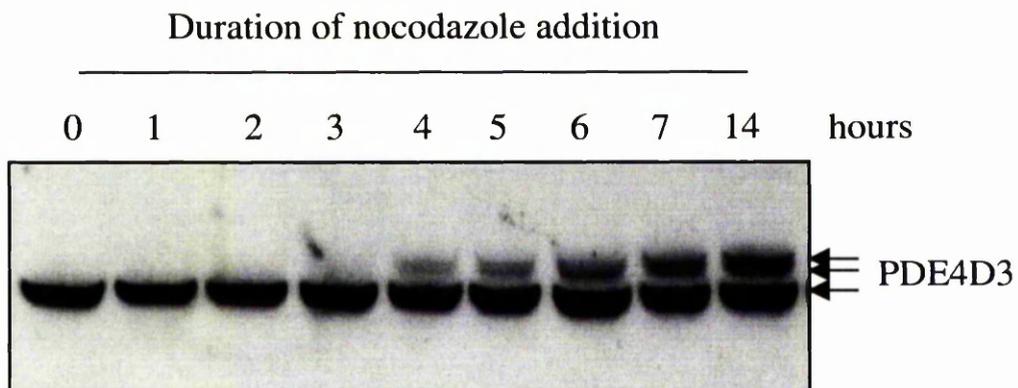


Figure 4.7. Changes in electrophoretic mobility of PDE4D3 in Rat-1 cells incubated with nocodazole for various times. Rat-1 cells were incubated with nocodazole (50 ng/ml media) over a 14 h time course and harvested in 3T3 lysis buffer, at intervals as shown. 100 μ g protein from each cell lysate was subjected to SDS-PAGE on an 8 % gel, transferred to nitrocellulose and immunoprobed with the PDE4D specific antiserum. The migration of the species of PDE4D3 protein is indicated.

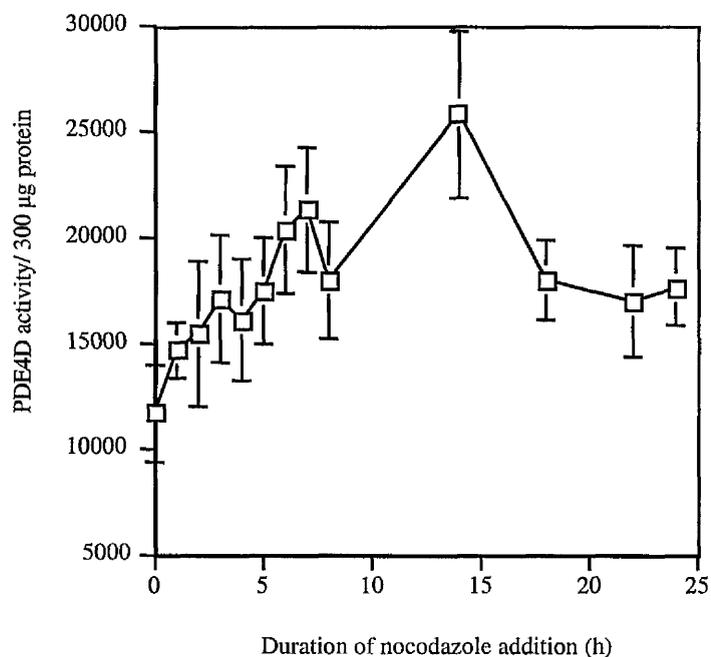


Figure 4.8. The increase in PDE4D activity as cells accumulate in mitosis. Asynchronous Rat-1 cells were incubated with nocodazole (50 ng/ml media) over a 24 h time course and harvested at the times indicated. PDE4D was isolated by immunoprecipitation from 300 µg cell lysate using the PDE4D specific antibody (*see section 2.3.10.*) and the enzymatic activity of PDE4D was measured (*see section 2.3.9.*). The results are expressed as the means \pm SE of five independent experiments.

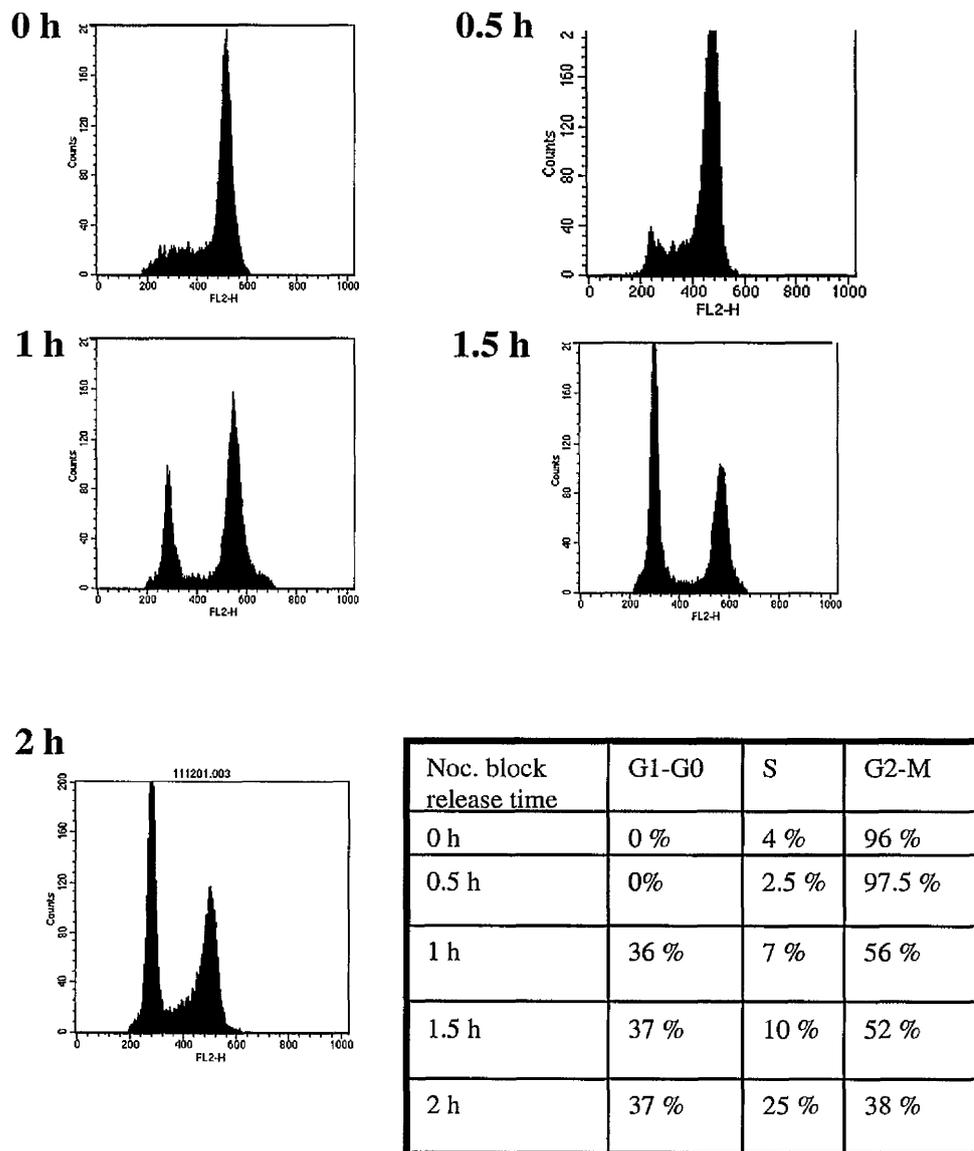


Figure 4.9. Redistribuition of Rat-1 cells through the cell cycle upon release of the nocodazole- induced mitotic block. Rat-1 cells subjected to nocodazole-induced mitotic arrest (*see section 2.1.4.5.*) were released from the block and harvested at half hour intervals as indicated (*see section 2.2.1.*). The distribution of a sample of 20000 cells through the cell cycle were determined by FACs analysis (*see section 2.2.2.*). The histograms represent the amount of DNA in the sampled population of cells and the proportion of cells in the phases of the cell cycle is indicated in the accompanying table.

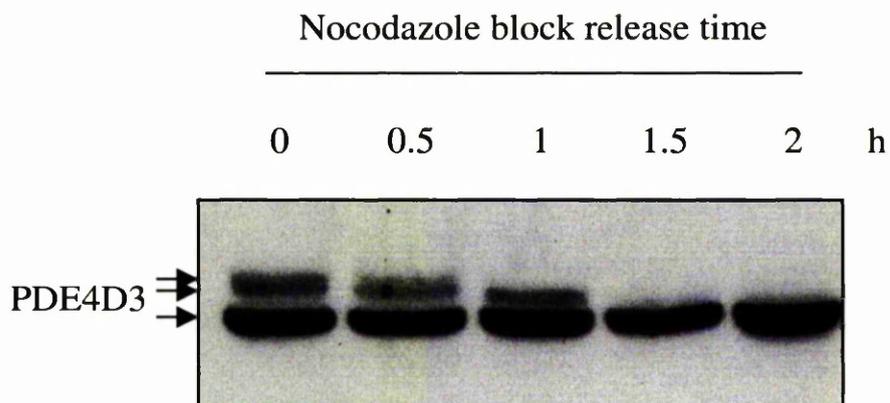


Figure 4.10. Increase in electrophoretic mobility of PDE4D3 protein as Rat-1 cells exit nocodazole-induced mitosis. Rat-1 cells arrested in mitosis, by the addition of nocodazole (50 ng/ml) for 14 h, were released into the next cell cycle and cells harvested at half hour intervals in 3T3 lysis buffer, as indicated. 100 μ g of cell lysates were separated by SDS-PAGE on an 8 % gel, transferred to nitrocellulose and immunoblotted with the PDE4D specific antibody. The electrophoretic mobility of the different species of PDE4D3 protein are indicated.

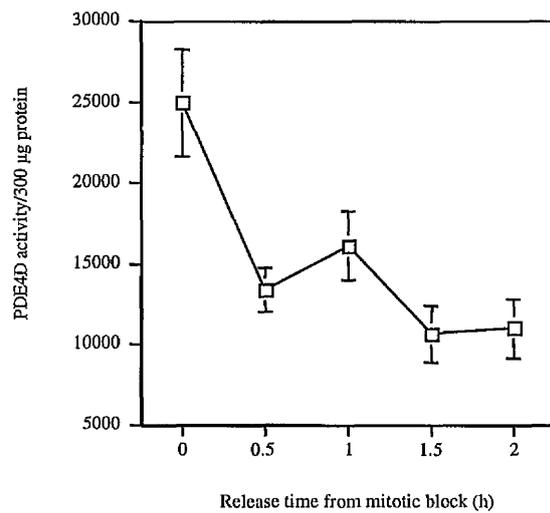


Figure 4.11. Decrease in PDE4D activity in cells released from nocodazole - induced mitotic arrest. Rat-1 cells arrested in mitosis by incubation with nocodazole (50 ng/ml media), were released from the mitotic block and harvested at 30 min intervals in 3T3 lysis buffer. The PDE4D protein was isolated by immunoprecipitation from 300 µg cell lysate (*see section 2.3.10.*) and the enzymatic activity of the protein determined (*see section 2.3.9.*). The results are expressed at the mean \pm SE of 4 independent experiments.

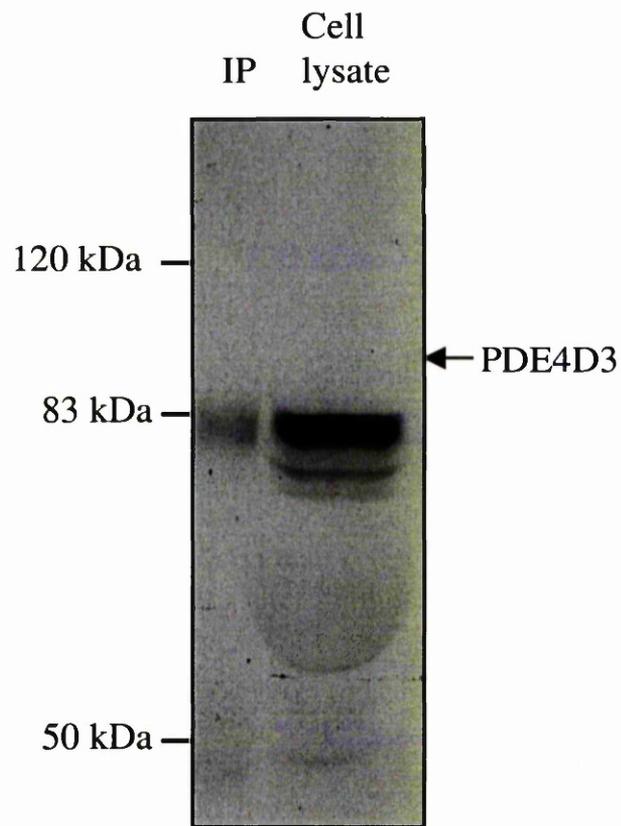


Figure 4.12. PDE4D3 is not ubiquitinated during mitosis. PDE4D3 protein was isolated by immunoprecipitation from 1 mg cell lysate from Rat-1 cells arrested in mitosis, using PDE4D specific antiserum (*see section 4.3.10.*). The immunoprecipitated protein (IP) and 100 μ g Rat-1 cell lysate were separated by SDS-PAGE on an 8 % gel, transferred to nitrocellulose and the proteins were immunoblotted with an anti ubiquitin-protein conjugate antibody. The molecular weights of the protein standards are indicated, as is the expected position of PDE4D3 migration (95 kDa).

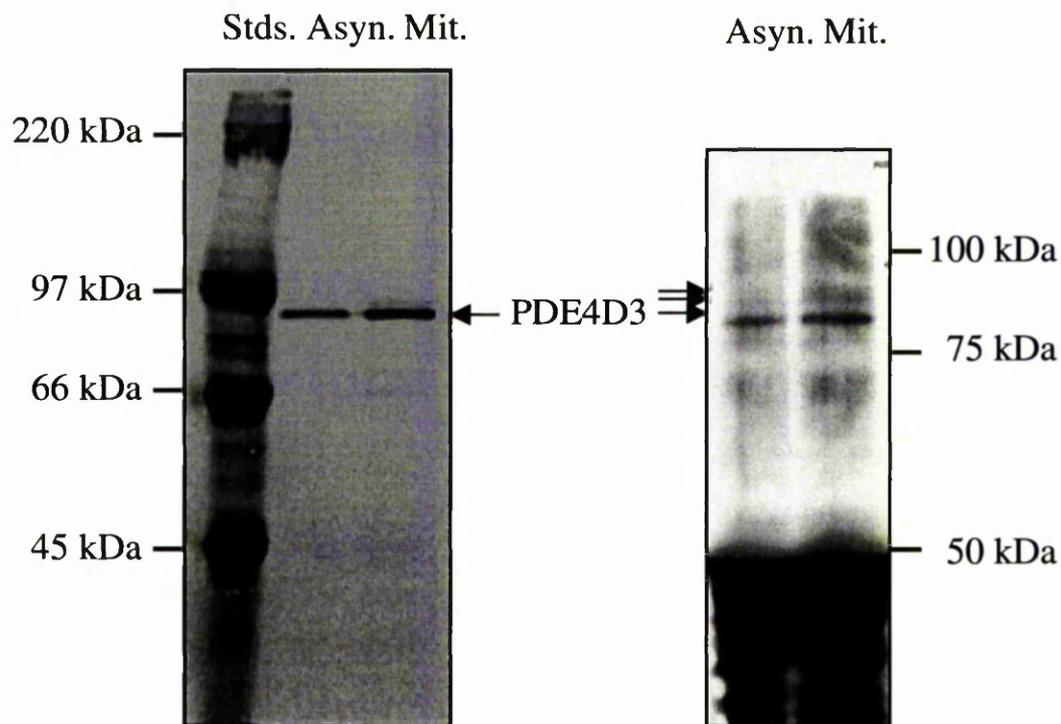


Figure 4.13. *In vivo* phosphorylation of PDE4D3 in asynchronous and mitotic cells. Rat-1 cells were left asynchronous (Asyn.) or incubated with 50 ng/ml media nocodazole for 14 h to arrest the cells in mitosis (Mit.). The cells were then incubated in phosphate free media, supplemented with 300 μ Ci/ml 32 P orthophosphate, for 2 h. The cells were lysed and PDE4D protein isolated by immunoprecipitation using the PDE4D specific antisera. The protein was separated by SDS-PAGE on an 8 % gel, transferred to nitrocellulose and visualised by exposing the nitrocellulose to a phosphorimage screen for 24 h (left-hand panel). The molecular weights of the standard proteins (Stds.) and the migration of the 32 P labelled PDE4D3 (95 kDa) are indicated. The blot was then probed with PDE4D specific anti serum (right-hand panel). In this figure the migration of the *stage 1*, *stage 2* and native forms of PDE4D3 are indicated, as is the migration of the molecular weight standards.

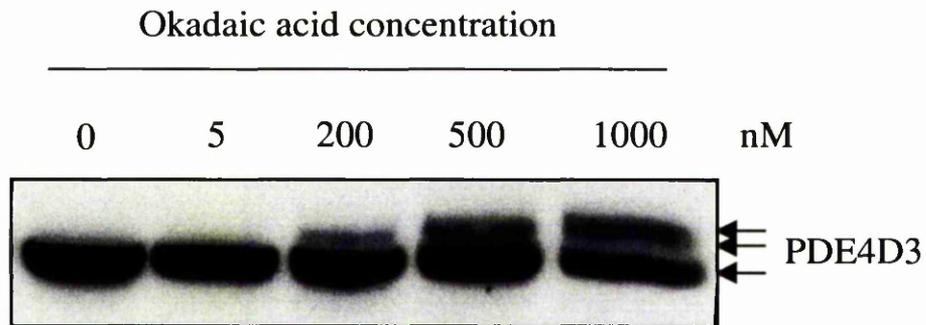


Figure 4.14. Okadaic acid maintains bandshifted PDE4D3 modification after release of cells from mitotic block. Rat-1 cells arrested in mitosis by incubation with nocodazole (50 ng/ml) were released from the mitotic block for 2 h in the presence of increasing concentrations of okadaic acid, as indicated. The cells were harvested in 3T3 lysis buffer and 100 μ g of protein from the cell lysates were separated by SDS-PAGE on an 8 % gel. The proteins were transferred to nitrocellulose and immunoblotted with a PDE4D specific antibody. The migration of the species of PDE4D3 are indicated.

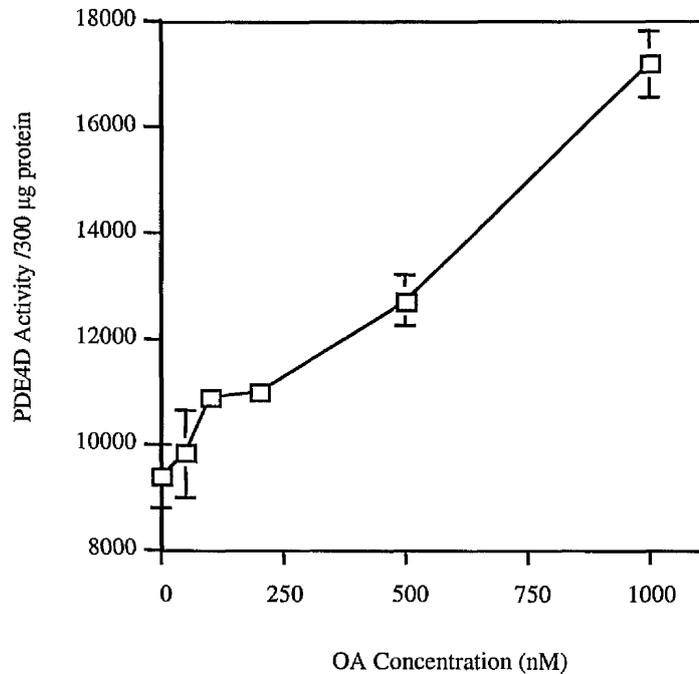


Figure 4.15. Okadaic acid maintains the elevated PDE4D activity after release of cells from mitotic block. Rat-1 cells arrested in mitosis by incubation with nocodazole (50 ng/ml media) were released from the mitotic block for 2 h in the presence of increasing concentration of okadaic acid, as indicated. PDE4D was isolated from 300 µg of the cell lysates by immunoprecipitation (*see section 2.3.10.*), using the PDE4D specific antibody, the enzymatic activity of the protein was then determined (*see section 2.3.9.*). Results are shown as the means \pm SE of four independent experiments.

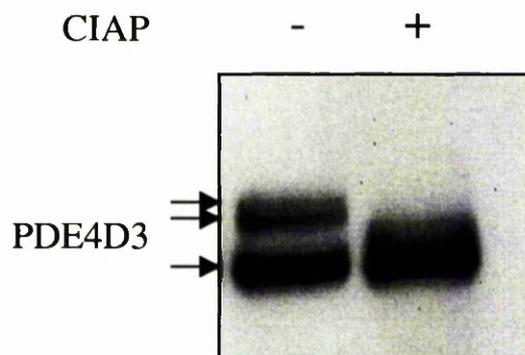


Figure 4.16. CIAP ablates the bandshifted species of PDE4D3 from nocodazole-induced mitotic lysate. Rat-1 cells arrested in mitosis were harvested and 100 μg of the lysate were incubated with (+) or without (-) 10 units calf intestinal alkaline phosphatase (CIAP) for 1 h (*see section 2.4.2.*). The protein was then subjected to SDS-PAGE on an 8 % gel, transferred to nitrocellulose and immunoblotted with the PDE4D specific antibody. The migration of the different species of PDE4D3 protein is indicated.

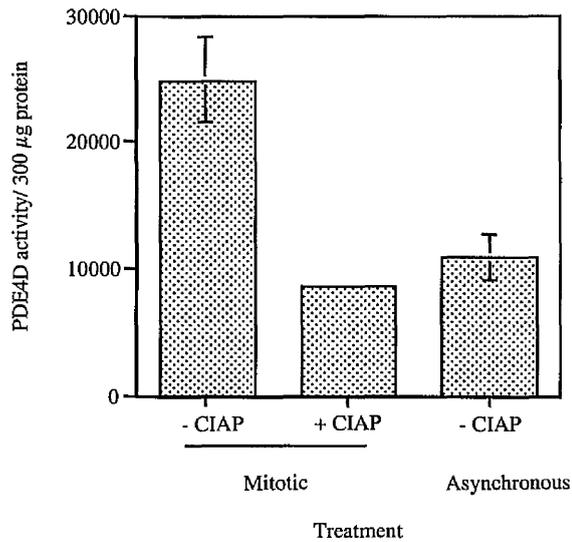


Figure 4.17. CIAP reduces the activity of PDE4D in nocodazole-induced mitotic cells. Lysate from Rat-1 cells arrested in mitosis was incubated in the absence or presence of 10 units calf intestinal alkaline phosphatase (CIAP) for 1 h (*see section 2.4.2.*). The PDE4D was then isolated from 300 µg of the treated mitotic lysates or from asynchronous lysate by immunoprecipitation, using the PDE4D specific antibody and the enzymatic activity of the protein was determined (*see section 2.3.9.*). The results are shown as the means \pm SE of three independent experiments.

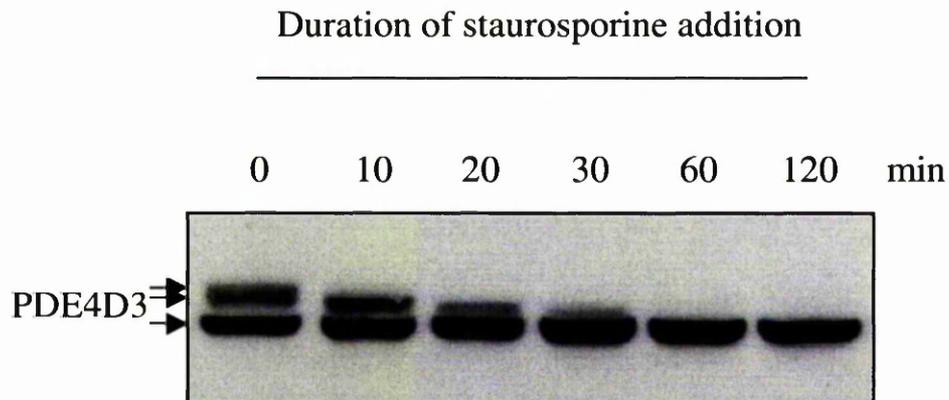


Fig 4.19. Staurosporine ablates the nocodazole-induced mitotic bandshift of PDE4D3 in a time dependent fashion. Rat-1 cells arrested in a nocodazole-induced mitosis were released from the block in the presence of 100 nM staurosporine for up to 2 h. Cells were harvested in 3T3 lysis buffer, at intervals as shown, and 100 μ g protein from of the cell lysates were subjected to SDS-PAGE on an 8 % gel. The proteins were transferred to nitrocellulose and PDE4D3 was detected by immunoblot analysis using a PDE4D specific antibody. The positions of the different PDE4D3 species are indicated.

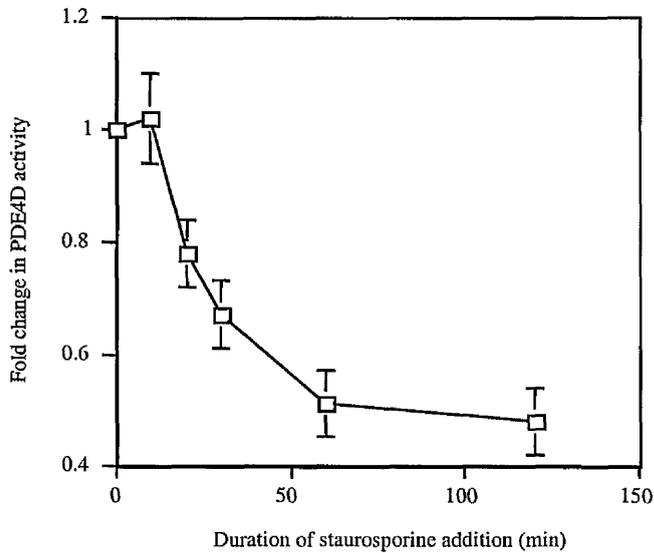


Figure 4.20. Staurosporine reduces the activity of PDE4D in nocodazole-induced mitotic cells. Rat-1 cells in nocodazole-induced mitosis were incubated with 100 nM staurosporine for up to 2 h. Cells were harvested in 3T3 lysis buffer at the time points indicated and PDE4D was isolated by immunoprecipitation from 300 μ g of cell lysate (see section 2.3.10.). The enzymatic activity of PDE4D was measured (see section 2.3.9.) and the results expressed as the fold differences in activity of PDE4D compared to 0 min staurosporine incubation. The results are represented as the means \pm SE of four independent experiments.

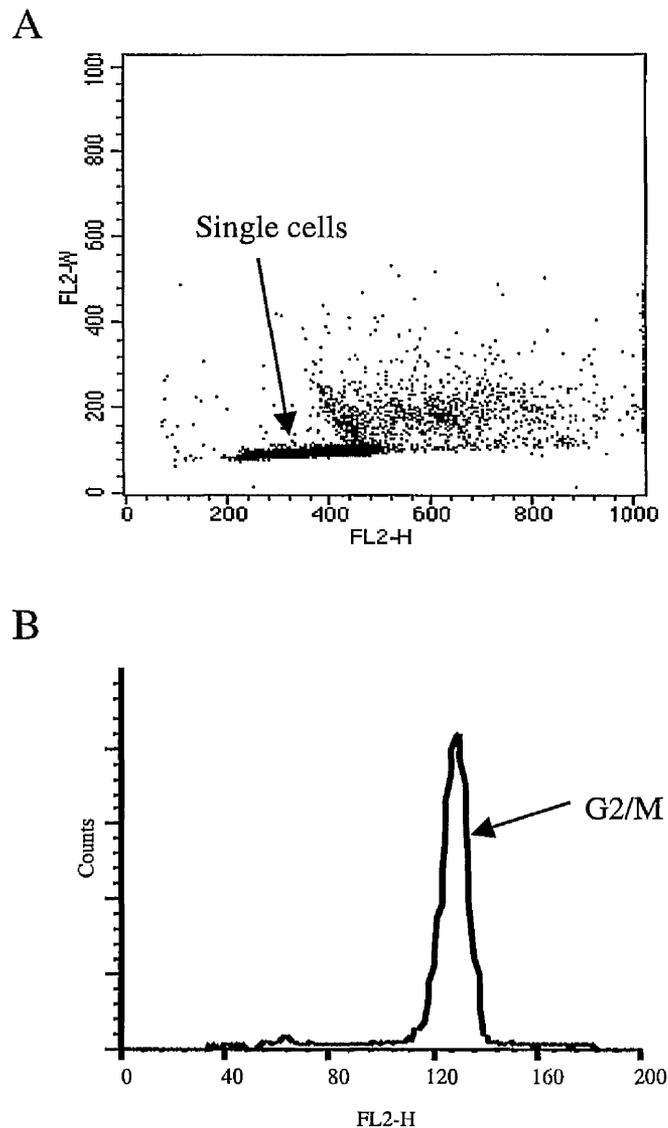


Figure 4.21. FACS analysis of Rat-1 cells arrested in mitosis and subjected to a further incubation with staurosporine. Rat-1 cells were subjected to nocodazole-induced mitosis (*see section 2.1.4.5.*) and were then incubated with 100 nM staurosporine for 2 h. The cells were harvested and stained with BrdU-FITC and propidium iodide (PI, *see section 2.2.3.*) prior to the collection and analysis of 20000 cells by FACS using the CELLQuest acquisition package (*see section 2.2.4.*). *Panel A*, analysis of multinucleated cells, cell clumps and cell debris was measured on a density plot of the PI labelled cells in the FL2-H vs FL2-W channels. The single cell population are indicated. *Panel B*, the distribution of the 20000 cells within the cell cycle was analysed on a histogram of PI incorporation in FL2-H vs counts, the G2/mitotic population are indicated.

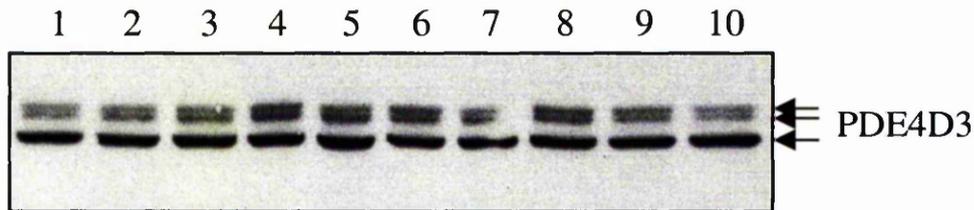


Figure 4.22. Commercially available specific kinase inhibitors do not ablate the PDE4D3 bandshift in nocodazole induce mitotic cells. Rat-1 cells incubated with nocodazole (50 ng/ml) for 14 h to arrest them in mitosis (*lane 1*) were subsequently incubated with 10 μ M H89 (*lane 2*), 10 μ M genistein (*lane 3*), 10 μ M 5,6-Dichloro-1- β -D-ribofuranosylbenzimidazole (DRB) (*lane 4*), 1 mM Wortmannin (*lane 5*), 10 μ M LY294002 (*lane 6*), 10 μ M U0126 (*lane 7*), 20 μ M Olomucine (*lane 8*), 10 μ M PD98059 (*lane 9*) and 10 μ M Bisindolylmaleimide II (*lane 10*) for 2 h prior to cell harvest. The cells were lysed in 3T3 lysis buffer and 100 μ g of protein from each cell lysate was separated by SDS-PAGE on an 8 % gel, transferred to nitrocellulose and immunoblotted with a PDE4D specific antibody. The migration of the PDE4D3 species are indicated.

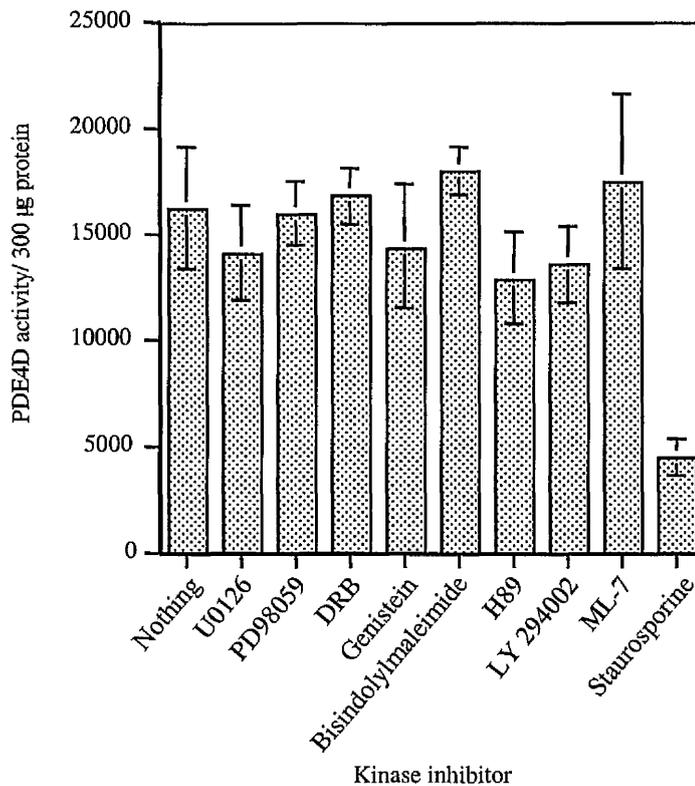


Figure 4.23. The increased activity of PDE4D in nocodazole-induced mitotic cells is insensitive to many commercially available specific kinase inhibitors. Nocodazole-induced mitotic Rat-1 cells were incubated with commercially available kinase inhibitors, as indicated (*for details of concentrations of inhibitors used see section 4.3.6.2.*), for 2 h prior to harvest in 3T3 lysis buffer. The PDE4D protein was isolated from 300 µg cell lysates by immunoprecipitation (*see section 2.3.10.*) using the PDE4D specific antiserum and the enzymatic activity of the protein analysed (*see section 2.3.9.*). The results are expressed as the means \pm SE of between 3-5 independent experiments.

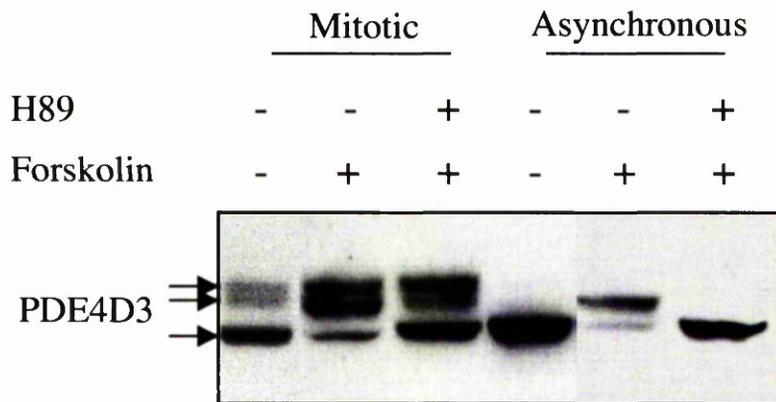


Figure 4.24. Change in electrophoretic mobility of PDE4D3 in mitotic and asynchronous cells upon stimulation or inhibition of PKA activity. Asynchronous Rat-1 cells or cells arrested in mitosis with nocodazole were incubated with 100 μ M forskolin with or without a preincubation with H89, as indicated. 100 μ g of protein from the cell lysates were separated by SDS-PAGE, on an 8 % gel, transferred to nitrocellulose and immunoprobed with the PDE4D specific antibody. The migration of the different species of PDE4D3 are indicated.

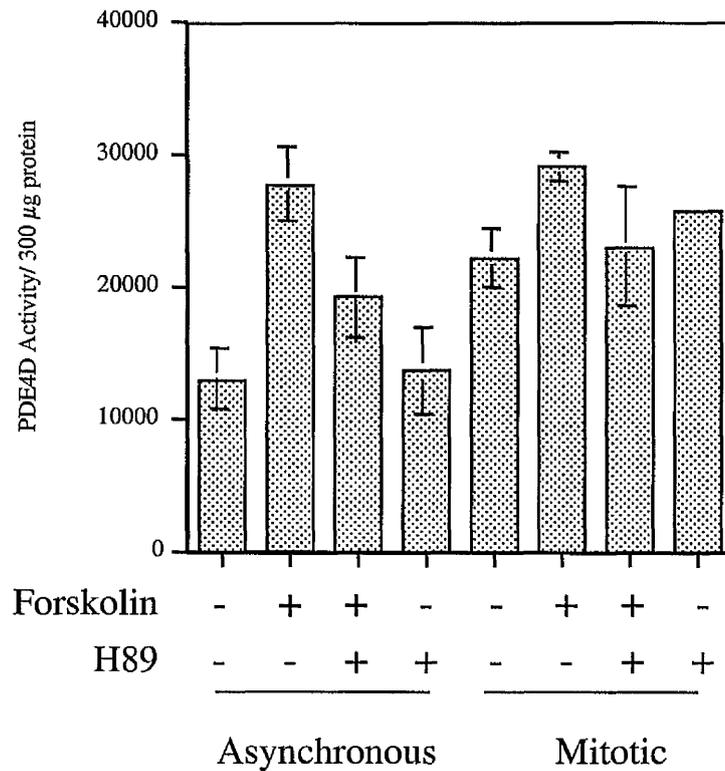


Figure 4.25. Changes in PDE4D activity upon treatment with forskolin and H89. Asynchronous or mitotically arrested Rat-1 cells were pre-incubated in the presence or absence of 10 μM H89 for 20 min, prior to a subsequent 15 min incubation in the presence or absence of 100 μM forskolin, as indicated. The PDE4D3 protein was then isolated from 300 μg cell lysate by immunoprecipitation (*see section 2.3.10.*) using the PDE4D specific antiserum and the enzymatic activity of the protein assayed (*see section 2.3.9.*). The results are means \pm SE of between 3-5 independent experiments.

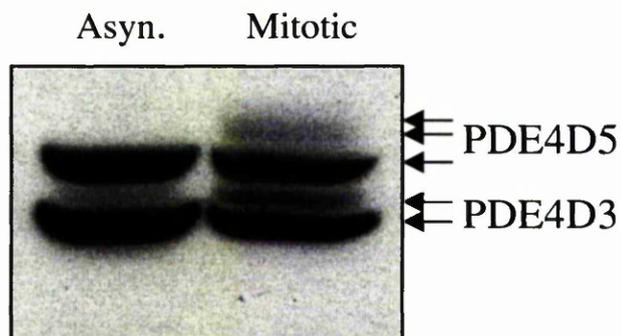


Figure 4.27. A proportion of endogenous PDE4D3/PDE4D5 in nocodazole induced mitotic HeLa cells has reduced electrophoretic mobilities. Asynchronous HeLa cells (Asyn.) and cells isolated in mitosis (Mitotic) with nocodazole incubation (50 ng/ml media for 14 h) were harvested in 3T3 lysis buffer and 100 μ g proteins from the cell lysate were separated by SDS-PAGE on an 8 % gel. The proteins were transferred to nitrocellulose which was immunoprobed with the PDE4D specific antiserum. The migration of the species of PDE4D3 and PDE4D5 are indicated.

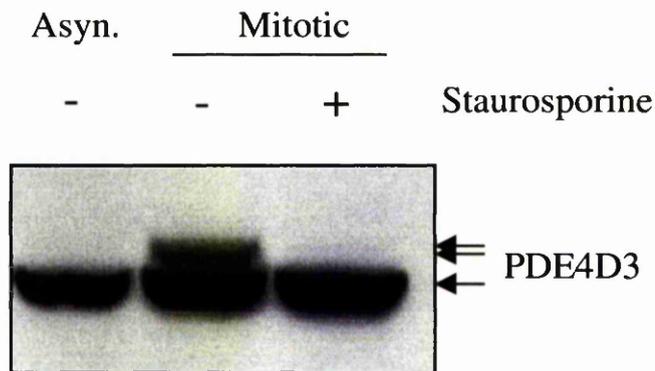


Figure 4.28. PDE4D3 Ser¹³/Ala mutant behaves as wild-type in nocodazole-induced mitosis. HeLa cells transfected with a construct encoding Ser¹³/Ala mutant PDE4D3 were either left asynchronous (Asyn.) or arrested in mitosis by incubation with nocodazole (50 ng/ml media for 14 h). The mitotic arrested cells were subjected to a further incubation with nocodazole for 2 h in the presence (+) or absence (-) of 100 nM staurosporine for 2 h. The cells were harvested in 3T3 lysis buffer and 100 μ g protein from these lysates were separated by SDS-PAGE on an 8 % gel. The proteins were transferred to nitrocellulose which was immunoblotted with the anti-VSV polyclonal antibody. The migration of the PDE4D3 species are indicated.

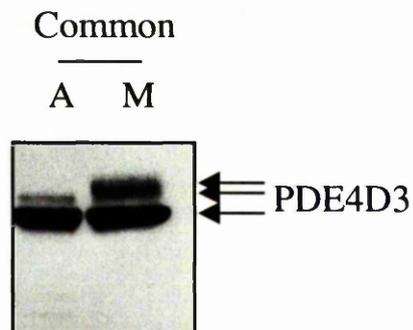
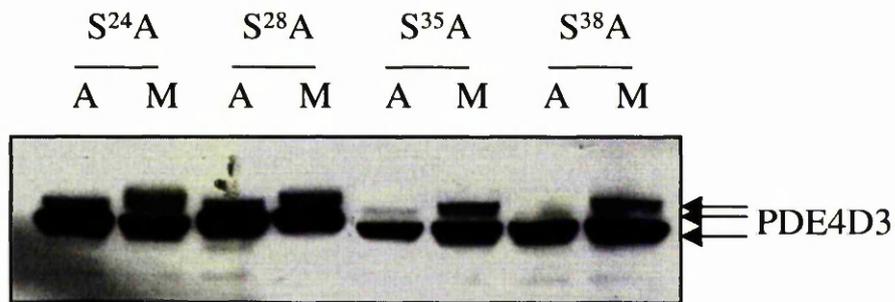
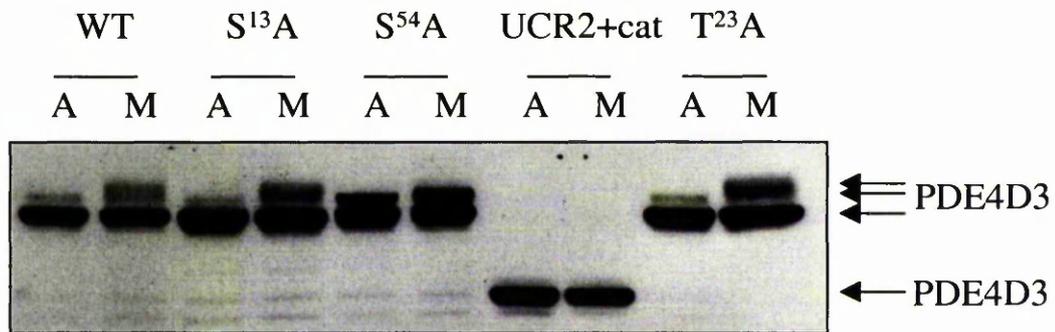


Figure 4.29. Analysis of electrophoretic mobilities of PDE4D mutants in mitosis. Mutant forms of PDE4D3 were expressed in HeLa cells, as indicated (*described in section 4.6.2.3.*). The cells were left asynchronous (A) or were arrested in mitosis 24 h after transfection, by incubation with 50 ng/ml media nocodazole (M). The cells were harvested in 3T3 lysis buffer and 100 μ g protein from these lysates were separated by SDS-PAGE on an 8 % gel. The proteins were transferred to nitrocellulose and then probed using the anti-VSV polyclonal antibody. The positions of the different species of PDE4D3 are indicated.

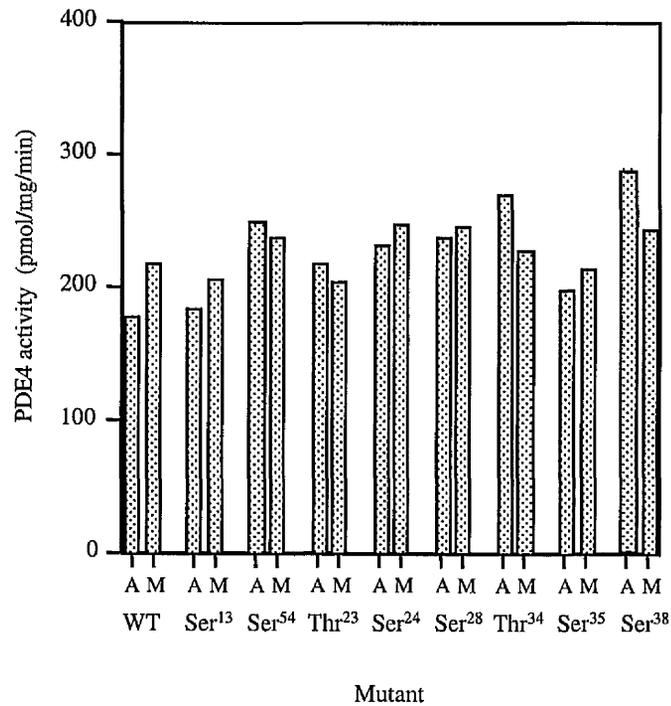


Figure 4.30. Mutant PDE4D3 protein activity in asynchronous and mitotic cells. Mutant constructs of PDE4D3 (See figure 4.31.) were transfected into HeLa cells (see section 2.1.3.), and the cells were subsequently left asynchronous (A) or subjected to nocodazole-induced mitotic arrest (M). The cells were harvested in 3T3 lysis buffer and the PDE activities of the cell lysates were measured (see section 2.3.9.). The results are representative of three independent experiments.

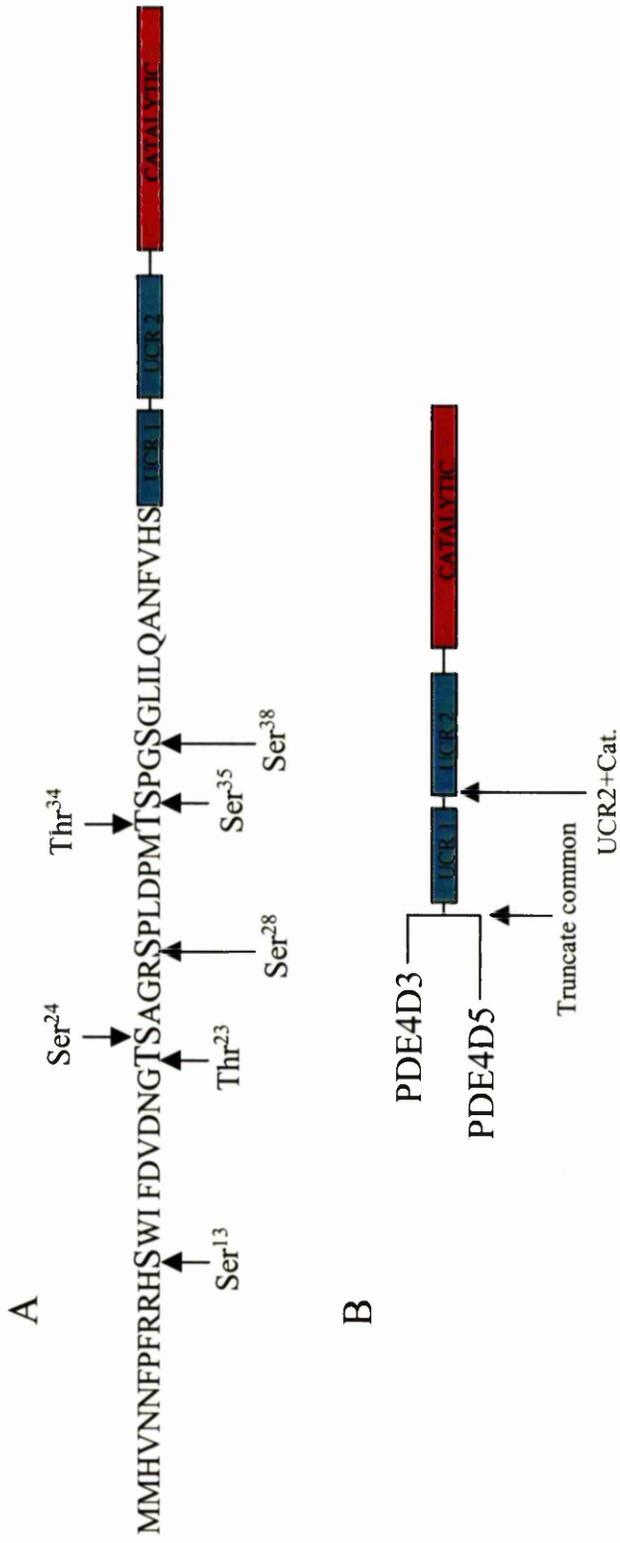


Figure 4.31. Mutant forms of PDE4D3 used in this study. Panel A, The serine (S) and threonine (T) residues of PDE4D3 that were mutated to alanine by Quickchange (see section 2.5.9.) are indicated, with each site mutated individually as described in section 4.6.2. **Panel B,** The sites at which PDE4D3 was truncated are indicated which generated a mutant lacking the unique N-terminal residues (Truncate common) and a mutant lacking the UCR1 region (UCR2+Cat) (see section 4.6.2.).

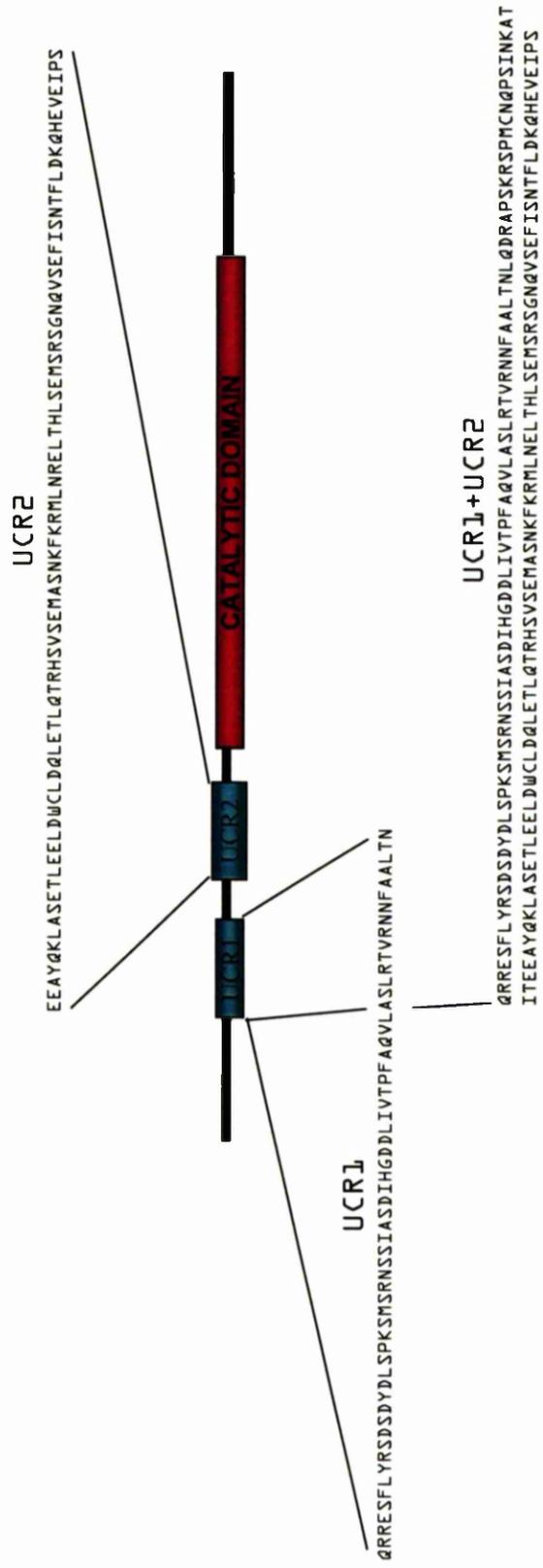


Figure 4.32. Domain sequences of GST-fused recombinant protein used for *in vitro* phosphorylation reactions. The UCR1 alone, UCR2 alone or UCR1 and UCR2 sequences indicated were generated as N-terminal GST fusion protein constructs by Ray Owens, Celltech, to be used in subsequent *in vitro* phosphorylation reactions.

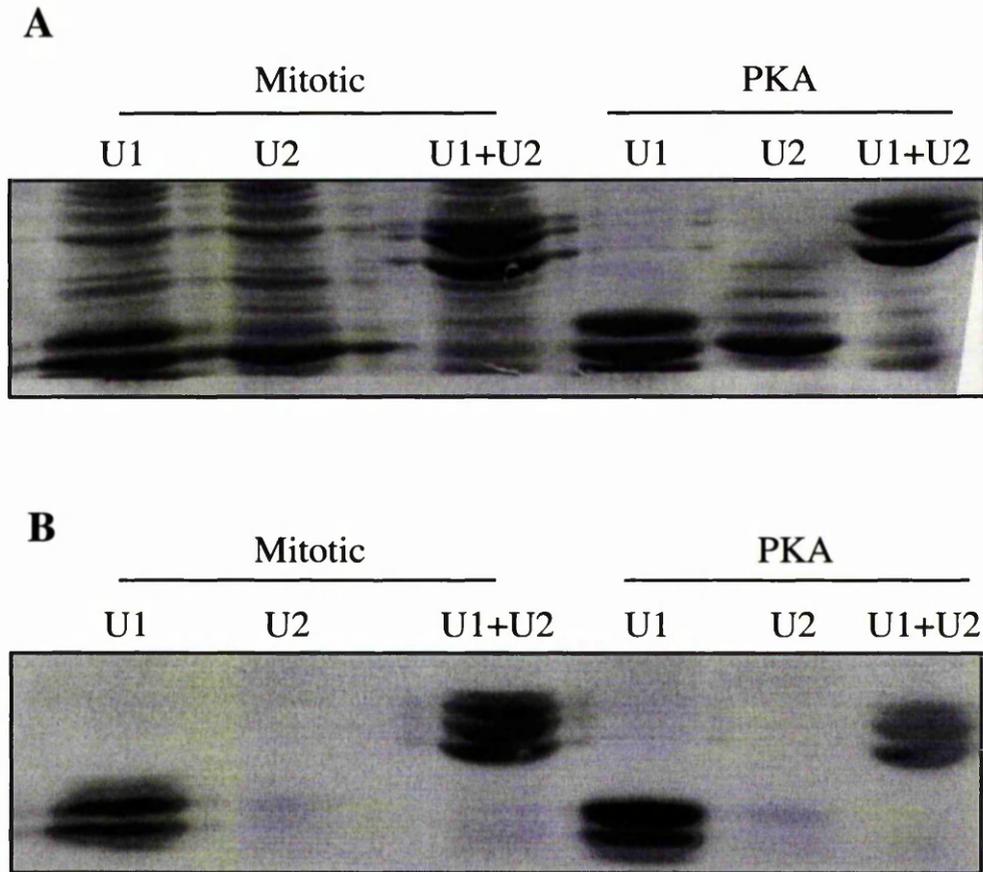


Figure 4.33. Phosphorylation of recombinant UCR1/UCR2 constructs by mitotic lysate and PKA. Recombinant proteins encoding UCR1 (U1) or UCR2 (U2) alone or both together (U1+U2) were expressed as GST fusions (*see section 2.4.3.*), purified and 100 μ l was subjected to an *in vitro* phosphorylation reaction, in the presence of 32 P-ATP. The reactions were carried out with lysate from cells isolated in mitosis (mitotic) or with purified PKA catalytic subunit (PKA, *see sections 2.4.5.1 and 2.4.5.2*) as indicated. The proteins were separated by SDS-PAGE on a 10 % gel and the proteins transferred to nitrocellulose. *Panel A*, the nitrocellulose was stained with Ponceau-S (*see section 2.3.8.2.*) to detect the recombinant protein. *Panel B*, the 32 P labelled proteins were detected by exposing the nitrocellulose to phosphorimage plate for 24 h (*see section 2.4.5.2.*).

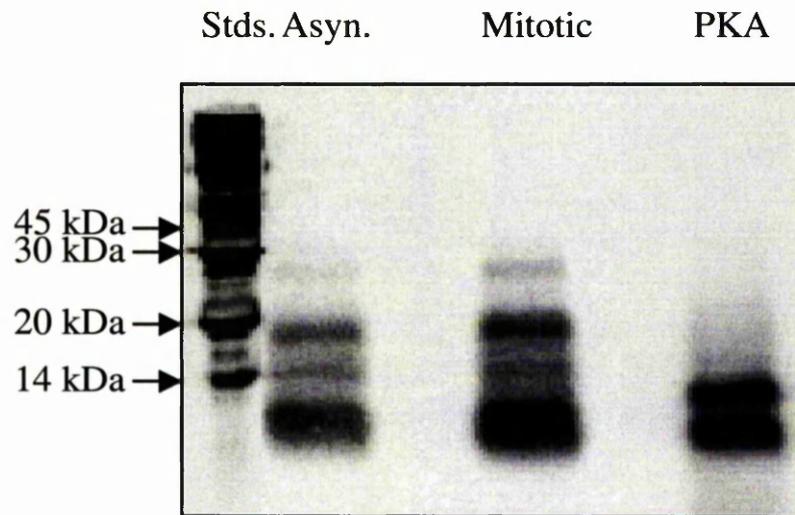


Figure 4.34. Peptides generated from *in vitro* phosphorylated PDE4D3 cleaved with cyanogen bromide. Full length recombinant PDE4D3 was phosphorylated *in vitro* with asynchronous (Asyn.) or mitotic lysate extracted from Rat-1 cells (*see section 2.5.4.2.*), or with purified PKA catalytic subunit (PKA, *see section 2.5.4.1.*), in the presence of γ [^{32}P]-ATP. The protein was then subjected to a cyanogen bromide peptide cleavage for 24 h and the peptides were separated by SDS-PAGE on a 16 % gel. The peptides were transferred to nitrocellulose and visualised by exposing the nitrocellulose to a phosphorimage plate for 48 h. The molecular weights of the protein standards (Stds.) are indicated.

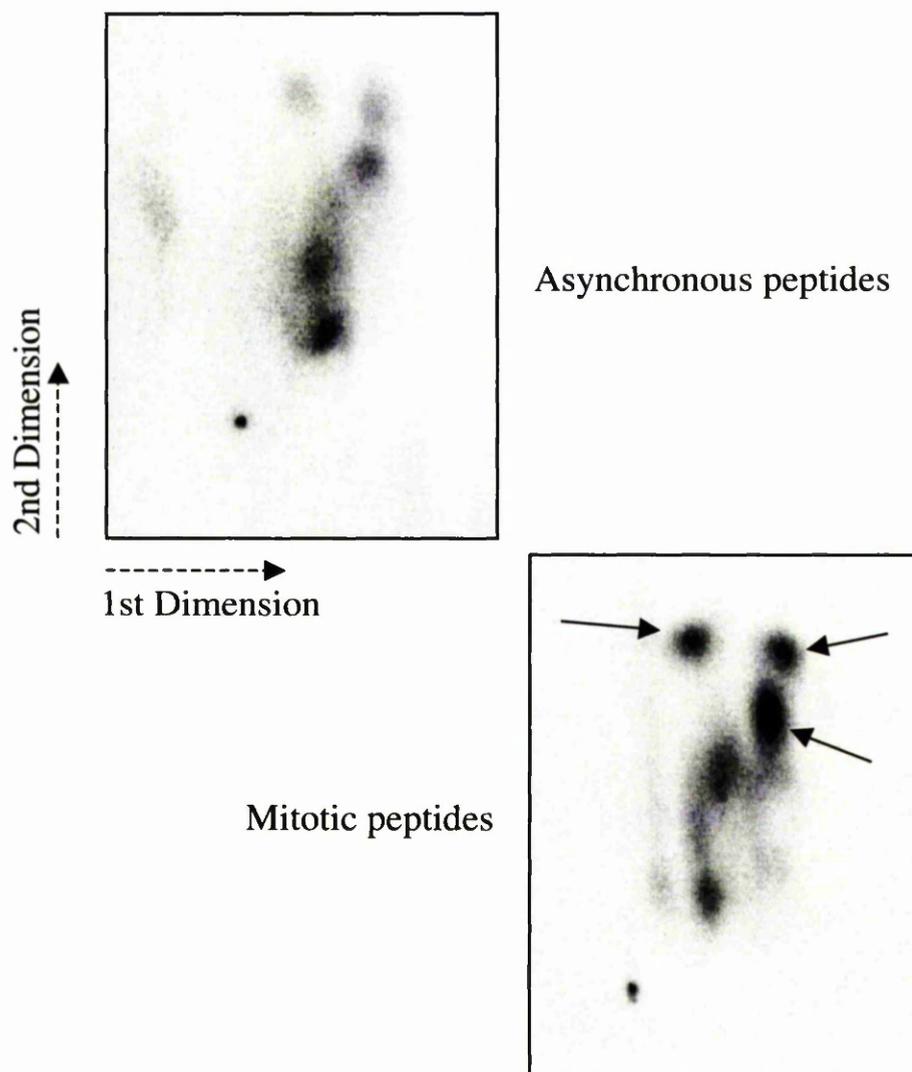


Figure 4.35. Separation of tryptically digested PDE4D3 phosphopeptides by 2D thin layer chromatography. Recombinant PDE4D3 protein was phosphorylated *in vitro* by kinases isolated from asynchronous or mitotic cell lysate (*see section 2.4.5.2.*), then digested with trypsin (*see section 2.4.6.*). The peptides generated were separated in the 1st dimension by electrophoresis and in the 2nd dimension by chromatography (*see section 2.4.6.*). The TLC plates were then exposed to a phosphorimage plate and the phosphopeptides that were consistently more highly phosphorylated by kinases in mitotic lysate are indicated with arrows. These results are representative of 4 independent experiments.

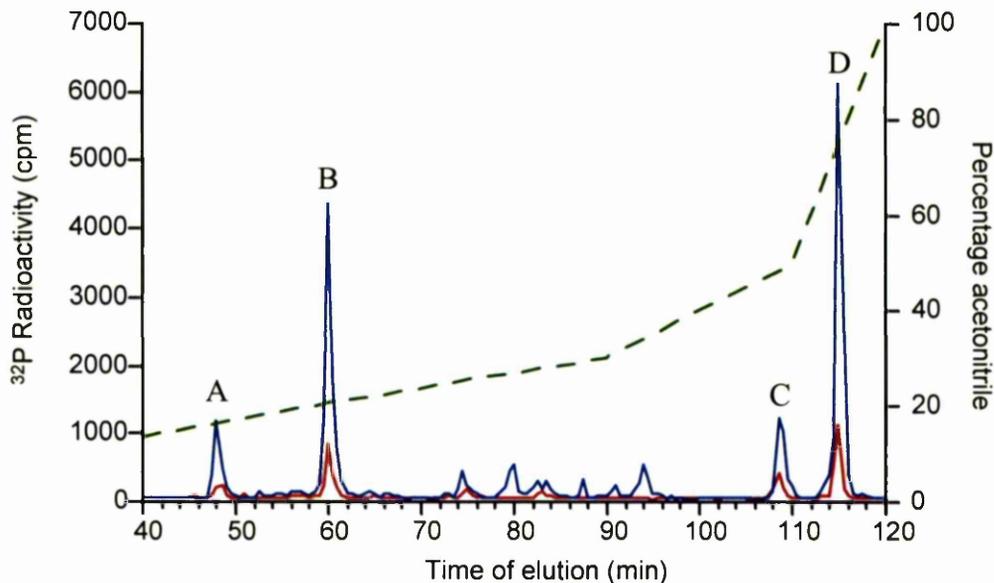


Figure 4.36. Separation of tryptically digested PDE4D3 phosphopeptides by HPLC. Recombinant PDE4D3 protein was phosphorylated with kinases isolated from asynchronous (Asyn. red trace) or mitotic cell lysate (Mit., blue trace) (*see section 2.4.5.2.*) and then digested with trypsin (*see section 2.4.7.1.*). The peptides were isolated from the tryptic digest (*see section 2.4.7.1.*) and separated by reverse phase HPLC (*see section 2.4.7.2.*) and eluted from the column with increasing concentrations of acetonitrile. The elution times and amounts of ^{32}P incorporated into each peptide are shown, the peptides used for further analysis are labelled A, B, C and D.

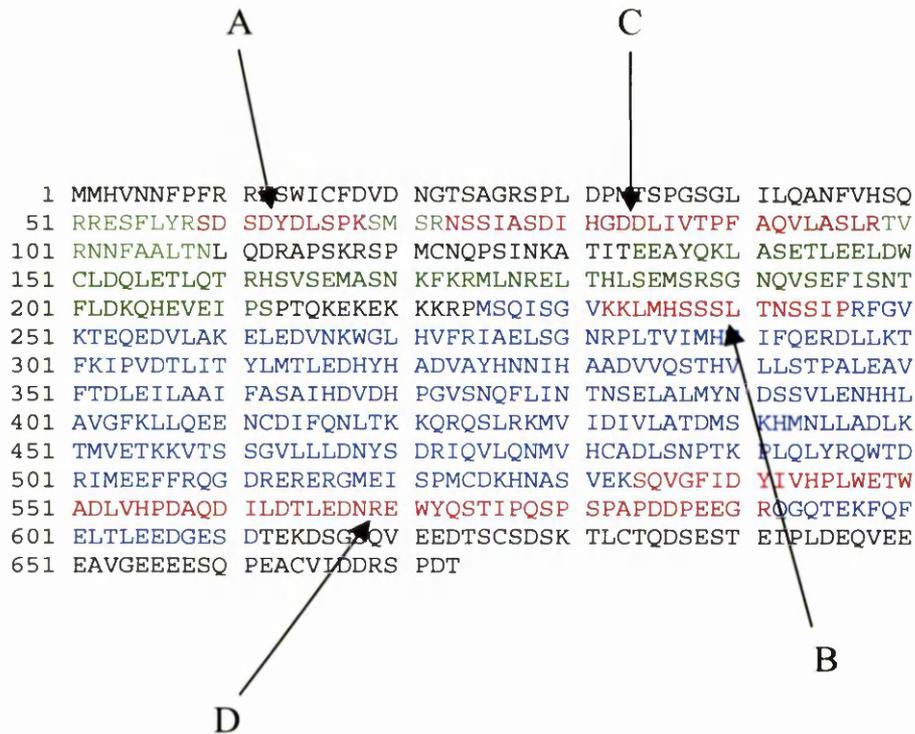


Figure 4.37. Peptides of PDE4D3 phosphorylated *in vitro* by kinases from mitotic lysate. The phosphopeptides generated by the phosphorylation of recombinant PDE4D3 with kinases isolated from mitotic cell lysate, once purified by HPLC, were identified by mass spectrometry and mapped to PDE4D3 sequence (*see section 4.7.4.*). The phosphopeptides are highlighted in red, and the arrow letter associated with each peptide refers to the peptide isolated on the HPLC trace (*see Fig. 4.36.*). The UCR1 domain is indicated in light green, UCR2 in dark green and the catalytic domain in blue. The remaining residues are within the unique, LR1, LR2 and C-terminal domains of PDE4D3. The numbers relate to the residue number in the PDE4D3 protein.

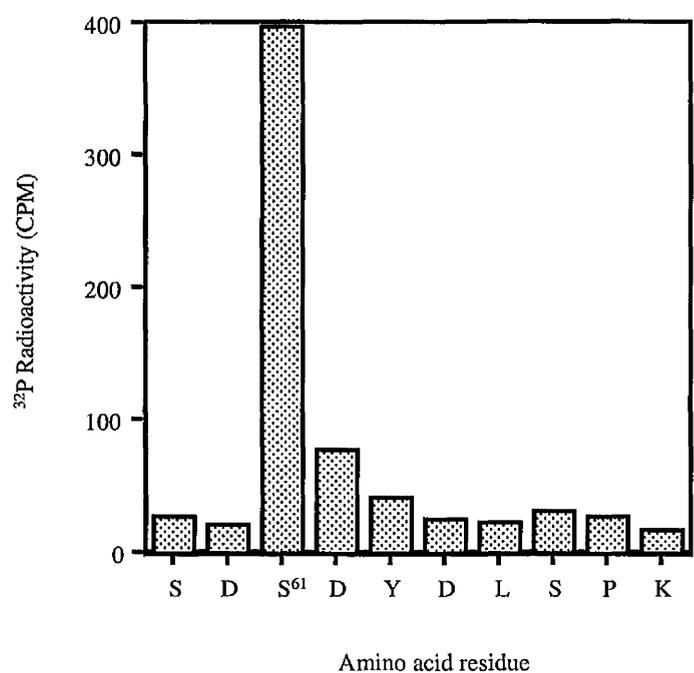


Figure 4.38a. Cycle burst amino acid analysis of residues phosphorylated in peptide A, found at the N-terminal of UCR1. The peptide of PDE4D3 phosphorylated by kinases present in lysate from cells arrested in mitosis, (*see section 4.8.4.*) once identified by mass spectrometry analysis (*see section 4.8.4.1.*), was sequenced by Edman degradation and the levels of ³²P incorporated into each residue was measured. The amino acids are represented by their single letter nomenclature and the level of ³²P incorporated into each residue and Ser⁶¹ is indicated.

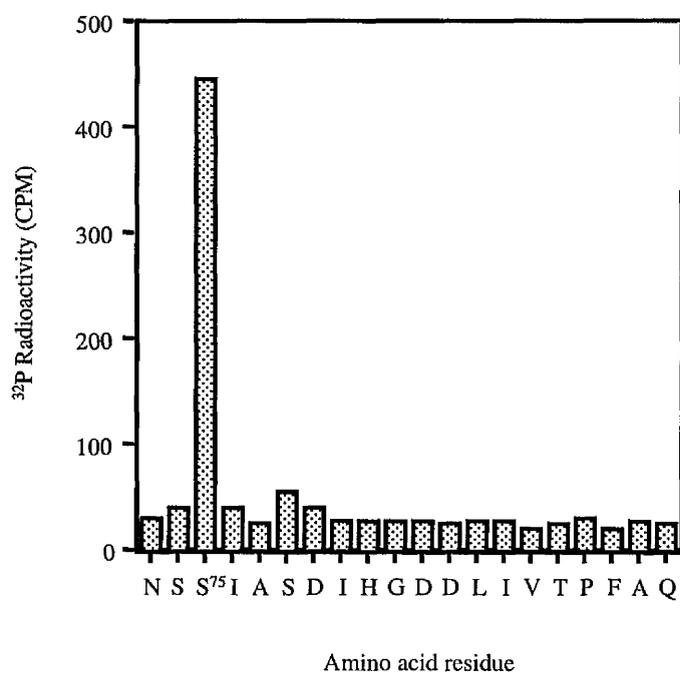


Figure 4.38b. Cycle burst amino acid analysis of residues phosphorylated in peptide C, found at the C-terminal of UCR1. The peptide of PDE4D3 phosphorylated by kinases present in lysate from cells arrested in mitosis, (*see section 4.8.4.*) once identified by mass spectrometry analysis (*see section 4.8.4.1.*), was sequenced by Edman degradation and the levels of ³²P incorporated into each residue was measured. The amino acids are represented by their single letter nomenclature and the level of ³²P incorporated into each residue is indicated, and the Ser⁷⁵ residue is numbered.

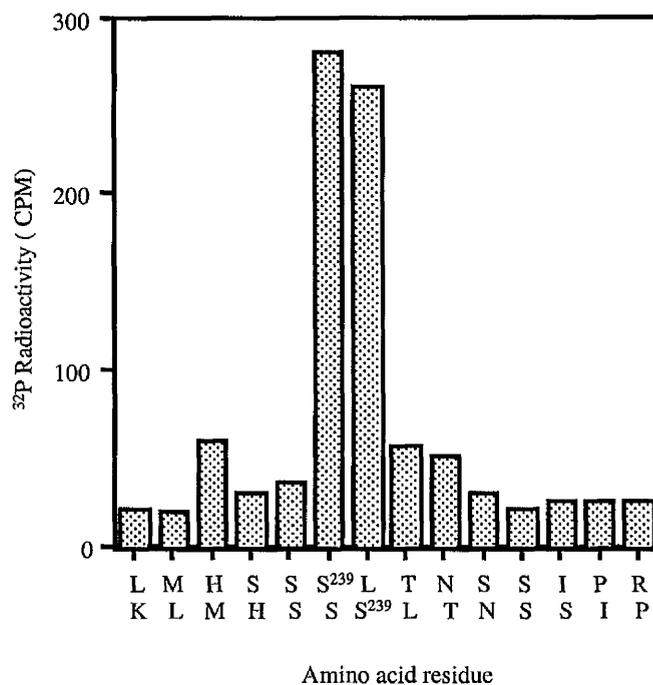


Figure 4.38c. Cycle burst amino acid analysis of residues phosphorylated in peptide B, found at the N-terminal of the catalytic domain. The peptide of PDE4D3 phosphorylated by kinases present in lysate from cells arrested in mitosis, (*see section 4.8.4.*) once identified by mass spectrometry analysis (*see section 4.8.4.1.*), was sequenced by Edman degradation and the levels of ³²P incorporated into each residue was measured. The amino acids are represented by their single letter nomenclature and the level of ³²P incorporated into each residue is indicated. The two sequences of amino acids are shown as there are two lysine residues located next to one another and some of the peptides generated by tryptic digest contain this residue, whereas other lack it. Two peaks of radiolabelled serines (Ser²³⁹) are therefore detected, however, both map to the final serine residue in the triplet within the sequence.

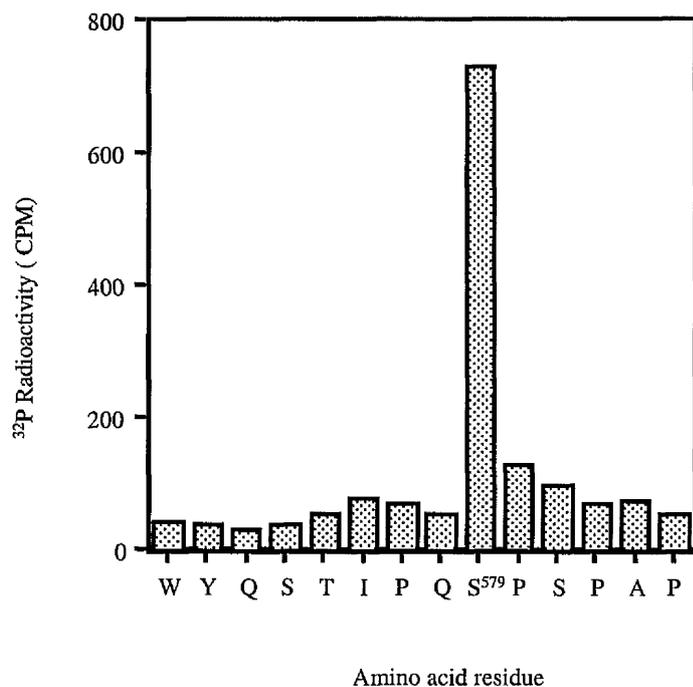


Figure 4.38d. Cycle burst amino acid analysis of residues phosphorylated in peptide D found at the C-terminal of the catalytic domain. The peptide of PDE4D3 phosphorylated by kinases present in lysate from cells arrested in mitosis, (*see section 4.8.4.*) once identified by mass spectrometry analysis (*see section 4.8.4.1.*), was sequenced by Edman degradation and the levels of ³²P incorporated into each residue was measured. The amino acids are represented by their single letter nomenclature and the level of ³²P incorporated into each residue and Ser⁵⁷⁹ are indicated.

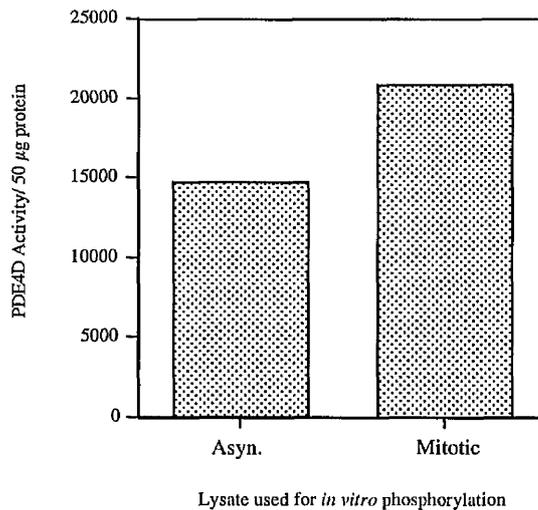


Figure 4.39. Changes in PDE4D activity after *in vitro* phosphorylation with kinases isolated from asynchronous and mitotic lysate. 50 µg PDE4D3 protein expressed in HEK-293 cells was isolated by immunoprecipitation using the VSV polyclonal antibody (*see section 2.3.10.*) and was subjected to 'cold' *in vitro* phosphorylation using asynchronous (Asyn.) or mitotic lysates, (*see section 2.4.5.2.*). The activity of the PDE4D3 protein after phosphorylation was determined.

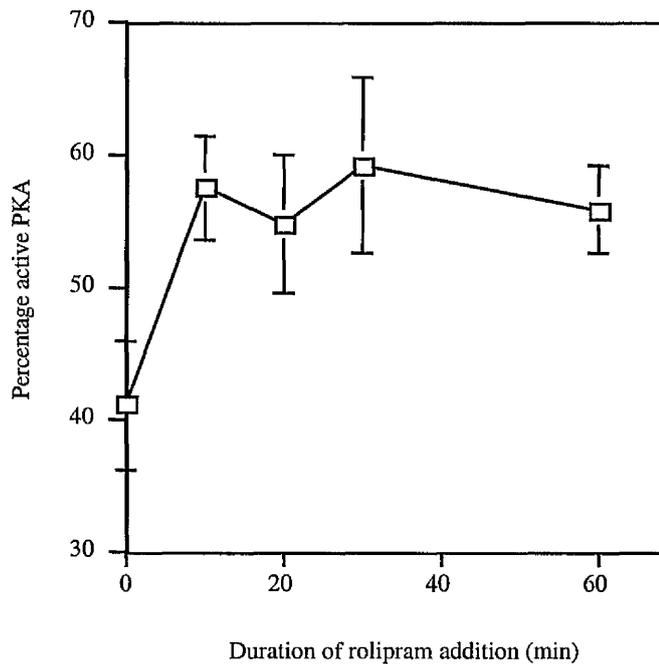


Figure 4.40. Increase in proportion of active PKA in cells arrested in mitosis after incubation with rolipram. Rat-1 cells arrested in mitosis, through incubation with 50 ng/ml nocodazole for 14 h, were incubated with 10 μ M rolipram for up to 60 mins. Cells were harvested in extraction buffer (*see section 2.4.1.1.*) at the time points indicated and the proportion of active PKA in these cell extracts were determined (*see section 2.4.1.*). The PKA activity is shown as a percentage of total PKA which can be activated in the cells and is the means \pm SE of four independent experiments.

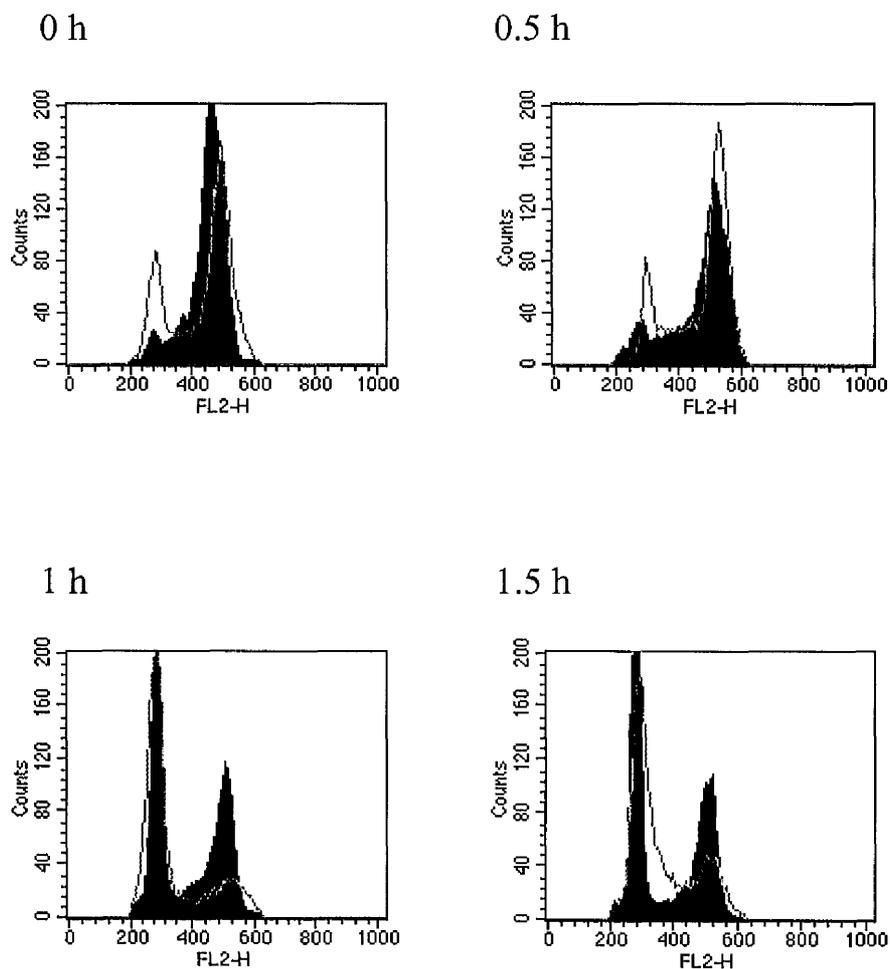


Figure 4.41. The effect of rolipram on cell cycle distribution after the release of cells from nocodazole-induced mitosis. Rat-1 cells were released from a nocodazole induced mitotic arrest (*see section 2.1.4.5.*) in the presence (filled, purple histogram) or absence (unfilled, green histogram) of 10 μ M rolipram. Cells were harvested at 30 min intervals post release and their DNA content determined by FACs analysis (*see sections 2.2.1. and 2.2.2.*). The histograms were produced using the CELLQuest acquisition package and represent the DNA content of a population of 20000 cells analysed.

Inhibitor	Specificity
Genistein	Protein Tyrosine Kinases
5,6-Dichloro-1- β - D- ribofuranosylbenzimidazole	Casein kinase II
Wortmannin	Phosphatidylinositol 3- Kinase
LY294002	Phosphatidylinositol 3- Kinase
U0129	MAPK
Olomucine	Cdk1/cyclinB, Cdk2/CyclinA, Cdk2/CyclinE
Roscovitine	Cdk1/CyclinB, Cdk2/Cyclin A, Cdk2/Cyclin E
Chelerythrine chloride	Protein kinase C
Bisindolylmaleimide	Protein kinase C
ML7	Myosin light chain Kinase
PD98059	Map kinase kinase (MEK)

Table 4.1. Panel of kinase inhibitors. A series of commercially available kinase inhibitors were incubated on Rat-1 cells isoalted in mitosis in an attempt to block the phosphorylation of PDE4D3 (*see section 4.3.6.2.*). The specific inhibitors used and their target kinases are laid out above.

Residue	Position and phosphorylation motif	Probability	Residue	Position and phosphorylation motif	Probability
Serine	13 FRRHSWICF	0.997	Threonine	181 NRELTHLSE	0.871
	24 DNGTSAGRS	0.669		213 PSPTQKEK	0.938
	28 SAGRSPLDP	0.996		252 FGVKTEQED	0.665
	35 DPMTSPGSG	0.778		455 TMVETKKVT	0.965
	49 NFVHSQRRE	0.991		499 YRQWTDRLM	0.710
	54 QRRESFLYR	0.981		603 QFELTLEED	0.874
	59 FLYRSDSDY	0.992		611 GESDTEKDS	0.954
	61 YRSDSDYDL	0.997		624 VEEDTSCSD	0.966
	66 DYDLSPKSM	0.981		640 DSESTEIPL	0.682
	69 LSPKMSMRN	0.992	Tyrosine	63 SDSDYDLSP	0.973
	70 PKMSMRNSS	0.809		137 TEEAYQKLA	0.970
	74 MSRNSSIAS	0.996		196 QVSEYISNT	0.761
	75 SRNSSIASD	0.957		319 LEDHYHADV	0.551
	78 SSIASDIHG	0.518		325 ADVAYHNNI	0.745
	116 DRAPSKRSP	0.992			
	119 PSKRSPMCN	0.929			
	142 QKLASETLE	0.585			
	163 QTRHSVSEM	0.997			
	164 RHSVSEMAS	0.824			
	169 SEMASNKFK	0.617			
	212 VEIPSPTQK	0.781			
	226 KRPMQISG	0.997			
	279 IAELSGNRP	0.550			
	343 HVLLSTPAL	0.654			
	393 YNDSSVLEN	0.920			
	425 KQRQSLRKM	0.991			
	460 KKVTSSGVL	0.931			
	521 GMEISPMCD	0.662			
	530 KHNASVEKS	0.981			
	534 SVEKSQVGF	0.529			
	579 TIPQSPSPA	0.983			
	580 PQSPSPAPD	0.927			
	610 EDGESDTEK	0.991			
616 TEKDSGSQV	0.949				
617 KDSGSQVEE	0.994				
625 EEDTSCSDS	0.995				
639 QDSESTEIP	0.992				

Table 4.2. Probability of residue phosphorylation using NetPhos. The sequence of the Rat PDE4D3 isoform was submitted to the NetPhos prediction form, online (*see section 4.5.1.1.*), and the probability that a residue was phosphorylated was calculated. The sequences in bold are those later identified as being phosphorylated by kinases from mitotic lysates (*see section 4.7.*).

Kinase	Phosphorylated residue	Motif	Kinase	Phosphorylated residue	Motif
CaMII	S-13 S-54 S-61 S-75 S-116 T-181 S-226 T-285 T-499	RRHSWIC RRESFLY RSDSDYD RNSSIAS RAPSKRS RELTHLS RPMSQIS RPLTVIM RQWTDRI	GSK3 C-terminal +4 S must be prephosphorylated	S-24 T-34 S-71 S-165 S-194 S-239 S-530 T-575 T-612 S-625	NGTSAGRS DPMTSPGS KSMSRNSS HSVSEMAS NQVSEYIS HSSSLTNS HNASVEKS YQSTIPQS ESDTEKDS EDTSCSDS
CKI N-terminal T/S must be phosphorylated	S-28 S-38 S-69 S-75 T-99 S-119 T-160 S-169 S-184 S-198 S-229 T-241 T-310 S-440 T-455 T-489 S-534 S-579 S-616 S-627 T-634 T-640	SAGRSPLD TSPGSLI SPKSMSR SRNSSIAS SLRTVRN SKRSPMC TLQTRHS SEMASNKF THLSEMS SEYISNTF SQISGVK SSSLTNSC TLITYLM TDMSKHM TMVETKKV SNPTKPL SVEKSQVG TIPQSPSP TEKDSGSQ TSCSDSK TLCTQDS SESTEIP	CKII	S-28 S-59 T-131 T-144 S-163 T-200 T-214 T-252 T-314 T-352 T-381 S-393 T-451 T-549 T-564 T-603 S-610 S-618 S-62	AGRSPLD LYRSDSD NKATITE ASETLEE TRHSVSE ISNTFLD PSPTQKE GVKTEQE YLMTLED AVFTDLE LINTNSE NDSSVLE DLKTMVE LWETWAD ILDILED FELTLBE DGESDTE DSGSQVE EDTSCSD
MLCK	S-226	KKRPMSQIS	P70s6k	S-226	KRPMSQIS
PKA	S-13 S-54 S-61 S-75 S-116 S-163 T-181 S-226 T-285 S-425 T-499	RRHSWIC RRESFLY RSDSDYD RNSSIAS RAPSKRS RHSVSE RELTHLS RPMSQIS RPLTVIM RQSLRK RQWTDRI	PKC	S-49 S-66 S-96 S-116 S-169 T-214 T-300 T-419 S-425 T-455 S-470 T-499 T-595 T-612	FVHSQRR YDLSPKS VLASLRT RAPSKRS EMASNKF PSPTQKE LLKTFKI QNLTKKQ QRQSLRK MVETKKV DNYSDDRI RQWTDRI QQQTBKF ESDTEKD

PKG	S-13 S-54 T-459	RRHSWIC RRESFLY KKVTSSG	Cdk1	No identified residues	
-----	-----------------------	-------------------------------	------	------------------------	--

Table 4.3. Predicted phosphorylation sites of PDE4D3 using PhosphoBase. The Rat sequence of PDE4D3 was inserted into the prediction submission form on the PhosphoBase programme (*see section 4.5.1.1.*) and the predicted phosphorylation sites within the protein were given. The sequences in red correspond to those later identified as being targeted for phosphorylation by kinases active in mitotic lysates (*see section 4.7.*).

Molecular Weight (Daltons)	Peptide Sequence
16662.365	CDKHNASVEKSQVGFIDYIVHPLWETWA DLVHPDAQDILD TLEDNREWYQSTIPQSP SPAPDDQEDGRQGQTEKFQFEL TLEEDGE SDTEKDSGSQVEEDTSCSDSKTLCTQDSE STEIPLDEQVEEEAVAEESQPQTGVADD CCPDT
8111.52	TLEDHYHADVAYHNNIHAADV VQSTHVL LSTPALEAVFTDLEILAAIFASAIHDVDHP GVSNQFLINTNSELALM
5916.86	HSSSLTNSCIPRFGVKTEQEDVLAKELEDV NKWGLHVFRIELSGNRPLTVIM
5502.895	SRNSSIASDIHGDDLIVTPFAQVLASLRTV RNNFAALTNLQDRAPSKRSPM
5247.51	CNQPSINKATITEEAYQKLASETLEELDW CLDQLETLQTRHSVSEM
4826.479	YNDSSVLENHHLAVGFKLLQEENC DIFQN LTKKQRQSLRKM
4525.343	SRSGNQVSEYISNTFLDKQHEVEIPSPTQK EKEKKRPM
4141.37	TSPGSGLILQANFVHSQRRESFLYRSDSDY DLSPKSM
3511.671	HVNTFPFRRHSWICFDVDNGTSAGRSPLD PM
3002.616	VETKKVTSSGVLLLDNYS DRIQVLQNM
2987.66	HTIFQERDLLKTFKIPVDTLITYLM
2837.452	VHCADLSNPTKPLQLYRQWT DRIM
1893.895	EEFFRQGDRERERGM
1294.675	LNRELTHLSEM
1042.625	SQISGVKKLM
1013.551	AIDIVLATDM
970.557	NLLADLKTM
933.526	ASNKFKRM
528.299	EISPM

Table 4.4. Predicted peptides generated upon cyanogen bromide cleavage of PDE4D3.

The molecular weights and sequences of the peptides generated by cleavage of PDE4D3 with cyanogen bromide were calculated using the ExPASy-PeptideMass prediction web site at <http://ca.expasy.org/cgi-bin/peptide-mass.pl>. The highlighted peptides are those previously identified as being phosphorylated by PKA.

Chapter 5

Characterisation of Phosphodiesterase 7 (PDE7)

5.1 Introduction

T lymphocytes are activated by antigen bound to the major histocompatibility complex (MHC) on the antigen presenting cell interacting with the CD3 T cell receptor complex on surface of T cell (Geppert and Lipsky, 1986). This interaction alone induces expression of low levels of interleukin 2 (IL-2, June et al., 1989), an effect that is enhanced synergistically upon the co-stimulation of the T cell CD28 receptor by the antigen-presenting cell (Thompson et al., 1989). The co-stimulation of the two receptors causes the levels of cAMP to decrease, an effect brought about by an increase in PDE activity in the T cells (Takemoto et al., 1978). It is this decrease in cAMP that initiates the induction of high levels of IL-2 (Mary et al., 1987; Skalhegg et al., 1994). IL-2 acts in an autocrine fashion to stimulate T cell proliferation (Giembycz et al., 1996; Lingk et al., 1990) and to increase the expression of cytokines such as TNF α (Shames et al., 2001), IL-13 (Kanda and Watanabe, 2001) and IL-4 (Borger et al., 1996) and to stimulate their exocytosis (Shahinian et al., 1993) when bound to its cognate receptor. T cell activation is associated with inflammatory diseases (Kay, 2000) and PDE4 inhibitors have been identified as viable targets for therapeutic intervention (Rogers and Giembycz, 1998). Side effects such as emesis were associated with first generation PDE4 inhibitors and thus the next generation of more selective PDE4 inhibitors are required to target inflammatory diseases. This prompted the study of PDE profiles and function within T lymphocytes to identify new therapeutic targets.

Upon inhibition of PDE4 and PDE3 in T lymphocytes it was noted that there was a 25% residual cAMP specific hydrolytic activity in the cytosolic fraction of the cell (Robicsek et al., 1991; Tenor et al., 1995). This was referred to as the cAMP specific, IBMX-insensitive activity in the cell and has been attributed to PDE7 (Ichimura and Kase, 1993); to which there were no specific inhibitors. PDE7 activity has been suggested to be involved in signalling cascades that initiate proliferation and stimulate IL-2 release from T cells inducing their full activation (Giembycz et al., 1996). Both CD4⁺ and CD8⁺ T cells express PDE7 (Giembycz et al., 1996; Glavas et al., 2001). Levels of PDE7 activity are low in peripheral T lymphocytes, but when they are activated there is a rapid increase in PDE7A1 and PDE7A3 mRNA and protein levels (Glavas et al., 2001). Inhibition of PDE7, by down-regulating expression of the protein using anti-sense oligonucleotides, decreases the amount of IL-2 (Li et al., 1999) and IL-13 (Kanda and Watanabe, 2001) cytokine expression in activated T lymphocytes and inhibits the proliferation of T cells (Li et al., 1999). With PDE7 contributing significantly to mechanisms involved in the full activation

of T cells it could provide a potential therapeutic target. Specific inhibitors might be expected to decrease IL-2 production and thus, prevent excessive cellular proliferation perhaps without the side effects associated with PDE4 inhibition (Barnes et al., 2001).

The first synthetic inhibitors which targeted PDE7 activity were benzyl derivatives of 2,1,3-Benzo-and benzothienol[3,2-*a*]-thiadiazine2,2-dioxides (*Fig. 5.1.*). These showed inhibition of recombinant PDE7 expressed in *Saccharomyces cerevisiae*, with IC₅₀ values of around 10 μM. However, these compounds exhibited high cross-reactivity with PDE3 and PDE4 isoforms and so were not suitable for explicit selectivity (Martinez et al., 2000). The next generation of PDE7 inhibitors were designed around a guanine based structure (*Fig 5.1.*) with 8 -bromo-9 -substitution (Barnes et al., 2001). These proved to be potent PDE7 inhibitors, the most selective having an IC₅₀ of 1 μM for PDE7, while only very weakly (~10 %) inhibiting PDE3 and PDE4 activity at a concentration of 10 μM (Barnes et al., 2001).

Four PDE7 isoforms have been identified, three originating from the PDE7A gene and one from the PDE7B gene. The PDE7A protein was initially identified by complementation analysis in cAMP-specific PDE-deficient *Saccharomyces cerevisiae* (Michaeli et al., 1993). Further identification of this protein from both T cell lines and skeletal muscle uncovered two splice variants, PDE7A1 (accession number AAA35644) and PDE7A2 (accession number AAB65772, Bloom and Beavo, 1996; Han et al., 1997). These two proteins have mobilities of 57 kDa and 50 kDa, respectively, and differ from one another in their extreme N-termini (*Fig. 5.2., Panel A*). The N-terminus of PDE7A2 encompasses a hydrophobic region that localises the protein to particulate cell fractions, whereas the PDE7A1 N-terminus is much more hydrophilic and a more even distribution of the protein between cytosolic and membrane fractions is found (Han et al., 1997). A third PDE7A splice variant has recently been identified in T-cells, PDE7A3 (accession number AAK57640, Glavas et al., 2001). It has the same N-terminus as PDE7A1 but differs at the C-terminus. It has an apparent molecular weight of 50 kDa (*Fig. 5.2., Panel B*).

Results

5.2. Expression of PDE7A isoforms in cells

5.2.1 Screening cell lines for endogenous PDE7A protein

PDE7A1 is the most abundant PDE7 isoform expressed in T cell lines (Glavas et al., 2001; Bloom and Beavo, 1996). In order to establish which cell lines would be appropriate to study the activity and sub-cellular distribution of PDE7A, a series of cell lines were screened with PDE7A specific polyclonal rabbit antisera, provided by Celltech Plc. The antiserum was raised against a synthetic peptide, ELNSQLLPQENRLS, which equates to a sequence located at the extreme C-termini of the PDE7A1 and PDE7A2 splice variants, but not PDE7A3. The cell lines screened ranged from T cells (Molt-3, Jurkat J6 and HuT-78), B cells and monocytes (U-937) to kidney (HEK-293, COS-1 and COS-7) and fibroblast cell lines (F442A, *Fig. 5.3.*). A summary of the expression of the PDE7A isoforms in the different cell lines is presented in Table 5.1. In agreement with previously published observations (Glavas et al., 2001; Bloom and Beavo, 1996), PDE7A was only expressed at high levels in T cell lines where the most abundant isoform was PDE7A1 (57 kDa). No cell lines studied expressed PDE7A2 (50 kDa) at high levels, but immunoreactive bands were evident in COS-1, COS-7 and Jurkat J6 cells.

5.2.2. Expression of recombinant PDE7A protein in a mammalian system

I was supplied with several DNA plasmid constructs generated by Dr. Ray Owens at Celltech Plc. The first of these constructs, referred to as pSM2, contained the human PDE7A1 cDNA sequence cloned into the BamHI/XbaI sites of the polylinker region of the pcDNA3.1 expression vector (Invitrogen), with a FLAG sequence fused to the N-terminus of the protein. The second construct supplied, referred to as pBMC, contained the human PDE7A2 cDNA cloned into the BamHI site within the polylinker region of the pVL1392 baculovirus transfer vector (PharMingen). Celltech Plc had previously characterised these PDE7A isoforms as proteins expressed in insect cells. However, when they attempted to express the PDE7A proteins in COS-1 and Chinese hamster ovary (CHO) cells, no expression was detected by activity studies or by western blotting (personal communication, R Owens). PDE7A mRNA transcripts were detected in the transfected COS-1 and CHO cells by RT-PCR, which led the investigators to believe that PDE7A protein translation required a cofactor and this might be absent in these cell lines (personal communication, R. Owens). This suggestion of selective translation of PDE7 in cells

containing the mRNA transcripts had previously been proposed by Bloom and Beavo, since they also observed PDE7A mRNA, but detected no PDE7A protein in skeletal muscle and B cell lines (Bloom and Beavo, 1996).

5.2.2.1. Cloning PDE7A2 into the pcDNA3.

As the human PDE7A2 cDNA was supplied in the baculovirus transfer vector pVL1392, the PDE7A2 cDNA had to be subcloned into a mammalian expression vector, to allow expression of the protein in mammalian cell lines.

The PDE7A2 open reading frame (ORF) cDNA was excised from the pVL1392 vector using the BamHI endonuclease (Materials and methods 2.5.3.1). The PDE7A2 cDNA fragment was isolated by agarose gel electrophoresis, purified from the gel (Materials and methods 2.5.3.1 and 2.5.3.3) and ligated into purified, BamHI digested, pcDNA3 vector (Materials and methods 2.5.4), giving rise to the plasmid pCS1. To confirm the subcloning of the PDE7A2 cDNA into pcDNA3 had occurred in the correct orientation the pCS1 construct was sequenced (Materials and methods 2.5.8) and was found to be correct (*data not shown*).

5.2.2.2. Transfection of COS-7 cells with PDE7A constructs

To characterise the PDE7A proteins, the PDE7A1 containing construct, pSM2, and the PDE7A2 containing construct, pCS1, were transfected into COS-7 cells using the DEAE-Dextran method (Materials and methods 2.1.3.1). Transfected cells were incubated for 24 – 48 h, to allow for expression of the protein, before being harvested and processed for immunoblotting. As can be seen in Fig. 5.4., COS-1 cells transfected with the PDE7A1 construct expressed the protein well when compared to mock transfected cells. The PDE7A2 construct, however, did not produce any detectable immunoreactive protein (*Fig. 5.4.*).

In an attempt to express the PDE7A2 construct in COS-7 cells, different transfection methods were utilised, including calcium phosphate mediated transfection (Materials and methods 2.3.1.2.) and several commercially available lipid based transfections procedures, including lipofectAMINE™, Dotap™ and Superfect™ reagents (Materials and methods 2.3.1.3 and manufacturer's instructions). When the transfected cell lysates were analysed by immunoblotting (Materials and methods 2.3.5.) none of the methods of transfection allowed the expression of PDE7A2 (*Fig. 5.5.*).

5.2.2.3. *PDE7A mRNA is detected in COS-7 cells*

As Celltech Plc. had previously confirmed the expression of PDE7A mRNA from the pSM2 plasmid by RT-PCR analysis, I endeavoured to perform similar analysis of COS-1 cells transfected with pCS1, using primers specific for PDE7A isoforms, to check whether expression at the mRNA level could be observed. The RT-PCR reactions from pCS1 transfected COS-7 total RNA, using specific PDE7A primers (W1075 and W1070, *see Fig. 5.6., Panel A*), supplied by Celltech Plc, were carried out. PCR products of approximately 600 bases were amplified from RNA extracted from both mock and transfected COS-7 cells (*Fig. 5.6., Panel B*). This indicated that transcripts of PDE7A were endogenously present in COS-7 cells and it was therefore impossible to determine whether the PDE7A2 construct was functional.

5.2.2.4. *Attempt to transfect T-cell lines with PDE7A1*

T cells are known to express PDE7A1 (Ichimura and Kase, 1993; Bloom and Beavo, 1996) and as the levels of PDE7A1 protein had previously been shown to be increased upon the activation of T cells (Glavas et al., 2001) I endeavoured to study the effects of overexpression of PDE7A1 in T cell lines. I attempted to introduce the pSM2 construct into Jurkat J6 and Hut-78 T-cell lines. However, these cells proved difficult to transfect using many different transfection methods including calcium phosphate-mediated transfection (Materials and methods 2.3.1.2.) and several commercially available lipid based transfections procedures, which included lipofectAMINE™, Dotap™ and Superfect™ reagents (Materials and methods 2.3.1.3 and manufacturer's instructions). The levels of PDE7A1 protein in these cells utilising these transfection methods never increased above that of the endogenously expressed protein (*Fig. 5.7.*). Therefore, COS-1 and COS-7 cell lines were used to study expression and characterisation of PDE7A1.

5.2.2.5. *Subcellular localisation of PDE7A1 in mammalian cells*

PDE7A1 has previously been shown to be distributed between the particulate and cytosolic fraction of a cell when analysed in brain, kidney, lung and skeletal muscle (Han et al., 1997). To confirm that PDE7A1, when overexpressed in the COS-1 cells, was localising to similar cellular compartments as the endogenous protein in primary cells crude subcellular fractionations of COS-1 cells transfected with the pSM2 construct (Materials and methods 2.3.1.2) were probed with the PDE7 specific antiserum (*Fig. 5.8.*). These results indicate

that the majority of the PDE7A1 protein was localised to the cytosolic fraction of the cell, with a small proportion localising to the low speed P1 and high speed P2 fraction.

5.3. Analysis of PDE7A1 Protein Activity

As the transient overexpression of PDE7A2 proved fruitless, further work was carried out on the characterisation of the PDE7A1 protein. In order to elucidate which effectors control and regulate the activity of PDE7A1 within mammalian cells it is necessary to be able to determine the activity of the PDE7A1 enzyme. There are no commercially available inhibitors of PDE7, so its activity has been determined as the cAMP, specific IBMX-insensitive activity within the cell, as it has been described by others (Michaeli et al., 1993). However, in light of the characterisation of the 'new' PDE families (PDE8, PDE9, PDE10 and PDE11) it has become apparent that PDE8, PDE9 and PDE11 are all insensitive to IBMX inhibition therefore analysis of PDE activity under these conditions does not allow detection of PDE7 activity specifically. Only very recently have inhibitors been synthesised that exhibit PDE7 specificity (Barnes et al., 2001), but unfortunately these were not available for use at this stage of my study. The activities of PDE7A1 were therefore determined on isolated protein.

5.3.1. Modification of PDE assay to optimise the detection of PDE7 activity

Our laboratory has an established assay method for determining the activity of PDE4 from cellular lysates, as described in section 2.3.9. of the Materials and Methods. However, the concentration of cAMP used was closer to the K_m values for PDE4, namely 2 μM (Materials and methods 2.3.9.) than that of PDE7. As both COS-1 and COS-7 cells appear to have high levels of endogenous PDE4 protein (*Fig. 5.9.*), this assay would pick up alterations in PDE4 activities as well as those of PDE7. Therefore, it was necessary to modify the standard PDE assay used in the laboratory to maximise the sensitivity of the assay to detect PDE7 activity. PDE7A has a K_m value of 0.2 μM for cAMP (Michaeli et al., 1993) and PDE4 proteins have K_m values for cAMP in the ranges of 1.5 – 8 μM (Bolger et al., 1997; Huston et al., 1997; McPhee et al., 1995). A range of cAMP concentrations was utilised in the PDE assay to maximise detection of PDE7 and minimise detection of PDE4 activities (*Fig. 5.10.*). The activity of PDE7 was detected to a greater extent than the activity of PDE4 when a concentration of 0.05 μM cAMP was used in the PDE assay. This concentration of cAMP was therefore utilised in further PDE assays.

5.4. Characterisation of PDE7 specific inhibitors

After optimisation of the PDE assay for the specific detection of PDE7, presumed selective inhibitors for PDE7 were made available from Celltech Plc. Therefore full characterisation of the specificities of the PDE7 selective inhibitors for different PDE families was performed.

5.4.1. Production of PDE7 specific inhibitors.

The PDE7 inhibitors CT6351 and CT6236 supplied by Celltech Plc. were different to the compounds that had been previously published by the Celltech group (Barnes et al., 2001). The structures of the CT6251 and CT6236 compounds are shown in Figure 5.11. I would have liked to have discussed the chemistry behind the synthesis of these inhibitor compounds and the IC₅₀ values obtained by Celltech Plc for them, but due to confidentiality agreements, these details have not been provided to our group.

5.4.2. Characterisation of PDE7 inhibitors in mammalian cells

The PDE7 inhibitors CT6351 and CT6236 had previously been characterised by Celltech Plc on insect cell-expressed cAMP specific PDE proteins (personal communication, R-Owens). Studies of recombinant PDE proteins from insect cells only allow characterisation of the protein in isolation. In mammalian cells there are profiles of PDE isoforms expressed, therefore the cross reactivities of the inhibitor compounds can be analysed. The IC₅₀ values obtained by Celltech for the PDE7 inhibitors, CT6251 and CT6236, on the PDE7 and PDE4 isoforms are shown in Table 5.2. I analysed the IC₅₀ values of the CT6351 and CT6236 inhibitor compounds for PDE7A1 and PDE4D3 recombinant protein expressed in mammalian cells. The values obtained for PDE7A1 and PDE4D3 were 0.1 $\mu\text{M} \pm 0.02$ and 1.3 μM respectively for the CT6251 compound (*Fig. 5.12., Panel A & 5.12., Panel B*) and for CT6236 were 0.65 μM and >50 μM for PDE7A1 and PDE4D3 respectively (*Fig. 5.13., Panel A & 5.13., Panel B*). The CT6251 compound was not selective enough to inhibit PDE7 activity in cells specifically, whereas the CT6236 compound had enough specificity for PDE7 to allow determination of the PDE7 activity in a cell in isolation from PDE4.

5.5. Modification of PDE7 within cells

As the increases of PDE7A1 activity has only been associated with its increased expression upon T cell activation an investigation was carried out in an attempt to identify any post-translational modification PDE7A1 might be subjected to. Phosphodiesterase activities are altered by phosphorylation (see section 1.2.5 and those within section 1.3.), by binding to adapter proteins such as AKAPs (see section 1.3.4.2) and by binding phospholipids (see section 1.3.4.5.), so these were all taken into consideration.

5.5.1. Prediction of phosphorylation sites within PDE7A1

Phosphorylation of PDEs has been the most extensively studied post-translational mechanism by which these enzyme activities are modulated (Beavo, 1995; Shibata et al., 1991; Sette and Conti, 1996; Tetsuka et al., 1995; Paglia et al., 2001; Rybalkin et al., 2001; Ahmad et al., 2000; Hoffmann et al., 1999; MacKenzie et al., 2000). Therefore, the potential phosphorylation sites within PDE7 were analysed using the web-based analysis package, PhosphoBase v2.0 to determine whether there are potential target sites for phosphorylation. This is a database of phosphorylation sites provided by the Center for Biological Sequence Analysis (Kreegipuu et al., 1999). It is a service which implements a prediction algorithm based on substrate consensus sequences of some of the more commonly known protein kinases. As mentioned in chapter 4, the results from these predicted protein phosphorylation sequence sites have to be interpreted with caution as many sequences that do not correspond to a consensus motif can be phosphorylated and not all consensus phosphorylation sequences are indeed phosphorylated. The sites on PDE7A1 identified by these services were, therefore, only used as tentative guidelines for the potential phosphorylation sites of the protein. As can be seen in Table 5.3., there are several candidate kinases which have been identified as potentially being able to phosphorylate sites in PDE7A1, these include PKA, PKC, Calmodulin dependent kinase II (CaMKII), Casein kinase I and II (CKI and CKII) and GSK-3.

5.5.2. Stimulation of cells in an attempt to phosphorylate PDE7A1

As described in the introduction and as demonstrated in chapter 4 several modifications of phosphodiesterases including phosphorylation can alter the activity of the enzyme (Ahmad et al., 2000; Rybalkin et al., 2001).

Cells expressing PDE7A1 were stimulated with agonists of kinase signalling cascades and alterations in the activity of PDE7 in cells was detected by isolation of PDE7A1 by immunoprecipitation and the activity of the immunoprecipitate was assayed (*Fig. 5.14.*). Forskolin treatment of cells led to a 1.5 fold stimulation of PDE7A1 activity. Whereas the stimulation of cells with other agonists such as ionomycin, EGF and PMA showed no change in PDE7A1 activity (*Fig. 5.14.*).

5.5.3. Attempted *in vitro* phosphorylation of PDE7A1

Work in our laboratory and others has shown that PDE4 isoforms are phosphorylated by PKA (Hoffmann et al., 1998; Sette and Conti, 1996) and more recently it has been shown that one of the PDE7B splice variants, PDE7B2 can potentially be phosphorylated by PKA (Sasaki et al., 2002). There are 12 predicted sites for PKA phosphorylation of PDE7A1 (*Table 5.3.*) and challenge of cells with forskolin did appear to increase PDE7 activity (see section 5.5.2.2.). This *in vitro* phosphorylation of PDE7A1 with PKA was attempted. Some method development was required to ensure PDE7A1 isolation was optimal for phosphorylation.

5.5.3.1. Efficacy of the PDE7A antibody in the isolation of PDE7A from cell lysates

PDE7A protein needed to be isolated from cell lysate at levels high enough to provide an adequate target for phosphorylation of the protein in an *in vitro* system. Therefore the efficacy of the PDE7A antibody for immunoprecipitation of the PDE7A1 protein from transfected cells was assessed (Materials and methods 2.3.10). As the protein migrated similarly to the IgG heavy chains, it was necessary to use a mouse monoclonal anti-FLAG antibody directed against the epitope tag at the N-terminus of the protein. As can be seen in *Fig. 5.15.*, PDE7A1 was successfully immunoprecipitated from cells over-expressing it.

5.5.3.2. *In vitro* phosphorylation of PDE7A1

PDE7A1 was isolated from transfected COS-1 cells and both endogenous PDE7A1 and PDE7A2 were isolated from Molt-3 cells by immunoprecipitation using the PDE7A antiserum. These proteins were subjected to an *in vitro* kinase assay using the purified PKA catalytic sub-unit (Materials and methods 2.4.5.1). The reaction incorporated ³²P into the PDE7A1 and PDE7A2 protein in the presence and absence of the PKA catalytic subunit (*Fig. 5.16.*). This suggested that a kinase was co-immunoprecipitating with the

PDE7A1 protein and phosphorylating the protein even in the absence of the PKA. Therefore the phosphorylation of PDE7A isoforms could not be attributed conclusively to a PKA dependent mechanism.

5.5.4. In vivo phosphorylation of PDE7A1

Recently, PDE7B isoforms have been reported to be phosphorylated *in vivo* (Sasaki et al., 2002). In order to determine whether PDE7A1 was targeted for phosphorylation *in vivo*, COS-7 cells were transfected with the pSM2 construct and subjected to whole cell labelling (Materials and methods 2.4.4.). Phosphorylation of the transfected protein was observed, well above that observed in mock-transfected cells (*Fig. 5.17.*), suggesting that PDE7A1 can indeed be potentially phosphorylated under physiological conditions.

5.5.5. Attempted identification of kinase which co-immunoprecipitates with PDE7A antibody.

As PDE7A1 was subjected to phosphorylation *in vitro*, in the absence of a recombinant kinase an investigation as to which kinase might be co-immunoprecipitating with PDE7A1 was carried out.

5.5.5.1. Immunoprobe of the PDE7A1 immunoprecipitate

The polyclonal anti-PDE7A antibody used to immunoprecipitate PDE7A1 protein and the monoclonal anti-FLAG antibody used in the isolation of the FLAG-tagged PDE7A1 protein from cells appeared to bind non-specifically to many proteins within the cell lysate (*Fig. 5.18.*). Therefore, to reduce the amount of non-specific proteins bound these antibodies during immunoprecipitation a series of stringent washes of the immunoprecipitates were carried out (*Fig. 5.18.*). It was found that even with high concentrations of salt and SDS in the final washes lots of protein remained bound to the PDE7A1/beads/antibody, suggesting that these proteins might be binding specifically to PDE7A1.

I set out to determine whether any of these proteins, which appeared to bind specifically to PDE7A1, could be a kinase able to phosphorylate PDE7A1 in the *in vitro* phosphorylation reactions. In the first instance, PDE7A1 immunoprecipitates were immunoprobed with a goat pan-PKC antibody. This identified a protein that migrated at around 90 kDa in the

immunoprecipitates (*Fig. 5.19.*), suggesting that PKC isoforms could be binding specifically to PDE7A1.

5.5.5.2. *Coimmunoprecipitation of RACK1 with PDE7A1*

Our laboratory has previously reported a potential effect of the activation of PKC causing an alteration in the activity of the IBMX-insensitive fraction of PDE activity in CHO cells (Spence et al., 1995). We have also shown that the PKC adaptor protein, RACK1 (receptor for activated C-kinase) can interact with the PDE4D5 isoform (Yarwood et al., 1999). Therefore, further studies were carried out to investigate whether PKC was targeting PDE7A1 for phosphorylation and, more specifically, whether RACK-1 interacted with PDE7A1.

PDE7A1 was isolated from cells by immunoprecipitation using the PDE7A antiserum and the proteins were probed with an anti-RACK1 monoclonal antibody. RACK1 appeared to co-immunoprecipitate with the PDE7A1 protein from the pSM2 transfected COS-1 cells (*Fig. 5.20.*), suggesting that an interaction between PDE7A1 and RACK1 occurs within cells. There was a small amount of RACK1 protein detected in the immunoprecipitate from mock transfected cells, suggesting either a small amount of endogenous PDE7A was being immunoprecipitated from the COS1 cells and the RACK1 was co-immunoprecipitating with it or else a small amount of RACK1 binds non-specifically to the PDE7 specific antiserum.

5.5.5.3. *RACK1-GST pulldown of in vitro expressed PDE7A1*

To remove the possibility of endogenous PDE7A protein interfering with the immunoprecipitation reaction and in an attempt to determine whether there was a specific interaction between PDE7A1 and RACK1, an *in vitro* pulldown reaction between PDE7A1 and RACK1 was carried out. PDE7A1 protein was generated by an *in vitro* expression system that incorporated ³⁵S into the protein. This labelled protein was then used in a pulldown experiment with a recombinant RACK1-GST fusion protein (Materials and methods 2.4.7.). Although RACK1-GST did bind to the PDE7A1 protein (*Fig. 5.21.*), the control pull-down reaction in which GST alone was used to bind PDE7A1, also appeared to interact with PDE7A1. This suggests that the PDE7A1 in this reaction did not bind to RACK1 specifically and that the interaction seen to occur between PDE7A1 and RACK1 was due to a non-specific protein interaction. Therefore no conclusions can be drawn about the ability of RACK1 to interact with PDE7A1.

5.6. Conclusions

The PDE7 family of phosphodiesterases is generated from two genes, PDE7A and PDE7B. There are three PDE7A splice variants two of which, PDE7A1 and PDE7A3, have been associated with the activation of T cells (Li et al., 1999; Glavas et al., 2001; Bloom and Beavo, 1996) and the third splice variant, PDE7A2, is relatively uncharacterised (Han et al., 1997; Wang et al., 2000). Screening a variety of cell lines confirmed that PDE7A1 was expressed endogenously in T cells, as PDE7A1 protein was detected in HuT-78, Jurkat J6 and Molt-3 cells, all of which are derived from T cells (Ichimura and Kase, 1993). PDE7A2 is not expressed at high levels in many cell lines, although it has been detected in skeletal muscle, heart, embryo and kidney primary cells (Wang et al., 2000). There were low levels of PDE7A2 protein detected in COS-1, COS-7 and HEK-293 cells, all of which are kidney derived cell lines and there were also low levels of immunoreactive PDE7A2 detected in HuT-78, Jurkat J6 and Molt-3 cell lines.

At the outset of this investigation, relatively little was known about the PDE7 isoforms. I wished to perform characterisation studies of PDE7A in mammalian cells, which required isolation of high levels of PDE7 protein from these cells. Previous attempts by workers at Celltech Plc to over-express both PDE7A1 and PDE7A2 in mammalian cells had failed. Utilising several methods of transfection and recloning the PDE7A2 cDNA into a mammalian expression vector I was also unable to overexpress PDE7A2. However, over-expression of PDE7A1 protein was achieved in all but the immune cell lines as they were difficult to transfect. The distribution of the over-expressed PDE7A1 suggested similar compartmentalisation as had been detected previously in primary cells by the Beavo group (Bloom and Beavo, 1996). Therefore further characterisation of the protein was attempted.

With PDE7 isoforms identified as a relatively novel phosphodiesterase various groups are attempting to assess the functions of PDE7A within cells. It has been shown that PDE7A isoforms contribute to the activation of T cells (Bloom and Beavo, 1996), although the mechanisms of their activation have been linked only to alterations in their expression levels (Glavas et al., 2001). It was hoped, therefore, that this study would elucidate mechanisms of control of enzymatic activity brought about by post-translational modifications of PDE7A isoforms. This might then lead to further understanding of the involvement of PDE7 in the activation of T lymphocytes (Li et al., 1999). The effect of subjecting COS-1 cells overexpressing PDE7A1, to different chemical stimuli on the phosphorylation state and activity of PDE7A1 were studied.

PDE7A is phosphorylated *in vivo* in cells and a kinase that co-immunoprecipitates with PDE7A1 phosphorylates the protein *in vitro*. However, the kinase responsible for this phosphorylation modification, within the limits of this study at the time it was carried out, was not identified. To determine whether phosphorylation of PDE7A1 affected the enzymatic activity of the protein the standard PDE assay was modified to maximise the detection of PDE7 activity. This required reduction of the concentration of cAMP within the assay from levels which were close to the V_{MAX} of the PDE7 isoforms (2 μ M) to amounts nearer to their K_m values (0.05 μ M). Previously, PDE7 activity had been characterised as the cAMP specific IBMX-insensitive PDE activity within a cell (Ichimura and Kase, 1993; Michaeli et al., 1993). As an increasing number of PDE families, such as PDE8, PDE9 and PDE11, are being identified which have reduced sensitivities to the general PDE inhibitor IBMX (Hayashi et al., 1998; Fisher et al., 1998; Fawcett et al., 2000), it is becoming apparent that the initial observations regarding the IBMX-insensitive fraction of T lymphocytes (Ichimura and Kase, 1993) are unlikely to be due to just one family of PDE. Currently there are no commercially available PDE7 inhibitors, however, inhibitor compounds were made available by Celltech Plc. and one of these, CT6236, was determined to be highly selective for PDE7 over other cAMP specific phosphodiesterases.

In forskolin stimulated cells isolated PDE7A1 was found to have slightly elevated activity, when compared to the activity of PDE7A1 from unstimulated cells. This suggests that PKA could potentially be regulating the activity of PDE7A1, as it does members of the PDE4 family (Sette and Conti, 1996; Hoffmann et al., 1998).

PDE7A isoforms aid the full activation of T cells (Glavas et al., 2001) through stimulating the induction of IL-2 expression and increasing cellular proliferation (Li et al., 1999). Incubation of T cells with phorbol esters also stimulates expression of IL-2 (Klein et al., 1983; Sander et al., 1991; Reem et al., 1984), induces DNA synthesis (Di Pauli and Rassat, 1983) and increase T cell proliferation (Gause et al., 1988). It was speculated that a PKC dependent mechanism could induce the alterations in PDE7A1 activity in T cell activation as our laboratory have shown PMA stimulation of CHO cells alters the IBMX insensitive fraction of PDE activity (Spence et al., 1995). Further investigations of PKC dependent effects on PDE7A1 activity were carried out. A kinase of approximately 90 kDa, detected with a pan-PKC antibody, apparently co-immunoprecipitated with PDE7A1, leading to further consideration that PKC could be phosphorylating the protein in the *in vitro* phosphorylation reactions. A direct interaction between the receptor for activated C-kinase, RACK1 and a PDE4D isoform has been reported linking the PDE isoform into a complex with active PKC (Yarwood et al., 1999). However, the investigation as to whether

PDE7A1 could form an interaction with the RACK1/ PKC complex, showed no apparent interaction of PDE7A1 with the scaffolding protein. From these investigations it can only be concluded that the initial interaction apparent between RACK1 and PDE7A1 was due to either non-specific interactions with antibodies or a non-specific binding of PDE7A1 to the GST protein tag, and no direct interaction of the proteins was ever shown. Therefore, although PDE7A1 is subjected to phosphorylation in cells under physiological conditions identification of the candidate kinase was not achieved.

Due to problems related to the availability of selective inhibitors and difficulties experienced in obtaining high levels of expression of the PDE7A2 isoform at the end of my first year I changed to working on the PDE4 enzymes. However, with the current technology available in proteomics and, in particular, in light of the work I have consequently carried out and presented in Chapters 3 and 4 on the analysis of phosphorylation sites, it would be possible to set out to identify the co-immunoprecipitated protein and phosphorylation sites on PDE7A1. These are likely to be important processes to making novel insights into PDE7 activation.

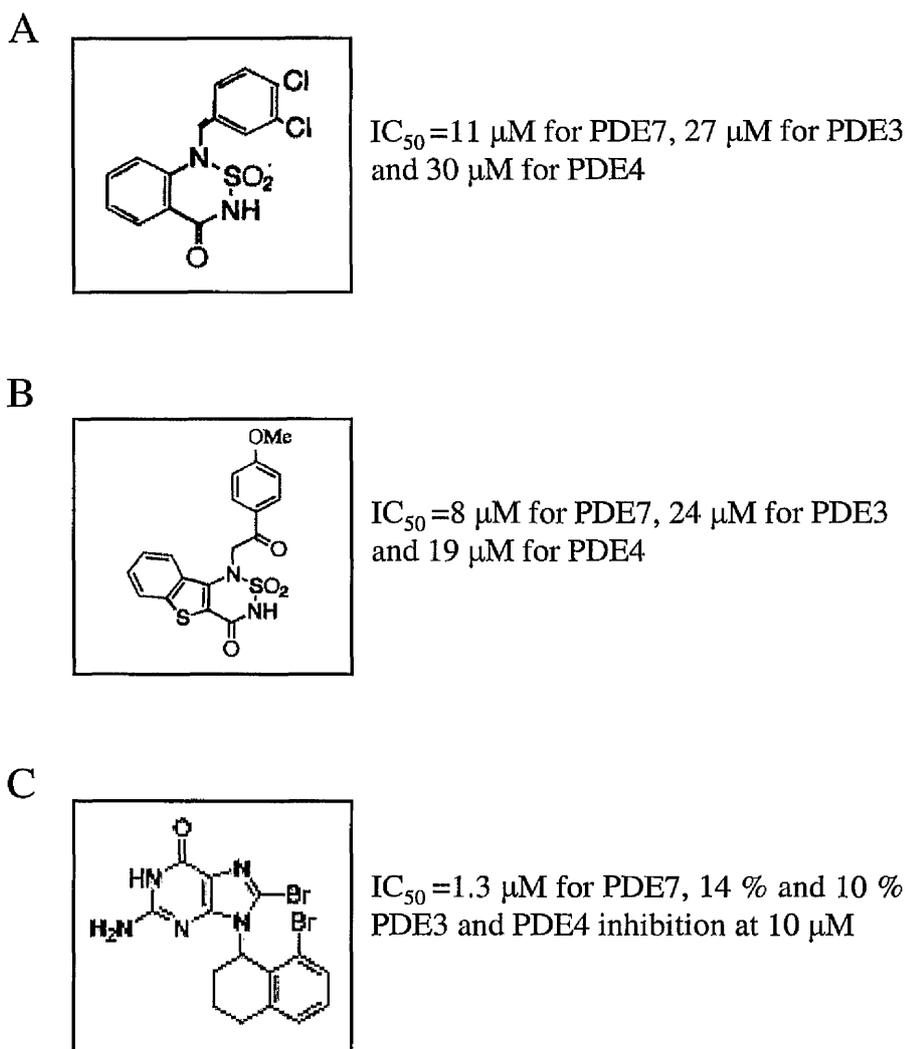


Figure 5.1. Synthetic selective inhibitors of PDE7. Although the benzyl derivatives of 2,1,3-benzo (A) and benzothienol[3,2-a]thiadiazine 2,2-dioxides (B) target PDE7 activity with high potency, they also cross react with the other cAMP specific phosphodiesterase families, PDE4 and PDE3 (Martinez et al., 2000). The IC_{50} values are indicated for PDE7, PDE3 and PDE4. Guanine based analogues were synthesised by the Celltech group producing the final compound with high potency and selectivity for PDE7 (C) (Barnes et al., 2001). The IC_{50} value for PDE7 is indicated, as is the percentage of PDE3 and PDE4 inhibited with 10 μ M of the same compound.

A

```

      10      20      30      40      50      60      70
MEVCYQLPVLPLDRPVPQHVLSRRGAI SFSSSSALFGCPNPRQLSQRRGAI SYDSSDQTALYIRMLGDVRRVRSRAGF PDE7A1
      |||||
      MGITLIWCLALVLIKWITSKRRRGAI SYDSSDQTALYIRMLGDVRRVRSRAGF PDE7A2
      |      |      |      |      |      |
      80      90      100     110     120     130     140     150
ESERRGSHPHYIDFRIFHSQSEIEVSVSARNIRRLLSFQRYLRSSRFFRGTA VSNLNLDDDDYNGQAKCMLEKVGNW PDE7A1
.....
ESERRGSHPHYIDFRIFHSQSEIEVSVSARNIRRLLSFQRYLRSSRFFRGTA VSNLNLDDDDYNGQAKCMLEKVGNW PDE7A2
      |      |      |      |      |      |      |      |
      160     170     180     190     200     210     220     230
NFDIFLFDRLTNGNSLVSLTFHLFSLHGLIEYFHLDMMLKRRFLVMIQEDYHSQNPYHNAVHAADV TQAMHCYLKEP PDE7A1
.....
NFDIFLFDRLTNGNSLVSLTFHLFSLHGLIEYFHLDMMLKRRFLVMIQEDYHSQNPYHNAVHAADV TQAMHCYLKEP PDE7A2
      |      |      |      |      |      |      |      |
      130     140     150     160     170     180     190     200
      240     250     260     270     280     290     300
KLANSVTPWDILLSLIAAATHDLDPGVNQPFLLIKTNHYLATLYKNTSVLENHHWRS AVGLLRESGLF SHLPLESRQ PDE7A1
.....
KLANSVTPWDILLSLIAAATHDLDPGVNQPFLLIKTNHYLATLYKNTSVLENHHWRS AVGLLRESGLF SHLPLESRQ PDE7A2
      |      |      |      |      |      |      |      |
      210     220     230     240     250     260     270     280
      310     320     330     340     350     360     370     380
QMETQIGALILATDISRQNEYLSLFRSHLDRGDLCELETRRHLVLMALKCADICNPCRTWELSKQWSEKVTEEFF PDE7A1
.....
QMETQIGALILATDISRQNEYLSLFRSHLDRGDLCELETRRHLVLMALKCADICNPCRTWELSKQWSEKVTEEFF PDE7A2
      |      |      |      |      |      |      |      |
      290     300     310     320     330     340     350
      390     400     410     420     430     440     450     460
HQGDIEKKYHLGVSPLCDRHTESTIANIQIGFMTYLVEPLFTEWARF SNTRLSQTMLGHVGLNKASWKGLQREQSSSE PDE7A1
.....
HQGDIEKKYHLGVSPLCDRHTESTIANIQIGFMTYLVEPLFTEWARF SNTRLSQTMLGHVGLNKASWKGLQREQSSSE PDE7A2
      |      |      |      |      |      |      |      |
      360     370     380     390     400     410     420     430
      470     480
DTDAAFELNSQLLPQENRLS PDE7A1
.....
DTDAAFELNSQLLPQENRLS PDE7A2
      |      |
      440     450

```

B

```

      390     400     410     420     430     440     450     460
HQGDIEKKYHLGVSPLCDRHTESTIANIQIGFMTYLVEPLFTEWARF SNTRLSQTMLGHVGLNKASWKGLQREQSSSE PDE7A1
.....
HQGDIEKKYHLGVSPLCDRHTESTIANIQIGNYTYLDIAG PDE7A3
      |      |      |      |      |      |      |      |
      390     400     410     420     430     440     450     460
      470     480
DTDAAFELNSQLLPQENRLS PDE7A1

```

Figure 5.2. Alignment of PDE7A1, PDE7A2 and PDE7A3 peptide sequences. *Panel A.* The peptide sequence of PDE7A1 (accession number AAA35644) and PDE7A2 (accession number AAB65772) are aligned with one another using the GeneJockey v2.2II software. *Panel B.* The C-terminal peptide sequences of PDE7A1 and PDE7A3 (accession number AAK57640) are aligned with one another using the GeneJockey v2.2II software. The N-terminal sequences of the proteins up to residue 415 are identical, the extreme C-terminal residues of PDE7A3 differ from those in PDE7A1 and the protein is truncated at residue 244.

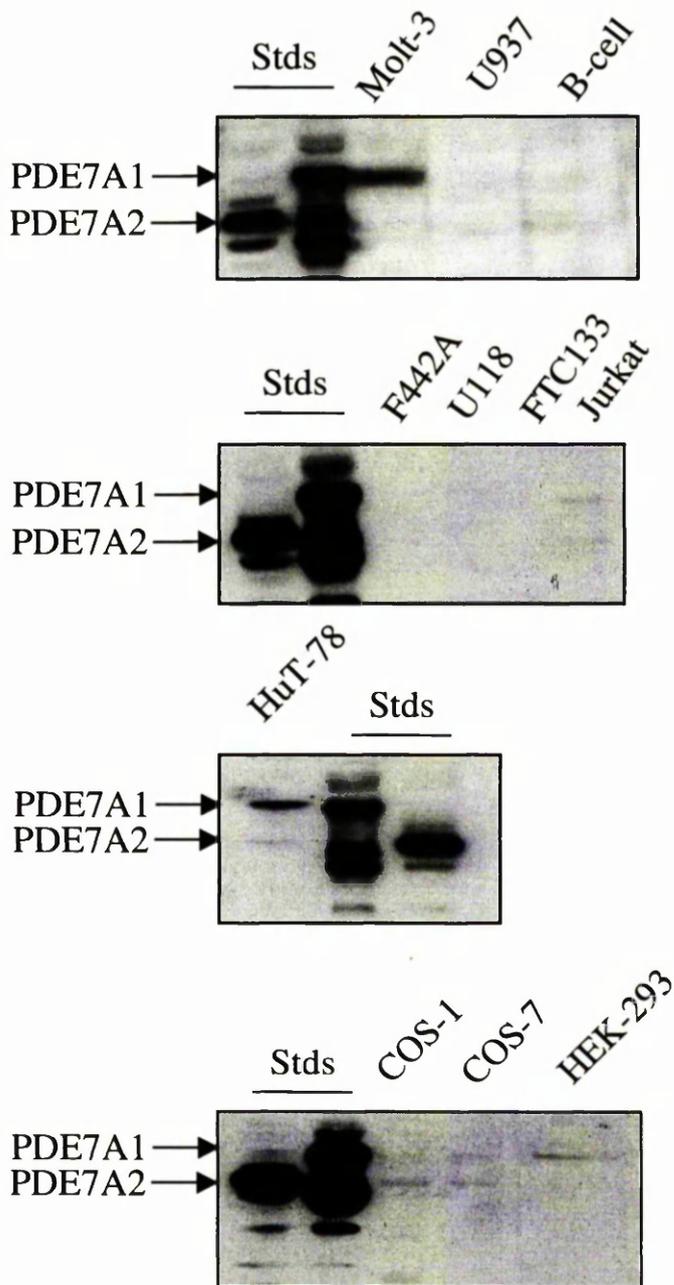


Figure 5.3. Screening cell lines for PDE7A isoforms. 50 μ g cell lysates from multiple cell lines, as indicated, and 5 μ g standard PDE7A1 and PDE7A2 proteins were separated by SDS-PAGE on a 10 % gel. The proteins were transferred to nitrocellulose and immunoprobed with PDE7A specific antiserum. The migration of PDE7A1 (57 kDa) and PDE7A2 (50 kDa) isoforms on each blot are indicated. A summary of the cell lines and their origins are presented in table 5.1..



Figure 5.4. Transfection of COS-1 cells with PDE7A1 and PDE7A2 cDNA constructs. COS-1 cells were transfected with constructs containing PDE7A1 or PDE7A2 cDNA, or were subjected to a mock transfection using the DEAE-Dextran method (*see section 2.1.2.*). The cells were left to express the proteins for 48 h and were then harvested in KHEM. 25 μ g of protein from the cell lysate and 5 μ g of the PDE7A1 and PDE7A2 protein standards (Stds), expressed in insect cells, were separated by SDS-PAGE on a 10 % gel and transferred to nitrocellulose. The proteins were then immunoprobed using PDE7A specific antiserum. The positions of the PDE7A1 (57 kDa) and PDE7A2 (50 kDa) proteins are indicated.

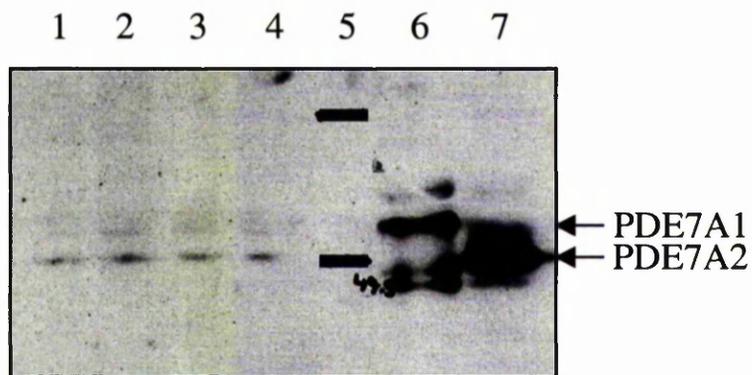


Figure 5.5. Attempted lipid-based transfection of COS-7 cells with pCS1. COS-7 cells were left untransfected (*lane 1*) or transfected with the pCS1 construct using LipofectAMINE™ (*lane 2*), Dotap™ (*lane 3*) or Superfect™ (*lane 4*) reagents as described in section 2.1.3. and according to manufacturer's instructions. The cells were harvested in 3T3 lysis buffer and 100 μg protein from these lysates were separated by SDS-PAGE on a 10 % gel, along with the protein standards (*lane 5*). The upper protein standard migrated with a molecular weight of 86 kDa, and the lower marker migrated at 47.5 kDa. 5 μg of PDE7A1 (57 kDa) and PDE7A2 (50 kDa) recombinant protein were also separated on the same gel (*lanes 6 & 7 respectively*). The proteins were transferred onto nitrocellulose and then immunoprobed using the PDE7A specific antiserum.

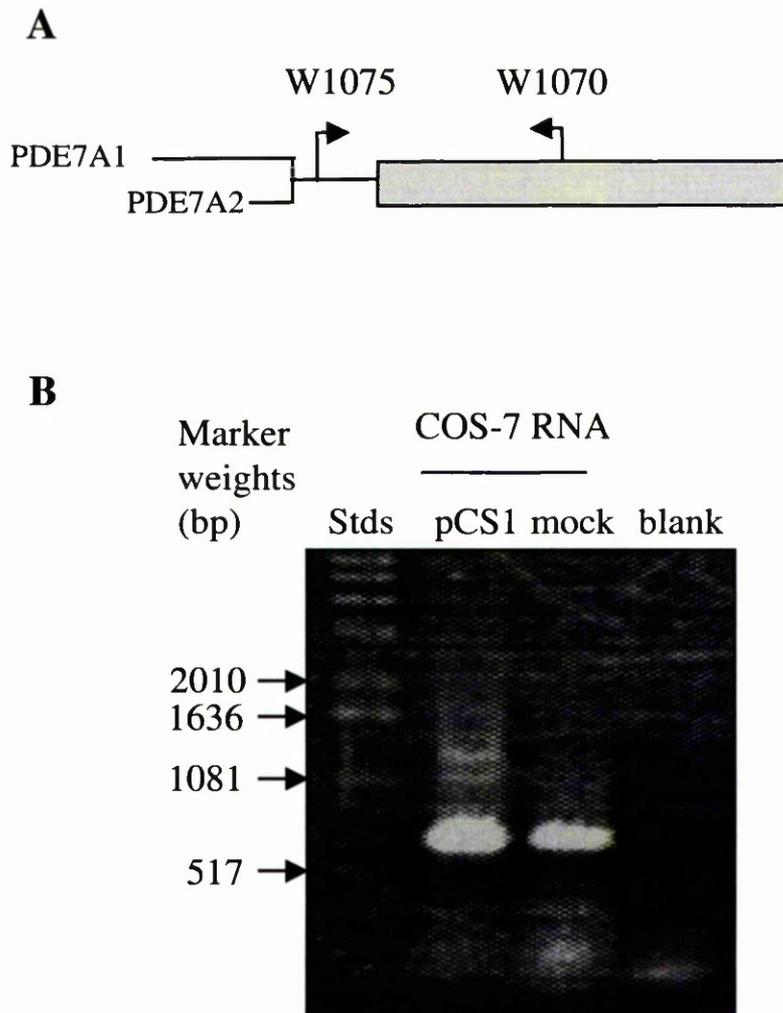


Figure 5.6. RT-PCR analysis of pCS1 transfected COS-7 cells. *Panel A.* The forward primer W1075 and the reverse primer W1070, both indicated above, were used for RT-PCR analysis of mRNA transcripts of PDE7A. The DNA fragment produced by RT-PCR had a predicted weight of 600 base pairs (bp). *Panel B.* Total RNA was extracted from COS-7 cells transfected with the construct containing PDE7A2 (pCS1) or subjected to a mock transfection (mock) (*see section 2.5.10.1.*). First strand cDNA synthesis was carried out (*see section 2.5.10.2.*) and the W1075 and W1070 primers were used to amplify PDE7A cDNA. A reaction containing no cDNA was also carried out (blank). The DNA fragments produced were separated on a 1.5 % agarose gel, alongside a 1 kilobase DNA ladder. The sizes of the markers are indicated in base-pairs.

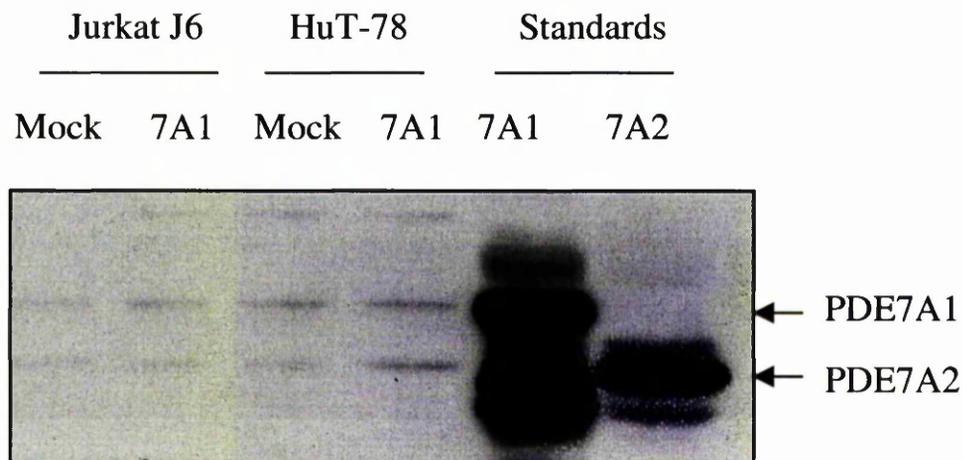


Figure 5.7. Attempted transfection of Jurkat J6 and HuT-78 cells with PDE7A1 containing construct. Jurkat J6 and HuT-78 cells were transfected with the pSM2 construct, which contains the PDE7A1 cDNA (7A1), or subjected to a mock transfection without a vector (Mock), using the lipofectAMINE™ lipid based transfection reagent (*see section 2.1.3.*). The cells were allowed to express the protein for 36 h and then harvested in 3T3 lysis buffer. Then 50 μg of protein from the cell lysate and 5 μg of the PDE7A1 and PDE7A2 recombinant protein standards were separated by SDS-PAGE on a 10 % gel. The proteins were transferred to nitrocellulose and immunoprobed using the PDE7A specific antiserum. The position of PDE7A1 (57 kDa) and PDE7A2 (50 kDa) migration are indicated.

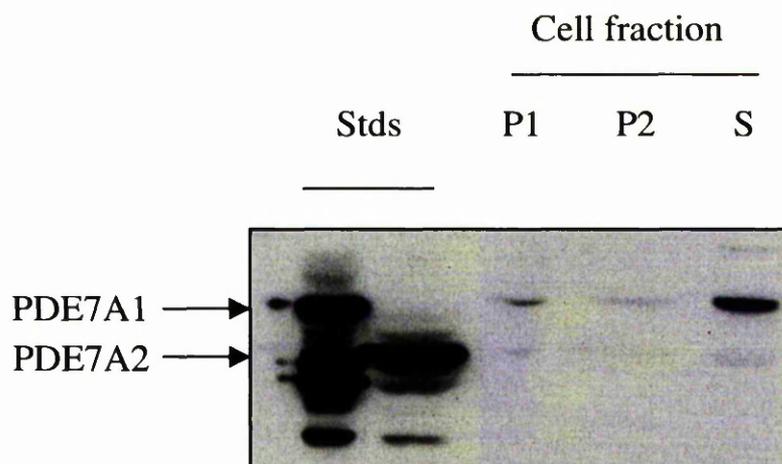


Figure 5.8. Subcellular localisation of PDE7A1 in COS-1 cells. COS-1 cells transfected with the pSM2 construct, which contains the PDE7A1 cDNA, were harvested in KHEM buffer and subjected to crude subcellular fractionation (*see section 2.3.1.2.*). 50 μ g protein from the low speed (2000 g, fixed angle rotor, 15 min) cell pellet (P1), the high speed (75000 g fixed angle rotor, 45 min) cell pellet (P2) and the residual cytosolic fraction (S) together with 5 μ g recombinant protein standards (Stds.) were separated by SDS-PAGE on a 10 % gel. The proteins were transferred to nitrocellulose and immunoprobed with a PDE7A specific antiserum. The positions of PDE7A1 (57 kDa) and PDE7A2 (50 kDa) are indicated.

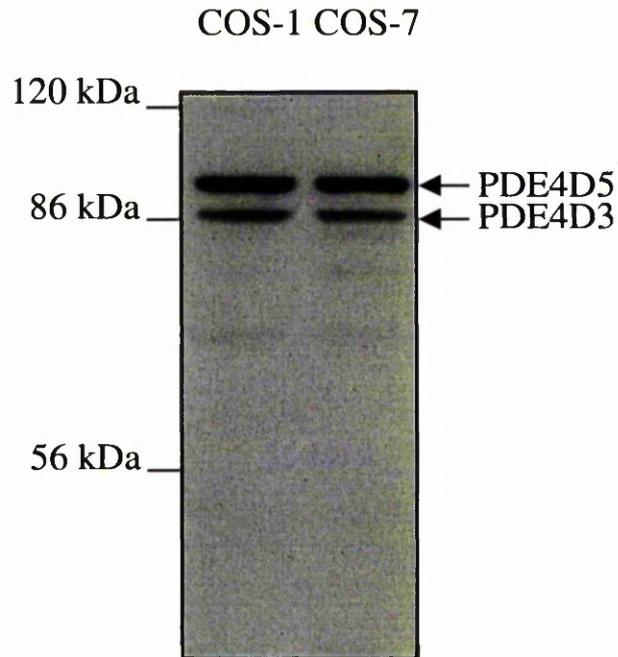


Figure 5.9. Expression of endogenous PDE4 isoforms in COS cell lines. COS-1 and COS-7 cells were harvested in 3T3 lysis buffer and 100 μ g protein from the cell lysates were separated by SDS-PAGE on a 10 % gel. The proteins were transferred to nitrocellulose and were then immunoprobed with a PDE4D specific antibody (*see section 3.2.4.*), the positions of the PDE4D5 (105 kDa) and PDE4D3 (95 kDa) proteins are indicated, as are the molecular weights of the protein standard markers.

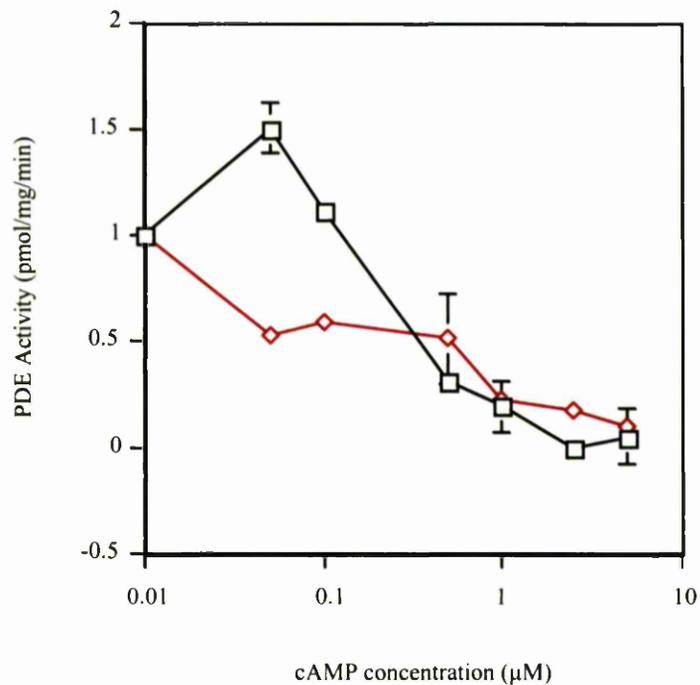
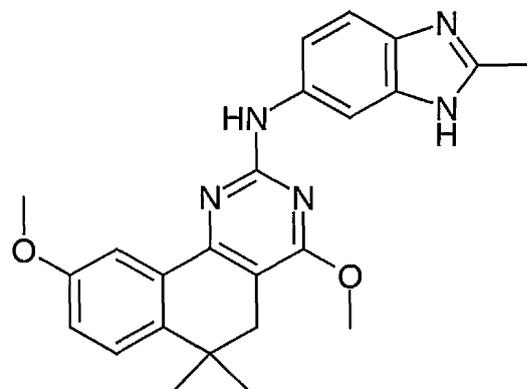
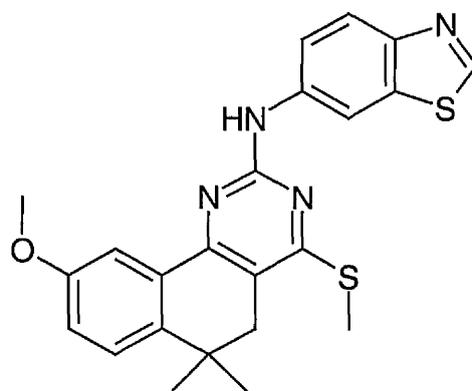


Figure 5.10. Detection of PDE7 and PDE4 enzymatic activity in the presence of varying cAMP concentrations. Constructs containing PDE7A1 (□) or PDE4D3 (◇) cDNA were transfected into COS-1 cells and expressed in the cells for 24 h. The cells were then harvested in KHEM buffer and the lysates used for PDE assay analysis (*see section 2.3.9.*). Increasing concentrations of cAMP were used in the PDE assay, as indicated. The results are expressed as the means \pm SE of 5 independent experiments.



CT6251



CT6236

Figure 5.11. Chemical structures of CT6251 and CT6236. The chemical structures of the PDE7 selective inhibitor compounds CT6251 and CT6236 were supplied by Celltech Plc. However, the basis of these inhibitor compounds cannot be discussed due to confidentiality agreements.

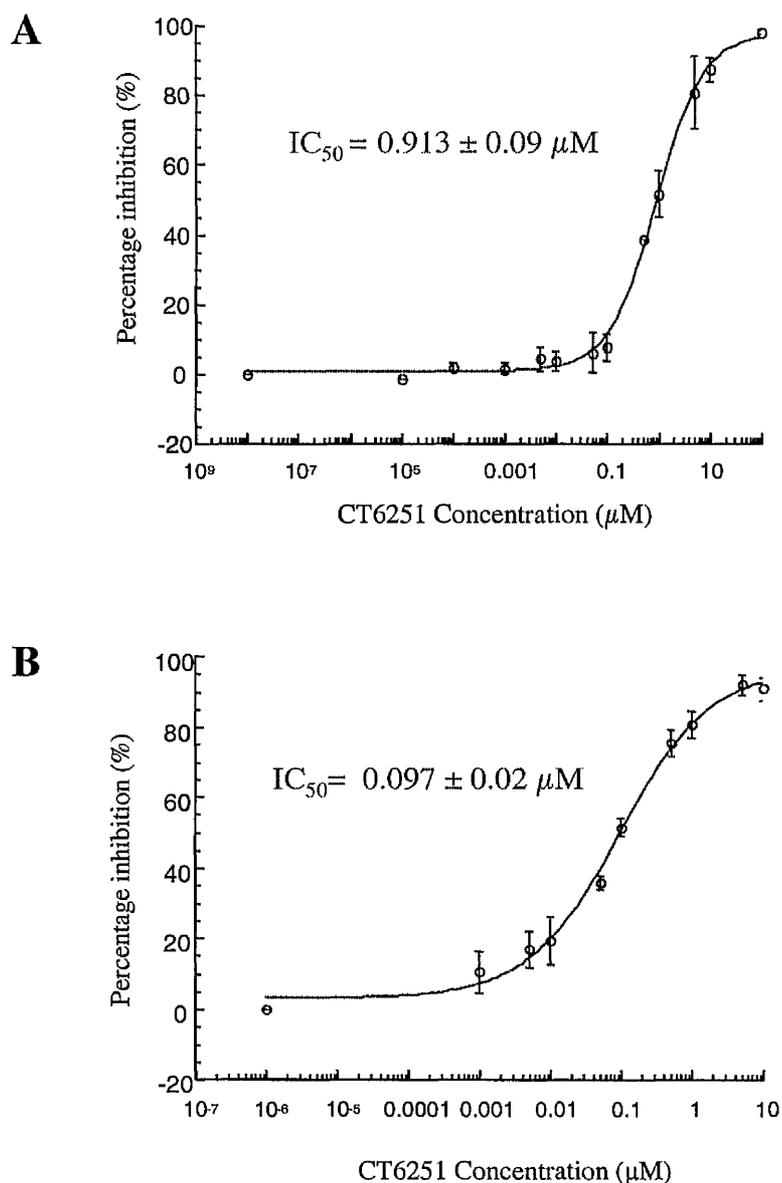


Figure 5.12. IC_{50} values of CT6251 for PDE4 and PDE7. *Panel A*, Cell lysate from COS-1 cells overexpressing PDE4D3, was used in PDE assays (*see section 2.3.9.*) in the presence of increasing concentrations of the inhibitor compound, CT6251, as indicated. The percentage of the total PDE4D3 activity suppressed by CT6251 was calculated and from the equation of the line of best fit for these points the IC_{50} value was calculated. The IC_{50} value (in μM) for CT6251 on PDE4D3 and the SE of this value, from 3 independent experiments is indicated. *Panel B*, Cell lysate from COS-1 cells over-expressing PDE7A1 was used in the same IC_{50} analysis for the CT6251 compound and the IC_{50} values (in μM) were calculated from the line of best fit from 4 independent experiments

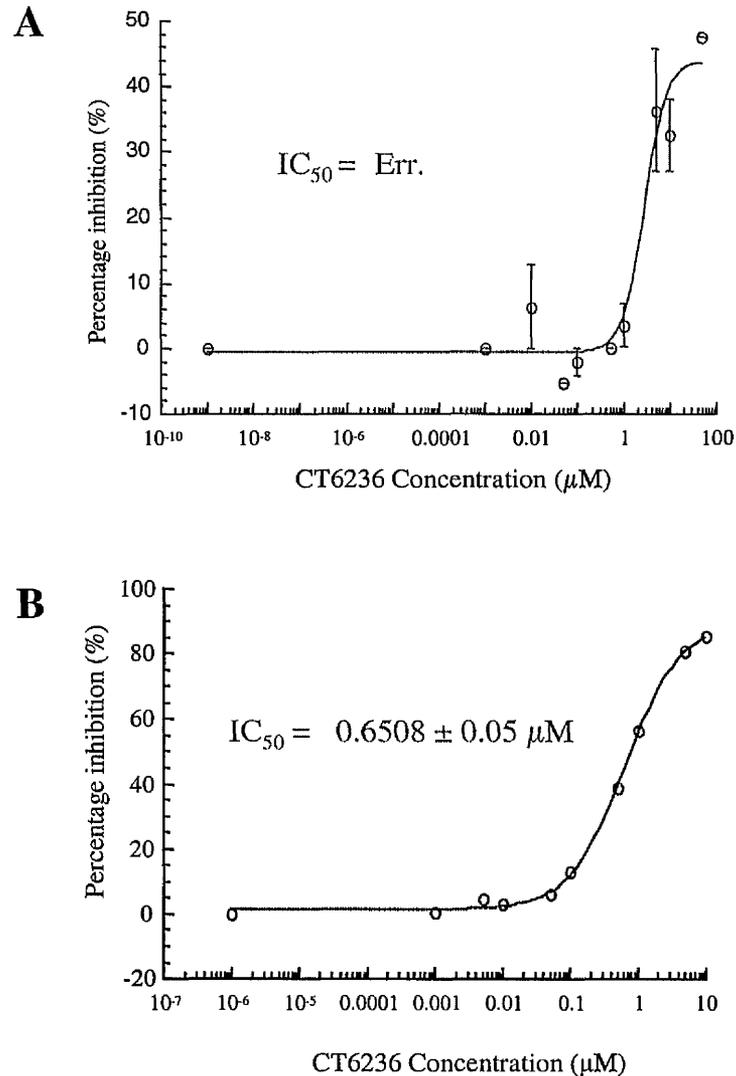


Figure 5.13. IC₅₀ values of CT6236 for PDE4 and PDE7. *Panel A*, Cell lysate from COS-1 cells overexpressing PDE4D3, was used in PDE assays (*see section 2.3.9.*) in the presence of increasing concentrations of the inhibitor compound, CT6236, as indicated. The percentage of the total PDE4D3 activity suppressed by CT6236 was calculated and from the equation of the line of best fit for these points the IC₅₀ value was calculated. The IC₅₀ value (in μM) for CT6236 on PDE4D3 and the SE of this value, from two independent experiments is indicated. *Panel B*, Cell lysate from COS-1 cells overexpressing PDE7A1 was used in the same IC₅₀ analysis for the CT6236 compound and the IC₅₀ values (in μM) were calculated from the line of best fit from two independent experiments

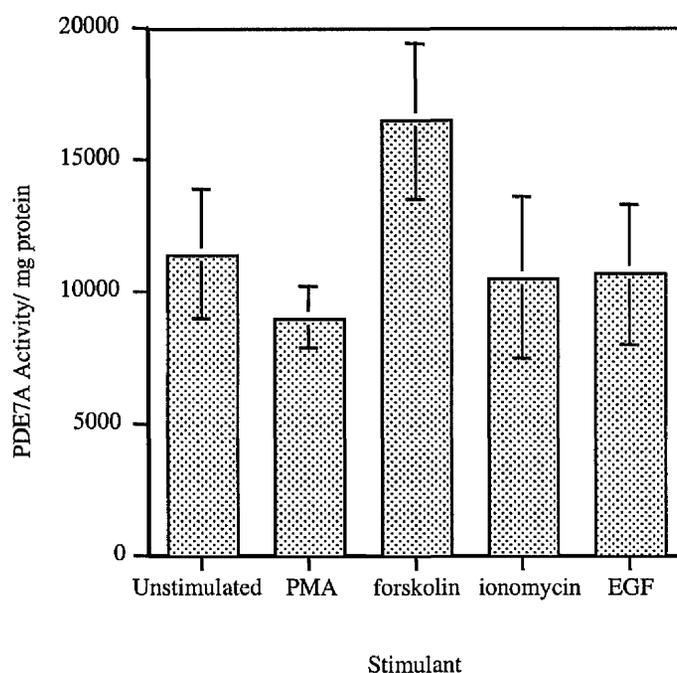


Figure 5.14. Activity changes of PDE7A1 upon stimulation of cells with agonists of kinase signalling cascades. COS-1 cells were transfected with pSM2, the construct containing the cDNA for PDE7A1, and stimulated with agonists of kinase signalling cascades, such as 100 nM PMA, 10 μ M forskolin, 10 μ M ionomycin and 50ng/ml EGF, as indicated, for 20 min. The cells were then harvested in KHEM and PDE7A1 was isolated from 1 mg protein from these cell lysates by immunoprecipitation using PDE7 specific antiserum (*see section 2.3.10.*). The enzymatic activity of the isolated protein was then determined by PDE assay (*see section 2.3.9.*). The results are expressed as the means \pm SE of three independent experiments.

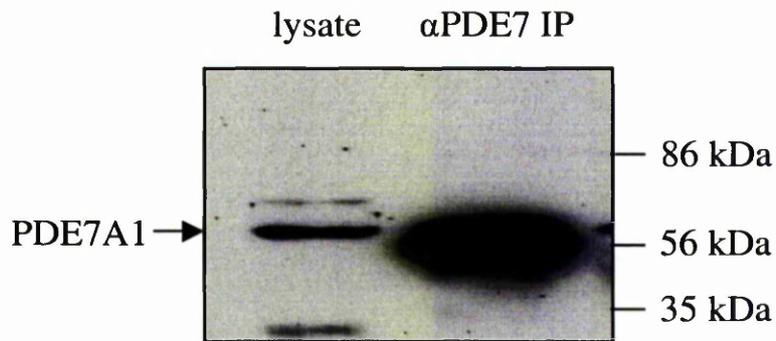


Figure 5.15. Rabbit anti-PDE7A antibody successfully immunoprecipitates PDE7A1 from COS-1 cell lysate. COS-1 cells transfected with the PDE7A1 plasmid, pSM2 (*see section 2.1.2.*), were allowed to express the protein for 24 h and were then harvested in KHEM buffer. The PDE7A1 protein was isolated by immunoprecipitation from 1 mg of the cell lysate, using the PDE7A specific antiserum (α PDE7 IP). The proteins were separated by SDS-PAGE on a 10 % gel alongside 50 μ g protein from pSM2 transfected COS-1 whole cell lysate. The protein were transferred to nitrocellulose and immunoprobed with the monoclonal anti-FLAG antibody, the migration of the PDE7A1 protein (57 kDa) and the molecular weight standards are indicated.

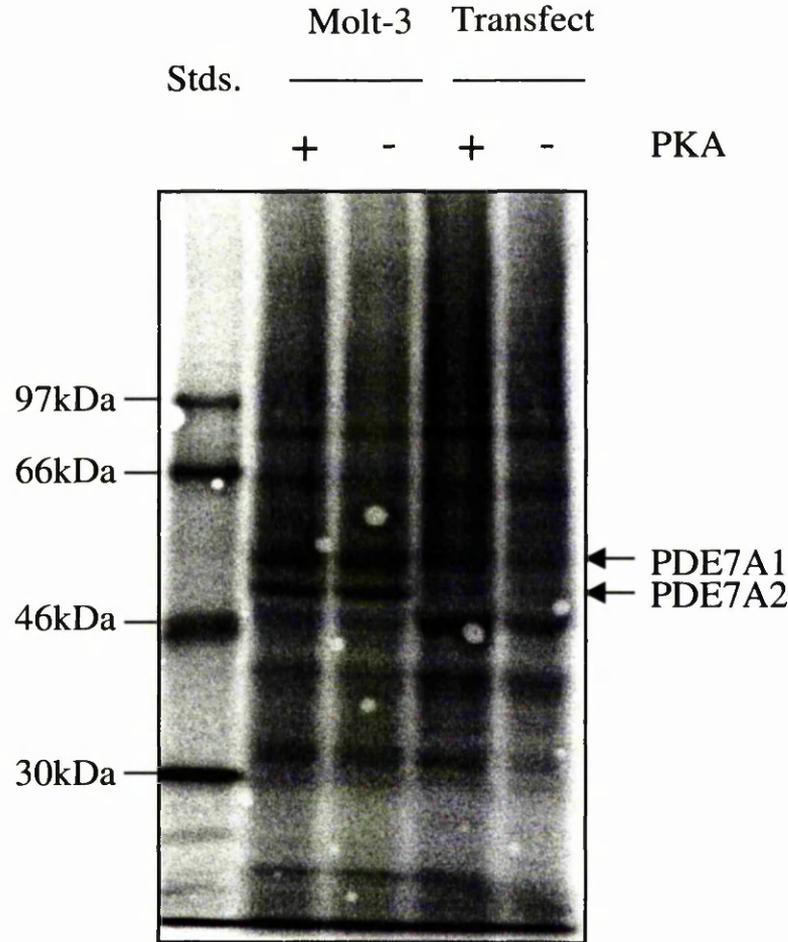


Figure 5.16. *In vitro* phosphorylation of PDE7A1 and PDE7A2. Molt-3 cells and COS-1 cells, transfected with pSM2 (Transfect), were harvested in 3T3 lysis buffer and the PDE7A isoforms were isolated by immunoprecipitation (*see section 2.3.10.*), from 1 mg of protein from these lysates, using PDE7A specific antiserum. The proteins were subjected to an *in vitro* phosphorylation reaction using $\gamma[^{32}\text{P}]\text{ATP}$ in the presence or absence of the purified catalytic sub-unit of PKA (*see section 2.4.5.1.*). The phosphorylated proteins and 10 μl of the radiolabelled protein standards (Stds.) were separated by SDS-PAGE on a 10 % gel and then transferred to nitrocellulose. The nitrocellulose was exposed to a phosphorimage screen for 2 days, and the proteins visualised using the BioRad system (*see section 2.4.5.4.*). The migration of the molecular weight standards and the PDE7A1 (57 kDa) and PDE7A2 (50 kDa) isoforms are indicated.

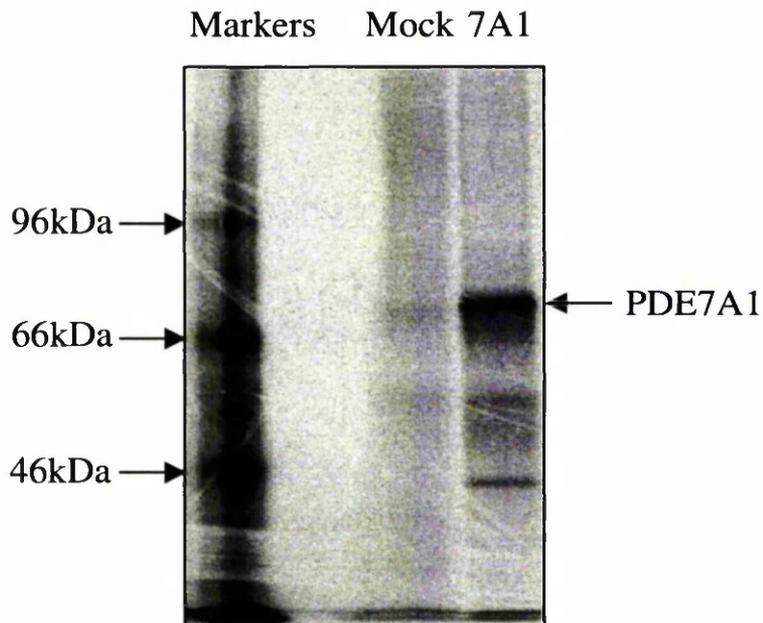


Figure 5.17. Whole cell labelling of COS-7 cells transfected with the pSM2 construct. COS-7 cells were either transfected with the PDE7A1 containing construct, pSM2 (7A1), or subjected to a mock transfection (Mock). The cells were allowed to express the protein for 24 h and were then labelled with 300 $\mu\text{Ci/ml}$ ^{32}P - orthophosphate overnight (*see section 2.4.4.*). The cells were harvested in 3T3 lysis buffer and the PDE7A1 protein was isolated from 1 mg of protein from these cell lysates by immunoprecipitation using the anti-FLAG antibody. The immunoprecipitated proteins were separated by SDS-PAGE on a 10 % gel, transferred to nitrocellulose and exposed to a phosphorimage screen overnight (*see section 2.4.4.*). The migration of the radiolabelled protein markers and PDE7A1 (57 kDa) are indicated.

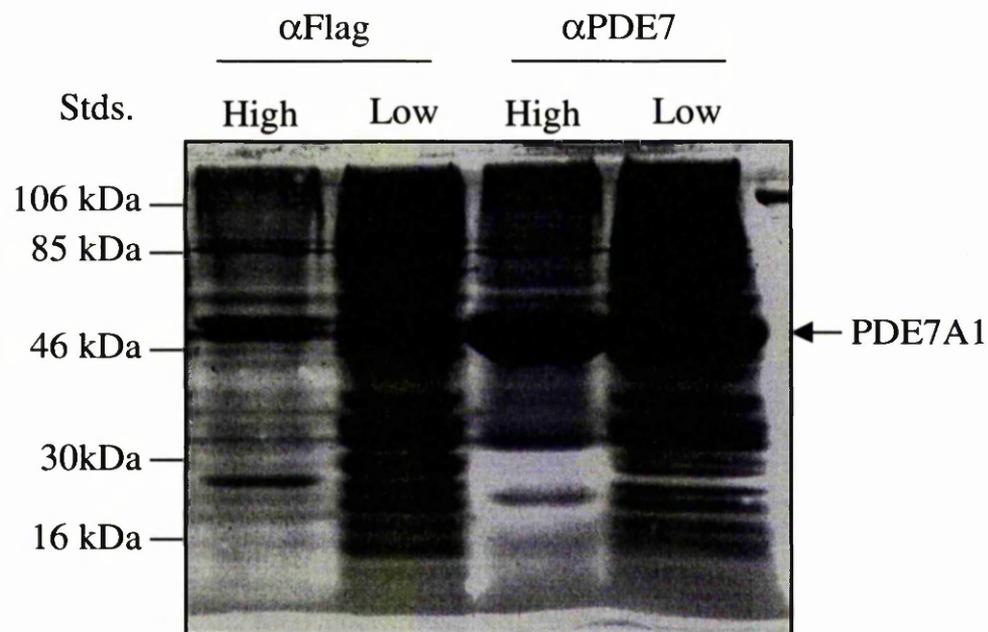


Figure 5.18. High salt and SDS washes remove non specific bound protein from immunoprecipitates of PDE7A1. PDE7A1 protein was isolated from 1 mg COS-1 cell lysate transfected with the pSM2 construct, using the monoclonal anti-FLAG antibody (α FLAG) or PDE7A specific antiserum (α PDE7). The protein bound beads were then subjected either to a stringent wash, which include a 0.5M NaCl, 0.1% SDS and a 0.01% NaPa wash (High) or subjected to the original wash procedure with lysis buffer (Low). The proteins bound to the beads were separated by SDS-PAGE on a 10 % gel and the gel was silver stained (*see section 2.3.7.*). The migration of the molecular weights standards and the PDE7A1 protein (57 kDa) is indicated.

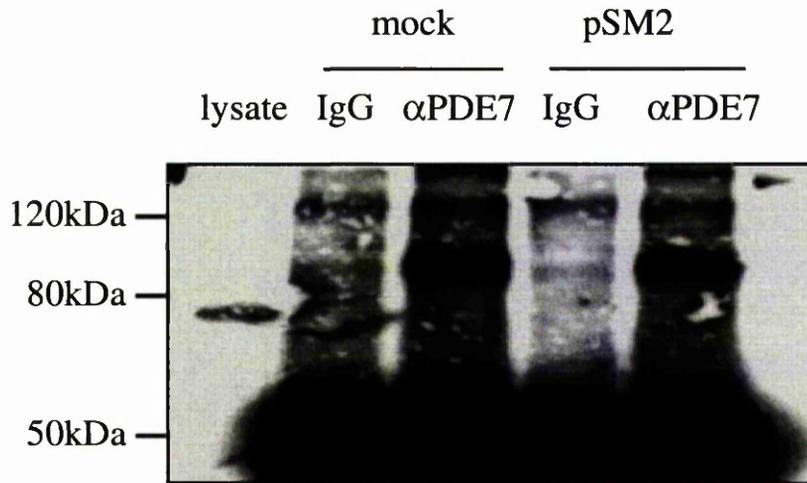


Figure 5.19. A protein which cross reacts with the pan-PKC antibody co-immunoprecipitates with PDE7A1 protein. PDE7A1 protein was isolated by immunoprecipitation using the PDE7 specific antiserum (α PDE7) from 1 mg COS-1 cell lysate transfected with the PDE7A1 containing construct, pSM2, or from mock transfected cells or pre-immune sera from rabbit (IgG). The isolated protein was subjected to SDS-PAGE on a 10 % gel, transferred to nitrocellulose and probed with the goat polyclonal Pan-PKC antibody. 100 μ g Whole cell lysate was used as a standard to determine where the PKC isoforms from COS-1 cells migrated. The migration of the molecular weight standards are also indicated.

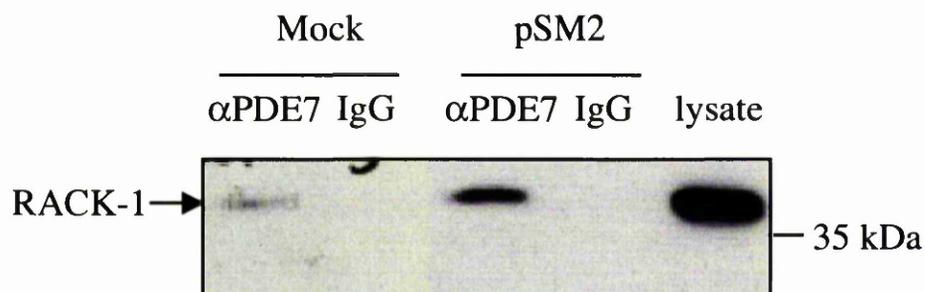


Figure 5.20. RACK-1 appears to coimmunoprecipitate with PDE7A1. PDE7A1 was isolated from 1 mg COS-1 cell lysates which were transfected with the pSM2 construct (pSM2), or mock transfected (Mock) by immunoprecipitation using the PDE7 antiserum (α PDE7) or rabbit preimmune sera (IgG) (as described in section 2.3.10.). The isolated proteins were separated by SDS-PAGE on a 10 % gel, transferred to nitrocellulose and immunoprobed using monoclonal antibody raised against RACK-1. Whole cell lysate from COS-1 cells was used as a control to confirm RACK-1 was expressed in these cells (lysate). The migration of the RACK-1 protein (36 kDa) and the 35 kDa molecular weight marker is indicated.

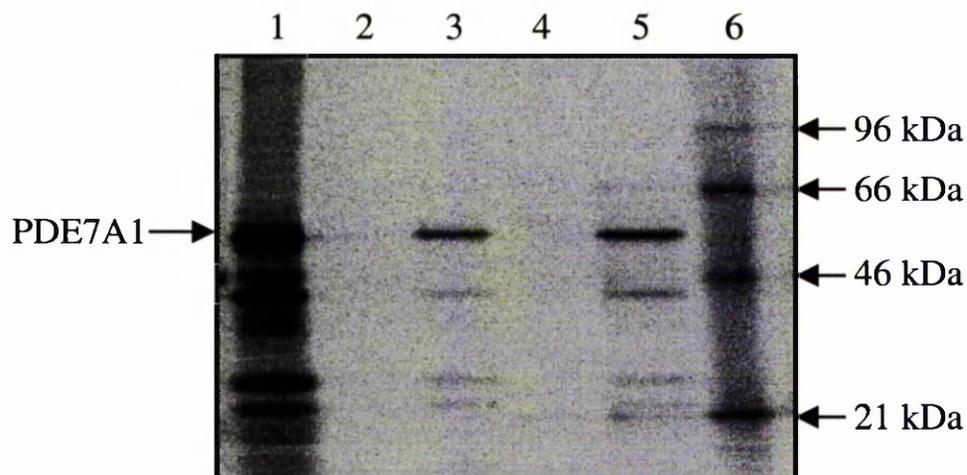


Figure 5.21. GST-RACK-1 pulldown of *in vitro* synthesised PDE7A1 protein. Recombinant RACK-1-GST protein was incubated with *in vitro* synthesised PDE7A1 protein, for 1 h at 4 °C, prior to the addition of GSH-sepharose beads for a further 1 h (*see section 2.4.7.*). The beads were then washed and boiled in laemllis sample buffer before the proteins were subjected to SDS-PAGE on a 10 % gel. The proteins were transferred to nitrocellulose and exposed to a phosphorimage screen for 3 days. Lane 1 contains the *in vitro* synthesised PDE7A1 protein products. Lane 2 contains the GSH-sepharose beads alone. Lane 3 contains the PDE7A1 protein bound to GST/GSH beads alone. Lane 4 contains RACK-1-GST bound to the GSH beads. Lane 5 contains the *in vitro* synthesised PDE7A1 bound to RACK-1-GST/GSH beads. Lane 6 contains the radiolabelled molecular weight markers. The migration of the molecular weight markers and the migration of PDE7A1 (57 kDa) are indicated.

Cell Line	Cell Origin	PDE7A1 Detected	PDE7A2 Detected
B-cell	Human atopic B cells	NO	NO
COS-1 & COS-7 ATCC: CRL 1650 & CRL 1651	African green monkey kidney	NO	Low levels
F442A	Fibroblast, preadipocyte	NO	NO
FTC133 ECACC 94060901	Human thyroid follicular carcinoma	NO	NO
HEK-293 ATCC: CRL 1573	Human embryo kidney	NO	Low levels
HuT-78 ATCC: TIB 161	Human peripheral blood cutaneous lymphoma T-cell	Yes	Low levels
Jurkat J6 ATCC BS TCL 110	human leukaemia T-cell	Low levels	Low levels
Molt-3 ECACC 90021901	Human leukemia, acute lymphoblastic T-cell	Yes	Low levels
U118 ATCC HTB-15	Human glioblastoma astrocytoma	NO	NO
U397 CRL-1593.2	Human monocyte	NO	NO

Table 5.1. Summary of the expression of PDE7A1 and PDE7A2 protein in different cell lines. The indicated cell lines were harvested in 3T3 lysis buffer and 100 µg of protein from the cell lysates were separated by SDS-PAGE on a 10 % gel. The proteins were then transferred onto nitrocellulose and immunoprobed with PDE7A specific antiserum (*see Fig. 5.3.*). The table indicates the name and origin of the cell line analysed and it also specifies whether PDE7A1 and/or PDE7A2 was detected by immunoblotting in each cell line.

Isoform	PDE3	PDE4	PDE7
CT6251 IC ₅₀	>1.3 μM	N/A	0.014 μM
CT6236 IC ₅₀	>1.3 μM	>1.3 μM	0.117 μM

Table 5.2. The IC₅₀ values of the PDE7 selective inhibitors CT6251 and CT6236. The above table details the IC₅₀ values obtained by Celltech Plc for the inhibitor compounds, CT6251 and CT6236. These IC₅₀ values were calculated on recombinant proteins expressed in insect cells. The IC₅₀ value for the CT6251 compound on PDE4 was not given (N/A) due to contractual commitments to which Celltech Plc were bound.

Kinase	Phosphorylated residue	Motif	Kinase	Phosphorylated residue	Motif
CaMII	S-45 S-73 S-84 S-113 S-459	RQLSQRR RVRSRAG RRGSHPY RLLSFQR REQSSSE	GSK3 C-terminal +4 S must be prephosphorylated	S-28 S-52 T-165 S-296 S-331 T-369 S-373	GAISFSSS GAISYDSS DRLTNGNS LRESGLFS EYLSLFRS PCRTWELS WELSKQWS
CKI N-terminal T/S must be phosphorylated	S-32 S-56 S-130 S-169 S-300 S-324 S-335 S-373 T-381 S-437 T-464	SFSSSSAL SYDSSDQT TAVNSNL TNGNSLVS SGLFSHLP TDIRSQN SLFRSHLD TWELSKQW SEKVTEEF TRLSQTM SSEDTDAA	CKII	S-95 T-238 S-279 S-335 S-459	IFHSQSE NSVTPWD KNTSVLE LFRSHLD REQSSSE
			Cdk1	No identified Residues	
			PKG	S-84	RRGSHPY
MLCK	No identified residues		P70s6k	No identified residues	
PKA	S-45 S-73 S-84 S-113 S-121 T-127 T-165 S-296 T-406 S-432 S-437 S-459	RQLSQRR RVRSRAG RRGSHPY RLLSFQR RSSRFF RGTAVS RLTNGN RESGLF RHTESI RFSNTR RLSQTM REQSSSE	PKC	S-22 S-45 S-79 S-104 S-120 S-377 S-450	HVLSRRG RQLSQRR GFESERR VSVSARN YLRSSRF KQWSEKV NKASWKG

Table 5.3. Predicted phosphorylation sites of PDE7A1 using PhosphoBase. The sequence of PDE7A1 was inserted into the prediction submission form on the PhosphoBase programme and the predicted phosphorylation sites within the protein were given.

Chapter 6

General discussion and future directions

Phosphodiesterases make up a large family of key enzymes involved in the regulation of intracellular concentration of cAMP, which is central to many physiological processes including cell differentiation, survival, inflammatory processes and lipolysis.

It has been known for many years that cAMP and its downstream signal transducing kinase, PKA are involved in influencing cell proliferation. Increases in PKA activity, in particular, have been associated with the arrest of cells in the cell cycle prior to the G1/S transition. Fluctuations of PKA activity have also been associated with processes involved in the onset, progression through and exit from mitosis. PDEs antagonise PKA activity since they degrade cAMP. Thus, an intimate relationship exists between PDE isoforms and PKA, which involves multiple positive and negative feedback loops and common binding proteins.

As with many systems, most studies of PDE isoforms in mammalian somatic cells have focussed on asynchronous populations of cells, with little attention having been paid to the possibility that PDEs might be regulated during the cell cycle. Given that cAMP and PKA have established important roles in progression through the cell cycle, I set out to determine whether specific PDEs could play a regulatory role. This notion initiated the majority of the work of this thesis, namely that described in chapter 3 and chapter 4, in which a study of phosphodiesterase activity through the cell cycle was undertaken.

The initial conclusion drawn from the work presented here indicates that the activity of certain cAMP-specific PDEs do indeed fluctuate through the cell cycle in Rat-1 fibroblasts. Particularly interesting was the finding that there was an increase in total PDE activity during nocodazole-induced mitosis. This was shown to be essentially attributable to alterations in PDE4 isoform reactivity, in studies that were initially based on rolipram sensitivity. More detailed analysis of the enzymatic activities of PDE4 family members revealed that it was alterations in the PDE4D3 isoform that underpinned such changes in PDE4 activity. This increase in PDE4D3 activity was especially interesting because it coincided with the lowest PKA activity observed throughout the cell cycle, suggesting that the increased PDE4D3 activity might be responsible for this decreased PKA activity. In support of this hypothesis, inhibition of PDE4 enzymes, using rolipram, was shown to drastically increase PKA activity during mitosis.

Further work identified that this activation of PDE4D3 was brought about by the phosphorylation of the protein. Concomitant with this elevation of activity, phosphorylation of PDE4D3 induced a change in its electrophoretic mobility when

analysed by SDS-PAGE. Initial observations suggested that these two events were manifestations of the same or related phosphorylation events for several reasons. Firstly, they were both sensitive to the general kinase inhibitor, staurosporine, but insensitive to a whole range of other more specific kinase inhibitors, including ones to PKA and the ERK pathway, the only two kinases previously known to phosphorylate PDE4D3. Secondly, both the band-shifts and the increased activity can be prolonged over a comparable time-course by high concentrations of okadaic acid, following a release from a mitotic block. Thirdly, they could both be reversed using calf intestinal alkaline phosphatase.

However, the *in vivo* phosphorylation of PDE4D3 provided the first indication that the activatory phosphorylation of PDE4D3 occurs independently of the phosphorylation of PDE4D3 that altered its electrophoretic mobility. From metabolic labelling of cells with ^{32}P it appears that, although PDE4D3 was phosphorylated in mitosis the incorporation of ^{32}P into the *stage 1* and *stage 2* species of PDE4D3 occurred at such low levels that it was not detectable by phosphorimage analysis. As the activation of PDE4D3 was also brought about by a phosphorylation event, this suggests that the phosphorylation of 'native' PDE4D3 observed by *in vivo* phosphorylation was related to the activatory phosphorylation.

Forskolin stimulation of mitotic cells led to further indication that the mitotic activation and 'band-shifts' of PDE4D3 were not manifestations of the same phosphorylation event. When mitotic cells were stimulated with forskolin the increase in the amount of immunoreactive PDE4D3 migrating with lower electrophoretic mobility was a much higher proportion than the small increase in the activity of PDE4D3 observed. In contrast to this, the challenge of asynchronous cells with forskolin caused an increase in the activity of PDE4D3 that was proportional to the amount of PDE4D3 with altered electrophoretic mobility.

The HPLC analysis of the residues of PDE4D3 phosphorylated by kinases in mitotic lysates also suggested that incorporation of ^{32}P occurs to different extents, depending on the serine residue. This analysis also provided the initial evidence as to the identity of the residues phosphorylated in mitosis that were responsible for the increase the activity of PDE4D3 and those that alter the migration of PDE4D3 by SDS-PAGE.

HPLC analysis of PDE4D3 peptides phosphorylated by mitotic lysates identified four serine residues, Ser⁶¹, Ser⁷⁵, Ser²³⁹ and Ser⁵⁷⁹ as incorporating ^{32}P . Three of these sites (Ser⁶¹, Ser⁷⁵ and Ser²³⁹) are residues of PDE4D3 that have never previously been shown to

be phosphorylated. With the HPLC analysis there was, presumably similar amounts of peptides but the levels of ^{32}P incorporated into each site were variable. It was shown that Ser⁶¹ and Ser⁷⁵ both incorporated lower levels of ^{32}P than the Ser²³⁹ and Ser⁵⁷⁹ residues. This indicated that the kinases that target Ser⁶¹ and Ser⁷⁵ were less active than the kinases that target Ser²³⁹ and Ser⁵⁷⁹. Alternatively, the lower levels of ^{32}P incorporation could be due to the fact that Ser⁶¹ and Ser⁷⁵ do not lie within ideal consensus motifs for the candidate kinases or that dephosphorylation of these sites was very active.

It is likely that high levels of phosphorylation were responsible for conferring the activated state of PDE4D3 as, in mitotic cells PDE4D3 activity was only slightly increased when treated with forskolin. This suggests that the auto-inhibition of PDE4D3, exhibited in the unmodified protein was almost entirely ablated when PDE4D3 was subjected to mitotic phosphorylation. This leads to the suggestion that it could be the Ser²³⁹ and/or Ser⁵⁷⁹, which via HPLC analysis were shown to incorporate the highest levels of ^{32}P , that are phosphorylated in order to activate PDE4D3. Phosphorylation of Ser⁵⁷⁹ has previously been shown by our group to be the site that is phosphorylated by ERK (Hoffmann et al., 1999), leading to a decrease in PDE4D3 activity. The occurrence of this inhibitory phosphorylation is due to an effect mediated by the UCR1 and UCR2 domains of PDE4D3. Thus it is unlikely that phosphorylation of Ser⁵⁷⁹ is responsible for PDE4D3 activation. Therefore, I propose that the phosphorylation of Ser²³⁹, located within the N-terminus of the catalytic domain by a kinase activated in mitosis, confers activation upon PDE4D3. Increasingly this region of the catalytic domain has been suggested to interact with the auto-inhibitory UCR2. Thus if this 'model' was valid, it utilises the same route to PDE4D3 activation as PKA. However, with PKA it is phosphorylation of UCR1 that appears to disrupt the UCR2/catalytic inhibitory coupling. Thus the proposal for mitotic phosphorylation of Ser²³⁹ would achieve the same ends, but by disrupting the target for UCR2 interaction in the catalytic unit. Hence, this model also explains why the mitotic and PKA phosphorylations do not give additive effects.

Mitotic phosphorylation led to the change in electrophoretic mobility of PDE4D3. However, only a small amount of PDE4D3 was modified. This was evident because only 35 % of the immunoreactive PDE4D3 migrated with the *stage 1* and *stage 2* forms of the protein, which both have reduced electrophoretic mobilities when analysed by SDS-PAGE, compared to 'native' PDE4D3. These shifted forms of PDE4D3 were not detected by *in vivo* phosphorylation of the protein, although both *stage 1* and *stage 2* forms of PDE4D3 are present in the mitotic cell. It is proposed that the phosphorylations that induce changes in the electrophoretic mobility of PDE4D3 are brought about by kinases for which

PDE4D3 is a poor substrate for kinases that have low activity in mitotic lysate. Relating this to the identification, by HPLC, of the serine residues phosphorylated to a lesser extent than Ser²³⁹ and Ser⁵⁷⁹ by the mitotic kinases would suggest that Ser⁶¹ and Ser⁷⁵ are the residues in PDE4D3 that are phosphorylated and bring about the shift in the electrophoretic mobility of PDE4D3. The proposed model for the phosphorylation of PDE4D3 during mitosis is presented in Figure 6.1.

Important work that needs attention in the short term clearly includes the in-depth characterisation of each of the three novel phosphorylation sites, Ser⁶¹, Ser⁷⁵ and Ser²³⁹ and further studies of the phosphorylation of Ser⁵⁷⁹. This could be carried out through the generation of phospho-specific antibodies that detect phosphorylation of these sites in isolation of each other. This would enable analysis of the kinetics of phosphorylation of these sites as cells accumulate and leave mitosis. These antibodies could also be used to monitor the phosphorylation of the serine residues in *in vitro* kinase reactions. Where they could aid the identification of the kinase which target these sites. The phospho-specific antibodies would also confirm the identification of the residues phosphorylated in the *stage 1* and *stage 2* forms of PDE4D3.

Mutational analysis of the serine residues at positions 61, 75 and 239 of the PDE4D3 amino acid sequence would enable confirmation of the identity of the residues required to be phosphorylated in order to activate PDE4D3. It would also provide distinction between these residues and those involved in the alteration in the electrophoretic mobility of PDE4D3. The serine residues need to be mutated both singly and in combination with each other and also with the previously identified PKA and ERK phosphorylation sites. These should ideally be produced as both alanine substitutions that would be predicted to mimic the unphosphorylated states, and as aspartate substitutions that may behave more as phosphomimetic mutants. As well as allowing the effects of each residue on PDE4D3 activity and its electrophoretic mobility need to be assessed and will also enable functional analyses of PDE4D3 activity to be performed. In this respect, it would be interesting to see what effect these mutations have on various parameters such as the distribution of cells in the cell cycle, the rate of exit of the cells from mitosis and the activity of PKA at different stages of the cell cycle. It has already been shown within this study that rolipram-mediated inhibition of PDE4 leads to an increase in PKA activity in mitosis and an increase in the rate at which cells leave mitosis. However, due to the lack of PDE4 isoform-specific inhibitors these observations can not be associated definitively with the mitotic increase in PDE4D3 activity.

Also of crucial importance, although possibly more challenging, is the elucidation of the mitotic kinases phosphorylating these novel sites on PDE4D3. This could then shed much more light on the physiological role of these novel phosphorylation events and how PDE4D3 activity might be controlled through the cell cycle. The identification of the residues in PDE4D3 phosphorylated during mitosis has enabled us to analyse the consensus sequences in which they lie enabling us to predict the candidate kinases. However, using this as a starting point the key experiments would now involve the utilisation of a panel of recombinant protein kinases for *in vitro* phosphorylation of PDE4D3, to determine if the Ser⁶¹, Ser⁷⁵ or Ser³⁷⁹ were the substrate residues. Upon identification of the candidate kinases further investigations would then need to be carried out in order to ascertain whether the kinases target PDE4D3 *in vivo* during the cell cycle.

Once the candidate kinases have been identified immuno-depletion of the mitotic lysates, using antibodies specific to the kinases, would provide lysate that could be used for *in vitro* phosphorylation of PDE4D3. With the lack of the kinase in the lysate it would enable determination as to whether the kinase altered the activity or the electrophoretic mobility of PDE4D3.

Another important investigation that needs to be carried out involves the study of physiological processes that take place during mitosis and the effect that the inhibition of PDE4 has on these. One such mitotic process with which PKA has been associated is the control of the formation of the nuclear envelope. As I have already shown that the inhibition of PDE4 appears to increase the rate at which cells leave mitosis, it would be interesting to investigate why this occurs. Following work carried out by Steens et al. (Steen et al., 2000) and Lamb et al. (Lamb et al., 1991), the changes in nuclear lamin assembly should be investigated to assess whether it is the target for a PDE4-mediated control mechanism during mitosis. The kinetics of the rates of nuclear envelope reformation upon exit from mitosis and analysis of the cytoskeletal dynamics should also be visualised by confocal microscopy. A currently proposed model of how the activity of PDE4D3 during mitosis affects the transition of cells from G2/M and into the next G1 are shown in Figure 6.2.

The body of work presented here is an important contribution to the field of cell cycle progression and the control of mitosis. It is the first demonstration of a mechanism by which PKA activity might be regulated as cells pass the G2 checkpoint and proceed into mitosis. On a more general level, the work contributes to the ever expanding larger picture of how a typical cell functions and divides: the picture that will ultimately allow us to

devise specific therapies for the treatment of human health conditions such as cancer, to name but one obvious example.

The work carried out on the characterisation of PDE7A1 as presented in this thesis in chapter 5 is too preliminary as yet to formulate any conclusions from. What can be gleaned from the study is that PDE7A1 appears to be phosphorylated by an as yet unidentified kinase. This observation is novel in the characterisation of PDE7A1 and with the technologies used in the characterisation of PDE4D3 phosphorylation during mitosis it would now be feasible to carry out a similar study in order to identify the residues of PDE7A1 which exhibit the potential to be phosphorylated.

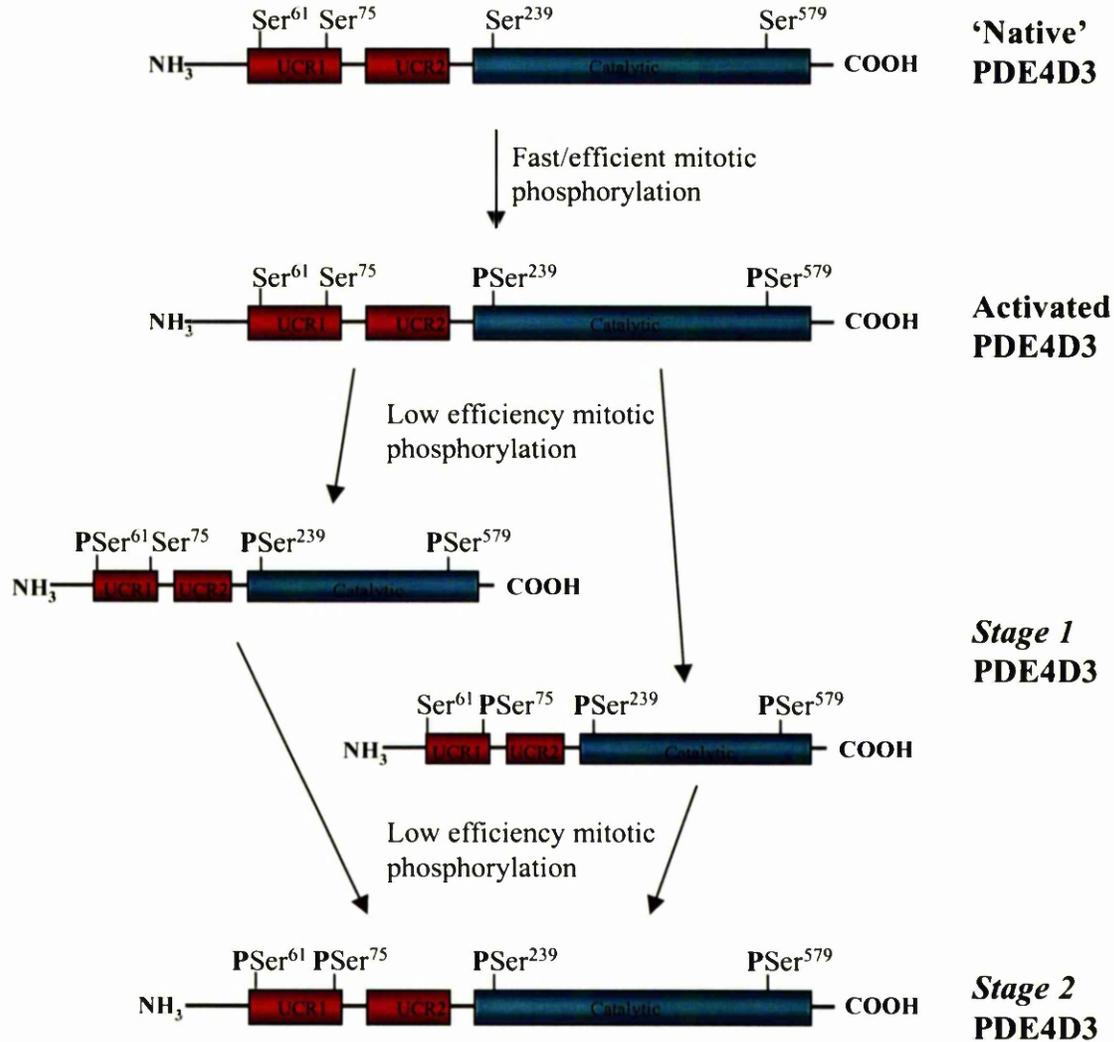


Figure 6.1. Proposed mechanism of PDE4D3 phosphorylation in mitosis. It is proposed that 'native' PDE4D3 is phosphorylated by kinases activated in mitosis with high efficiency on residues Ser²³⁹ and Ser⁵⁷⁹. This leads to an increase in the enzymatic activity of PDE4D3. PDE4D3 is then subjected to phosphorylation by a less efficient kinase, in mitosis, at either residue Ser⁶¹ or Ser⁷⁵. This causes the protein to migrate with a slightly reduced electrophoretic mobility when analysed by SDS-PAGE, which has been termed the *stage 1* form of PDE4D3. Another inefficient kinase also targets PDE4D3 during mitosis, phosphorylating the protein at either Ser⁶¹ or Ser⁷⁵, which changes the electrophoretic mobility of PDE4D3 further still. This final phosphorylation causes PDE4D3 to migrate with a mobility that has been termed *stage 2*.

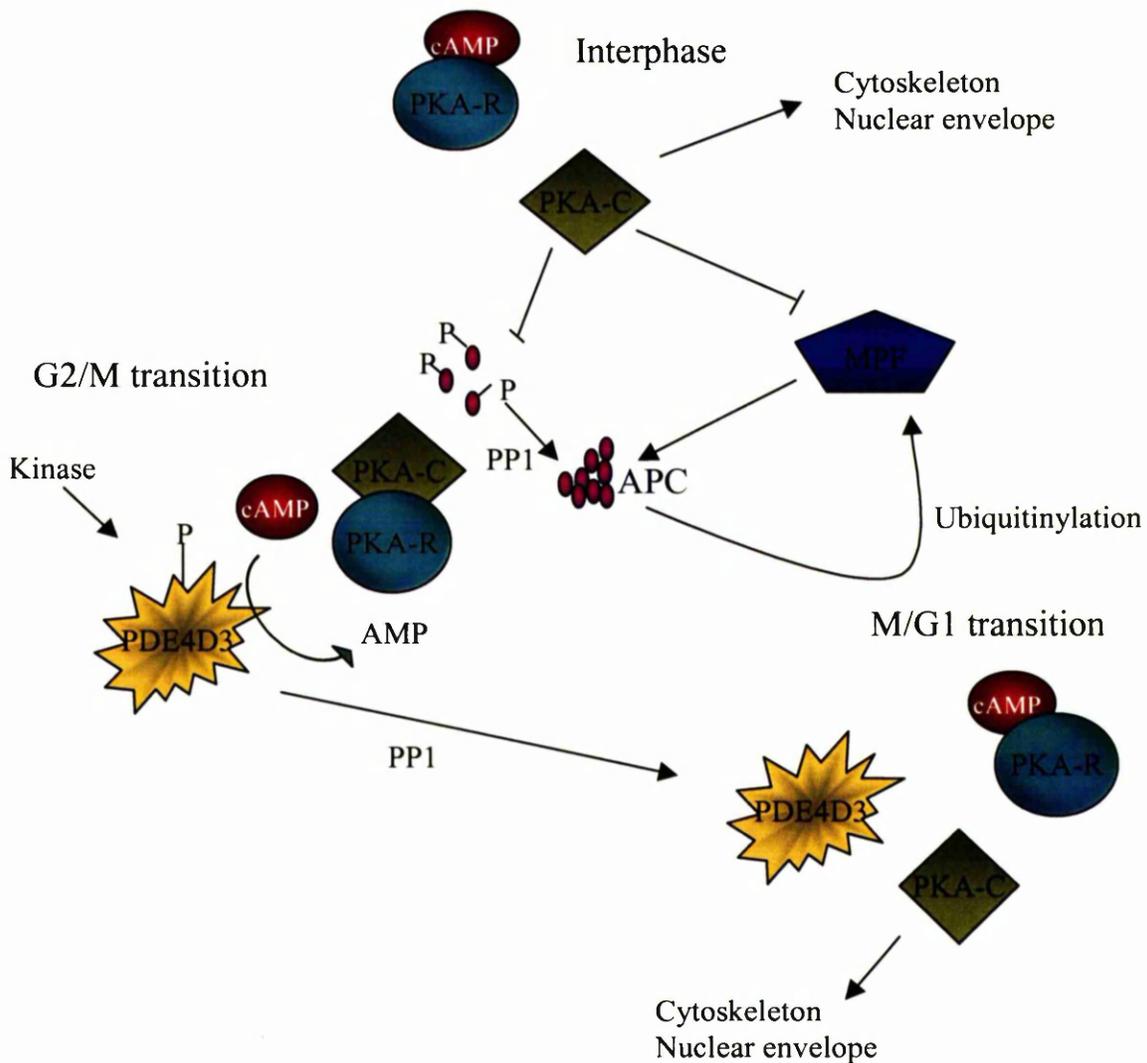


Figure 6.2. Involvement of PDE4D3 in the progression of cells through mitosis. The mechanisms by which the activation of PDE4D3 controls the progression of cells through mitosis is governed by the influence it has on the levels of cAMP in the cell. In interphase cells PDE4D3 activity is low, consequently the levels of cAMP are high and PKA is active. PKA activity maintains the cell nucleus and an ordered cytoskeleton. PKA phosphorylates the regulatory subunits of the anaphase promoting complex (APC), which prevents the formation of the active APC, and also phosphorylates the maturation promoting factor (MPF), preventing its premature activation. Upon the G2/M transition, PDE4D3 is phosphorylated by an as yet unidentified kinase and the activity of the PDE increases. Cyclic AMP in the cell is hydrolysed, causing re-association of the regulatory and catalytic subunits of PKA. The APC subunits are dephosphorylated by protein phosphatase 1 (PP1) and the active APC forms, this then targets multiple substrates for ubiquitinylation, instigating their proteasome mediated degradation. Dephosphorylation of nuclear lamins and the cytoskeletal elements causes nuclear envelope breakdown, and cytoskeletal re-arrangements and the cells pass through mitosis. The kinase which phosphorylates PDE4D3 is then inactivated and PDE4D3 is dephosphorylated by PP1 as cells make the M/G1 transition. The levels of cAMP increase, activating PKA and initiating the reformation of the cytoskeleton and the nuclear envelope.

References

- Abraham,R.T., Acquarone,M., Andersen,A., Asensi,A., Belle,R., Berger,F., Bergounioux,C., Brunn,G., Buquet-Fagot,C., Fagot,D., and . (1995). Cellular effects of olomoucine, an inhibitor of cyclin-dependent kinases. *Biol. Cell* 83, 105-120.
- Adams,R.R., Carmena,M., and Earnshaw,W.C. (2001). Chromosomal passengers and the (aurora) ABCs of mitosis. *Trends Cell Biol.* 11, 49-54.
- Ahmad,F., Cong,L.N., Stenson,H.L., Wang,L.M., Rahn,L.T., Pierce,J.H., Quon,M.J., Degerman,E., and Manganiello,V.C. (2000). Cyclic nucleotide phosphodiesterase 3B is a downstream target of protein kinase B and may be involved in regulation of effects of protein kinase B on thymidine incorporation in FDCP2 cells. *J. Immunol.* 164, 4678-4688.
- Ammit,A.J. and Panettieri,R.A., Jr. (2001). Invited Review: The circle of life: cell cycle regulation in airway smooth muscle. *J. Appl. Physiol* 91, 1431-1437.
- Anghileri,P., Branduardi,P., Sternieri,F., Monti,P., Visintin,R., Bevilacqua,A., Alberghina,L., Martegani,E., and Baroni,M.D. (1999). Chromosome separation and exit from mitosis in budding yeast: dependence on growth revealed by cAMP-mediated inhibition. *Exp. Cell Res.* 250, 510-523.
- Artemyev,N.O., Arshavsky,V.Y., and Cote,R.H. (1998). Photoreceptor phosphodiesterase: interaction of inhibitory gamma subunit and cyclic GMP with specific binding sites on catalytic subunits. *Methods* 14, 93-104.
- Baillie,G., MacKenzie,S.J., and Houslay,M.D. (2001). Phorbol 12-myristate 13-acetate Triggers the Protein Kinase A-Mediated Phosphorylation and Activation of the PDE4D5 cAMP Phosphodiesterase in Human Aortic Smooth Muscle Cells through a Route Involving Extracellular Signal Regulated Kinase (ERK). *Mol. Pharmacol.* 60, 1100-1111.
- Baillie,G.S., MacKenzie,S.J., McPhee,I., and Houslay,M.D. (2000). Sub-family selective actions in the ability of Erk2 MAP kinase to phosphorylate and regulate the activity of PDE4 cyclic AMP-specific phosphodiesterases. *Br. J. Pharmacol.* 131, 811-819.
- Baker,P.E., Fahey,J.V., and Munck,A. (1981). Prostaglandin inhibition of T-cell proliferation is mediated at two levels. *Cell Immunol.* 61, 52-61.
- Banner,K.H., Dimitriou,G., Kinali,M., Page,C.P., and Greenough,A. (2000). Evidence to suggest that the phosphodiesterase 4 isoenzyme is present and involved in the proliferation of umbilical cord blood mononuclear cells. *Clin. Exp. Allergy* 30, 706-712.
- Banner,K.H., Roberts,N.M., and Page,C.P. (1995). Differential effect of phosphodiesterase 4 inhibitors on the proliferation of human peripheral blood mononuclear cells from normals and subjects with atopic dermatitis. *Br. J. Pharmacol.* 116, 3169-3174.
- Barnes,M.J., Cooper,N., Davenport,R.J., Dyke,H.J., Galleway,F.P., Galvin,F.C., Gowers,L., Haughan,A.F., Lowe,C., Meissner,J.W., Montana,J.G., Morgan,T., Picken,C.L., and Watson,R.J. (2001). Synthesis and structure-activity relationships of guanine analogues as phosphodiesterase 7 (PDE7) inhibitors. *Bioorg. Med. Chem. Lett.* 11, 1081-1083.

- Beard, M.B., O'Connell, J.C., Bolger, G.B., and Houslay, M.D. (1999). The unique N-terminal domain of the cAMP phosphodiesterase PDE4D4 allows for interaction with specific SH3 domains. *FEBS Lett.* *460*, 173-177.
- Beavo, J.A. (1995). Cyclic nucleotide phosphodiesterases: functional implications of multiple isoforms. *Physiol Rev.* *75*, 725-748.
- Beavo, J.A., Hardman, J.G., and Sutherland, E.W. (1970). Hydrolysis of cyclic guanosine and adenosine 3',5'-monophosphates by rat and bovine tissues. *J. Biol. Chem.* *245*, 5649-5655.
- Bellen, H.J., Gregory, B.K., Olsson, C.L., and Kiger, J.A., Jr. (1987). Two *Drosophila* learning mutants, *dunce* and *rutabaga*, provide evidence of a maternal role for cAMP on embryogenesis. *Dev. Biol.* *121*, 432-444.
- Biedler, J.L., Helson, L., and Spengler, B.A. (1973). Morphology and growth, tumorigenicity, and cytogenetics of human neuroblastoma cells in continuous culture. *Cancer Res.* *33*, 2643-2652.
- Billington, C.K., Joseph, S.K., Swan, C., Scott, M.G., Jobson, T.M., and Hall, I.P. (1999). Modulation of human airway smooth muscle proliferation by type 3 phosphodiesterase inhibition. *Am. J. Physiol* *276*, L412-L419.
- Birnbaumer, L., Abramowitz, J., and Brown, A.M. (1990). Receptor-effector coupling by G proteins. *Biochim. Biophys. Acta* *1031*, 163-224.
- Bito, H., Deisseroth, K., and Tsien, R.W. (1996). CREB phosphorylation and dephosphorylation: a Ca(2+)- and stimulus duration-dependent switch for hippocampal gene expression. *Cell* *87*, 1203-1214.
- Black, E.J., Clark, W., and Gillespie, D.A. (2000). Transient deactivation of ERK signalling is sufficient for stable entry into G0 in primary avian fibroblasts. *Curr. Biol.* *10*, 1119-1122.
- Blain, S.W., Montalvo, E., and Massague, J. (1997). Differential interaction of the cyclin-dependent kinase (Cdk) inhibitor p27Kip1 with cyclin A-Cdk2 and cyclin D2-Cdk4. *J. Biol. Chem.* *272*, 25863-25872.
- Blomhoff, H.K., Blomhoff, R., Stokke, T., deLange, D.C., Brevik, K., Smeland, E.B., Funderud, S., and Godal, T. (1988). cAMP-mediated growth inhibition of a B-lymphoid precursor cell line Reh is associated with an early transient delay in G2/M, followed by an accumulation of cells in G1. *J. Cell Physiol* *137*, 583-587.
- Bloom, T.J. and Beavo, J.A. (1996). Identification and tissue-specific expression of PDE7 phosphodiesterase splice variants. *Proc. Natl. Acad. Sci. U. S. A* *93*, 14188-14192.
- Bolger, G.B., Erdogan, S., Jones, R.E., Loughney, K., Scotland, G., Hoffmann, R., Wilkinson, I., Farrell, C., and Houslay, M.D. (1997). Characterization of five different proteins produced by alternatively spliced mRNAs from the human cAMP-specific phosphodiesterase PDE4D gene. *Biochem. J.* *328 (Pt 2)*, 539-548.
- Bolger, G.B., McPhee, I., and Houslay, M.D. (1996). Alternative splicing of cAMP-specific phosphodiesterase mRNA transcripts. Characterization of a novel tissue-specific isoform, RNPDE4A8. *J. Biol. Chem.* *271*, 1065-1071.

214
Bonfoco,E., Li,E., Kolbinger,F., and Cooper,N.R. (2001). Characterization of a novel proapoptotic caspase-2- and caspase-9- binding protein. *J. Biol. Chem.* 276, 29242-29250.

Borger,P., Kauffman,H.F., Postma,D.S., and Vellenga,E. (1996). Interleukin-4 gene expression in activated human T lymphocytes is regulated by the cyclic adenosine monophosphate-dependent signaling pathway. *Blood* 87, 691-698.

Bos,J.L. (1989). ras oncogenes in human cancer: a review. *Cancer Res.* 49, 4682-4689.

Bos,J.L. (1998). All in the family? New insights and questions regarding interconnectivity of Ras, Rap1 and Ral. *EMBO J.* 17, 6776-6782.

Bos,J.L., de Rooij,J., and Reedquist,K.A. (2001). Rap1 signalling: adhering to new models. *Nat. Rev. Mol. Cell Biol.* 2, 369-377.

Boucher,M.J., Duchesne,C., Laine,J., Morisset,J., and Rivard,N. (2001). cAMP protection of pancreatic cancer cells against apoptosis induced by ERK inhibition. *Biochem. Biophys. Res. Commun.* 285, 207-216.

Brennan,P., Babbage,J.W., Burgering,B.M., Groner,B., Reif,K., and Cantrell,D.A. (1997). Phosphatidylinositol 3-kinase couples the interleukin-2 receptor to the cell cycle regulator E2F. *Immunity.* 7, 679-689.

Brewis,N.D., Street,A.J., Prescott,A.R., and Cohen,P.T.W. (1993). PPX, a novel serine/threonine phosphatase localised to centrosomes. *EMBO J.* 12, 987-996.

Browne,C.L., Bower,W.A., Palazzo,R.E., and Rebhun,L.I. (1990). Inhibition of mitosis in fertilized sea urchin eggs by inhibition of the cyclic AMP-dependent protein kinase. *Exp. Cell Res.* 188, 122-128.

Bumbasirevic,V., Skaro-Milic,A., Mircic,A., and Djuricic,B. (1995). Apoptosis induced by microtubule disrupting drugs in normal murine thymocytes in vitro. *Scanning Microsc.* 9, 509-516.

Bunemann,M. and Hosey,M.M. (1999). G-protein coupled receptor kinases as modulators of G-protein signalling. *Journal of Physiology* 517, 5-23.

Burk,R.R. (1968). *Nature* 219, 1272-1275.

Butcher,R.W. and Sutherland,E.W. (1962). Adenosine 3',5'-phosphate in biological materials. *J. Biol. Chem.* 237, 1244-1250.

Byers,D., Davis,R.L., and Kiger,J.A., Jr. (1981). Defect in cyclic AMP phosphodiesterase due to the dunce mutation of learning in *Drosophila melanogaster*. *Nature* 289, 79-81.

Byus,C.V., Hayes,J.S., Brendel,K., and Russell,D.H. (1976). Correlation between cAMP, activation of cAMP-dependent protein kinase(s), and rate of glycogenolysis in isolated rat hepatocytes. *Life Sci.* 19, 329-335.

Cantrell,D.A. (2001). Phosphoinositide 3-kinase signalling pathways. *J. Cell Sci.* 114, 1439-1445.

Cartledge,J. and Eardley,I. (1999). Sildenafil. *Expert. Opin. Pharmacother.* 1, 137-147.

Charbonneau,H. (1990). Structure-function relationships among cyclic nucleotide phosphodiesterases. In *Cyclic Nucleotide Phosphodiesterases: Structure, Function,*

Regulation and Drug Action, J.A.Beavo and M.D.Houslay, eds. (Chichester: Wiley), pp. 267-298.

Chen,M.X., McPartlin,A.E., Brown,L., Baker,H.M., and Cohen,P.T.W. (1994). A novel human protein serine/threonine phosphatase which possesses four tetratricopeptide repeat motifs and localises to the nucleus. *EMBO J.* 14, 4278-4290.

Chijiwa,T., Mishima,A., Hagiwara,M., Sano,M., Hayashi,K., Inoue,T., Naito,K., Toshioka,T., and Hidaka,H. (1990). Inhibition of forskolin-induced neurite outgrowth and protein phosphorylation by a newly synthesized selective inhibitor of cyclic AMP-dependent protein kinase, N-[2-(p-bromocinnamylamino)ethyl]-5-isoquinolinesulfonamide (H-89), of PC12D pheochromocytoma cells. *J. Biol. Chem.* 265, 5267-5272.

Cho,R.J., Huang,M., Campbell,M.J., Dong,H., Steinmetz,L., Sapinoso,L., Hampton,G., Elledge,S.J., Davis,R.W., and Lockhart,D.J. (2001). Transcriptional regulation and function during the human cell cycle. *Nat. Genet.* 27, 48-54.

Christoffersen,J., Smeland,E.B., Stokke,T., Tasken,K., Andersson,K.B., and Blomhoff,H.K. (1994). Retinoblastoma protein is rapidly dephosphorylated by elevated cyclic adenosine monophosphate levels in human B-lymphoid cells. *Cancer Res.* 54, 2245-2250.

Ciechanover,A., Orian,A., and Schwartz,A.L. (2000). The ubiquitin-mediated proteolytic pathway: mode of action and clinical implications. *J. Cell Biochem. Suppl* 34, 40-51.

Clay,F.J., McEwen,S.J., Bertoncello,I., Wilks,A.F., and Dunn,A.R. (1993). Identification and cloning of a protein kinase-encoding mouse gene, Plk, related to the polo gene of *Drosophila*. *Proc. Natl. Acad. Sci. U. S. A* 90, 4882-4886.

Cohen,P., Holmes,C.F., and Tsukitani,Y. (1990). Okadaic acid: a new probe for the study of cellular regulation. *Trends Biochem. Sci.* 15, 98-102.

Conti,M., Andersen,C.B., Richard,F.J., Shitsukawa,K., and Tsafirri,A. (1998). Role of cyclic nucleotide phosphodiesterases in resumption of meiosis. *Mol. Cell Endocrinol.* 145, 9-14.

Cook,S.J. and McCormick,F. (1993). Inhibition by cAMP of Ras-dependent activation of Raf. *Science* 262, 1069-1072.

Cooper,D.M., Mons,N., and Karpen,J.W. (1995). Adenylyl cyclases and the interaction between calcium and cAMP signalling. *Nature* 374, 421-424.

Cordeiro-Stone,M. and Kaufman,D.G. (1985). Kinetics of DNA replication in C3H 10T1/2 cells synchronized by aphidicolin. *Biochemistry* 24, 4815-4822.

Cospedal,R., Lobo,M., and Zachary,I. (1999). Differential regulation of extracellular signal-regulated protein kinases (ERKs) 1 and 2 by cAMP and dissociation of ERK inhibition from anti-mitogenic effects in rabbit vascular smooth muscle cells. *Biochem. J.* 342 (Pt 2), 407-414.

Crews,C.M., Alessandrini,A., and Erikson,R.L. (1992). The primary structure of MEK, a protein kinase that phosphorylates the ERK gene product. *Science* 258, 478-480.

- Crews,C.M. and Erikson,R.L. (1992). Purification of a murine protein-tyrosine/threonine kinase that phosphorylates and activates the Erk-1 gene product: relationship to the fission yeast *byr1* gene product. *Proc. Natl. Acad. Sci. U. S. A* 89, 8205-8209.
- Crossen,P.E., Gerner,E.W., Bell,C.W., and Trent,J.M. (1986). Analysis of the length of S-phase required to show sister chromatid differential staining. *Cell Tissue Kinet.* 19, 527-532.
- Cunningham,L.W. (1954). Kinetic properties of crystalline diisopropyl phosphoryl trypsin. *J. Biol. Chem.* 211, 13-17.
- Davis,R.J. (1995). Transcriptional regulation by MAP kinases. *Mol. Reprod. Dev.* 42, 459-467.
- Davis,R.L. and Kiger,J.A., Jr. (1981). Dunce mutants of *Drosophila melanogaster*: mutants defective in the cyclic AMP phosphodiesterase enzyme system. *J. Cell Biol.* 90, 101-107.
- Davis,R.L., Takayasu,H., Eberwine,M., and Myers,J. (1989). Cloning and characterisation of human homologues of the *Drosophila* *dunce+* gene. *Proc. Natl. Acad. Sci. U. S. A* 86, 3640-3648.
- de Rooij,J., Rehmann,H., van Triest,M., Cool,R.H., Wittinghofer,A., and Bos,J.L. (2000). Mechanism of regulation of the Epac family of cAMP-dependent RapGEFs. *J. Biol. Chem.* 275, 20829-20836.
- de Rooij,J., Zwartkruis,F.J., Verheijen,M.H., Cool,R.H., Nijman,S.M., Wittinghofer,A., and Bos,J.L. (1998). Epac is a Rap1 guanine-nucleotide-exchange factor directly activated by cyclic AMP. *Nature* 396, 474-477.
- Degerman,E., Belfrage,P., and Manganiello,V.C. (1997). Structure, localization, and regulation of cGMP-inhibited phosphodiesterase (PDE3). *J. Biol. Chem.* 272, 6823-6826.
- Di Pauli,R. and Rassat,J. (1983). T cell lines and variant subclones with differing susceptibility to tumor promoters. *J. Immunol.* 130, 2732-2736.
- Diehl,J.A., Zindy,F., and Sherr,C.J. (1997). Inhibition of cyclin D1 phosphorylation on threonine-286 prevents its rapid degradation via the ubiquitin-proteasome pathway. *Genes Dev.* 11, 957-972.
- Diviani,D., Lattion,A.L., and Cotecchia,S. (1997). Characterization of the phosphorylation sites involved in G protein- coupled receptor kinase- and protein kinase C-mediated desensitization of the alpha1B-adrenergic receptor. *J. Biol. Chem.* 272, 28712-28719.
- Dodge,K.L., Khouangsathiene,S., Kapiloff,M.S., Mouton,R., Hill,E.V., Houslay,M.D., Langeberg,L.K., and Scott,J.D. (2001). mAKAP assembles a protein kinase A/PDE4 phosphodiesterase cAMP signaling module. *EMBO J.* 20, 1921-1930.
- Donaldson,M.M., Tavares,A.A., Hagan,I.M., Nigg,E.A., and Glover,D.M. (2001). The mitotic roles of Polo-like kinase. *J. Cell Sci.* 114, 2357-2358.
- Doskeland,S.O., Maronde,E., and Gjertsen,B.T. (1993). The genetic subtypes of cAMP-dependent protein kinase--functionally different or redundant? *Biochim. Biophys. Acta* 1178, 249-258.

- Drees,M., Zimmermann,R., and Eisenbrand,G. (1993). 3',5'-Cyclic nucleotide phosphodiesterase in tumor cells as potential target for tumor growth inhibition. *Cancer Res.* 53, 3058-3061.
- Dudai,Y., Jan,Y.N., Byers,D., Quinn,W.G., and Benzer,S. (1976). *dunce*, a mutant of *Drosophila* deficient in learning. *Proc. Natl. Acad. Sci. U. S. A* 73, 1684-1688.
- Ebina,M., Takahashi,T., Chiba,T., and Motomiya,M. (1993). Cellular hypertrophy and hyperplasia of airway smooth muscles underlying bronchial asthma. A 3-D morphometric study. *Am. Rev. Respir. Dis.* 148, 720-726.
- Ekholm,D., Mulloy,J.C., Gao,G., Degerman,E., Franchini,G., and Manganiello,V.C. (1999). Cyclic nucleotide phosphodiesterases (PDE) 3 and 4 in normal, malignant, and HTLV-I transformed human lymphocytes. *Biochem. Pharmacol.* 58, 935-950.
- Epstein,P.M., Mills,J.S., Hersh,E.M., Strada,S.J., and Thompson,W.J. (1980). Activation of cyclic nucleotide phosphodiesterase from isolated human peripheral blood lymphocytes by mitogenic agents. *Cancer Res.* 40, 379-386.
- Erdogan,S. and Houslay,M.D. (1997). Challenge of human Jurkat T-cells with the adenylate cyclase activator forskolin elicits major changes in cAMP phosphodiesterase (PDE) expression by up-regulating PDE3 and inducing PDE4D1 and PDE4D2 splice variants as well as down-regulating a novel PDE4A splice variant. *Biochem. J.* 321 (Pt 1), 165-175.
- Essayan,D.M., Kagey-Sobotka,A., Lichtenstein,L.M., and Huang,S.K. (1997). Differential regulation of human antigen-specific Th1 and Th2 lymphocyte responses by isozyme selective cyclic nucleotide phosphodiesterase inhibitors. *J. Pharmacol. Exp. Ther.* 282, 505-512.
- Exton,J.H. (1994). Phosphatidylcholine breakdown and signal transduction. *Biochim. Biophys. Acta* 1212, 26-42.
- Eyler,Y.L., Lantz,L.M., and Lewis,A.M., Jr. (1994). Flow cytometric detection of DNA tumor virus nuclear oncogene products in unfixed cells: saponin FACS of viral oncogene products. *J. Virol. Methods* 46, 23-27.
- Fantes,P. and Brooks,R. (1993). *The Cell Cycle.*, D.Rickwood and B.D.Hames, eds. (New York: Oxford University Press).
- Fawcett,L., Baxendale,R., Stacey,P., McGrouther,C., Harrow,I., Soderling,S., Hetman,J., Beavo,J.A., and Phillips,S.C. (2000). Molecular cloning and characterization of a distinct human phosphodiesterase gene family: PDE11A. *Proc. Natl. Acad. Sci. U. S. A* 97, 3702-3707.
- Feliciello,A., Gallo,A., Mele,E., Porcellini,A., Troncone,G., Garbi,C., Gottesman,M.E., and Avvedimento,E.V. (2000). The localization and activity of cAMP-dependent protein kinase affect cell cycle progression in thyroid cells. *J. Biol. Chem.* 275, 303-311.
- Feliciello,A., Gottesman,M.E., and Avvedimento,E.V. (2001). The biological functions of A-kinase anchor proteins. *J. Mol. Biol.* 308, 99-114.
- Fernandez,A., Cavadore,J.C., Demaille,J., and Lamb,N. (1995). Implications for cAMP-dependent protein kinase in the maintenance of the interphase state. *Prog. Cell Cycle Res.* 1, 241-253.

- Fisher,D.A., Smith,J.F., Pillar,J.S., St Denis,S.H., and Cheng,J.B. (1998). Isolation and characterization of PDE9A, a novel human cGMP-specific phosphodiesterase. *J. Biol. Chem.* 273, 15559-15564.
- Florio,C., Martin,J.G., Styhler,A., and Heisler,S. (1994). Antiproliferative effect of prostaglandin E2 in cultured guinea pig tracheal smooth muscle cells. *Am. J. Physiol* 266, L131-L137.
- Florio,S.K., Prusti,R.K., and Beavo,J.A. (1996). Solubilization of membrane-bound rod phosphodiesterase by the rod phosphodiesterase recombinant delta subunit. *J. Biol. Chem.* 271, 24036-24047.
- Ford,H.L. and Pardee,A.B. (1998). The S phase: Beginning, Middle, and End: A Perspective. *Journal of Cellular Biochemistry Supplements* 30/31, 1-7.
- Fraker,P.J., King,L.E., Lill-Elghanian,D., and Telford,W.G. (1995). Quantification of apoptotic events in pure and heterogeneous populations of cells using the flow cytometer. *Methods Cell Biol.* 46, 57-76.
- Francis,S.H. and Corbin,J.D. (1994). Structure and function of cyclic nucleotide-dependent protein kinases. *Annu. Rev. Physiol* 56, 237-272.
- Freedman,N.J., Liggett,S.B., Drachman,D.E., Pei,G., Caron,M.G., and Lefkowitz,R.J. (1995). Phosphorylation and desensitization of the human beta 1-adrenergic receptor. Involvement of G protein-coupled receptor kinases and cAMP- dependent protein kinase. *J. Biol. Chem.* 270, 17953-17961.
- Frost,V., Morley,S.J., Mercep,L., Meyer,T., Fabbro,D., and Ferrari,S. (1995). The phosphodiesterase inhibitor SQ 20006 selectively blocks mitogen activation of p70S6k and transition to S phase of the cell division cycle without affecting the steady state phosphorylation of eIF-4E. *J. Biol. Chem.* 270, 26698-26706.
- Frye,R.A. (1992). Involvement of G proteins, cytoplasmic calcium, phospholipases, phospholipid-derived second messengers, and protein kinases in signal transduction from mitogenic cell surface receptors. *Cancer Treat. Res.* 63, 281-299.
- Fujishige,K., Kotera,J., Michibata,H., Yuasa,K., Takebayashi,S., Okumura,K., and Omori,K. (1999). Cloning and characterization of a novel human phosphodiesterase that hydrolyzes both cAMP and cGMP (PDE10A). *J. Biol. Chem.* 274, 18438-18445.
- Gallant,P., Fry,A.M., and Nigg,E.A. (1995). Protein kinases in the control of mitosis: focus on nucleocytoplasmic trafficking. *J. Cell Sci. Suppl* 19, 21-28.
- Gause,W.C., Takashi,T., Mountz,J.D., Finkelman,F.D., and Steinberg,A.D. (1988). Activation of CD 4-. *J. Immunol.* 141, 2240-2245.
- Geilen,C.C., Wieprecht,M., Wieder,T., and Reutter,W. (1992). A selective inhibitor of cyclic AMP-dependent protein kinase, N-[2- bromocinnamyl(amino)ethyl]-5-isoquinolinesulfonamide (H-89), inhibits phosphatidylcholine biosynthesis in HeLa cells. *FEBS Lett.* 309, 381-384.
- Geppert,T.D. and Lipsky,P.E. (1986). Accessory cell-T cell interactions involved in anti-CD3-induced T4 and T8 cell proliferation: analysis with monoclonal antibodies. *J. Immunol.* 137, 3065-3073.

- Gether,U. (2000). Uncovering molecular mechanisms involved in activation of G protein-coupled receptors. *Endocr. Rev.* *21*, 90-113.
- Gether,U., Lin,S., and Kobilka,B.K. (1995). Fluorescent labeling of purified beta 2 adrenergic receptor. Evidence for ligand-specific conformational changes. *J. Biol. Chem.* *270*, 28268-28275.
- Giembycz,M.A., Corrigan,C.J., Kay,A.B., and Barnes,P.J. (1994). Inhibition of CD4 and CD8 T-lymphocyte proliferation and cytokine secretion by isozyme selective phosphodiesterase (PDE) inhibitors: correlation with cyclic AMP concentrations. *Clin. Exp. Allergy* *24*, 995A.
- Giembycz,M.A., Corrigan,C.J., Seybold,J., Newton,R., and Barnes,P.J. (1996). Identification of cyclic AMP phosphodiesterases 3, 4 and 7 in human CD4+ and CD8+ T-lymphocytes: role in regulating proliferation and the biosynthesis of interleukin-2. *Br. J. Pharmacol.* *118*, 1945-1958.
- Glavas,N.A., Ostenson,C., Schaefer,J.B., Vasta,V., and Beavo,J.A. (2001). T cell activation up-regulates cyclic nucleotide phosphodiesterases 8A1 and 7A3. *Proc. Natl. Acad. Sci. U. S. A* *98*, 6319-6324.
- Gluzman,Y. (1981). SV40-transformed simian cells support the replication of early SV40 mutants. *Cell* *23*, 175-182.
- Gordon,J.A. (1991). Use of vanadate as protein-phosphotyrosine phosphatase inhibitor. *Methods Enzymol.* *201*, 477-482.
- Goren,E.N. and Rosen,O.M. (1972). Purification and properties of a cyclic nucleotide phosphodiesterase from bovine heart. *Arch. Biochem. Biophys.* *153*, 384-397.
- Grange,M., Sette,C., Cuomo,M., Conti,M., Lagarde,M., Prigent,A.F., and Nemoz,G. (2000). The cAMP-specific phosphodiesterase PDE4D3 is regulated by phosphatidic acid binding. Consequences for cAMP signaling pathway and characterization of a phosphatidic acid binding site. *J. Biol. Chem.* *275*, 33379-33387.
- Graves,L.M., Bornfeldt,K.E., Raines,E.W., Potts,B.C., Macdonald,S.G., Ross,R., and Krebs,E.G. (1993). Protein kinase A antagonizes platelet-derived growth factor-induced signaling by mitogen-activated protein kinase in human arterial smooth muscle cells. *Proc. Natl. Acad. Sci. U. S. A* *90*, 10300-10304.
- Greene,W.C. and Leonard,W.J. (1986). The human interleukin-2 receptor. *Annu. Rev. Immunol.* *4*, 69-95.
- Greulich,H. and Erikson,R.L. (1998). An analysis of Mek1 signaling in cell proliferation and transformation. *J. Biol. Chem.* *273*, 13280-13288.
- Grieco,D., Avvedimento,E.V., and Gottesman,M.E. (1994). A role for cAMP-dependent protein kinase in early embryonic divisions. *Proc. Natl. Acad. Sci. U. S. A* *91*, 9896-9900.
- Grieco,D., Porcellini,A., Avvedimento,E.V., and Gottesman,M.E. (1996). Requirement for cAMP-PKA pathway activation by M phase-promoting factor in the transition from mitosis to interphase. *Science* *271*, 1718-1723.
- Guipponi,M., Scott,H.S., Kudoh,J., Kawasaki,K., Shibuya,K., Shintani,A., Asakawa,S., Chen,H., Lalioti,M.D., Rossier,C., Minoshima,S., Shimizu,N., and Antonarakis,S.E. (1998). Identification and characterization of a novel cyclic nucleotide phosphodiesterase

gene (PDE9A) that maps to 21q22.3: alternative splicing of mRNA transcripts, genomic structure and sequence. *Hum. Genet.* *103*, 386-392.

Ha,K.Y., Yeol,C.J., Jeong,Y., Wolgemuth,D.J., and Rhee,K. (2002). Nek2 Localizes to Multiple Sites in Mitotic Cells, Suggesting Its Involvement in Multiple Cellular Functions during the Cell Cycle. *Biochem. Biophys. Res. Commun.* *290*, 730-736.

Haas,A.L. and Bright,P.M. (1985). The immunochemical detection and quantitation of intracellular ubiquitin-protein conjugates. *J. Biol. Chem.* *260*, 12464-12473.

Hamilton,B.T. and Snyder,J.A. (1982). Rapid completion of mitosis and cytokinesis in PtK cells following release from nocodazole arrest. *Eur. J. Cell Biol.* *28*, 190-194.

Hamm,H.E. (1998). The many faces of G protein signaling. *J. Biol. Chem.* *273*, 669-672.

Han,P., Fletcher,C.F., Copeland,N.G., Jenkins,N.A., Yaremko,L.M., and Michaeli,T. (1998). Assignment of the mouse Pde7A gene to the proximal region of chromosome 3 and of the human PDE7A gene to chromosome 8q13. *Genomics* *48*, 275-276.

Han,P., Zhu,X., and Michaeli,T. (1997). Alternative splicing of the high affinity cAMP-specific phosphodiesterase (PDE7A) mRNA in human skeletal muscle and heart. *J. Biol. Chem.* *272*, 16152-16157.

Hanuske-Abel,H.M., Park,M.H., Hanuske,A.R., Popowicz,A.M., Lalande,M., and Folk,J.E. (1994). Inhibition of the G1-S transition of the cell cycle by inhibitors of deoxyhypusine hydroxylation. *Biochim. Biophys. Acta* *1221*, 115-124.

Hannak,E., Kirkham,M., Hyman,A.A., and Oegema,K. (2001). Aurora-A kinase is required for centrosome maturation in *Caenorhabditis elegans*. *J. Cell Biol.* *155*, 1109-1116.

Hansen,G., Jin,S., Umetsu,D.T., and Conti,M. (2000). Absence of muscarinic cholinergic airway responses in mice deficient in the cyclic nucleotide phosphodiesterase PDE4D. *Proc. Natl. Acad. Sci. U. S. A* *97*, 6751-6756.

Hardie, D. G., Campbell, D. G., Caudwell, F. B., and Haystead, T. A. J. Analysis of sites phosphorylated *in vivo* and *in vitro*. *Protein phosphorylation a practical approach* *123*, 61-85. 1993.

Ref Type: Generic

Harrison,T., Graham,F., and Williams,J. (1977). Host-range mutants of adenovirus type 5 defective for growth in HeLa cells. *Virology* *77*, 319-329.

Hawes,B.E., Kil,E., Green,B., O'Neill,K., Fried,S., and Graziano,M.P. (2000). The melanin-concentrating hormone receptor couples to multiple G proteins to activate diverse intracellular signaling pathways. *Endocrinology* *141*, 4524-4532.

Hayashi,M., Matsushima,K., Ohashi,H., Tsunoda,H., Murase,S., Kawarada,Y., and Tanaka,T. (1998). Molecular cloning and characterization of human PDE8B, a novel thyroid-specific isozyme of 3',5'-cyclic nucleotide phosphodiesterase. *Biochem. Biophys. Res. Commun.* *250*, 751-756.

Hayashi,S., Morishita,R., Matsushita,H., Nakagami,H., Taniyama,Y., Nakamura,T., Aoki,M., Yamamoto,K., Higaki,J., and Ogihara,T. (2000). Cyclic AMP inhibited proliferation of human aortic vascular smooth muscle cells, accompanied by induction of p53 and p21. *Hypertension* *35*, 237-243.

- Hayne,C., Tzivion,G., and Luo,Z. (2000). Raf-1/MEK/MAPK pathway is necessary for the G2/M transition induced by nocodazole. *J. Biol. Chem.* 275, 31876-31882.
- Helbing,C.C., Wellington,C.L., Gogela-Spehar,M., Cheng,T., Pinchbeck,G.G., and Johnston,R.N. (1998). Quiescence versus apoptosis: Myc abundance determines pathway of exit from the cell cycle. *Oncogene* 17, 1491-1501.
- Hengst,L. and Reed,S.I. (1996). Translational control of p27Kip1 accumulation during the cell cycle. *Science* 271, 1861-1864.
- Herbert,J.M., Augereau,J.M., Gleye,J., and Maffrand,J.P. (1990). Chelerythrine is a potent and specific inhibitor of protein kinase C. *Biochem. Biophys. Res. Commun.* 172, 993-999.
- Hetman,J.M., Soderling,S.H., Glavas,N.A., and Beavo,J.A. (2000). Cloning and characterization of PDE7B, a cAMP-specific phosphodiesterase. *Proc. Natl. Acad. Sci. U. S. A* 97, 472-476.
- Hidaka,H., Hayashi,H., Kohri,H., Kimura,Y., Hosokawa,T., Igawa,T., and Saitoh,Y. (1979). Selective inhibitor of platelet cyclic adenosine monophosphate phosphodiesterase, cilostamide, inhibits platelet aggregation. *J. Pharmacol. Exp. Ther.* 211, 26-30.
- Hoffmann,R., Baillie,G.S., MacKenzie,S.J., Yarwood,S.J., and Houslay,M.D. (1999). The MAP kinase ERK2 inhibits the cyclic AMP-specific phosphodiesterase HSPDE4D3 by phosphorylating it at Ser579. *EMBO J.* 18, 893-903.
- Hoffmann,R., Wilkinson,I.R., McCallum,J.F., Engels,P., and Houslay,M.D. (1998). cAMP-specific phosphodiesterase HSPDE4D3 mutants which mimic activation and changes in rolipram inhibition triggered by protein kinase A phosphorylation of Ser-54: generation of a molecular model. *Biochem. J.* 333 (Pt 1), 139-149.
- Hohmann,P., DenHaese,G., and Greene,R.S. (1993). Mitotic CDC2 kinase is negatively regulated by cAMP-dependent protein kinase in mouse fibroblast cell free extracts. *Cell Prolif.* 26, 195-204.
- Holden,C.A., Chan,S.C., and Hanifin,J.M. (1986). Monocyte localization of elevated cAMP phosphodiesterase activity in atopic dermatitis. *J. Invest Dermatol.* 87, 372-376.
- Honda,R., Ohba,Y., Nagata,A., Okayama,H., and Yasuda,H. (1993). Dephosphorylation of human p34cdc2 kinase on both Thr-14 and Tyr-15 by human cdc25B phosphatase. *FEBS Lett.* 318, 331-334.
- Honkanen,R.E., Zwiller,J., Daily,S.L., Khatra,B.S., Dukelow,M., and Boynton,A.L. (1991). Identification, purification, and characterization of a novel serine/threonine protein phosphatase from bovine brain. *J. Biol. Chem.* 266, 6614-6619.
- Houslay,M.D. (1991). Gi-2 is at the centre of an active phosphorylation/dephosphorylation cycle in hepatocytes: the fine-tuning of stimulatory and inhibitory inputs into adenylate cyclase in normal and diabetic states. *Cell Signal.* 3, 1-9.
- Houslay,M.D. (2001). PDE4 cAMP-specific phosphodiesterases. *Prog. Nucleic Acid Res. Mol. Biol.* 69, 249-315.
- Houslay,M.D. and Kolch,W. (2000). Cell-type specific integration of cross-talk between extracellular signal-regulated kinase and cAMP signaling. *Mol. Pharmacol.* 58, 659-668.

- Houslay, M.D. and Milligan, G. (1997). Tailoring cAMP-signalling responses through isoform multiplicity. *Trends Biochem. Sci.* 22, 217-224.
- Howard, A. and Pelc, S. (1953). Synthesis of deoxyribonucleic acid in normal and irradiated cells and its relation to chromosome breakage. *Heredity* 6, 261-273.
- Hurley, J.H. (1998). The adenylyl and guanylyl cyclase superfamily. *Curr. Opin. Struct. Biol.* 8, 770-777.
- Hurley, J.H. (1999). Structure, mechanism, and regulation of mammalian adenylyl cyclase. *J. Biol. Chem.* 274, 7599-7602.
- Huston, E., Lumb, S., Russell, A., Catterall, C., Ross, A.C., Steele, M.R., Bolger, G.B., Perry, M., Owens, R., and Houslay, M.D. (1997). Molecular cloning and transient expression in COS7 cells of a novel human PDE4B cyclic nucleotide phosphodiesterase, HSPDE4B3. *Biochem. J.* 328, 549-558.
- Huston, E., Pooley, L., Julien, P., Scotland, G., McPhee, I., Sullivan, M., Bolger, G., and Houslay, M.D. (1996). The human cyclic AMP-specific phosphodiesterase PDE-46 (HSPDE4A4B) expressed in transfected COS7 cells occurs as both particulate and cytosolic species that exhibit distinct kinetics of inhibition by the antidepressant rolipram. *J. Biol. Chem.* 271, 31334-31344.
- Hutchins, J.R.A., Huges, M., and Clarke, P.R. (2000). Substrate specificity determinants of the checkpoint protein kinase Chk1. *FEBS Lett.* 466, 91-95.
- Ichimura, M. and Kase, H. (1993). A new cyclic nucleotide phosphodiesterase isozyme expressed in the T- lymphocyte cell lines. *Biochem. Biophys. Res. Commun.* 193, 985-990.
- Indolfi, C., Avvedimento, E.V., Di Lorenzo, E., Esposito, G., Rapacciuolo, A., Giuliano, P., Grieco, D., Cavuto, L., Stingone, A.M., Ciullo, I., Condorelli, G., and Chiariello, M. (1997). Activation of cAMP-PKA signaling in vivo inhibits smooth muscle cell proliferation induced by vascular injury. *Nat. Med.* 3, 775-779.
- Ip, J.H., Fuster, V., Badimon, L., Badimon, J., Taubman, M.B., and Chesebro, J.H. (1990). Syndromes of accelerated atherosclerosis: role of vascular injury and smooth muscle cell proliferation. *J. Am. Coll. Cardiol.* 15, 1667-1687.
- Ishii, K., Kumada, K., Toda, T., and Yanagida, M. (1996). Requirement for PP1 phosphatase and 20S cyclosome/APC for the onset of anaphase is lessened by the dosage increase of a novel gene *sds23+*. *EMBO J.* 15, 6629-6640.
- Ito, M. (2000). Factors controlling cyclin B expression. *Plant Mol. Biol.* 43, 677-690.
- Izquierdo, P.M., Reif, K., and Cantrell, D. (1995). The regulation and function of p21ras during T-cell activation and growth. *Immunol. Today* 16, 159-164.
- Jenkins, M.K. and Johnson, J.G. (1993). Molecules involved in T-cell costimulation. *Curr. Opin. Immunol.* 5, 361-367.
- Jin, S.L., Bushnik, T., Lan, L., and Conti, M. (1998). Subcellular localization of rolipram-sensitive, cAMP-specific phosphodiesterases. Differential targeting and activation of the splicing variants derived from the PDE4D gene. *J. Biol. Chem.* 273, 19672-19678.

- Jin,S.L., Richard,F.J., Kuo,W.P., D'Ercole,A.J., and Conti,M. (1999). Impaired growth and fertility of cAMP-specific phosphodiesterase PDE4D- deficient mice. *Proc. Natl. Acad. Sci. U. S. A* *96*, 11998-12003.
- Johnson-Mills,K., Arauz,E., Coffey,R.G., Krzanowski,J.J., Jr., and Polson,J.B. (1998). Effect of CI-930 [3-(2H)-pyridazinone-4,5-dihydro-6-[4-(1H-imidazolyl) phenyl]-5-methyl-monohydrochloride] and rolipram on human coronary artery smooth muscle cell proliferation. *Biochem. Pharmacol.* *56*, 1065-1073.
- Johnson,P.R., Roth,M., Tamm,M., Hughes,M., Ge,Q., King,G., Burgess,J.K., and Black,J.L. (2001). Airway smooth muscle cell proliferation is increased in asthma. *Am. J. Respir. Crit Care Med.* *164*, 474-477.
- Johnston,J.A., Bacon,C.M., Finbloom,D.S., Rees,R.C., Kaplan,D., Shibuya,K., Ortaldo,J.R., Gupta,S., Chen,Y.Q., Giri,J.D., and . (1995). Tyrosine phosphorylation and activation of STAT5, STAT3, and Janus kinases by interleukins 2 and 15. *Proc. Natl. Acad. Sci. U. S. A* *92*, 8705-8709.
- Jordan,M.A., Thrower,D., and Wilson,L. (1992). Effects of vinblastine, podophyllotoxin and nocodazole on mitotic spindles. Implications for the role of microtubule dynamics in mitosis. *J. Cell Sci.* *102 (Pt 3)*, 401-416.
- Juilfs,D.M., Fulle,H.J., Zhao,A.Z., Houslay,M.D., Garbers,D.L., and Beavo,J.A. (1997). A subset of olfactory neurons that selectively express cGMP-stimulated phosphodiesterase (PDE2) and guanylyl cyclase-D define a unique olfactory signal transduction pathway. *Proc. Natl. Acad. Sci. U. S. A* *94*, 3388-3395.
- June,C.H., Jackson,K.M., Ledbetter,J.A., Leiden,J.M., Lindsten,T., and Thompson,C.B. (1989). Two distinct mechanisms of interleukin-2 gene expression in human T lymphocytes. *J. Autoimmun.* *2 Suppl*, 55-65.
- Kakiuchi,S. and Yamazaki,R. (1970). Calcium dependent phosphodiesterase activity and its activating factor (PAF) from brain studies on cyclic 3',5'-nucleotide phosphodiesterase (3). *Biochem. Biophys. Res. Commun.* *41*, 1104-1110.
- Kakkar,R., Raju,R.V.S., and Sharma,R.K. (1999). Calmodulin-dependent cyclic nucleotide phosphodiesterase. *Cellular and molecular life sciences* *55*, 1164-1186.
- Kanda,N. and Watanabe,S. (2001). Regulatory roles of adenylate cyclase and cyclic nucleotide phosphodiesterases 1 and 4 in interleukin-13 production by activated human T cells. *Biochem. Pharmacol.* *62*, 495-507.
- Kandli,M., Feige,E., Chen,A., Kilfin,G., and Motro,B. (2000). Isolation and characterization of two evolutionarily conserved murine kinases (Nek6 and nek7) related to the fungal mitotic regulator, NIMA. *Genomics* *68*, 187-196.
- Kaplan,D.R., Bergmann,C.A., Gould,D., and Landmeier,B. (1988). Membrane-associated interleukin 2 epitopes on the surface of human T lymphocytes. *J. Immunol.* *140*, 819-826.
- Kato,J.Y., Matsuoka,M., Polyak,K., Massague,J., and Sherr,C.J. (1994). Cyclic AMP-induced G1 phase arrest mediated by an inhibitor (p27Kip1) of cyclin-dependent kinase 4 activation. *Cell* *79*, 487-496.
- Kawasaki,H., Springett,G.M., Mochizuki,N., Toki,S., Nakaya,M., Matsuda,M., Housman,D.E., and Graybiel,A.M. (1998). A family of cAMP-binding proteins that directly activate Rap1. *Science* *282*, 2275-2279.

- Kay,A.B. (2000). Overview of 'allergy and allergic diseases: with a view to the future'. *Br. Med. Bull.* 56, 843-864.
- Keryer,G., Yassenko,M., Labbe,J.C., Castro,A., Lohmann,S.M., Evain-Brion,D., and Tasken,K. (1998). Mitosis-specific phosphorylation and subcellular redistribution of the RIIalpha regulatory subunit of cAMP-dependent protein kinase. *J. Biol. Chem.* 273, 34594-34602.
- Kimura,M., Kotani,S., Hattori,T., Sumi,N., Yoshioka,T., Todokoro,K., and Okano,Y. (1997). Cell cycle-dependent expression and spindle pole localization of a novel human protein kinase, Aik, related to Aurora of *Drosophila* and yeast Ipl1. *J. Biol. Chem.* 272, 13766-13771.
- King,R.W., Deshaies,R.J., Peters,J.M., and Kirschner,M.W. (1996). How proteolysis drives the cell cycle. *Science* 274, 1652-1659.
- King,R.W., Peters,J.M., Tugendreich,S., Rolfe,M., Hieter,P., and Kirschner,M.W. (1995). A 20S complex containing CDC27 and CDC16 catalyzes the mitosis-specific conjugation of ubiquitin to cyclin B. *Cell* 81, 279-288.
- Kishimoto,N. and Yamashita,I. (2000). Cyclic AMP regulates cell size of *Schizosaccharomyces pombe* through Cdc25 mitotic inducer. *Yeast* 16, 523-529.
- Klee,C.B. and Krinks,M.H. (1978). Purification of cyclic 3',5'-nucleotide phosphodiesterase inhibitory protein by affinity chromatography on activator protein coupled to Sepharose. *Biochemistry* 17, 120-126.
- Klein,B., Rey,A., Jourdan,M., and Serrou,B. (1983). The role of interleukin 1 and interleukin 2 in human T colony formation. *Cell Immunol.* 77, 348-356.
- Knudsen,E.S., Buckmaster,C., Chen,T.T., Feramisco,J.R., and Wang,J.Y. (1998). Inhibition of DNA synthesis by RB: effects on G1/S transition and S- phase progression. *Genes Dev.* 12, 2278-2292.
- Koff,A., Giordano,A., Desai,D., Yamashita,K., Harper,J.W., Elledge,S., Nishimoto,T., Morgan,D.O., Franza,B.R., and Roberts,J.M. (1992). Formation and activation of a cyclin E-cdk2 complex during the G1 phase of the human cell cycle. *Science* 257, 1689-1694.
- Kook,S., Shim,S.R., Kim,J.I., Ahnn,J.H., Jung,Y.K., Paik,S.G., and Song,W.K. (2000). Degradation of focal adhesion proteins during nocodazole-induced apoptosis in rat-1 cells. *Cell Biochem. Funct.* 18, 1-7.
- Kotani,S., Tanaka,H., Yasuda,H., and Todokoro,K. (1999). Regulation of APC activity by phosphorylation and regulatory factors. *J. Cell Biol.* 146, 791-800.
- Kotani,S., Tugendreich,S., Fujii,M., Jorgensen,P.M., Watanabe,N., Hoog,C., Hieter,P., and Todokoro,K. (1998). PKA and MPF-activated polo-like kinase regulate anaphase-promoting complex activity and mitosis progression. *Mol. Cell* 1, 371-380.
- Kovala,T., Lorimer,I.A., Brickenden,A.M., Ball,E.H., and Sanwal,B.D. (1994). Protein kinase A regulation of cAMP phosphodiesterase expression in rat skeletal myoblasts. *J. Biol. Chem.* 269, 8680-8685.
- Koyama,H., Bornfeldt,K.E., Fukumoto,S., and Nishizawa,Y. (2001). Molecular pathways of cyclic nucleotide-induced inhibition of arterial smooth muscle cell proliferation. *J. Cell Physiol* 186, 1-10.

- Krause,D.S. and Deutsch,C. (1991). Cyclic AMP directly inhibits IL-2 receptor expression in human T cells: expression of both p55 and p75 subunits is affected. *J. Immunol.* *146*, 2285-2296.
- Kreegipuu,A., Blom,N., and Brunak,S. (1999). PhosphoBase, a database of phosphorylation sites: release 2.0. *Nucleic Acids Res.* *27*, 237-239.
- Kronemann,N., Nockher,W.A., Busse,R., and Schini-Kerth,V.B. (1999). Growth-inhibitory effect of cyclic GMP- and cyclic AMP-dependent vasodilators on rat vascular smooth muscle cells: effect on cell cycle and cyclin expression. *Br. J. Pharmacol.* *126*, 349-357.
- Krude,T. (1999). Mimosine arrests proliferating human cells before onset of DNA replication in a dose-dependent manner. *Exp. Cell Res.* *247*, 148-159.
- Krymskaya,V.P., Penn,R.B., Orsini,M.J., Scott,P.H., Plevin,R.J., Walker,T.R., Eszterhas,A.J., Amrani,Y., Chilvers,E.R., and Panettieri,R.A., Jr. (1999). Phosphatidylinositol 3-kinase mediates mitogen-induced human airway smooth muscle cell proliferation. *Am. J. Physiol* *277*, L65-L78.
- Kupetz,I.S. and Jeter,J.R., Jr. (1985). Cell-cycle-specific activity of cyclic nucleotide phosphodiesterase in *Physarum polycephalum*. *Cell Tissue Kinet.* *18*, 159-168.
- Kurokawa,K. and Kato,J. (1998). Cyclic AMP delays G2 progression and prevents efficient accumulation of cyclin B1 proteins in mouse macrophage cells. *Cell Struct. Funct.* *23*, 357-365.
- Kwon,T.K., Nagel,J.E., Buchholz,M.A., and Nordin,A.A. (1996). Characterization of the murine cyclin-dependent kinase inhibitor gene p27Kip1. *Gene* *180*, 113-120.
- L'Allemain,G., Lavoie,J.N., Rivard,N., Baldin,V., and Pouyssegur,J. (1997). Cyclin D1 expression is a major target of the cAMP-induced inhibition of cell cycle entry in fibroblasts. *Oncogene* *14*, 1981-1990.
- Laemmli,U.K., Beguin,F., and Gujer-Kellenberger,G. (1970). A factor preventing the major head protein of bacteriophage T4 from random aggregation. *J. Mol. Biol.* *47*, 69-85.
- Laird,A.D., Morrison,D.K., and Shalloway,D. (1999). Characterization of Raf-1 activation in mitosis. *J. Biol. Chem.* *274*, 4430-4439.
- Lamb,N.J., Cavadore,J.C., Labbe,J.C., Maurer,R.A., and Fernandez,A. (1991). Inhibition of cAMP-dependent protein kinase plays a key role in the induction of mitosis and nuclear envelope breakdown in mammalian cells. *EMBO J.* *10*, 1523-1533.
- Lane,H.A. and Nigg,E.A. (1996). Antibody microinjection reveals an essential role for human polo-like kinase 1 (Plk1) in the functional maturation of mitotic centrosomes. *J. Cell Biol.* *135*, 1701-1713.
- Leblond,C.P. and El Alfy,M. (1998). The eleven stages of the cell cycle, with emphasis on the changes in chromosomes and nucleoli during interphase and mitosis. *Anat. Rec.* *252*, 426-443.
- Lee,J.H., Johnson,P.R., Roth,M., Hunt,N.H., and Black,J.L. (2001). ERK activation and mitogenesis in human airway smooth muscle cells. *Am. J. Physiol Lung Cell Mol. Physiol* *280*, L1019-L1029.

- Lefebvre,G., Raval,G., and Gay,R. (1980). [Variations in cyclic AMP level and specific activities of adenylate cyclase and cyclic AMP phosphodiesterase during the cell cycle of an Actinomycete (author's transl)]. *Biochim. Biophys. Acta* 632, 26-34.
- Lefkowitz,R.J. (1998). G protein-coupled receptors. III. New roles for receptor kinases and beta-arrestins in receptor signaling and desensitization. *J. Biol. Chem.* 273, 18677-18680.
- Leighfield,T.A. and Van Dolah,F.M. (2001). Cell Cycle regulation in a dinoflagellate, *Amphidinium operculatum*: identification of the diel entraining cue and a possible role for cyclic AMP. *Journal of Experimental Marine Biology and Ecology* 262, 177-197.
- Leitman,D.C., Fiscus,R.R., and Murad,F. (1986). Forskolin, phosphodiesterase inhibitors, and cyclic AMP analogs inhibit proliferation of cultured bovine aortic endothelial cells. *J. Cell Physiol* 127, 237-243.
- Li,A. and Blow,J.J. (2001). The origin of CDK regulation. *Nat. Cell Biol.* 3, E182-E184.
- Li,L., Yee,C., and Beavo,J.A. (1999). CD3- and CD28-dependent induction of PDE7 required for T cell activation. *Science* 283, 848-851.
- Li,Y. and Rubin,C.S. (1995). Mutagenesis of the regulatory subunit (RII beta) of cAMP-dependent protein kinase II beta reveals hydrophobic amino acids that are essential for RII beta dimerization and/or anchoring RII beta to the cytoskeleton. *J. Biol. Chem.* 270, 1935-1944.
- Lim,J., Pahlke,G., and Conti,M. (1999). Activation of the cAMP-specific phosphodiesterase PDE4D3 by phosphorylation. Identification and function of an inhibitory domain. *J. Biol. Chem.* 274, 19677-19685.
- Ling,Y.H., Tornos,C., and Perez-Soler,R. (1998). Phosphorylation of Bcl-2 is a marker of M phase events and not a determinant of apoptosis. *J. Biol. Chem.* 273, 18984-18991.
- Lingk,D.S., Chan,M.A., and Gelfand,E.W. (1990). Increased cyclic adenosine monophosphate levels block progression but not initiation of human T cell proliferation. *J. Immunol.* 145, 449-455.
- Liu,H. and Maurice,D.H. (1998). Expression of cyclic GMP-inhibited phosphodiesterases 3A and 3B (PDE3A and PDE3B) in rat tissues: differential subcellular localization and regulated expression by cyclic AMP. *Br. J. Pharmacol.* 125, 1501-1510.
- Liu,H. and Maurice,D.H. (1999). Phosphorylation-mediated activation and translocation of the cyclic AMP- specific phosphodiesterase PDE4D3 by cyclic AMP-dependent protein kinase and mitogen-activated protein kinases. A potential mechanism allowing for the coordinated regulation of PDE4D activity and targeting. *J. Biol. Chem.* 274, 10557-10565.
- Liu,H., Palmer,D., Jimmo,S.L., Tilley,D.G., Dunkerley,H.A., Pang,S.C., and Maurice,D.H. (2000a). Expression of phosphodiesterase 4D (PDE4D) is regulated by both the cyclic AMP-dependent protein kinase and mitogen-activated protein kinase signaling pathways. A potential mechanism allowing for the coordinated regulation of PDE4D activity and expression in cells. *J. Biol. Chem.* 275, 26615-26624.
- Liu,Y., Vidanes,G., Lin,Y.C., Mori,S., and Siede,W. (2000b). Characterization of a *Saccharomyces cerevisiae* homologue of *Schizosaccharomyces pombe* Chk1 involved in DNA-damage-induced M-phase arrest. *Mol. Gen. Genet.* 262, 1132-1146.

- Loesberg,C., van Wijk,R., Zandbergen,J., van Aken,W.G., van Mourik,J.A., and de Groot,P.G. (1985). Cell cycle-dependent inhibition of human vascular smooth muscle cell proliferation by prostaglandin E1. *Exp. Cell Res.* 160, 117-125.
- Loughney,K., Hill,T.R., Florio,V.A., Uher,L., Rosman,G.J., Wolda,S.L., Jones,B.A., Howard,M.L., McAllister-Lucas,L.M., Sonnenburg,W.K., Francis,S.H., Corbin,J.D., Beavo,J.A., and Ferguson,K. (1998). Isolation and characterization of cDNAs encoding PDE5A, a human cGMP-binding, cGMP-specific 3',5'-cyclic nucleotide phosphodiesterase. *Gene* 216, 139-147.
- Lovely,J.R. and Threlfall,R.J. (1978). Adenylate cyclase and cyclic AMP phosphodiesterase activity during the mitotic cycle of *Physarum polycephalum*. *Biochem. Biophys. Res. Commun.* 85, 579-584.
- Lovely,J.R. and Threlfall,R.J. (1979). The activity of guanylate cyclase and cyclic GMP phosphodiesterase during synchronous growth of the acellular slime mould *Physarum polycephalum*. *Biochem. Biophys. Res. Commun.* 86, 365-370.
- MacKenzie,S.J., Baillie,G.S., McPhee,I., Bolger,G.B., and Houslay,M.D. (2000). ERK2 mitogen-activated protein kinase binding, phosphorylation, and regulation of the PDE4D cAMP-specific phosphodiesterases. The involvement of COOH-terminal docking sites and NH2-terminal UCR regions. *J. Biol. Chem.* 275, 16609-16617.
- MacKenzie,S.J. and Houslay,M.D. (2000). Action of rolipram on specific PDE4 cAMP phosphodiesterase isoforms and on the phosphorylation of cAMP-response-element-binding protein (CREB) and p38 mitogen-activated protein (MAP) kinase in U937 monocytic cells. *Biochem. J.* 347, 571-578.
- MacKenzie,S.J., Yarwood,S.J., Peden,A.H., Bolger,G.B., Vernon,R.G., and Houslay,M.D. (1998). Stimulation of p70S6 kinase via a growth hormone-controlled phosphatidylinositol 3-kinase pathway leads to the activation of a PDE4A cyclic AMP-specific phosphodiesterase in 3T3-F442A preadipocytes. *Proc. Natl. Acad. Sci. U. S. A* 95, 3549-3554.
- Manganiello,V.C., Taira,M., Degerman,E., and Belfrage,P. (1995). Type III cGMP-inhibited cyclic nucleotide phosphodiesterases (PDE3 gene family). *Cell Signal.* 7, 445-455.
- Manganiello,V.C., Tanaka,T., and Murashima,S. (1990). Cyclic GMP-stimulated cyclic nucleotide phosphodiesterases. In *Isoenzymes of Cyclic Nucleotide Phosphodiesterases*, J.A.Beavo and M.D.Houslay, eds. (New York: Wiley), pp. 61-85.
- Marchmont,R.J. and Houslay,M.D. (1980). Insulin trigger, cyclic AMP-dependent activation and phosphorylation of a plasma membrane cyclic AMP phosphodiesterase. *Nature* 286, 904-906.
- Martinez,A., Castro,A., Gil,C., Miralpeix,M., Segarra,V., Domenech,T., Beleta,J., Palacios,J.M., Ryder,H., Miro,X., Bonet,C., Casacuberta,J.M., Azorin,F., Pina,B., and Puigdomenech,P. (2000). Benzyl derivatives of 2,1,3-benzo- and benzothienof[3,2-a]thiadiazine 2,2-dioxides: first phosphodiesterase 7 inhibitors. *J. Med. Chem.* 43, 683-689.
- Mary,D., Aussel,C., Ferrua,B., and Fehlmann,M. (1987). Regulation of interleukin 2 synthesis by cAMP in human T cells. *J. Immunol.* 139, 1179-1184.

- Matousovic,K., Grande,J.P., Chini,C.C., Chini,E.N., and Dousa,T.P. (1995). Inhibitors of cyclic nucleotide phosphodiesterase isozymes type-III and type-IV suppress mitogenesis of rat mesangial cells. *J. Clin. Invest* 96, 401-410.
- Matousovic,K., Tsuboi,Y., Walker,H., Grande,J.P., and Dousa,T.P. (1997). Inhibitors of cyclic nucleotide phosphodiesterase isozymes block renal tubular cell proliferation induced by folic acid. *J. Lab Clin. Med.* 130, 487-495.
- Matsushime,H., Roussel,M.F., Ashmun,R.A., and Sherr,C.J. (1991). Colony-stimulating factor 1 regulates novel cyclins during the G1 phase of the cell cycle. *Cell* 65, 701-713.
- McPhee,I., Pooley,L., Lobban,M., Bolger,G., and Houslay,M.D. (1995). Identification, characterization and regional distribution in brain of RPDE-6 (RNPDE4A5), a novel splice variant of the PDE4A cyclic AMP phosphodiesterase family. *Biochem. J.* 310 (Pt 3), 965-974.
- Michaeli,T., Bloom,T.J., Martins,T., Loughney,K., Ferguson,K., Riggs,M., Rodgers,L., Beavo,J.A., and Wigler,M. (1993). Isolation and characterization of a previously undetected human cAMP phosphodiesterase by complementation of cAMP phosphodiesterase- deficient *Saccharomyces cerevisiae*. *J. Biol. Chem.* 268, 12925-12932.
- Mikhailov,A. and Gundersen,G.G. (1998). Relationship between microtubule dynamics and lamellipodium formation revealed by direct imaging of microtubules in cells treated with nocodazole or taxol. *Cell Motil. Cytoskeleton* 41, 325-340.
- Milligan,G. (1998). New Aspects of G-protein-coupled receptor signalling and regulation. *Trends in endocrinology and metabolism* 9, 13-19.
- Minowada,J., Onuma,T., and Moore,G.E. (1972). Rosette-forming human lymphoid cell lines. I. Establishment and evidence for origin of thymus-derived lymphocytes. *J. Natl. Cancer Inst.* 49, 891-895.
- Mitchinson,J.M. (1971). *The Biology of the Cell Cycle*. Cambridge University Press).
- Modiano,J.F., Domenico,J., Szepesi,A., Lucas,J.J., and Gelfand,E.W. (1994). Differential requirements for interleukin-2 distinguish the expression and activity of the cyclin-dependent kinases Cdk4 and Cdk2 in human T cells. *J. Biol. Chem.* 269, 32972-32978.
- Molinari,M. (2000). Cell cycle checkpoints and their inactivation in human cancer. *Cell Prolif.* 33, 261-274.
- Monfar,M., Lemon,K.P., Grammer,T.C., Cheatham,L., Chung,J., Vlahos,C.J., and Blenis,J. (1995). Activation of pp70/85 S6 kinases in interleukin-2-responsive lymphoid cells is mediated by phosphatidylinositol 3-kinase and inhibited by cyclic AMP. *Mol. Cell Biol.* 15, 326-337.
- Montminy,M. (1997). Transcriptional regulation by cyclic AMP. *Annu. Rev. Biochem.* 66, 807-822.
- Morena,A.R., Boitani,C., de Grossi,S., Stefanini,M., and Conti,M. (1995). Stage and cell-specific expression of the adenosine 3',5' monophosphate- phosphodiesterase genes in the rat seminiferous epithelium. *Endocrinology* 136, 687-695.
- Morgan,D.O. (1999). Regulation of the APC and the exit from mitosis. *Nat. Cell Biol.* 1, E47-E53.

- Morisaki,H., Fujimoto,A., Ando,A., Nagata,Y., Ikeda,K., and Nakanishi,M. (1997). Cell cycle-dependent phosphorylation of p27 cyclin-dependent kinase (Cdk) inhibitor by cyclin E/Cdk2. *Biochem. Biophys. Res. Commun.* *240*, 386-390.
- Murphy, B. J and Scott, J. D. Functional anchoring of the cAMP-dependent protein kinase. *Trends Cardiovasc.Med.* *8*[2], 89-95. 1998.
Ref Type: Generic
- Musa,N.L., Ramakrishnan,M., Li,J., Kartha,S., Liu,P., Pestell,R.G., and Hershenson,M.B. (1999). Forskolin inhibits cyclin D1 expression in cultured airway smooth- muscle cells. *Am. J. Respir. Cell Mol. Biol.* *20*, 352-358.
- Naderi,S., Gutzkow,K.B., Christoffersen,J., Smeland,E.B., and Blomhoff,H.K. (2000). cAMP-mediated growth inhibition of lymphoid cells in G1: rapid down- regulation of cyclin D3 at the level of translation. *Eur. J. Immunol.* *30*, 1757-1768.
- Nair,K.G. (1966). Purification and properties of 3',5'-cyclic nucleotide phosphodiesterase from dog heart. *Biochemistry* *5*, 150-157.
- Nakayama,K.I., Hatakeyama,S., and Nakayama,K. (2001). Regulation of the cell cycle at the G1-S transition by proteolysis of cyclin E and p27Kip1. *Biochem. Biophys. Res. Commun.* *282*, 853-860.
- Naro,F., Zhang,R., and Conti,M. (1996). Developmental regulation of unique adenosine 3',5'-monophosphate- specific phosphodiesterase variants during rat spermatogenesis. *Endocrinology* *137*, 2464-2472.
- Neer,E.J. (1995). Heterotrimeric G proteins: organizers of transmembrane signals. *Cell* *80*, 249-257.
- Nemoz,G., Sette,C., and Conti,M. (1997). Selective activation of rolipram-sensitive, cAMP-specific phosphodiesterase isoforms by phosphatidic acid. *Mol. Pharmacol.* *51*, 242-249.
- Nigg,E.A. (2001). Mitotic kinases as regulators of cell division and its checkpoints. *Nat. Rev. Mol. Cell Biol.* *2*, 21-32.
- Nigg,E.A., Blangy,A., and Lane,H.A. (1996). Dynamic changes in nuclear architecture during mitosis: on the role of protein phosphorylation in spindle assembly and chromosome segregation. *Exp. Cell Res.* *229*, 174-180.
- Noguchi,K., Murata,T., and Cho-Chung,Y.S. (1998). 8-chloroadenosine 3',5'-monophosphate (8-Cl-cAMP) selectively eliminates protein kinase A type I to induce growth inhibition in c-ras- transformed fibroblasts. *Eur. J. Cancer* *34*, 1260-1267.
- Nurse,P. (2000). A long twentieth century of the cell cycle and beyond. *Cell* *100*, 71-78.
- O'Connell,J.C., McCallum,J.F., McPhee,I., Wakefield,J., Houslay,E.S., Wishart,W., Bolger,G., Frame,M., and Houslay,M.D. (1996). The SH3 domain of Src tyrosyl protein kinase interacts with the N- terminal splice region of the PDE4A cAMP-specific phosphodiesterase RPDE-6 (RNPDE4A5). *Biochem. J.* *318* (Pt 1), 255-261.
- Oberholte,R., Bhakta,S., Alvarez,R., Bach,C., Zuppan,P., Mulkins,M., Jarnagin,K., and Shelton,E.R. (1993). The cDNA of a human lymphocyte cyclic-AMP phosphodiesterase (PDE IV) reveals a multigene family. *Gene* *129*, 239-247.

- Oberholte,R., Ratzliff,J., Baecker,P.A., Daniels,D.V., Zuppan,P., Jarnagin,K., and Shelton,E.R. (1997). Multiple splice variants of phosphodiesterase PDE4C cloned from human lung and testis. *Biochim. Biophys. Acta* *1353*, 287-297.
- Oh,W.J., Joe,C.O., and Choi,K.H. (1996). Regulation of the activity of M-phase promoting factor through protein kinase A-mediated pathway in LP1-1 cells. *Biochem. Mol. Biol. Int.* *39*, 991-999.
- Ohi,R. and Gould,K.L. (1999). Regulating the onset of mitosis. *Curr. Opin. Cell Biol.* *11*, 267-273.
- Ohtsubo,M., Theodoras,A.M., Schumacher,J., Roberts,J.M., and Pagano,M. (1995). Human cyclin E, a nuclear protein essential for the G1-to-S phase transition. *Mol. Cell Biol.* *15*, 2612-2624.
- Osinski,M.T., Rauch,B.H., and Schror,K. (2001). Antimitogenic actions of organic nitrates are potentiated by sildenafil and mediated via activation of protein kinase A. *Mol. Pharmacol.* *59*, 1044-1050.
- Osinski,M.T. and Schror,K. (2000). Inhibition of platelet-derived growth factor-induced mitogenesis by phosphodiesterase 3 inhibitors: role of protein kinase A in vascular smooth muscle cell mitogenesis. *Biochem. Pharmacol.* *60*, 381-387.
- Page,K., Li,J., Wang,Y., Kartha,S., Pestell,R.G., and Hershenson,M.B. (2000). Regulation of cyclin D(1) expression and DNA synthesis by phosphatidylinositol 3-kinase in airway smooth muscle cells. *Am. J. Respir. Cell Mol. Biol.* *23*, 436-443.
- Paglia,M.J., Mou,H., and Cote,R.H. (2001). Regulation of photoreceptor phosphodiesterase (PDE6) by phosphorylation of its inhibitory {gamma} subunit re-evaluated. *J. Biol. Chem.*
- Pan,X., Arauz,E., Krzanowski,J.J., Fitzpatrick,D.F., and Polson,J.B. (1994). Synergistic interactions between selective pharmacological inhibitors of phosphodiesterase isozyme families PDE III and PDE IV to attenuate proliferation of rat vascular smooth muscle cells. *Biochem. Pharmacol.* *48*, 827-835.
- Pardee,A.B. (1989). G1 events and regulation of cell proliferation. *Science* *246*, 603-608.
- Pastan,I.H., Johnson,G.S., and Anderson,W.B. (1975). Role of cyclic nucleotides in growth control. *Annu. Rev. Biochem.* *44*, 491-522.
- Patel,R., Holt,M., Philipova,R., Moss,S., Schulman,H., Hidaka,H., and Whitaker,M. (1999). Calcium/calmodulin-dependent phosphorylation and activation of human Cdc25-C at the G2/M phase transition in HeLa cells. *J. Biol. Chem.* *274*, 7958-7968.
- Patel,T.B., Du,Z., Pierre,S., Cartin,L., and Scholich,K. (2001). Molecular biological approaches to unravel adenylyl cyclase signaling and function. *Gene* *269*, 13-25.
- Petzelt,C.P., Kodirov,S., Taschenberger,G., and Kox,W.J. (2001). Participation of the Ca(2+)-calmodulin-activated Kinase II in the control of metaphase-anaphase transition in human cells. *Cell Biol. Int.* *25*, 403-409.
- Piaggio,G., Farina,A., Perrotti,D., Manni,I., Fuschi,P., Sacchi,A., and Gaetano,C. (1995). Structure and growth-dependent regulation of the human cyclin B1 promoter. *Exp. Cell Res.* *216*, 396-402.

- Pines, J. and Hunter, T. (1989). Isolation of a human cyclin cDNA: evidence for cyclin mRNA and protein regulation in the cell cycle and for interaction with p34cdc2. *Cell* 58, 833-846.
- Pohl, S.L. (1981). Cyclic nucleotides and lipolysis. *Int. J. Obes.* 5, 627-633.
- Polyak, K., Kato, J.Y., Solomon, M.J., Sherr, C.J., Massague, J., Roberts, J.M., and Koff, A. (1994a). p27Kip1, a cyclin-Cdk inhibitor, links transforming growth factor-beta and contact inhibition to cell cycle arrest. *Genes Dev.* 8, 9-22.
- Polyak, K., Lee, M.H., Erdjument-Bromage, H., Koff, A., Roberts, J.M., Tempst, P., and Massague, J. (1994b). Cloning of p27Kip1, a cyclin-dependent kinase inhibitor and a potential mediator of extracellular antimitogenic signals. *Cell* 78, 59-66.
- Pooley, L., Shakur, Y., Rena, G., and Houslay, M.D. (1997). Intracellular localization of the PDE4A cAMP-specific phosphodiesterase splice variant RD1 (RNPDE4A1A) in stably transfected human thyroid carcinoma FTC cell lines. *Biochem. J.* 321 (Pt 1), 177-185.
- Prouty, S.M., Hanson, K.D., Boyle, A.L., Brown, J.R., Shichiri, M., Follansbee, M.R., Kang, W., and Sedivy, J.M. (1993). A cell culture model system for genetic analyses of the cell cycle by targeted homologous recombination. *Oncogene* 8, 899-907.
- Puck, T.T., Waldren, C.A., and Hsie, A.W. (1972). Membrane dynamics in the action of dibutyryl adenosine 3':5'-cyclic monophosphate and testosterone on mammalian cells. *Proc. Natl. Acad. Sci. U. S. A* 69, 1943-1947.
- Pulverer, B.J., Kyriakis, J.M., Avruch, J., Nikolakaki, E., and Woodgett, J.R. (1991). Phosphorylation of c-jun mediated by MAP kinases. *Nature* 353, 670-674.
- Ramakrishnan, M., Musa, N.L., Li, J., Liu, P.T., Pestell, R.G., and Hershenson, M.B. (1998). Catalytic activation of extracellular signal-regulated kinases induces cyclin D1 expression in primary tracheal myocytes. *Am. J. Respir. Cell Mol. Biol.* 18, 736-740.
- Ramstad, C., Sundvold, V., Johansen, H.K., and Lea, T. (2000). cAMP-dependent protein kinase (PKA) inhibits T cell activation by phosphorylating ser-43 of raf-1 in the MAPK/ERK pathway. *Cell Signal.* 12, 557-563.
- Ravanko, K., Jarvinen, K., Paasinen-Sohns, A., and Holttä, E. (2000). Loss of p27Kip1 from cyclin E/cyclin-dependent kinase (CDK) 2 but not from cyclin D1/CDK4 complexes in cells transformed by polyamine biosynthetic enzymes. *Cancer Res.* 60, 5244-5253.
- Reem, G.H., Cook, L.A., and Palladino, M.A. (1984). Regulation of interleukin-2 synthesis in human thymocytes. *J. Biol. Response Mod.* 3, 195-205.
- Rena, G., Begg, F., Ross, A., MacKenzie, C., McPhee, I., Campbell, L., Huston, E., Sullivan, M., and Houslay, M.D. (2001). Molecular cloning, genomic positioning, promoter identification, and characterization of the novel cyclic amp-specific phosphodiesterase PDE4A10. *Mol. Pharmacol.* 59, 996-1011.
- Robicsek, S.A., Blanchard, D.K., Djeu, J.Y., Krzanowski, J.J., Szentivanyi, A., and Polson, J.B. (1991). Multiple high-affinity cAMP-phosphodiesterases in human T-lymphocytes. *Biochem. Pharmacol.* 42, 869-877.
- Rogers, D.F. and Giembycz, M.A. (1998). Asthma therapy for the 21st century. *Trends Pharmacol. Sci.* 19, 160-164.

Roovers,K. and Assoian,R.K. (2000). Integrating the MAP kinase signal into the G1 phase cell cycle machinery. *Bioessays* 22, 818-826.

Rubin, C. S., Rangel Aldao, R., Sarker, D., Erlichman, J., and Fleischer, N. Characterisation and comparison of membrane-associated and cytosolic cAMP-dependent protein kinases; physicochemical and immunological studies on bovine cerebral cortex protein kinases. *J.Biol.Chem.* 254, 3797-3805. 1979.
Ref Type: Generic

Rybalkin,S.D., Rybalkina,I.G., Feil,R., Hofmann,F., and Beavo,J.A. (2001). Regulation of cGMP-specific phosphodiesterase (PDE5) phosphorylation in smooth muscle cells. *J. Biol. Chem.*

Sadhu,K., Hensley,K., Florio,V.A., and Wolda,S.L. (1999). Differential expression of the cyclic GMP-stimulated phosphodiesterase PDE2A in human venous and capillary endothelial cells. *J. Histochem. Cytochem.* 47, 895-906.

Salanova,M., Chun,S.Y., Iona,S., Puri,C., Stefanini,M., and Conti,M. (1999). Type 4 cyclic adenosine monophosphate-specific phosphodiesterases are expressed in discrete subcellular compartments during rat spermiogenesis. *Endocrinology* 140, 2297-2306.

Sanchez,D., Labarca,P., and Darszon,A. (2001). Sea urchin sperm cation-selective channels directly modulated by cAMP. *FEBS Lett.* 503, 111-115.

Sander,B., Cardell,S., Moller,G., and Moller,E. (1991). Differential regulation of lymphokine production in mitogen-stimulated murine spleen cells. *Eur. J. Immunol.* 21, 1887-1892.

Sano,R., Miki,T., Suzuki,Y., Shimada,F., Taira,M., Kanatsuka,A., Makino,H., Hashimoto,N., and Saito,Y. (2001). Analysis of the insulin-sensitive phosphodiesterase 3B gene in type 2 diabetes. *Diabetes Res. Clin. Pract.* 54, 79-88.

Sasaki,T., Kotera,J., and Omori,K. (2002). Novel alternative splice variants of rat phosphodiesterase 7B showing unique tissue-specific expression and phosphorylation. *Biochem. J.* 361, 211-220.

Sasaki,T., Kotera,J., Yuasa,K., and Omori,K. (2000). Identification of human PDE7B, a cAMP-specific phosphodiesterase. *Biochem. Biophys. Res. Commun.* 271, 575-583.

Sauer,K. and Lehner,C.F. (1995). The role of cyclin E in the regulation of entry into S phase. *Prog. Cell Cycle Res.* 1, 125-139.

Savini,F., Berardi,S., Tatone,D., and Spoto,G. (1995). Phosphodiesterase in human colon carcinoma cell line CaCo-2 in culture. *Life Sci.* 56, L421-L425.

Schmitt,J.M. and Stork,P.J. (2000). beta 2-adrenergic receptor activates extracellular signal-regulated kinases (ERKs) via the small G protein rap1 and the serine/threonine kinase B-Raf. *J. Biol. Chem.* 275, 25342-25350.

Schmitt,J.M. and Stork,P.J. (2001). Cyclic AMP-mediated inhibition of cell growth requires the small G protein Rap1. *Mol. Cell Biol.* 21, 3671-3683.

Scott,J.D. (1991). Cyclic nucleotide-dependent protein kinases. *Pharmacol. Ther.* 50, 123-145.

- Scott,J.D., Stofko,R.E., McDonald,J.R., Comer,J.D., Vitalis,E.A., and Mangili,J.A. (1990). Type II regulatory subunit dimerization determines the subcellular localization of the cAMP-dependent protein kinase. *J. Biol. Chem.* *265*, 21561-21566.
- Scott,P.H., Belham,C.M., al Hafidh,J., Chilvers,E.R., Peacock,A.J., Gould,G.W., and Plevin,R. (1996). A regulatory role for cAMP in phosphatidylinositol 3-kinase/p70 ribosomal S6 kinase-mediated DNA synthesis in platelet-derived-growth- factor-stimulated bovine airway smooth-muscle cells. *Biochem. J.* *318 (Pt 3)*, 965-971.
- Seth,A., Alvarez,E., Gupta,S., and Davis,R.J. (1991). A phosphorylation site located in the NH2-terminal domain of c-Myc increases transactivation of gene expression. *J. Biol. Chem.* *266*, 23521-23524.
- Sette,C. and Conti,M. (1996). Phosphorylation and activation of a cAMP-specific phosphodiesterase by the cAMP-dependent protein kinase. Involvement of serine 54 in the enzyme activation. *J. Biol. Chem.* *271*, 16526-16534.
- Sewing,A., Burger,C., Brusselbach,S., Schalk,C., Lucibello,F.C., and Muller,R. (1993). Human cyclin D1 encodes a labile nuclear protein whose synthesis is directly induced by growth factors and suppressed by cyclic AMP. *J. Cell Sci.* *104 (Pt 2)*, 545-555.
- Shacter,E., Stadtman,E.R., Jurgensen,S.R., and Chock,P.B. (1988). Role of cAMP in cyclic cascade regulation. *Methods Enzymol.* *159*, 3-19.
- Shahinian,A., Pfeffer,K., Lee,K.P., Kundig,T.M., Kishihara,K., Wakeham,A., Kawai,K., Ohashi,P.S., Thompson,C.B., and Mak,T.W. (1993). Differential T cell costimulatory requirements in CD28-deficient mice. *Science* *261*, 609-612.
- Shakur,Y., Wilson,M., Pooley,L., Lobban,M., Griffiths,S.L., Campbell,A.M., Beattie,J., Daly,C., and Houslay,M.D. (1995). Identification and characterization of the type-IVA cyclic AMP-specific phosphodiesterase RD1 as a membrane-bound protein expressed in cerebellum. *Biochem. J.* *306 (Pt 3)*, 801-809.
- Shames,B.D., McIntyre,R.C., Jr., Bensard,D.D., Pulido,E.J., Selzman,C.H., Reznikov,L.L., Harken,A.H., and Meng,X. (2001). Suppression of tumor necrosis factor alpha production by cAMP in human monocytes: dissociation with mRNA level and independent of interleukin- 10. *J. Surg. Res.* *99*, 187-193.
- Sheaff,R.J., Groudine,M., Gordon,M., Roberts,J.M., and Clurman,B.E. (1997). Cyclin E-CDK2 is a regulator of p27Kip1. *Genes Dev.* *11*, 1464-1478.
- Sherr,C.J. (1993). Mammalian G1 cyclins. *Cell* *73*, 1059-1065.
- Shibata,H., Robinson,F.W., Soderling,T.R., and Kono,T. (1991). Effects of okadaic acid on insulin-sensitive cAMP phosphodiesterase in rat adipocytes. Evidence that insulin may stimulate the enzyme by phosphorylation. *J. Biol. Chem.* *266*, 17948-17953.
- Shichijo,M., Shimizu,Y., Hiramatsu,K., Inagaki,N., Tagaki,K., and Nagai,H. (1997). Cyclic AMP-elevating agents inhibit mite-antigen-induced IL-4 and IL-13 release from basophil-enriched leukocyte preparation. *Int. Arch. Allergy Immunol.* *114*, 348-353.
- Skalhegg,B.S., Rasmussen,A.M., Tasken,K., Hansson,V., Jahnsen,T., and Lea,T. (1994). Cyclic AMP sensitive signalling by the CD28 marker requires concomitant stimulation by the T-cell antigen receptor (TCR/CD3) complex. *Scand. J. Immunol.* *40*, 201-208.

- Skalhegg,B.S. and Tasken,K. (2000). Specificity in the cAMP/PKA signaling pathway. Differential expression,regulation, and subcellular localization of subunits of PKA. *Front Biosci.* 5, D678-D693.
- Smith,C.J., Vasta,V., Degerman,E., Belfrage,P., and Manganiello,V.C. (1991). Hormone-sensitive cyclic GMP-inhibited cyclic AMP phosphodiesterase in rat adipocytes. Regulation of insulin- and cAMP-dependent activation by phosphorylation. *J. Biol. Chem.* 266, 13385-13390.
- Smith,K.A. (1984). Interleukin 2. *Annu. Rev. Immunol.* 2, 319-333.
- Smits,V.A. and Medema,R.H. (2001). Checking out the G(2)/M transition. *Biochim. Biophys. Acta* 1519, 1-12.
- Soderling,S.H., Bayuga,S.J., and Beavo,J.A. (1998). Cloning and characterization of a cAMP-specific cyclic nucleotide phosphodiesterase. *Proc. Natl. Acad. Sci. U. S. A* 95, 8991-8996.
- Soderling,S.H. and Beavo,J.A. (2000). Regulation of cAMP and cGMP signaling: new phosphodiesterases and new functions. *Curr. Opin. Cell Biol.* 12, 174-179.
- Solberg,R., Sandberg,M., Natarajan,V., Torjesen,P.A., Hansson,V., Jahnsen,T., and Tasken,K. (1997). The human gene for the regulatory subunit RI alpha of cyclic adenosine 3', 5'-monophosphate-dependent protein kinase: two distinct promoters provide differential regulation of alternately spliced messenger ribonucleic acids. *Endocrinology* 138, 169-181.
- Souness,J.E., Hassall,G.A., and Parrott,D.P. (1992). Inhibition of pig aortic smooth muscle cell DNA synthesis by selective type III and type IV cyclic AMP phosphodiesterase inhibitors. *Biochem. Pharmacol.* 44, 857-866.
- Spada,A., Lania,A., Mantovani,S., and Ballare,E. (1997). Cyclic AMP and calcium in the transduction of hypothalamic neurohormone action in human pituitary tumors. *Horm. Res.* 47, 235-239.
- Spadari,S., Focher,F., Sala,F., Ciarrocchi,G., Koch,G., Falaschi,A., and Pedrali-Noy,G. (1985). Control of cell division by aphidicolin without adverse effects upon resting cells. *Arzneimittelforschung.* 35, 1108-1116.
- Spence,S., Rena,G., Sweeney,G., and Houslay,M.D. (1995). Induction of Ca²⁺/calmodulin-stimulated cyclic AMP phosphodiesterase (PDE1) activity in Chinese hamster ovary cells (CHO) by phorbol 12- myristate 13-acetate and by the selective overexpression of protein kinase C isoforms. *Biochem. J.* 310 (Pt 3), 975-982.
- Stacey,P., Rulten,S., Dapling,A., and Phillips,S.C. (1998). Molecular cloning and expression of human cGMP-binding cGMP-specific phosphodiesterase (PDE5). *Biochem. Biophys. Res. Commun.* 247, 249-254.
- Steen,R.L., Martins,S.B., Tasken,K., and Collas,P. (2000). Recruitment of protein phosphatase 1 to the nuclear envelope by A- kinase anchoring protein AKAP149 is a prerequisite for nuclear lamina assembly. *J. Cell Biol.* 150, 1251-1262.
- Stein,J.C., Farooq,M., Norton,W.T., and Rubin,C.S. (1987). Differential expression of isoforms of the regulatory subunit of type II cAMP-dependent protein kinase in rat neurons, astrocytes, and oligodendrocytes. *J. Biol. Chem.* 262, 3002-3006.

Stephen,J., Osborne,M.P., Spencer,A.J., and Warley,A. (1990). From HeLa cell division to infectious diarrhoea. *Scanning Microsc.* 4, 781-786.

Stewart,A.G., Harris,T., Fernandes,D.J., Schachte,L.C., Koutsoubos,V., Guida,E., Ravenhall,C.E., Vadiveloo,P., and Wilson,J.W. (1999). Beta2-adrenergic receptor agonists and cAMP arrest human cultured airway smooth muscle cells in the G(1) phase of the cell cycle: role of proteasome degradation of cyclin D1. *Mol. Pharmacol.* 56, 1079-1086.

Stryer,L., Hurley,J.B., and Fung,B.K. (1983). Transducin and the cyclic GMP phosphodiesterase of retinal rod outer segments. *Methods Enzymol.* 96, 617-627.

Sullivan,M., Olsen,A.S., and Houslay,M.D. (1999). Genomic organisation of the human cyclic AMP-specific phosphodiesterase PDE4C gene and its chromosomal localisation to 19p13.1, between RAB3A and JUND. *Cell Signal.* 11, 735-742.

Sullivan,M., Rena,G., Begg,F., Gordon,L., Olsen,A.S., and Houslay,M.D. (1998). Identification and characterization of the human homologue of the short PDE4A cAMP-specific phosphodiesterase RD1 (PDE4A1) by analysis of the human HSPDE4A gene locus located at chromosome 19p13.2. *Biochem. J.* 333 (Pt 3), 693-703.

Sundstrom,C. and Nilsson,K. (1976). Establishment and characterization of a human histiocytic lymphoma cell line (U-937). *Int. J. Cancer* 17, 565-577.

Sutherland,E.W. and Rall,T.W. (1958). Fractionation and characterisation of a cyclic adenine ribonucleotide formed by tissue particles. *J. Biol. Chem.* 232, 1077-1091.

Tachibana,K., Hirota,S., Iizasa,H., Yoshida,H., Kawabata,K., Kataoka,Y., Kitamura,Y., Matsushima,K., Yoshida,N., Nishikawa,S., Kishimoto,T., and Nagasawa,T. (1998). The chemokine receptor CXCR4 is essential for vascularization of the gastrointestinal tract. *Nature* 393, 591-594.

Takemoto,D.J., Lee,W.N., Kaplan,S.A., and Appleman,M.M. (1978). Cyclic AMP phosphodiesterase in human lymphocytes and lymphoblasts. *J. Cyclic. Nucleotide. Res.* 4, 123-132.

Tamaoki,T., Nomoto,H., Takahashi,I., Kato,Y., Morimoto,M., and Tomita,F. (1986). Staurosporine, a potent inhibitor of phospholipid/Ca⁺⁺dependent protein kinase. *Biochem. Biophys. Res. Commun.* 135, 397-402.

Tasken,K.A., Collas,P., Kemmner,W.A., Witczak,O., Conti,M., and Tasken,K. (2001). Phosphodiesterase 4D and protein kinase a type II constitute a signaling unit in the centrosomal area. *J. Biol. Chem.* 276, 21999-22002.

Taussig,R. and Gilman,A.G. (1995). Mammalian membrane-bound adenylyl cyclases. *J. Biol. Chem.* 270, 1-4.

Tavare, J. M. and Issad, T. Two-dimensional phosphopeptide mapping of receptor tyrosine kinases. *Protein kinase protocols* 124, 67-85. 2001.
Ref Type: Generic

Taylor,S.S., Knighton,D.R., Zheng,J., Ten Eyck,L.F., and Sowadski,J.M. (1992). Structural framework for the protein kinase family. *Annu. Rev. Cell Biol.* 8, 429-462.

Tenor,H., Staniciu,L., Schudt,C., Hatzelmann,A., Wendel,A., Djukanovic,R., Church,M.K., and Shute,J.K. (1995). Cyclic nucleotide phosphodiesterases from purified human CD4⁺ and CD8⁺ T lymphocytes. *Clin. Exp. Allergy* 25, 616-624.

- Tetsuka,T., Kusano,E., Takeda,S., Homma,S., Yoshida,I., Ando,Y., and Asano,Y. (1995). Activation of protein kinase C stimulates cAMP phosphodiesterase in rat renal collecting tubule. *Am. J. Physiol* 268, F808-F814.
- Thompson,C.B., Lindsten,T., Ledbetter,J.A., Kunkel,S.L., Young,H.A., Emerson,S.G., Leiden,J.M., and June,C.H. (1989). CD28 activation pathway regulates the production of multiple T-cell- derived lymphokines/cytokines. *Proc. Natl. Acad. Sci. U. S. A* 86, 1333-1337.
- Thompson,W.J. and Appleman,M.M. (1971). Cyclic nucleotide phosphodiesterase and cyclic AMP. *Ann. N. Y. Acad. Sci.* 185, 36-41.
- Thyberg,J. and Moskalewski,S. (1989). Subpopulations of microtubules with differential sensitivity to nocodazole: role in the structural organization of the Golgi complex and the lysosomal system. *J. Submicrosc. Cytol. Pathol.* 21, 259-274.
- Toledo,L.M. and Lydon,N.B. (1997). Structures of staurosporine bound to CDK2 and cAPK--new tools for structure-based design of protein kinase inhibitors. *Structure.* 5, 1551-1556.
- Tomlinson,P.R., Wilson,J.W., and Stewart,A.G. (1995). Salbutamol inhibits the proliferation of human airway smooth muscle cells grown in culture: relationship to elevated cAMP levels. *Biochem. Pharmacol.* 49, 1809-1819.
- Toribio,M.L., Gutierrez-Ramos,J.C., Pezzi,L., Marcos,M.A., and Martinez,C. (1989). Interleukin-2-dependent autocrine proliferation in T-cell development. *Nature* 342, 82-85.
- Tournier,S., Raynaud,F., Gerbaud,P., Lohmann,S.M., Doree,M., and Evain-Brion,D. (1991). Association of type II cAMP-dependent protein kinase with p34cdc2 protein kinase in human fibroblasts. *J. Biol. Chem.* 266, 19018-19022.
- Tramontano,D., Moses,A.C., and Ingbar,S.H. (1988). The role of adenosine 3',5'-monophosphate in the regulation of receptors for thyrotropin and insulin-like growth factor I in the FRTL5 rat thyroid follicular cell. *Endocrinology* 122, 133-136.
- Tsou,K.C., Hong,D.H., Varello,M., Wheeler,J.E., Giuntoli,R., Mangan,C., and Mikuta,J. (1986). Determination of cell cycle DNA and 5'-nucleotide phosphodiesterase in endometrial cancer. *Ann. N. Y. Acad. Sci.* 468, 316-328.
- Tsou,K.C., Morris,H.P., Lo,K.W., and Muscato,J.J. (1974). 5'-Nucleotide phosphodiesterase activity in rat hepatoma. *Cancer Res.* 34, 1295-1298.
- Tsoukas,C.D., Landgraf,B., Bentin,J., Valentine,M., Lotz,M., Vaughan,J.H., and Carson,D.A. (1985). Activation of resting T lymphocytes by anti-CD3 (T3) antibodies in the absence of monocytes. *J. Immunol.* 135, 1719-1723.
- Tsuboi,Y., Shankland,S.J., Grande,J.P., Walker,H.J., Johnson,R.J., and Dousa,T.P. (1996). Suppression of mesangial proliferative glomerulonephritis development in rats by inhibitors of cAMP phosphodiesterase isozymes types III and IV. *J. Clin. Invest* 98, 262-270.
- Tsuchikane,E., Fukuhara,A., Kobayashi,T., Kirino,M., Yamasaki,K., Kobayashi,T., Izumi,M., Otsuji,S., Tateyama,H., Sakurai,M., and Awata,N. (1999). Impact of cilostazol on restenosis after percutaneous coronary balloon angioplasty. *Circulation* 100, 21-26.

Tsuiki,H., Nitta,M., Tada,M., Inagaki,M., Ushio,Y., and Saya,H. (2001). Mechanism of hyperploid cell formation induced by microtubule inhibiting drug in glioma cell lines. *Oncogene* 20, 420-429.

Tsygankova,O.M., Saavedra,A., Rebhun,J.F., Quilliam,L.A., and Meinkoth,J.L. (2001). Coordinated regulation of Rap1 and thyroid differentiation by cyclic AMP and protein kinase A. *Mol. Cell Biol.* 21, 1921-1929.

Van Der Geer, P, Luo, K, Sefton, B. M, and Hunter, T. Phosphopeptide mapping and phosphoamino acid analysis on cellulose thin-layer plates. Protein phosphorylation a practical approach 123, 32-59. 1993.
Ref Type: Generic

van Oirschot,B.A., Stahl,M., Lens,S.M., and Medema,R.H. (2001). Protein Kinase A Regulates Expression of p27kip1 and Cyclin D3 to Suppress Proliferation of Leukemic T Cell Lines. *J. Biol. Chem.* 276, 33854-33860.

Verde,I., Pahlke,G., Salanova,M., Zhang,G., Wang,S., Coletti,D., Onuffer,J., Jin,S.L., and Conti,M. (2001). Myomegalin is a novel protein of the golgi/centrosome that interacts with a cyclic nucleotide phosphodiesterase. *J. Biol. Chem.* 276, 11189-11198.

Verdoodt,B., Decordier,I., Geleyns,K., Cunha,M., Cundari,E., and Kirsch-Volders,M. (1999). Induction of polyploidy and apoptosis after exposure to high concentrations of the spindle poison nocodazole. *Mutagenesis* 14, 513-520.

Verne,J., Fournier,E., Gervais,P., Hebert,S., and Richshoffer,N. (1973). Direct stimulant effect of cyclic AMP and dibutyryl cAMP on glycogenolysis by hepatocytes in histiotypic culture. *Biomedicine.* 19, 130-132.

Vicini,E. and Conti,M. (1997). Characterization of an intronic promoter of a cyclic adenosine 3',5'- monophosphate (cAMP)-specific phosphodiesterase gene that confers hormone and cAMP inducibility. *Mol. Endocrinol.* 11, 839-850.

Viscomi,C., Altomare,C., Bucchi,A., Camatini,E., Baruscotti,M., Moroni,A., and DiFrancesco,D. (2001). C terminus-mediated control of voltage and cAMP gating of hyperpolarization-activated cyclic nucleotide-gated channels. *J. Biol. Chem.* 276, 29930-29934.

Vossler,M.R., Yao,H., York,R.D., Pan,M.G., Rim,C.S., and Stork,P.J. (1997). cAMP activates MAP kinase and Elk-1 through a B-Raf- and Rap1-dependent pathway. *Cell* 89, 73-82.

Wacholtz,M.C., Minakuchi,R., and Lipsky,P.E. (1991). Characterization of the 3',5'-cyclic adenosine monophosphate-mediated regulation of IL2 production by T cells and Jurkat cells. *Cell Immunol.* 135, 285-298.

Wachtel,H. (1982). Characteristic behavioural alterations in rats induced by rolipram and other selective adenosine cyclic 3', 5'-monophosphate phosphodiesterase inhibitors. *Psychopharmacology (Berl)* 77, 309-316.

Walker,T.R., Moore,S.M., Lawson,M.F., Panettieri,R.A., Jr., and Chilvers,E.R. (1998). Platelet-derived growth factor-BB and thrombin activate phosphoinositide 3-kinase and protein kinase B: role in mediating airway smooth muscle proliferation. *Mol. Pharmacol.* 54, 1007-1015.

Walsh,D.A., Perkins,J.P., and Krebs,E.G. (1968). An adenosine 3',5'-monophosphate dependent protein kinase from rabbit skeletal muscle. *J. Biol. Chem.* **243**, 3763-3765.

Walworth,N.C. (2001). DNA damage: Chk1 and Cdc25, more than meets the eye. *Curr. Opin. Genet. Dev.* **11**, 78-82.

Wang,L., Liu,F., and Adamo,M.L. (2001a). Cyclic amp inhibits extracellular signal-regulated kinase and phosphatidylinositol 3-kinase/akt pathways by inhibiting rap1. *J. Biol. Chem.* **276**, 37242-37249.

Wang,P., Wu,P., Egan,R.W., and Billah,M.M. (2000). Cloning, characterization, and tissue distribution of mouse phosphodiesterase 7A1. *Biochem. Biophys. Res. Commun.* **276**, 1271-1277.

Wang,P., Wu,P., Egan,R.W., and Billah,M.M. (2001b). Human phosphodiesterase 8A splice variants: cloning, gene organization, and tissue distribution. *Gene* **280**, 183-194.

Weber,J.D., Raben,D.M., Phillips,P.J., and Baldassare,J.J. (1997). Sustained activation of extracellular-signal-regulated kinase 1 (ERK1) is required for the continued expression of cyclin D1 in G1 phase. *Biochem. J.* **326 (Pt 1)**, 61-68.

Weinberg,R.A. (1995). The retinoblastoma protein and cell cycle control. *Cell* **81**, 323-330.

Whitaker,M. (1997). Calcium and mitosis. *Prog. Cell Cycle Res.* **3**, 261-269.

Wright,J.H., Munar,E., Jameson,D.R., Andreassen,P.R., Margolis,R.L., Seger,R., and Krebs,E.G. (1999). Mitogen-activated protein kinase activity is required for the G(2)/M transition of the cell cycle in mammalian fibroblasts. *Proc. Natl. Acad. Sci. U. S. A* **96**, 11335-11340.

Wright,P.A., Lemoine,N.R., Goretzki,P.E., Wyllie,F.S., Bond,J., Hughes,C., Roher,H.D., Williams,E.D., and Wynford-Thomas,D. (1991). Mutation of the p53 gene in a differentiated human thyroid carcinoma cell line, but not in primary thyroid tumours. *Oncogene* **6**, 1693-1697.

Yamashita,Y.M., Nakaseko,Y., Kumada,K., Nakagawa,T., and Yanagida,M. (1999). Fission yeast APC/cyclosome subunits, Cut20/Apc4 and Cut23/Apc8, in regulating metaphase-anaphase progression and cellular stress responses. *Genes Cells* **4**, 445-463.

Yamashita,Y.M., Nakaseko,Y., Samejima,I., Kumada,K., Yamada,H., Michaelson,D., and Yanagida,M. (1996). 20S cyclosome complex formation and proteolytic activity inhibited by the cAMP/PKA pathway. *Nature* **384**, 276-279.

Yan,C., Zhao,A.Z., Bentley,J.K., and Beavo,J.A. (1996). The calmodulin-dependent phosphodiesterase gene PDE1C encodes several functionally different splice variants in a tissue-specific manner. *J. Biol. Chem.* **271**, 25699-25706.

Yanagida,M., Yamashita,Y.M., Tatebe,H., Ishii,K., Kumada,K., and Nakaseko,Y. (1999). Control of metaphase-anaphase progression by proteolysis: cyclosome function regulated by the protein kinase A pathway, ubiquitination and localization. *Philos. Trans. R. Soc. Lond B Biol. Sci.* **354**, 1559-1569.

Yang,J., Winkler,K., Yoshida,M., and Kormbluth,S. (1999). Maintenance of G2 arrest in the *xenopus* oocyte: a role for 14-3-3 mediated inhibition of Cdc25 nuclear import. *EMBO J.* **18**, 2174-2183.

233
Yarwood,S.J., Steele,M.R., Scotland,G., Houslay,M.D., and Bolger,G.B. (1999). The RACK1 signaling scaffold protein selectively interacts with the cAMP-specific phosphodiesterase PDE4D5 isoform. *J. Biol. Chem.* 274, 14909-14917.

Zeilig,C.E., Johnson,R.A., Sutherland,E.W., and Friedman,D.L. (1976). Adenosine 3':5'-monophosphate content and actions in the division cycle of synchronized HeLa cells. *J. Cell Biol.* 71, 515-534.

Zerfass-Thome,K., Schulze,A., Zwerschke,W., Vogt,B., Helin,K., Bartek,J., Henglein,B., and Jansen-Durr,P. (1997). p27KIP1 blocks cyclin E-dependent transactivation of cyclin A gene expression. *Mol. Cell Biol.* 17, 407-415.

Zwartkruis,F.J. and Bos,J.L. (1999). Ras and Rap1: two highly related small GTPases with distinct function. *Exp. Cell Res.* 253, 157-165.



